

(200)

R 298

DEPARTMENT OF THE INTERIOR
UNITED STATES GEOLOGICAL SURVEY

INTERPRETATION OF AEROMAGNETIC
ANOMALIES IN SOUTHEASTERN MISSOURI

By

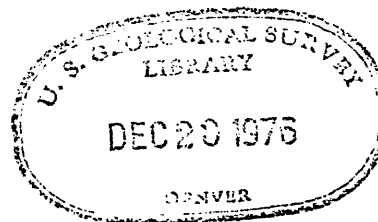
John W. Allingham

A study of the relations of aeromagnetic anomalies to the
Precambrian igneous geology and related mineral deposits

Prepared in cooperation with the
Missouri Geological Survey

Open-file Report 76-868

1976



This report is preliminary
and has not been edited or
reviewed for confromity with
U.S. Geological Survey standards
or nomenclature.

This report is the first draft of a manuscript which was written in 1966 and intended for more formal publication. It is released now (1976) in its original form to make the data available to the public.

CONTENTS

	PAGE
Abstract.....	1
Introduction.....	4
Geological and geophysical investigations.....	10
Acknowledgments.....	16
Physiography.....	18
Interpretative problems and results.....	28
Geologic setting.....	33
Igneous and sedimentary rocks.....	41
Volcanic rocks.....	44
Granitic rocks.....	47
Mafic rocks.....	49
Sedimentary rocks.....	50
Lamotte Sandstone.....	50a
Bonneterre Dolomite.....	51
Davis Formation.....	54
Derby-Doerun Dolomite.....	54a
Potosi Dolomite.....	55
Eminence Dolomite.....	57
Magnetic properties of the rocks.....	59
Measurements.....	61
Susceptibility.....	62
Remanent magnetism.....	70

CONTENTS (Continued)

PAGE

Structure.....	75
Faults.....	82
Joints.....	86a
Mineral deposits.....	87
Classification.....	93
Structural control.....	94
Domal and anticlinal structures.....	94
Ridge and basin structures.....	97
Fractures.....	100
Aeromagnetic survey.....	108
Collection and compilation of data.....	109
Field operations.....	109
Compilation of field data.....	110
Accuracy of position.....	110
Total-intensity map.....	113
Aeromagnetic anomalies.....	118
Interpretative techniques.....	120
Data and calculations.....	130
Characteristic anomalies.....	132

CONTENTS (Continued)	PAGE
Rock relations.....	152
Structural relations.....	158
Topographic anomalies.....	160
Roof pendants of volcanic rocks.....	169
Faults and basins.....	176
Relations to mineral deposits.....	185
Iron deposits.....	186
Pea Ridge anomaly.....	187
Cottoner Mountain anomaly.....	195
Kratz Spring anomaly.....	200
Shepherd Mountain anomaly.....	201
Iron Mountain anomaly.....	207
Lead and zinc deposits.....	208
Potosi area.....	210
The eastern mining area.....	221
Irondale anomaly.....	223
Bonne Terre area.....	225
Anomalies and mines.....	229
Analysis of anomalies.....	233
Detailed aeromagnetic data.....	245
Relations to regional features.....	249
Sources of volcanic rocks.....	250
Belle anomaly.....	252
Ironton anomaly.....	257
Indian Creek anomaly.....	260
Richwoods anomaly.....	265

CONTENTS (Continued)	PAGE
Avon anomaly.....	272
Gabbroic rocks.....	275
Subsurface structure and geophysical data.....	277
Resume and conclusions.....	291
References.....	294

TABLES

	PAGE
Table 1. Average susceptibility of rocks from the St. Francois Mountains.....	60
Table 2. Depths to buried Precambrian basement es- timated from aeromagnetic data.....	124
Table 3. Correlation of Precambrian topography and lowamplitude magnetic anomalies.....	167
Table 4. High-amplitude anomalies related to possible mineralized volcanic structures.....	251
Table 5. Ring-like magnetic anomalies in Missouri.....	256

ILLUSTRATIONS

PAGE

Figure 1. Index map of Missouri showing exposed Precambrian igneous rocks and major structural features.....	19
2. Geologic map of the St. Francois Mountains.....	34
2a. Aeromagnetic and geologic map of the lead mining district of southeastern Missouri.....	at end
3. Total-intensity aeromagnetic map of the St. Francois Mountains.....	35
<hr/>	
4. Generalized geologic section on the flanks of the St. Francois Mountains.....	40
5. Stratigraphic section of Precambrian and Cambrian rocks in the Bonne Terre area, Missouri.....	43
6. Plot of magnetite vs magnetic susceptibility of rocks from the St. Francois Mountains.....	64
7. Range of magnetic susceptibility of rocks from the St. Francois Mountains.....	66
8. Susceptibilities of granitic rocks in the St. Francois Mountains.....	68
9. Susceptibilities of volcanic rocks in the St. Francois Mountains.....	69
10. Remanent moments of samples of rhyolite near Stouts Creek before and after partial demagnetization.....	72
11. Random scatter of remanent vectors of granitic rocks from the St. Francois Mountains.....	74

ILLUSTRATIONS (Continued)

PAGE

12. Relations between sedimentary and basement structures.....	95
14. Use of Polar charts for two- and three dimensional analyses of aeromagnetic anomalies.....	121
15. Diagram showing the parameters used to compute the displacement of normal faults in basement rocks.....	126
16. Characteristic magnetic profiles across vertical fault zones.....	134
17. Width of the Simms Mountain fault zone estimated from aeromagnetic data.....	135
18. Characteristic total-intensity magnetic profiles over normal faults.....	136
19. Aeromagnetic interpretation of the Palmer fault zone.....	137
20. Magnetic effect of inclined contacts between granite and volcanic rocks.....	139
21. Characteristic total-intensity magnetic profiles in the magnetic meridian over vertical contacts showing the effects of varied rock susceptibilities.	140

ILLUSTRATIONS (Continued)

PAGE

22. Characteristic effects of ends of volcanic flows at different thicknesses and depths.....	141
23. Aeromagnetic profiles over contacts between granitic and volcanic rocks near Flatwoods area.....	142
24. Aeromagnetic profiles over volcanic flows near Minimum and Criswell, Missouri.....	143
25. Prismatic model used to approximate aeromagnetic anomalies of the type near Shirley, Missouri.....	145
26. Interpretation of the high-amplitude anomaly near Shirley, Missouri.....	146
27. Magnetic profiles over cylindrical models of infinite depth extent.....	147
28. Aeromagnetic anomaly associated with a plug-like feature near Pyatt.....	148
29. Magnetic profiles over erosional areas in volcanic flows.....	150
30. Aeromagnetic anomaly at Cedar Creek caused by an erosional discontinuity in volcanic flows.....	151
31. Aeromagnetic and geologic map of part of southeastern Missouri showing contrasting aeromagnetic patterns over granitic and volcanic rocks.....	153

ILLUSTRATIONS (Continued)

PAGE

32. Subsurface structure and lithology deduced from aeromagnetic profiles over the St. Francois Mountains.....	155
33. Topography of a granite knob showing the irregular three-dimensional model used in computations.....	161
34. The magnetic effect of topographic relief by three-dimensional techniques.....	162
35. Magnetic profiles computed from two-dimensional models showing the effect of topography.....	166
36. The magnetic expression of a rhyolite hill and a gabbro sill on granite terrain at Evans Mountain.....	170
37. The magnetic effect of volcanic rocks on gabbro terrain at Bald Knob.....	171
38. Subsurface structure of a roof pendant at Tin Mountain from aeromagnetic data.....	173
39. Magnetic profiles showing the effect of topography and deep-rooted subsurface structure of volcanic rocks at Crane Mountain.....	175
39a. Diagrammatic section showing aeromagnetic anomalies over the complex St. Genevieve fault zone.....	177
40. Aeromagnetic profile from Flat River to Cabanne Course, showing the effect of basement topography and major fault zones.....	179

ILLUSTRATIONS (Continued)

PAGE

41. Subsurface structure of the volcanic roof pendant and fault zone at Simms Mountain deduced from aeromagnetic data.....	180
42. Aeromagnetic profile over a ridge of trachyte and pyroclastic rocks at Buford Mountain.....	182
43. Computed magnetic profiles over models of representing (a) the shallow Bellevue basin and (b) the Farmington anticline.....	183
44. The high-amplitude aeromagnetic anomaly at Pea Ridge, Missouri, caused by a large magnetite-rich iron deposit.....	188
45. Second-vertical derivative of the Pea Ridge anomaly at 1/2-mile spacing suggesting an arcuate deposit.....	189
46. Second-vertical derivative of the Pea Ridge anomaly at 1/4-mile spacing suggesting a linear deposit....	191
47. Magnetic anomalies caused by volcanic rocks and magnetite body at Pea Ridge.....	192
48. Susceptibility measurements of rhyolite cored from the U.S. Bureau of Mines drill hole (BN-1) near Bourbon.....	194
49. The high-amplitude aeromagnetic anomaly at Cottoner Mountain near Marquand.....	196

ILLUSTRATIONS (Continued)

PAGE

50. Second-vertical derivative of the Mt. Cottoner anomaly near Marquand.....	198
51. Interpretation of a total-intensity aeromagnetic profile over a potential iron deposit at Cottoner Mountain.....	199
52. The Kratz Spring aeromagnetic anomaly, Union quadrangle that suggests a potential buried iron deposit.....	202
<hr/>	
52a. Susceptibility measurements of rhyolite core from drill holes at Shepherd Mountain, (a) Russell Mountain, and (b) Anderson Mountain. (c).....	203
<hr/>	
53. Total-intensity aeromagnetic anomaly at Potosi showing the distribution of residual lead and barite deposits.....	211
54. Second-vertical derivative of the Potosi anomaly at 3000-ft grid spacing showing the magnetic gradient that outlines the source rock.....	213
55. Second-vertical derivative of the Potosi anomaly at 2000-ft grid spacing.....	215
56. Second-vertical derivative of the Potosi anomaly at 1000-ft grid spacing.....	216
57. Potosi anomaly continued downward to 900 ft above sea level.....	217

ILLUSTRATIONS (Continued)	PAGE
58. Potosi anomaly continued downward to 100 ft below sea level, near the Precambrian surface.....	218
59. Magnetic profiles across the anomaly at Potosi showing the effect of downward continuation.....	219
60. Aeromagnetic and geologic map showing the major features of the main mining area near Bonne Terre, Missouri.....	222
61. Aeromagnetic (below) data showing correlation with Precambrian outcrop, subsurface topography, and faults (above) at Irondale, Missouri	224
63. Aeromagnetic profile showing the effect of topo- graphy and estimated depth to basement at Chicken Farm Knob.....	227
64. Aeromagnetic profiles over a granite knob at Bonne Terre showing low amplitude and continuity of the magnetic anomaly and its correlation with mine workings.....	230
65. Total-intensity aeromagnetic map of the Bonne Terre area, southeastern Missouri showing its relation to faults, mine workings, and buried knobs.....	232
66. Residual anomalies from the third-degree represen- tation of the geomagnetic field in the Bonne Terre area.....	235

ILLUSTRATIONS (Continued)

PAGE

67. Second-vertical derivative of the observed magnetic field in the Bonne Terre area.....	236
68. Aeromagnetic field in the Bonne Terre area continued downward to 100 ft below sea level, about average Precambrian surface level.....	237
69. Third-degree polynomial representation of the geomagnetic field in the Bonne Terre area.....	240
70. Profiles of derived magnetic fields over the rhyolite pendant of Switchback knob.....	242
71. Profiles of derived magnetic field over the rhyolite pendant of Chicken Farm Knob.....	243
72. Detailed total intensity aeromagnetic map of the Bonne Terre area having a 20-gamma contour interval.	246
73. Correlation of aeromagnetic data and mine workings at Leadwood, Missouri.....	248
74. The circular aeromagnetic anomaly at Belle, Missouri.	253
75. Magnetic profiles across the Belle anomaly showing dimensions of magnetically contrasting rock.....	254
76. Correlation of exposed igneous rocks and derived magnetic fields in the Ironton area.....	258
77. Susceptibility of trachytic rocks cored from a buried ridge near Indian Creek, Missouri.....	261

ILLUSTRATIONS (Continued)

PAGE

78. Correlation between aeromagnetic anomaly (solid) and subsurface topography (dashed) of Precambrian rocks near Indian Creek.....	263
79. Aeromagnetic profile over a ridge of trachyte of high susceptibility near Indian Creek.....	264
80. Aeromagnetic anomaly in the Richwoods area.....	266
81. Field of the Richwoods anomaly continued down- ward to 700 ft, about ground level.....	268
82. Field of the Richwoods anomaly continued down- ward to 600 ft below sea level, nearly the Precambrian surface level.....	269
83. Second-vertical derivative of the observed field in the Richwoods area.....	270
84. Profiles across the Richwoods aeromagnetic anomaly showing the effect of downward continuation on the total-intensity field.....	271
85. Subsurface structure and intrusive relation- ships near Avon.....	274
86. Relations of faults and earthquake epicenters at the margins of the St. Francois Mountains, Mississippi embayment, and western Kentucky.....	279
87. Magnetic lineaments and exposed Precambrian rocks in southeastern Missouri.....	282

ILLUSTRATIONS (Continued)	PAGE
88. Fracture systems, structural lineaments and contours on the buried Precambrian surface.....	283
89. Bouguer gravity, major subsurface magnetic units and inferred lithology.....	284
90. Fractures deduced from aeromagnetic and geologic information.....	288
91. Areas of postulated archipelago environment surrounding the St. Francois Mountains.....	289

Interpretation of aeromagnetic
anomalies in southeastern Missouri

by

John W. Allingham

U. S. Geological Survey

Washington, D. C.

ABSTRACT

Precambrian igneous rocks are exposed in the St. Francois Mountains, hilly core of the Ozark uplift. These rocks represent the top of a composite granite batholith that intruded a sequence of older volcanic rocks. Sheets of granophyre, granite porphyry, and thin roof pendants of resistant felsic volcanic rock (felsite) were incorporated into the granite terrain. Diabase and gabbro intruded mainly the contact between the granite and volcanic rock. The dominant fracture system has a rhombic pattern of northwesterly and northeasterly trend. Faulting near the granite-felsite isolated large blocks of coarse-grained granite that floor many shallow sedimentary basins. The Ozark region is characterized by its relatively flat landscape, thin flat-lying Paleozoic strata overlying an eroded igneous terrain of hills and knobs. Buried hills and ridges of granitic and volcanic rocks indirectly localized lead deposits in overlying Cambrian carbonate strata that flank the uplift. These igneous rocks also are host for iron and copper deposits.

The granitic rocks are distinguished by their magnetic properties, The coarse-grained granite is the least magnetic, whereas the fine-grained granophytic rock near the top of the batholith is more magnetic than some volcanic rocks. Most of the granitic rocks have low uniform magnetic susceptibility of about 1.7×10^{-3} emu/cm³, whereas volcanic rocks have higher susceptibilities because of local variations in amount of magnetite. Remanent magnetization of the granitic and volcanic rocks is negligible; thus, induction theory applies to most of the anomalies.

Large distinctive negative anomalies are associated with several shallow granite-floored basins containing Cambrian strata. Granite exposed at the in, basin rims have negligible or low susceptibility and reversed remanent magnetism. Faults and shear zones in igneous rocks produce magnetic lows that have amplitudes less than 100 gammas.

Hills and ridges of exposed igneous rock produce aeromagnetic anomalies of less than 200 gammas. Small amplitudes and limited lateral extent distinguish these low-amplitude anomalies from broad magnetic features related to major rock units. Anomalies associated with hills of volcanic rock have magnitudes twice as large as anomalies over comparable surfaces of granite. Anomalies resulting from hills of red granite range up to 100 gammas in amplitude, whereas anomalies resulting from hills of volcanic or fine-grained granophytic rock range up to 200 gammas. Some intermediate anomalies, 200-600 gammas in amplitude, are caused by a combination of topography and magnetic inhomogeneities of roof pendants. More magnetic volcanic and granophytic rock form dense, resistant hills on less magnetic granitic

terrain. Analyses of anomalies yielded the subsurface configuration of some isolated roof pendants of volcanic rocks.

Anomalies having amplitudes greater than 1000 gammas and limited areal extent indicate potential magnetite-rich iron deposits. Analyses of anomalies yield some dimensions and attitude of these deposits.

Analytical methods used in this study of aeromagnetic data emphasize low-amplitude anomalies associated with buried hills and ridges of basement rock. Computer techniques were used to continue the observed field downward towards its source, calculate vertical derivatives and separate residual anomalies. Continuation downward had the highest resolving power and correlates best with mine workings in areas of reliable subsurface control. The relations between lead deposits and analytically derived anomalies are useful guides for exploring stratigraphically favorable areas in the Ozark uplift.

Regional geology of the basement rocks is deduced from aeromagnetic anomalies by use of characteristic magnetic profiles over models representing common structures such as faults, contacts, prismatic, tabular and cylindrical rock units. Analysis of aeromagnetic data in southeastern Missouri shows that magnetic anomalies can be used to distinguish granitic from volcanic terrains, locate or extend faults and contacts between rock units, locate and define some buried basement hills and ridges, locate isolated volcanic roof pendants and determine their thickness, indicate magnetite-rich basement rocks. Analysis of magnetic data is not only helpful in disclosing regional structures but is also helpful in delineating sites favorable for mineral exploration in the Ozark uplift of southeast Missouri.

INTRODUCTION

The Ozark uplift in southeastern Missouri was aeromagnetically surveyed in cooperation with the Missouri Geological Survey from 1946 to 1948. The observed magnetic anomalies are a potential source of regional subsurface geologic information and might be used to guide mineral exploration.

Criteria to distinguish some rock units and to obtain geologic structure were developed from analyses of aeromagnetic anomalies over exposed igneous rocks in the St. Francois Mountains, over known structures and over mine workings in the lead district;

these data were extended to buried basement around the uplift to enhance knowledge of regional geology by delineating major features of the Precambrian surface and thereby aiding the search for deposits of iron and lead.

The mining district of southeastern Missouri has been one of the world's leading lead producers for almost a century. The site of the major first discovery of lead in 1820, Mine LaMotte, was mined until recently. The main producing area, locally called the Lead Belt, has yielded over eight million tons of lead from nearly three hundred million tons of ore. New reserves of lead are being developed and mined on the western flank of the St. Francois Mountains. This district is presently the largest lead producing area in the world and accounts for more than 30 percent of present annual U. S. production (1960).

Buried irregular Precambrian topography of igneous knobs and fault scarps controlled depositional sand ridges, gal reefs, slide breccias and zones of fracturing in the overlying Cambrian Bonneterre Formation. These sedimentary and tectonic structures are host for large deposits of disseminated galena. Precambrian rocks in the Ozark uplift are considered an important potential source of iron ore, especially since the discovery of the magnetite and hematite deposit at Pea Ridge. This southeastern region is still a major producing area for barite and accounts for about 40 percent of the total production in the United States (1960).

In 1946 the U.S. Geological Survey made an aeromagnetic survey in the Berryman-Potosi area to test its usefulness as a rapid means of examining large areas for economic mineral deposits and delineating regional structural features. The survey was premised on the known association of widespread disseminated lead deposits in sedimentary structures that were controlled by relief on the buried Precambrian surface. As a result of this successful test, the U.S. Geological Survey in cooperation with the Division of Geological Survey and Water Resources of the State of Missouri, aeromagnetically surveyed 17 15-minute quadrangles covering the eastern part of the Ozark uplift, including the lead mining district and the St. Francois Mountains. Aeromagnetic maps of this area were published in 1949 and 1950. As part of this program an interpretative study of the aeromagnetic data was undertaken in 1956 by the U.S. Geological Survey. The fundamental objective of this study was to relate surface configuration, rock type, regional and detailed structural features and mineral deposits to magnetic patterns in areas partly exposed Precambrian igneous rock and to extend the knowledge gained to data in areas of buried magnetic Precambrian rock. Several interpretive methods and techniques were used and compared in this work.

Geological and geophysical investigations

Professor Tolman in 1931 undertook a long range systematic study of the igneous rocks in the St. Francois Mountains, presented a general classification and description of the igneous rocks and subdivided them in an attempt to differentiate and interrelate the types of rocks. Recently, problems and current observations on the Precambrian rocks were outlined in a guidebook to the geology of the St. Francois Mountain area, edited by Hayes (1961). Anderson (1962) made a detailed study of ash flow tuffs in the Taum Sauk area of the St. Francois Mountains.

Structures in the Precambrian rocks were described by Graves (1938). Tarr (1936, p. 716-717) and James (1952, p. 650-651) described major features in the regional structural setting for lead deposits. Subsurface structure in the Bourbon area was investigated by Searight and others (1954) in connection with ground magnetic surveys.

Murphy and Mejia (1961, p. 129-136) recently discussed the geology of the Iron Mountain deposit. They favored the magmatic injection theory advocated earlier by Spurr (1927) and Ridge (1957).

Tarr (1936, p. 740-741) and James (1952, p. 654-657) described important relations between the lead deposits and Precambrian topography. The relations of ore-bearing sedimentary structures to the Precambrian surface recently were discussed in detail by Ohle and Brown (1954, p. 201-222), Snyder and Emery (1956, p. 1216) and Snyder and Odell (1958, p. 899-926).

In a summary of geophysical methods used in the search for lead deposits Scharon (1952) discussed magnetic surveys used to locate favorable buried knobs and ridges and electrical resistivity surveys used to measure depth to favorable strata and therein locate fractured zones.

In 1956, the writer collected igneous rocks in the St. Francois Mountains for a study of magnetic minerals physical properties and their application to aeromagnetic interpretation. Henderson (1957; 1958) used several of the small magnetic anomalies for his studies on dipole theory and application of a graphical method to three-dimensional bodies in the St. Francois Mountains. Analyses of aeromagnetic anomalies began in 1958. Some of the problems and interpretative results of this study were outlined in a brief report (Allingham, 1960, p. B-216-219).

Ganguli (1955), Neal (1956), and Gregson (1958) related their gravity surveys of parts of Franklin, Crawford, and Washington Counties to the volcanic rocks of the basement. Later Algermissen (1961) showed that some underground and surface gravity anomalies relate to buried igneous knobs. From a regional survey of the St. Francois Mountains, Gerlach and Scharon (1960) concluded that local anomalies correlate with buried Precambrian topography but do not correlate surface lithologies.

The paleomagnetic investigations of some Precambrian volcanic and granitic rocks in the St. Francois Mountains was made by Hays (1961) and Hsu (1962). Their results corroborated earlier measurements for aeromagnetic interpretation. Hays and Scharon (1963) showed some of the difficulties in attempting to relate measurements of remanent magnetism to ground surveys.

Acknowledgments

Aeromagnetic surveys in southeastern Missouri were made in cooperation with the Missouri Geological Survey which was then under the direction of E. L. Clark, State Geologist.

The staff of the Missouri Geological Survey under the direction of State Geologists, T. R. Beveridge and later W. C. Hayes, helped the writer in many ways, particularly in geologic compilation.

The author gratefully acknowledges the cooperation of officials and geologic staff of the St. Joseph Lead Company, the National Lead Company, American Zinc and Smelting Company, and the Ozark Mining Company, subsidiary of M. A. Hanna Company for furnishing subsurface samples from their drilling program and geologic information from exploration and mines. The writer is also indebted to the staff of the Geology Department of the Missouri School of Mines and Technology and the U. S. Bureau of Mines at Rolla for core samples and geologic information. H. L. Scharon, Professor of Geophysics, and Walter Hays, Research Assistant, Washington University at St. Louis, provided much information on rock magnetism from the Ironton area.

Gordon French of Rolla assisted in sampling igneous rocks in Washington County. James L. Connolly of Ironton, because of his knowledge of the Ozark region, guided and assisted the author during field sampling in 1956.

The writer especially acknowledges the assistance and counsel of colleagues and other personnel of the Geological Survey, who contributed directly to this study. A. L. Baldwin, Jr., and W. E. Huff, Jr. prepared and measured the magnetic properties of rock samples from southeast Missouri. Montgomery Higgins, J. C. Lowe, and B. L. White assisted in making numerical integrations and computations; together with Alan Niem and Natalie Tyson, they prepared magnetic input information, compiled and contoured computed data. R. G. Henderson provided guidance in applying mathematical procedures. James Marsheck and W. L. Anderson furnished computer programs and computations.

Geography

The mining region of southeastern Missouri is in the broad Interior Highlands Province of Fenneman (1938). This conspicuous physiographic feature is known as the Ozark plateau. The plateau surface is well dissected and only visible in the flat top ridges and hills. Mountains formerly buried beneath Upper Cambrian seas were uplifted during the Appalachian orogeny into an asymmetrical dome, known as the Ozark uplift.

Hills and knobs of exposed Precambrian igneous rock that form the core of the Ozark uplift, shown in figure 1, were named the St. Francois

Figure 1.--Near here

Mountains by Winslow (1896, p. 4). Aeromagnetic surveys interpreted in this report include the St. Francois Mountains and some of the shallow sedimentary basins that flank the uplift (fig. 2a) about 4,100 square miles were aeromagnetically surveyed by the U.S. Geological Survey in cooperation with the Missouri Geological Survey (fig. 2a). This area extends from parallel $37^{\circ}15'$ northward to $38^{\circ}15'$ and from meridian $91^{\circ}00'$ eastward to $90^{\circ}7\frac{1}{2}'$. The eastern boundary lies about 20 miles west of the Mississippi River.

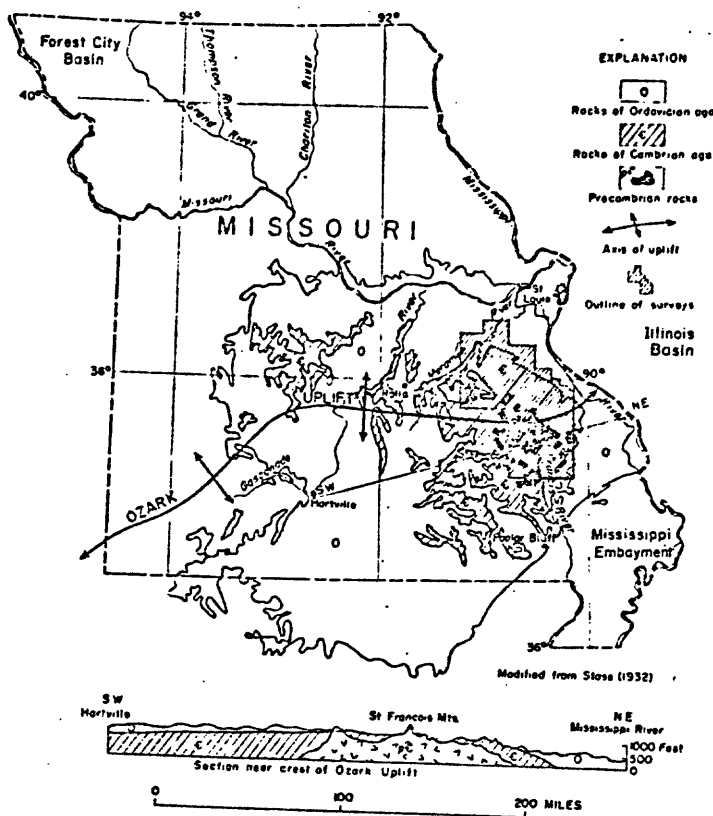


Figure 1.--Index map of Missouri showing exposed Precambrian igneous rocks and major structural features.

Relief of the ancient surface of Precambrian rocks was greater than the present relief. The valleys are now filled with sedimentary rocks that lap upon or cover the igneous knobs. This condition resulted in two distinct types of topography, a hilly upland area and gently rolling lowland areas. This area has a relief of 500 to 700 ft, as the hills exhibit their maximum relief near Taum Sauk Mountain. At an altitude of 1,772 ft, Taum Sauk is the highest point in the state. The intermontane valleys have an average altitude of 1,000 ft. Lowlands near Farmington average 900 ft. The nature of the buried Precambrian surface has been described by Graves (1938), French (1956) and later by Grenia (1960). Outcrops of igneous rocks at the borders of the Ozark region show that this area is underlain by a plateau of Precambrian igneous rocks. Although the topography of the exposed Precambrian surface shows considerable relief, direct evidence is lacking that the surface buried under Paleozoic formations has about the same relief.

In Missouri a number of wells penetrate the Precambrian surface and indicate a maximum depth in excess of 2,000 ft below this surface. Drilling at Sullivan showed that the Precambrian rocks are near surface or about 75 ft in depth, whereas at Bourbon and Pea Ridge the depth to the Precambrian surface is about 1,100 ft. Igneous knobs in the vicinity of Little Pilot Knob (fig. 2a) are flanked by Roubidoux and Gasconade sandstone and dolomite that exhibit a commonly observed peripheral initial dip. Drill hole information north of these knobs penetrated 1,400 ft of dolomite sandstone and shale and indicated a steep subsurface profile and high relief for these knobs. Additional information concerning the depth and nature of the Precambrian surface in southeast Missouri can be obtained from the aeromagnetic data.

Interpretative problems and results

The use of aeromagnetic anomalies to outline subsurface configurations of magnetic rock units is the most important contribution the magnetic method makes to regional geology and mineral exploration in southeastern Missouri. Many distributions of magnetic rock can be postulated to produce the observed anomalies; numerous assumptions about the variables can result in the ambiguity of multiple solutions. In order to eliminate some variables in magnetic computations, some knowledge of physical properties of the rocks are required. Areas of exposed rock and structural information permitted the sampling necessary for magnetic properties and direct correlation with geology.

The kind of interpretation, whether quantitative or qualitative depends upon the approach to the problem. Direct or indirect methods are used to interpret anomalies.

In the direct method of interpretation, fields are derived directly from the observed magnetic data and correlated with geology. These correlations then are extended to other areas. The method yields mainly qualitative results, which are particularly useful in shallow knob-and-basin or archipelago environment of the lead deposits. By direct correlation with geology, aeromagnetic information is used to differentiate some magnetically contrasting types of rock in the igneous basement. Granitic rock was distinguished from some volcanic rocks, and their areal extent and distribution is inferred from distinctive magnetic patterns, which are related to width and amplitude of anomalies. Shallow basin-like areas and some Precambrian knobs and ridges of low topographic relief are detected by examining aeromagnetic anomalies. Major fault zones that contain altered non-magnetic igneous rock are detected or extended beyond their mapped limits by magnetic data. These data can be used to guide mineral exploration, because continued or derived magnetic fields correlate with extensive lead deposits in the mining district. The direct method lacks the quantitative results of the indirect method of interpretation or modeling.

From known geological and assumed physical data such as the size, shape, depth of burial and magnetic characteristics of a rock unit, magnetic profiles are computed from a magnetic model. In the indirect method these parameters are changed until the computed profile fits the observed magnetic data. The method of modeling yields mainly quantitative structural information, such as the thickness or attitude of volcanic pendants.

Unknown geologic conditions may impose severe limitations on the methods of interpretations. Inhomogeneities in rock units or an uneven distribution of magnetic minerals caused by weathering or alteration may produce irregularities in magnetic data that are unrelated to size, shape or attitude of the units. The inhomogeneities in basement rocks and shallow burial of the Precambrian surface can introduce inaccuracies in determining depth to basement.

Two types of aeromagnetic anomalies are recognized by their areal extent, namely, broad regional anomalies and small local anomalies. The broad anomalies are related to large magnetically contrasting rock units, whereas the small anomalies are related to topography or small local variations in magnetite content of an otherwise homogeneous unit.

Before analyzing small local anomalies associated with small geologic features, the interpreter must isolate these anomalies from regional anomalies. An anomaly is isolated in two steps by removing the combined effects of the geomagnetic gradient and any regional anomaly. First the process of fitting a smoothed (polynomial) surface to the observed total intensity field by the method of least squares is performed by digital computers. Secondly, local (residual) anomalies are obtained by subtracting the smoothed surface from the observed field.

As Paleozoic strata in this region are nonmagnetic, the nature of the sand contact with the Precambrian surface is not disclosed by aeromagnetic data. Lead-bearing sedimentary structures may not be resolved because of the undetected smoothing effect of sand on an irregular basement surface.

The grid for computing derived fields such as downward continuation or second-vertical derivatives depends on an accurate estimate of the depth to the magnetic sources. Estimated depths to the magnetic basement are only accurate to 10 percent for some anomalies. Additional errors result from grid points interpolated by least squares method from irregularly distributed data. Limitations on the data are imposed by the spacing between flight lines and distance to the sources of anomalies. The resultant residual anomalies depend on the selection of the least-square fit of high-order surfaces that represent the regional anomaly field. Higher-order surfaces decrease the amplitude of some residual anomalies and affect the interpretation of the geometry of the source. The regional anomalies and trends reflect larger crustal blocks, whereas the local anomalies reflect small structural features such as volcanic necks, topographic relief on the basement surface, or fault traces.

GEOLOGIC SETTING

The earliest known geologic event in the Ozark region was extensive volcanism. Extrusion of volcanic flows and pyroclastic rocks was followed by intrusion of granite and iron mineralization. Emplacement of mafic dikes and sills was the Precambrian intrusive event. The area was then uplifted, tilted, and eroded to form the original St. Francois Mountains.

Exposed in a part of the uplift is the top of a granite batholith, which intruded volcanic rock and enclosed small bodies of granophyre and rock pendants of resistant extrusive rock. These extrusive rocks are part of the basement on which Paleozoic strata were deposited. Many hills of volcanic rock were steep-sided and conical in shape. Granite surfaces were generally undulating relative flat surfaces between the valleys.

The igneous rock units in the St. Francois Mountains shown in figure 2

Figure 2.--Near here

comprise a thick sequence of extensive prebatholithic rocks, slightly deformed rhyolite flows, welded tuffs, and interbedded pyroclastic units. The batholithic rocks are coarse-grained red and gray granite, and related phases of granite porphyry and granophyre.

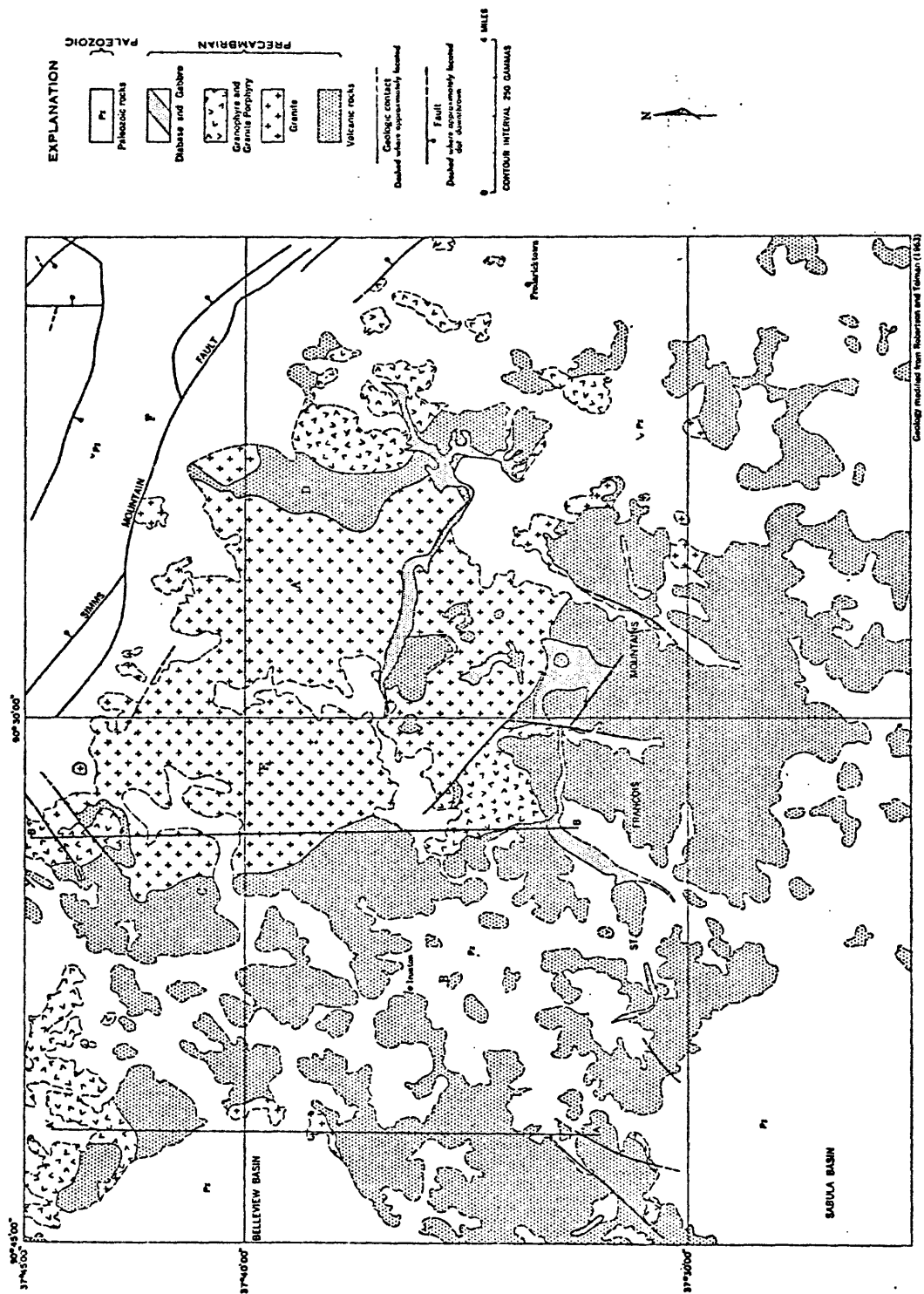


Figure 2.—Geologic map of the St. Francois Mountains.

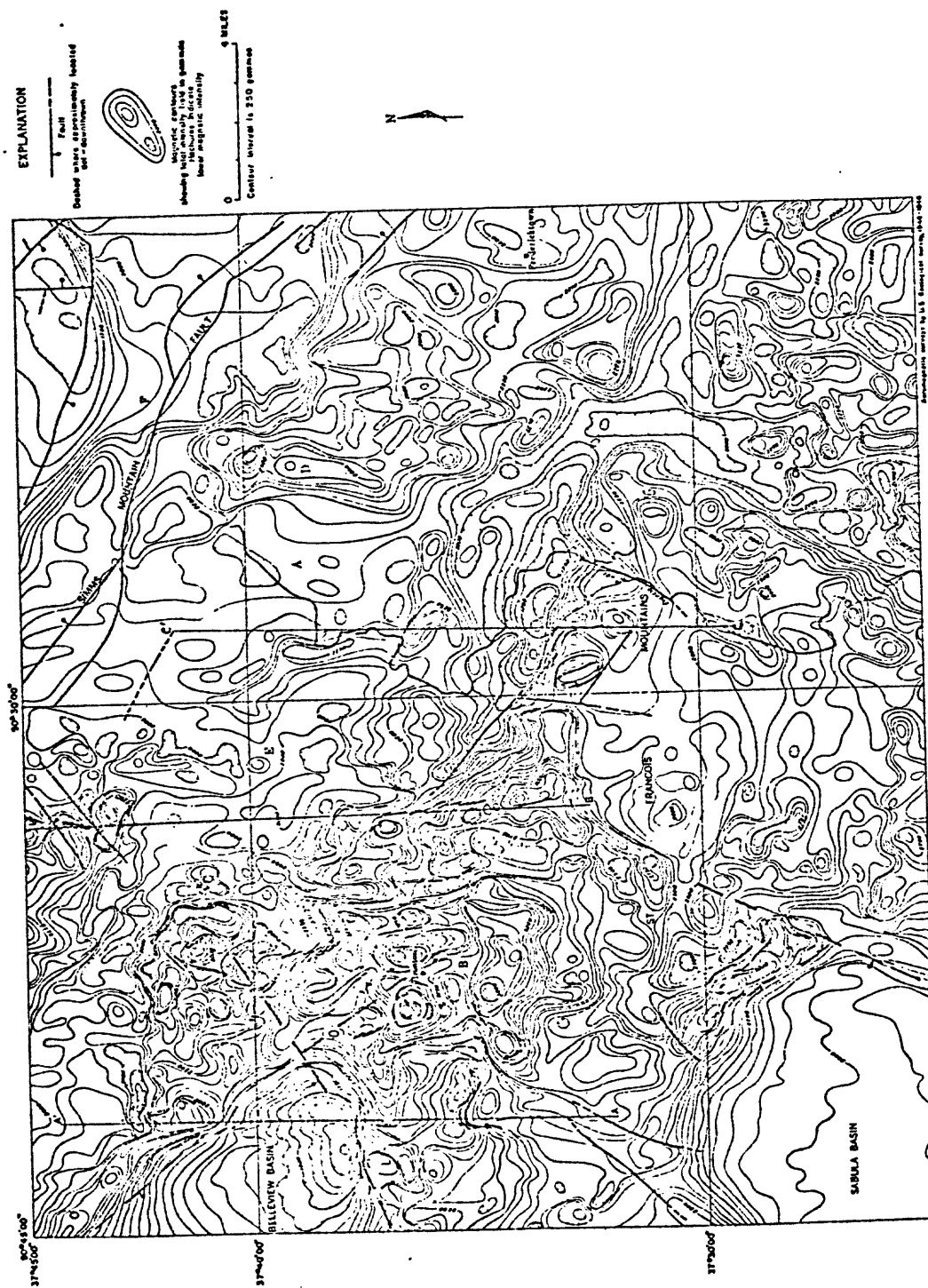


Figure 3.—Total-intensity aeromagnetic map of the St. Francois Mountains.

The fine-grained porphyry and granophyre are believed by the writer to be hypabyssal equivalents of the underlying granite. The coarse-grained granitic rocks contain few ferromagnesian minerals. Following emplacement of the granite, the region was intruded by sheet-like mafic dikes and sills of diabase.

This igneous terrain is part of a stable continental shield and is relatively undisturbed tectonically. Much of the region surrounding the mountains or hilly core of Precambrian rock is characterized by sedimentary formations of Cambrian and Lower Ordovician age that lap upon and bury ridges and knobs of Precambrian volcanic and granitic rock.

Boulder debris accumulated as talus on the slopes of knobs and hills before the Upper Cambrian seas deposited clastic sediments of the Lamotte Sandstone. Near the iron deposits, iron-bearing fragments and cobbles concentrated in these conglomerate beds. Haworth (1888, p. 285) postulated an archipelago of many small islands separated by valleys in which Cambrian strata were deposited. The Lamotte Sandstone, lowermost Upper Cambrian strata, fills the intermontane basins, obscures irregularities in the eroded igneous terrain and feathers out on the flanks of higher knobs. Deposition of the Lamotte Sandstone was marked by a sandy transition to carbonate deposition of the Bonneterre Dolomite. The Bonneterre strata fill the old valleys and capped many of the igneous hills. The basal beds of the overlying Bonneterre Formation contain depositional ridges, reefs, and slump breccias. These dolomitic rocks contain the most productive lead deposits.

The major faults and dominant fracture patterns trend northeast, northwest and west according to Graves (1938). Faults, particularly near the contact between granite and volcanic rock, isolated large blocks of downdropped granite that now underlay some shallow basins (B), (C), and (K) shown in Figure 3. Faulting and tilting of the basement rocks, prior to sedimentation, provided sufficient local

Figure 3 near here

relief of the development of a maturely dissected landscape of ridges and rounded knobs, the basic environment for the mineral deposits. Graves (1938, p. 142-152) postulated that a number of fault blocks developed within the Ozark dome. A drop of about 500 feet in the crustal block on the north side of the Simms Mountain fault has superimposed a southwest dip of nearly 2° on the district. Within the mined area a complex set of fractures trending northwestward was expressed by a number of small faults having both pre- and post-ore movement.

The generalized section in figure 4 shows the rocks that stratigraphically and structurally control the mineral deposits. Precambrian

Figure 4 near here

raphically and structurally control the mineral deposits. Precambrian rocks are host for iron and copper deposits. Lead deposits are partly controlled by (1) the pinchout line of the Lamotte Sandstone where it laps up on hills of basement rock, and by (2) depositional structures, such as sand ridges, reefs, and other sedimentary features of the overlying Bonneterre Dolomite. Some deposits of lead and barite are controlled by extensive fractures in the massive cherty Potosi Dolomite.

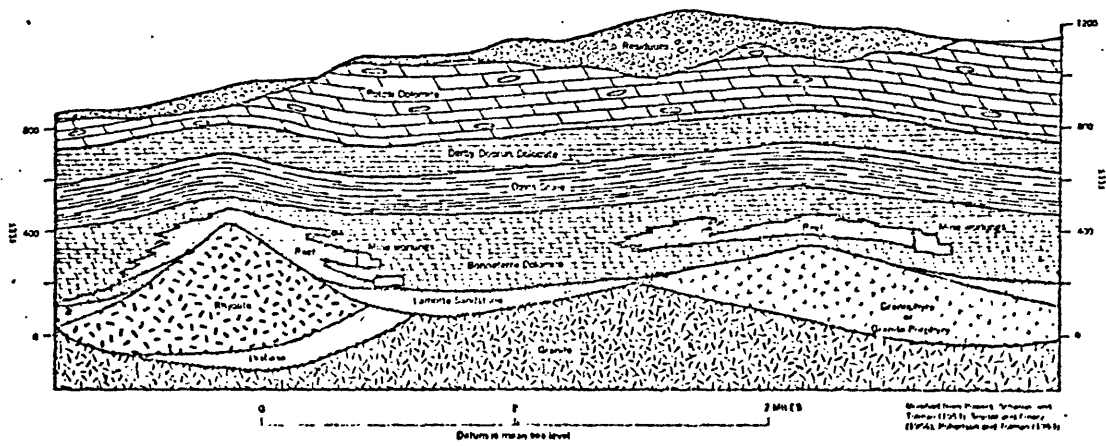


Figure 4.--Generalized geologic section on the flanks of the St. Francois Mountains.

40

Igneous and sedimentary rocks

An igneous and metamorphic complex of granite syenite, diorite, volcanic rock, gneiss, schist, and quartzite comprise the basement in Missouri upon which the overlying Paleozoic formations rest unconformably. Igneous rocks form the core of the St. Francois Mountains, a roughly circular area of about 800 square miles, centered near Ironton in Iron County. Bands of Paleozoic sedimentary rocks encircle the Precambrian rock and dip away from the central core in all directions. The igneous rocks are divided into three major groups: granitic rocks, volcanic rocks and mafic intrusive rocks. The granitic rocks comprise granite, granite porphyry or intrusive felsite and granophyre. The volcanic rocks are subdivided into two groups, Robertson and Tolman (1969). The lower group comprises flows of rhyolite, and some latite, trachyte, and andesite. The upper group consists mainly of ash-flow tuffs. The mafic intrusive rocks consist of diorite and diabase dikes. For detailed information about exposed Precambrian igneous rocks, the reader is referred to the report by Robertson and Tolman (1969).

The upper Cambrian sequence in the Ozark region consists of clastic carbonate strata of marine origin deposited around the igneous core of the Ozark uplift. The Cambrian beds comprise more than 1,500 feet of marine sandstone, siltstone, dolomite, and shale that surround the St. Francois Mountains and fill the intermontane valleys and larger basins. These strata are correlations of the upper Cambrian series of the Upper Mississippi Valley that were designated as St. Croixan by Walcott (1912, p. 257). Gradational boundaries and many facies changes are common in these rocks. Early classifications based on general lithic correlations resulted in disagreement and confusion.

Upper Cambrian formations overlying the maturely dissected Precambrian surface in ascending order are the Lamotte Sandstone, Bonneterre Dolomite, Davis Shale, Derby-Doerun Dolomite, Potosi Dolomite, and Eminence Formation of St. Croixan age (fig. 5). The lithology of the carbonate rocks is complicated by regional dolomitization and the effect of mineralizing fluids, and the local dolomitization, recrystallization, bleaching and solution of carbonate beds. The Bonneterre Dolomite was divided into 11 lithic units by J. E. Jewell and R. E. Wagner prior to 1947 and described in detail by Ohle and Brown (1954 p. 205). Despite alteration effects, Snyder and Odell (1958, p. 901-905) reconstructed the depositional environment, interpreted the facies relation and classified the lithic units of the lower part of the Bonneterre formation.

5

SERIES	FORMATION	SECTION	LITHOLOGY	THICKNESS in feet
Cambrian	Pleistocene and Recent		SOIL, residual chert	0 - 200
	Potosi dolomite		DOLOMITE, gray to brown, granular to coarsely crystalline, massive; abundant quartz druses; cherty	385
	Doe Run dolomite		DOLOMITE, argillaceous, cross-bedded; quartz druses	60
	Derby dolomite		DOLOMITE, shaly, calcareous	40
	Davis shale		SHALE, green dolomite, oolitic, conglomeratic; local edgewise conglomerate limestone, oolitic sandstone, glauconitic	165
	Upper dolomite		DOLOMITE, gray to white, dense, vuggy; lower part chocolate brown or mottled blue and white	80 to 100
			DOLOMITE, tan, coarsely crystalline, massive, locally oolitic; porous in lower part	100+
			DOLOMITE, gray, shaly; massive algal reefs of gray to brown shaly dolomite; Collenitic clastic detritus of oolite, pistolite, quartz sand, and volcanic grains 11 - limestone, tan gray spotted 9 - sedimentary breccia from slump of 7 or 12 beds	100 to 120
			DOLOMITE, tan, sugary to coarsely crystalline, even-bedded, green spotted, oolitic, lenticular	375 to 400
			DOLOMITE, gray, fine-grained, shaly partings; thin wavy bedding; nodular; brown and gray spots; small isolated algal reefs: "marble" beds at base	70 to 135
			DOLOMITE, tan to light gray, medium granular to coarsely crystalline; black shale; locally glauconitic;	
			DOLOMITE, tan to gray, sandy; irregular bedding;	
			SANDSTONE, white, fine to medium grained, friable in upper part, cross bedded to poorly bedded; well-rounded quartz grains; very porous and permeable; siltstone and thin dolomitic beds in upper part; residual basal grit and conglomerate	0 - 425
			a - DIABASE and GABBRO b - GRANITE c - GRANOPHYRE and GRANITE PORPHYRY d - RHYOLITE and PYROCLASTIC ROCKS	
Precambrian				

Figure 5 Stratigraphic section of Precambrian and Cambrian rocks in the Bonne Terre area, Missouri

Volcanic rocks

A series of felsic flows and pyroclastic rocks comprise the oldest igneous rocks exposed in southeastern Missouri. Mainly red and purple rhyolite, these rocks contain quartz and potash phenocrysts. In the past the volcanic rocks were called porphyry (Pumpelly, 1873, p. 3) but more recently, they have been designated felsite by Tolman and Meyer (1939).

Robertson and Tolman (1969) used a lithic marker, the Ketcherside Tuff, and the potash-soda ratio to separate older rhyolitic flows, designated the Middlebrook group, from stratigraphically younger flows and pyroclastic rocks of the Van East group. The volcanic rocks ^{are not} subdivided on the geologic map shown in Figure 2a.

Devitrified potash-rich rhyolitic flows and welded tuffs comprise the Middlebrook group. Some of these rocks are as mafic as quartz latite or andesite. Magnetite, the most abundant accessory in most felsites, occurs as crystals, irregular blebs and fine dust-like particles. It is commonly titaniferous in the more mafic rocks.

Flow units of the Van East group are typically devitrified glass at the base. The glass grades into porphyritic rhyolite having flow structures. Alignment of phenocrysts under stress of flowage produced banding. Welded tuff of the upper part contains pod-shaped quartz feldspar aggregates. Anderson (1962) believes these pods represent former gas or liquid cavities. The breccia phase at the top contains incompletely welded pumice fragments. Shard structures were partly obliterated by devitrification and flowage.

Some basal portions of flows are fragmental. Flow structures as thin bands parallel to the basal unit are common in porphyritic flows. In some instances flows are capped or separated by thin bedded tuff. At Taum Sauk Mountain thick welded tuff units containing flattened blebs of pumice and broken shards were recognized. Anderson and Sharon (1961, p. 121) observed at least six flow units exceeding a total thickness of 2500 ft in this area.

Flows of the Middlebrook group crop out near the center of the volcanic terrain that comprises the western two-thirds of igneous exposures in the St. Francois Mountains. Rocks of this group are exposed at Pilot Knob, Cedar Hill, Anderson, Shepherd, and Oak Mountains near Ironton. Pyroclastic rocks of the Ketcherside Tuff at the base of the Van East group were partly deposited unconformably in a shallow water environment on the surface of the Middlebrook rocks. Ash flows of the Van East group surround the Middlebrook rocks near Ironton. This relationship suggests doming of the volcanic rocks before erosion. The Van East group crops out typically at Stouts Creek, Grassy, Iron, Pine, Wolf, and Van East Mountains.

Near the granite contact, flows such as those south of Knob Lick and at Evans Mountain are bleached and more magnetic. A contact metamorphic phenomenon is believed to cause this bleaching and alteration. Meteoric or hydrothermal waters are believed to have bleached volcanic rock in the fault zone south of Wolf Mountain.

Granitic rocks

The exposed Precambrian granitic rocks comprise a composite batholith. Its contact with volcanic rocks is mainly concordant. The tabular sill-like upper part of the batholith intruded volcanic flows and pyroclastic rocks. Massive, structureless granite locally bleached the intruded volcanic rocks. K-Ar and Rb-Sr age determinations by Davis and others (1958, p. 180) indicate that the granite at Silvermine is about 1.4 billion years old. Using the potassium-argon method, Allen and others (1959) dated the granite at Silvermine and Graniteville at about 1.2 billion years.

Tolman and Koch (1936) suggested two stages of emplacement. Their six subdivisions of granite that were based on accessory minerals are regarded as different phases of the batholith. The marginal phases designated the Musco group, and younger coarsely crystalline phases assigned to the Bevos group represent the two stages of intrusion according to Robertson and Tolman. (1969) Rocks of the Musco group are usually dark red, fine grained, porphyritic, and granophyric, whereas rocks of the Bevos group are mainly light red to gray, coarse grained.

Granophyric and porphyritic granite near Fredericktown and northwest and northeast of Iron Mountain represents the Musco group. Granite near Graniteville, also north and east of Roselle, and the rhyolite porphyry southwest of Roselle represent the Bevos group.

Quartz, perthitic potash feldspar, sodic plagioclase, and biotite are the major constituents of the granite. Magnetite or martite, the most abundant accessory mineral, is usually less than 1% but may locally exceed 4%.

Granite of the Musco group was partly emplaced between the two groups of volcanic rocks. Concordant sill-like habit of these intrusive rocks is shown by nearly flat contacts at Buford and Stono Mountains and Mount Devon. Haworth (1883, p. 286-294) described the granite porphyry, which included the fine-grained and granophytic phases of the granitic rocks. He believed that the granite porphyry was intermediate between granite and felsite. Fine grained granite porphyry at Stono and Buford Mountains lies at the contact between coarse grained red granite and felsite. Snyder and Wagner (1961, p. 85) believe that these rocks are hypabyssal equivalents of the underlying granite. The writer agrees with their interpretation and also believes most of the fine grained granophytic and porphyritic granite bodies are hypabyssal equivalents of the main granite intrusion.

Rocks of the Bevost group represent the main phase of granitic intrusion. The concordant nature of these rocks is shown by their relation to relatively undisturbed, flat-lying roof pendants of volcanic rock at Evans, Mathews and Tin Mountains, and the ridge east of Flatwoods. Tabular or sheet-like bodies of granophyre locally mark the top of these rocks at Murphys Hill, and the area north and west of Buck Mountain.

Mafic Rocks

Basaltic, diabasic and gabbroic dikes, sills and bosses intruded both volcanic and granitic groups of rocks. Robertson and Tolman (1969) believe that the Skrainka diabase, the most common mafic rock, to be a differentiate of the batholith. The central part of some of the larger units contain coarse-grained gabbroic rock, which represent a cooling phase of these layered, sill-like bodies. The ratio of calcic plagioclase to augite, a mixture which gives the bluish gray rock a conspicuous diabasic texture, is about 2:1. Titaniferous magnetite readily separates from decomposed diabase and concentrates in rills on the residual granular soil.

At Hogan, Evans, Tin, and Halliday Mountains, diabase intruded the contact between granite and volcanic rocks as sills. Mafic dikes intruded nearly vertical fractures in the granite and overlying volcanic rocks.

Post-Devonian mafic rocks in numerous explosive volcanic vents near Avon and the Ste. Genevieve fault zone are described by Rust (1937) and Kidwell (1942, 1947).

In summary, Robertson and Tolman (1969) believe that two petrogenic eposhs were indicated by extrusion of Middlebrook felsites and emplacement of the granitic batholith. Felsites of the Van East group were/initial extrusive stage of magmatic intrusion. Two phases of the batholithic intrusion were the emplacement of the fine-grained granophyric and porphyritic rocks of the Musco group, and the intrusion of coarse-grained granite of the Bevos group. Mafic rocks, chemically related to the batholith, were then emplaced along fractures in the host rock.

Lamotte Sandstone

The Lamotte Sandstone, the oldest Cambrian formation exposed in Missouri, was named by Winslow (1894, p. 331-347) for Mine LaMotte in Madison County. The Lamotte Sandstone encircles all of the igneous knobs and rests on a maturely eroded crystalline basement of granite and volcanic rock. In the St. Francois Mountains its thickness ranges from a few feet over 450 ft. Sand deposition partly filled in irregularities on the Precambrian surface. The sandstone fills valleys and feathers out against igneous hills. Because of this relationship with the Precambrian basement its thickness changes over short distances; many of the small hills were not covered. Outcrops of sandstone dip away from hills at angles up to 12° which represents initial dip.

Bonneterre Dolomite

The Bonneterre Dolomite, at its type locality is about 390 feet thick although 448 feet was recorded in a drill hole (Buckley, 1909). Ohle and Brown (1954, p. 204) indicate a thickness of about 375-400 feet in the main mineralized belt, but thins gradually southward. The formation crops out on the floors of intermontane valleys in streams of deep dissection.

The formation is characteristically a buff to brown dolomite. In mineralized area, beds are almost completely dolomitized, but elsewhere they are partly limestone. The lithologic types were classified and the formation subdivided into zones prior to 1947 by Wagner and Jewell (Wagner, 1947). The formation was subdivided into eight characteristic units (fig. 5). Its basal bed is the sandy dolomitic phase overlying the Lamotte Sandstone. Dolomitization, recrystallization, and thinning by solution were the major effects of alteration. The formation contains several distinct sedimentary structures such as sand ridges, algal reefs and slide breccias (fig. 4).

Davis Formation

The Davis Formation comprises 150 to 190 feet of limestone dolomite shale and conglomerate. Limestone beds contain numerous intercalated green to brown shale beds and lenses. The dolomite limestone beds are generally coarsely crystalline and thinned bedded. Edgewise conglomerates make up part of the Davis but are irregular in distribution. Outcrops are not conspicuous nor abundant. The Davis Formation appears to be conformable on the Bonneterre dolomite.

The Derby-Doerun Dolomite, limited in distribution, is mainly developed within the mining district. Argillaceous and crystalline facies characteristic of the brownish gray to buff massive, noncherty Doerun Dolomite are gradational with the underlying Davis Formation. Its thickness near Potosi is about 75 feet, but the dolomite attains a maximum thickness of 110 feet in the mines near Doerun. Surface exposures of this formation are sparse.

In the type area of Washington County, the Potosi formation has a thickness between 250 to 390 ft according to Bridge (1930, p. 69). In St. Genevieve County, Weller and St. Clair (1928, p. 54) found the dolomite averages about 174 ft thick.

The Potosi is easily the most extensive formation in areal distribution. The Potosi dolomite crops out extensively south of the Palmer fault zone and northward in the bottom of Indian Creek. Road cuts and cliffs along stream banks present the largest exposures. Broken particles of druse or chert pave many stream beds. Numerous caves, pot holes sinks and other solution features are common in the dolomite.

Eminence Dolomite

In the Richwoods area Eminence formation averages 160 ft thick. In the Tiff Vineland area the average thickness is 200 ft. In the Berryman area it is also 190 to 200 feet, increasing lightly in thickness. Bridge (1930, p. 81) gives a maximum thickness in the Eminence region as 250 ft.

Magnetic properties of the rocks

Magnetic rocks in the St. Francois Mountains consist of rhyolite, and trachyte, dacite, andesite intruded by granite and related granophyre, intrusive felsite, and diabase. An areal distribution of representative oriented samples of all rock types were collected from outcrop and diamond-drill core. In addition the sources of separate anomalies were sampled to aid the interpretation of the aeromagnetic maps.

Total magnetization is the vector sum of remanent and induced magnetization. Susceptibility, the most important magnetic property of many rocks, is the ratio of the induced magnetization to the earth's geomagnetic field. Table 1 lists average susceptibilities of rocks in

Table 1 near here

the St. Francois Mountains. Natural remanent magnetization, another component of magnetization in rocks, may be greater than the induced magnetization, and its direction may not be parallel to the earth's present field. Before interpreting the aeromagnetic map, susceptibility and remanent magnetization of the rock units producing the anomalies were determined.

Table I. Average measured susceptibility of rocks from the
St. Francois Mountains

by

[W. E. Huff, Jr., Analyst]

	$K \times 10^{-3}$ emu/cm ³ *	Number of samples
Rhyolite	2.8	60
Granite, red	1.7	45
Trachyte	5.8	12
Andesite	8.0	8
Diabase	2.7	10
Granophyre	4.0	10
Tuff	1.01	8
Dolomite	1.005	6
Sandstone	1.005	4

* Two cores measured from each sample

Measurements

In the laboratory 2 to 4 cylindrical cores measuring one inch long and one inch in diameter were prepared for magnetic measurement from each oriented specimen. Susceptibility was measured using a bridge method. The instrument used for the measurement of magnetic susceptibility consists of a Maxwell bridge in one arm of which is an inductor whose core contains the rock sample. The accuracy of the magnetic measurement of the sample is about 2 percent in a testing field of 0.05 Oe.

The remanent magnetism of each cylinder was measured on a spinner magnetometer of the type described by Anderson (1961, p. C370-C372), and the results for each oriented sample were averaged.

In order to eliminate the effect of unstable or viscous magnetizations, the cores were demagnetized as described by Irving, Stott, and Ward (1961, p. 225-241).

The susceptibility of over 400 rock samples and the remanent magnetization of over 300 rock samples were measured and are shown in the Appendix.

Susceptibility

An abnormally high susceptibility for some sedimentary beds in southeastern Missouri was noted by Farnham and VanNostrand (1941). A similar high susceptibility for the Potosi Dolomite was observed by McEvilly (1956). His measurements showed that Potosi strata in Ste. Genevieve County have one-fifth the susceptibility of granite or about 0.16×10^{-3} emu/cm³. His susceptibility value for the Davis Shale compared with values obtained by Holmes (1950, p. 1143) for the Bonneterre Dolomite, about 0.04×10^{-3} emu/cm³.

From a series of susceptibility measurements of the sedimentary rocks (Table 1) it was concluded that the susceptibility of these strata can be disregarded in magnetic interpretation when considering the large amplitude anomalies being analyzed. The effect of the igneous rocks will in the predominately Ozark region where the sedimentary cover is thin and not in excess of 2,000 feet. For purposes of interpretation, the overlying sedimentary rocks in the shallow intermontane basins are considered nonmagnetic.

The susceptibility of rocks in the area is caused principally by varied content of accessory magnetite disseminated throughout large volumes of igneous rock. Examination of polished sections and X-ray data show that other ferromagnetic minerals, such as maghemite and titanomagnetite, also contribute to the magnetism of these rocks. Desborough and Amos (1961) discuss the presence of ilvaite and ulvöspinel in the diabase. Magnetic properties are a function of minerals of the $\text{FeO}-\text{Fe}_2\text{O}_3-\text{TiO}_2$ system and thus are a function of the chemical composition of rocks. The reader is referred to Nagata (1965) and Irving (1964, p. 10-38) for a comprehensive review of rock magnetism.

Slichter (1942) indicated the relative importance of magnetite, ilmenite, and specularite (specular hematite by susceptibility: magnetite, $300-800 \times 10^{-3}$ emu/cm³; ilmenite, $31-44 \times 10^{-3}$ emu/cm³; and specularite, $3-4 \times 10^{-3}$ emu/cm³). Magnetite is the most important mineral in rock magnetism by one to two orders of magnitude. In his study of the iron ores from the Kiruna district, Werner (1945, p. 50-58) demonstrated the dependence of magnetic susceptibility on the magnetite content of rocks. An empirical relation between susceptibility and magnetite content of rocks is shown in Figure 6.

Figure 6 near here

Data derived from igneous rocks of the St. Francois Mountains (open circles) are compared with an average value (smooth curve) of data compiled by G. E. Andreasen and J. R. Balsley of the U. S. Geological Survey, mainly from rocks of the Minnesota and Kiruna iron ranges and the Adirondack uplift. Magnetite content was determined from polished sections and by mineral separations. Susceptibility can be estimated by use of the curve, where the amount of magnetite is known from petrographic studies.

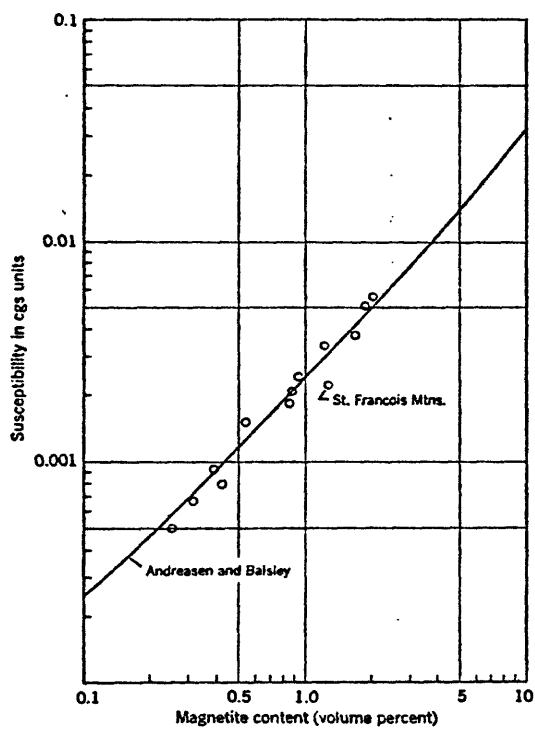


Figure 6.--Plot of magnetite vs magnetic susceptibility of rocks from the St. Francois Mountains.

Measurement of magnetic susceptibility eliminates one of the uncertainties in interpreting total-intensity anomalies. Susceptibility measurements of igneous rocks from the St. Francois Mountains, shown in Figure 7 in relation to rock type, have a more restricted range in

Figure 7 near here

values in contrast to the generalized data compiled by Dobrin (1960, p. 109). Red granite has a low-uniform-magnetite content and a susceptibility of 1.7×10^{-3} emu/cm³. Susceptibility measurements by McEvilly (1957) for granite near Jonca Creek was less than one-half this value. In comparison, dacite has a higher and more varied magnetite content than granite; its susceptibility is about 3.4×10^{-3} emu/cm³. Trachyte in the mining region has a higher susceptibility of 5×10^{-3} emu/cm³. Most of the bedded or crystal tuffs have negligible susceptibility similar to the Paleozoic strata.

The magnetic characteristics of the granite at Jonca Creek is about the same as the fine-grained granite (granite porphyry and granophyr) in the vicinity of Fredericktown. The susceptibility of the granitic rock underlying the Farmington anticline is between groups 1 and 2 (Fig. 8) This granite may be similar to the rocks that floor the shallow basins southwest of Ironton (Corridon-Hesterville areas).

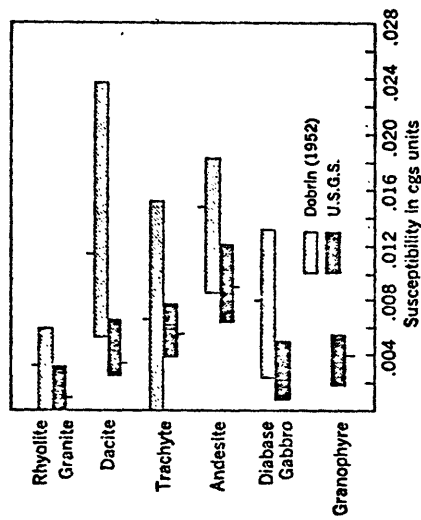


Figure 7.—Range of magnetic susceptibility of rocks from the St. Francois Mountains.

On the basis of magnetic susceptibility, granitic rocks in the St. Francois Mountains are divided into five groups, as shown in Figure 8.

Figure 8 near here

Each bar represents the average value of several samples. The first group is the very coarsely crystalline red granite of negligible (0.02×10^{-3} emu/cm³) to low (about 0.2×10^{-3} emu/cm³) susceptibility that is exposed in quarries at the margin of the basin at Bellevue, shown in Figure 2. These rocks represent the interior of the batholith and are in the position of an upthrown block or an eroded cupola. The second group of rocks from scattered localities within the main part of the exposed granite batholith is medium to coarse grained and uniformly magnetic. The susceptibility of these rocks is greater than 0.5×10^{-3} emu/cm³ but less than 1.0×10^{-3} emu/cm³. Group 3 is representative of more magnetic phases of the red granite and gray granite. These rocks are medium to fine grained; the grain size of the magnetite has not decreased over that of the other groups. Group 4 consists of granophytic rocks from near the roof of the batholith that are distributed in a north-south direction parallel to the western contact between the granite and the volcanic rocks. Group 5 consists of very fine-grained granophytic phases of the dark-red granite from localities east of the exposed red granite. These granitic rocks have susceptibilities comparable to those of the volcanic rocks. The granite is more magnetic at its outer margins and less magnetic in its interior.

Susceptibilities of volcanic rocks from four different localities are shown in Figure 9. Their magnetic susceptibility is

Figure 9 near here

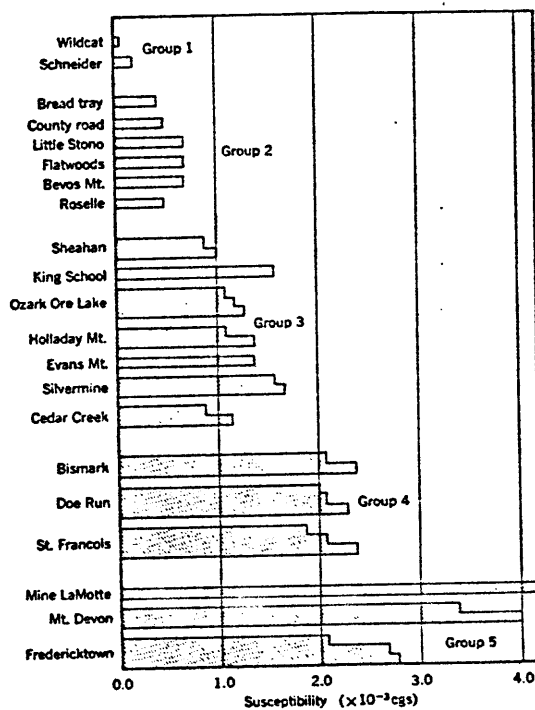


Figure 8.--Susceptibilities of granitic rocks in the St. Francois Mountains.

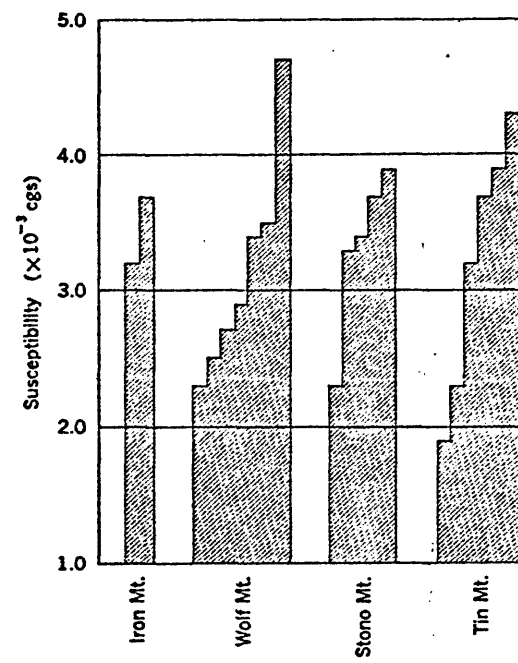


Figure 9.—Susceptibilities of volcanic rocks in the St. Francois Mountains.

about twice the average susceptibility of the granite used in magnetic computations of an area selected for detailed analysis.

Remanent magnetism

Two parameters of remanent magnetization that affect analysis of magnetic anomalies were examined in this study. The ratio of remanent magnetization to induced magnetization, designated as Q , may affect interpretation of anomalies where the rock has a high Q . The magnitude of remanent magnetism of volcanic rocks is known to considerably exceed the induced magnetism (Mumm, 1964; Ade-Hall, 1965). Where direction of remanent magnetization is not the same as the direction of the present geomagnetic field and the Q is greater than 1, the components of the induced and remanent magnetizations must be combined in calculating the total-intensity field. Green (1960) attributed the confused magnetic pattern obtained by magnetic surveys over volcanic rocks to the juxtaposition of normal and reversely magnetized rocks. Such patterns were observed in the Potosi and Berryman quadrangles and thereby precluded an examination of the magnetic properties of the volcanic rocks. A discussion of the complex causes and variations of remanent magnetism are beyond the scope of this paper, but Irving (1964) and Doell and Cox (1961) present excellent summaries on the subject.

The intensity and direction of remanent magnetization were measured on several one-inch cores from each oriented sample of igneous rock from the St. Francois Mountains. Measurements of a widespread rhyolite exposed in Stouts Creek were combined with those made by Hays (1961), and the results are shown in Figure 9. The measurements of brecciated and fragmental portions of the rhyolite were omitted, because the directions of remanent magnetizations were random and Q was very low. Before the direction of magnetization was computed, samples exhibiting poor stability characteristics, very low inclinations or nearly horizontal vectors, and low intensities were eliminated. The direction of magnetization was determined by the statistical method of Fisher (1953). In this instance the direction of remanence was close enough to the direction of the present geomagnetic field for scalar addition of the induced and remanent fields, but the low Q did not warrant further computations. The direction of remanent magnetism shown by Figure 10 however, could be used in paleomagnetic

Figure 10 near here

studies.

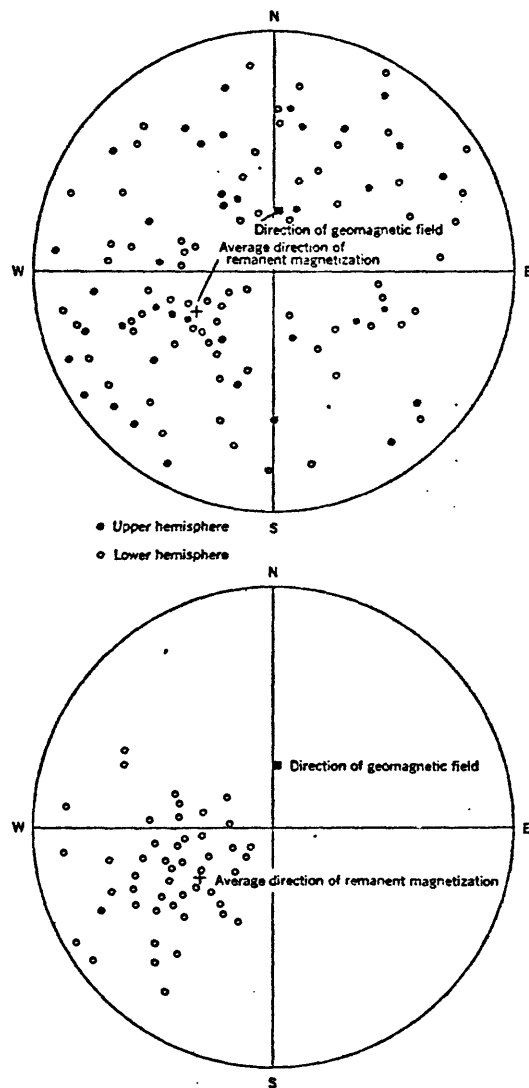


Figure 10.--Remanent moments of samples of rhyolite near Stouts Creek before and after partial demagnetization.

The directions of remanent magnetization are more grouped in the fine-grained rocks and may contribute materially to the total-intensity field. Fine-grained rocks, such as rhyolite or granophyre, have a greater intensity of remanent magnetization and a higher Q than granite. Granite has a negligible remanent magnetization. The directions of the remanent vectors of the coarse-grained granitic rocks have a random distribution as shown in Figure 11. This scatter

Figure 11 near here

may be due to the tectonic history of the rocks, mainly (a) shearing or pressure effects of tectonic stress, (b) changes in the structure of magnetic minerals due to deuteric alteration or weathering of the rocks, or (c) oxidation of magnetite grains.

Low intensities and random directions of the vectors eliminated remanent magnetism as a significant factor in the analyses of anomalies reviewed in this paper and showed that induction theory is applicable to these particular magnetic calculations.

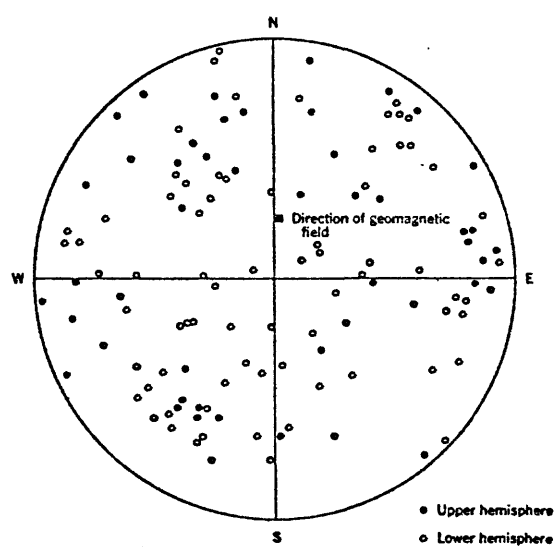


Figure 11.--Random scatter of remanent vectors of granitic rocks from the St. Francois Mountains.

Structure

The Precambrian igneous rocks of the basement, whose surface is irregular and nearly everywhere buried beneath a thin cover of Paleozoic sedimentary rocks, crop out in the St. Francois Mountains of southeastern Missouri (Eardley, 1962, p. 37; 52-53). Vertical movement in the igneous rocks, which form a wide stable platform in the interior lowlands, produced broad basins, arches, and domes. The sedimentary rocks were downwarped, faulted and crenulated.

Strata dipped radially from the high area of igneous rock in the St. Francois Mountains. The regional dip is about 10 to 20 feet per mile northward and northwestward from the center of the Ozark uplift. The main dip westward is also 10 to 20 feet per mile.

During the period between intrusion of mafic rocks and deposition of Upper Cambrian strata, the region was tilted southwestward and deeply eroded. Snyder and Wagner (1961, p. 92) demonstrate that the difference in altitude of the Lamotte sandstone at Knob Lick and Stegall Mountain to the southeast, about 1,700 ft, represents the amount of post-Lamotte tilting and faulting.

Faults

Most of the major structural features of the district are fault zones.

These zones consist of individual faults that form an intricate parallel, sub-parallel or branching patterns. The rock is fractured in different degrees of intensity. Locally it is shattered by closely spaced fractures or broken by widely spaced fractures. The Palmer and St. Genevieve fault zones are complex and show equally intricate patterns of faulting. Other major faults of the district, the Big River, Berryman, Shirley, Simms Mountain, and Wolf Creek, have a predominant northwesterly trend.

Post-batholithic faulting in the igneous rocks of the St. Francois Mountains trends N. 40° to 60° W. and N. 30° to 60° E.

The most intense faulting in southeastern Missouri is along a well-defined zone some 40 to 50 miles long extending in a northwest direction away from Mississippi River. The width of the zone called the St. Genevieve fault, is a maximum of 2 miles but is generally much less. The downdropped strata on the northeast side away from the center of the uplift forms a complexly faulted graben where the fault zone widens between undisturbed rocks.

The ^{St.}
Genevieve fault zone on the north and east sides of the
Farmington anticline consists of many parallel fractures and grabens.
Within the fault zone several large downdropped blocks preserved the
younger Paleozoic strata. Vertical displacements range from less than
100 ft to 1,200 ft in part of St. Genevieve County.

The Palmer Fault zone passes 2-1/2 miles north of Palmer and strikes
N. 75° W. and, in local areas, is very complex. The width of the fault
zone ranges from 2 to 5 miles. Dake (1930, p. 181) states that the
Palmer Fault zone can be traced in a northeasterly direction across the
Bonneterre quadrangle to the vicinity of French Village in St. Francois
County where it becomes part of the St. Genevieve fault zone. The
maximum throw in this zone is more than 400 ft on the west side of the
area. On the east side of the Potosi quadrangle, however, the throw is
not less than 800 ft; the movement is distributed through several faults.

The entire zone is characterized by a number of long very narrow dropped blocks between braided faults. The greatest movement along the Palmer fault zone is on the east side Sec. 26, T.36 N., R.2 E. (fig. 2a) Thus the movement along the Palmer fault is probably not less than 1200 feet. The most complicated structure is near Bel where 7 or 8 faults may be observed at a distance of less than 1/2 miles. Breccia zones, isolated masses, steeply inclined fault planes characterized the Palmer fault. The faults generally show no shift in direction due to topography, ridges or valleys. Faults are generally normal or gravity faults and are free from flexures that suggest active compression. Dake (1930, p. 184) suggested pre-Van Buren faulting along the Palmer River.

The Big River fault strikes N.40°E., the downthrown side northwest. It begins at the Cedar Creek fault, cuts the end of the Simms Mountain fault, and doubtless ends in the St. Genevieve fault complex to the northeast. Big River fault has a maximum displacement of about 120 ft.

The Simms Mountain fault strikes N. 65° W across the lead mining district for about 4 to 5 miles to a point southwest of Flat River. Its maximum displacement is about 600 feet, the downthrown side on the northeast. It is nearly vertical. The Simms Mountain fault extends southeastward and becomes part of the Mine LaMotte and Higdon fault system in Madison County. The Mine LaMotte fault has a displacement of at least 300 feet with the downthrown side to the northeast and the same alignment as that of the Simms Mountain fault. The Cedar Creek fault parallels the Simms Mountain fault and has its northeast side downthrown about 400 feet. This fault continues into Washington County as the Palmer Fault zone where its maximum displacement is 800 feet according to Dake (1932, p. 183).

The Shirley fault passes within 1-1/2 miles northeast of Shirley. The southwest side has been dropped where the maximum throw is not less than 300 feet. The throw on the Black fault is about 250 feet.

Many small faults pass through the mine workings in the Leadwood area and have displacements from a few feet upward to 100 ft in displacement. Many of these faults parallel the Simms Mountain fault zone. In the Ironton area, Graves (1938, p. 133-139) postulated three faults at the boundaries of the downdropped block of the Bellevue Valley, namely, the Ironton fault on the east side, the Munger fault on the south side, and the Hogan fault on the west side.

Joints

In the Precambrian volcanic rocks, joints are closely spaced.

Robertson and Tolman (1969) mentioned a major conjugate set that strikes N. 33° E. and N. 54° W. and a minor set that strikes N. 73° E. and N. 23° W. Joints in granite are widely spaced; they trend N. 45° E. and N. 65° W. and appear as secondary shears in the volcanic rocks.

According to Buckley (1908, p. 77) the major joints of the mining district strike N. 50° W. to nearly east-west. Major joints are nearly vertical. A less prominent group of joints strikes N. 30° to N. 80° E.

MINERAL DEPOSITS

The district is bounded on the southwest by the Simms Mountain fault, on the northwest and north by the Big River fault and on the east by the Farmington anticline where the Lamotte Sandstone is exposed. Faulting, tilting, and warping within the district resulted in a large trough-like shallow basin widening and flattening to the northwest. The lead district associated with this trough covers an area about 10 miles long and a maximum of 6 miles wide.

The lead deposits in the lower half of the Bonneterre Dolomite were partly localized by fracture pattern in the district. Mineral-bearing solutions entered the Bonneterre formation through fracture zones and spread laterally along permeable beds. The resulting mineral deposits are horizontal rather than vertical in extent. Galena is concentrated along the flat-lying shaly beds near contacts and on other permeable bedding produced during sedimentation.

Classification

Tarr (1936, p. 712-753, 832-866) classified the lead mines of southeastern Missouri as (1) disseminated, (2) bedded, and (3) vein deposits. Commonly galena is uniformly disseminated through all facies of the Bonneterre Dolomite as cubes or modified octahedrons. Vein deposits are simple fissures or joints in which the galena deposited with calcite and marcasite. Galena rarely replaces the walls of joints or fissures. Inclined veins are common in dense shattered dolomite. Vertical veins are not common in porous beds that contain disseminated lead.

Structural control

In the mining district three principal types of structures controlled the lead deposits. These structures were (1) domal and anticlinal structures related to buried Precambrian knobs and ridges; (2) ridge and basin structures of depositional origin; and (3) fracture zones (Fig. 12). Winslow (1896, p. 18) described one important controlling condition: sedimentary rocks were deposited in

Figure 12 near here

shallow basins from which numerous igneous hills protruded. He believed that steep dips surrounding the knobs resulted from sedimentation on an uneven sloping floor of an archipelago. Keyes (1910) believed that the ore was deposited in sagging strata to form basins and troughs. Buehler (1918, p. 396) stated that ore in the carbonaceous shaly dolomite outlined lagoon-like areas. The influence of buried ridges and knobs on some deposits was described by Tarr (1936, p. 740-741) and by James (1949, p. 654-657).

(fig. 2a)

Domal and anticlinal structures: At Mine LaMotte ore bodies in the Bonneterre Dolomite wrap around the knobs near the pinchout line of the sand on the basement hills according to Tarr (1936, p. 740-744). Some flat deposits were 10 to 15 ft thick, more than a thousand feet long, and from 2 to 300 ft wide. The lead deposits in the lower Bonneterre beds were as much as 50 ft thick, more continuous and abundant than those in the upper zones.

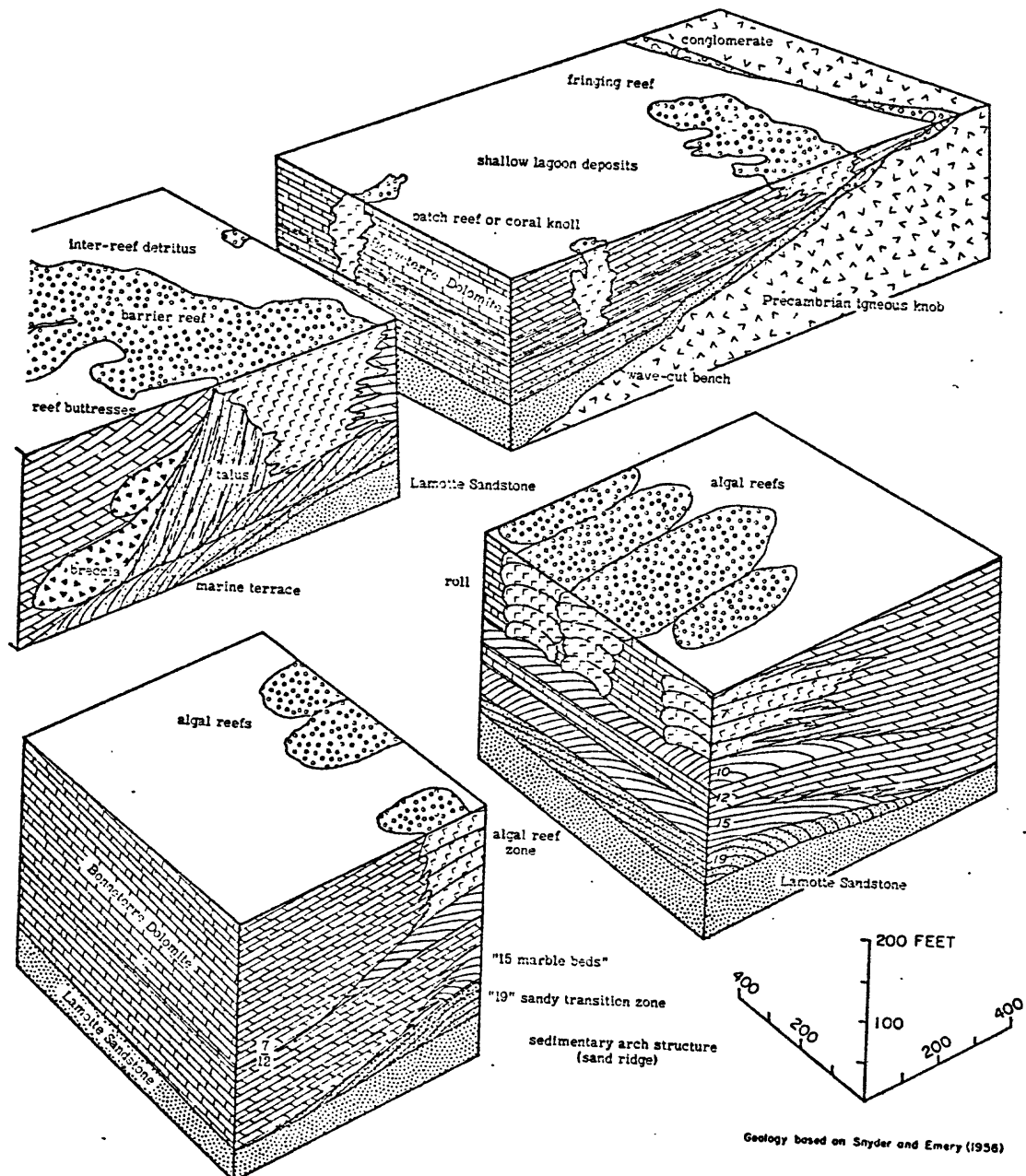


Figure 12.--Relations between sedimentary and basement structures.

Lead deposits in the Fredericktown area were related to the configuration of the Precambrian surface; the deposits lie on the flanks of protruding Precambrian igneous rocks exposed at the surface. Mineral deposits were similarly controlled by the pinchout line of the Lamotte Sandstone. James (1949, p. 22) concluded that in the Fredericktown area lead deposits were structurally high. The structures were the result of progressive burial of the mature Precambrian topography by Upper Cambrian sedimentary rocks, starting with the Lamotte sandstone. The beds developed initial dips in all directions away from the Precambrian highs. The knob structures trapped and concentrated the flow of mineral-bearing fluids, which moved upward and laterally through the lower Bonneterre strata containing beds and structure favorable for precipitation of galena.

Ridge and basin structures.--Ridge and basin structures are sedimentary arches, reefs, and breccias. The northeast ore trends in the Bonne Terre area are related to the arch structures of sedimentary origin. Northeast moving currents at the end of Lamotte time and at the beginning of Bonneterre time built ridges or bars of limy sediments, which feathered out northeastward. Some of these arch structures extended from the northeast side of Precambrian knobs, which were islands in the sea at that time. Lead deposited on the flanks of the sandy ridges, zone of interfingered clastic and carbonate fragments in the lower 200 feet of the Bonneterre formation. Reefs commonly grew outward from these sand ridges as observed in the Pacific atolls by Doan and others (1956).

The reef-like nature of the rolls and spotted rock forming bioherms is well developed in the Indian Creek mine where the algae grew abundantly around the margins of a ridge of volcanic rocks that projected high into the Bonneterre Dolomite (Bain, 1953). According to Ohle and Brown (1954, p. 935) the reefs are limited stratigraphically to the lower 200 feet of the Bonneterre Formation. These reefs developed on slightly elevated positions of the underlying sea floor, mainly on wave-cut benches on knobs, on saddles between projecting igneous ridges, or in sedimentary arch structures. These sedimentary features provide a complex structure for the deposition of galena. Wholly barren reefs are not common. In the Flat River area probably 20 to 30 percent of the total ore is in reef structures, at Leadwood less than 5 percent, at Bonne Terre 10 percent, and at Indian Creek mine 75 percent. But at Fredericktown and Mine LaMotte reef rock is almost absent, and all ore is in the lower beds. Tarr (1936, p. 719-721) and Ohle (1951, p. 903-904) described the reef rock in detail.

Many irregular layers of black shale in the lower part of the formation were important in controlling lead deposition. Much lead was disseminated in the shale. Massive layers of galena commonly replaced the dolomite adjacent to the shale. On the flanks of sand ridges, shale interfingers laterally with reef rock. Ohle (1959) believed that these features, termed fan structures, are sedimentary and that solution of carbonate strata accentuated pre-existing structure.

Snyder and Odell (1958, p. 899-926) showed that sedimentary breccias also were important controlling structures in the lower half of the Bonneterre formation. Four major breccia zones, each with over 6,000,000 tons of rock, were outlined. Individual ore bodies in the breccia zones range from several hundred over to 6,000 feet long. The breccias formed on the flanks of limy sand ridges by submarine slides into nearby depositional basins. Four basic types of material, argillaceous mud, sand-size sediment, algal deposits, and carbonate mud of the Bonneterre Dolomite, formed depositional ridges and basins. The ridges were composed of limy sand and reef deposits, whereas the basin sediments were fine-grained carbonate and argillaceous muds. Differential compaction over-steepened slopes between ridges and basin deposits and initiated the movement of unconsolidated strata. Repeated slides produced thick breccias in the lower part of the Bonneterre formation. Slides truncated and overlapped earlier slides resulting in continuous zones of breccia up to 130 feet thick. Thirty percent of the past production from the western part of the central lead belt came from sedimentary breccia ore bodies.

Fractures

Wagner (1947, p. 366-367) in his summary of lead belt geology stated that faulting on the ancient erosion surface of Precambrian volcanic rocks and granite resulted in a broad trough-like structure widening and flattening northwestward. This trough, roughly 10 miles long and 6 miles wide, contains the lead mining district, and corresponds to the structural block environment of James (1952, p. 650-660) whereby a combination of folding and faulting produced a reversal in the direction of dip within the block. James (1952, p. 658) described the structure as a block that was tilted upward by the faulting east of the Farmington anticline; the northwestern portions were upthrown by movement along the Big River fault zone and the southwestern parts were downthrown by movement on the Simms Mountain fault. The block was tilted southwesterly, but this dip was locally modified by an irregular hilly faulted floor on which the clastic carbonate beds were deposited. Few hills such as Bonneterre, Switchback, and Chicken Farm Knobs (Bonneterre, fig. 2a) extend into the overlying Bonneterre Dolomite. The extensive disseminated lead deposits in the Bonneterre Dolomite are rarely wider than 200 feet or higher than 50 feet. Galena is selectively disseminated in structurally and stratigraphically favorable beds, 20 to 30 feet thick, in the lower half of the Bonneterre Dolomite. Locally the mineral extends through a vertical interval of 200 feet.

James (1952, p. 650-660), in his summary of principal structural environments favorable for emplacement of galena, described the fault zone environment, which commonly consists of individual faults having intricate parallel, subparallel, and branching patterns. In the fault zone structural environment rock is brecciated by closely spaced fractures or broken into large blocks by widely spaced fractures. Palmer fault zone is an example of intricate faulting. The fault-zone type deposits were mined along the St. Genevieve, Big River, Palmer, Berryman, Shirley, and Simms Mountain fault zones. These mines, now abandoned, furnished most of the early lead production of the mining district. Sphalerite, barite, and smithsonite were commonly associated with the galena.

Aeromagnetic survey

The instrumentation and use of the airborne magnetometer and the results of some aeromagnetic surveys have been summarized by Balsley (1952, p. 313-349). The airborne magnetometer used in this survey consists of the flux-gate or saturatable inductor, a detecting mechanism self-oriented with respect to the earth's field, together with electronic oscillators and amplifiers necessary for its operation, and recording equipment necessary to indicate variations of the earth's total magnetic field. The instrument has a sensitivity of about 1 gamma in the earth's normal field of about 56,000 gammas. However a magnetic error of at least 1 gamma is introduced into the magnetic record because of the orientation of the aircraft with respect to the earth's magnetic field.

Collection and compilation of data

Field operations: The aeromagnetic survey was made in 1946 under the supervision of F. Keller, Jr., and J. R. Henderson and in 1948 by W. J. Dempsey and R. T. Duffner. Magnetic measurements were made by a continuously recording AN/ASQ-3A airborne magnetometer installed in a twin-engine airplane. North-south traverses were flown at 1/4 mile interval over the entire area and were tied together by 9 east-west base-line traverses used to correct for instrument drift and diurnal variation. A constant barometric altitude of 1,800 feet above sea level was maintained except in areas above 1,400 feet where the altitude of the aircraft was increased to clear all peaks by 500 feet. A recording radar altimeter continuously measured the distance from the plane to the ground. Aerial photographs were used for pilot guidance and the flight path of the aircraft was recorded by a Sonne gyrostabilized continuous-stripfilm camera. A vertical observation sight was used by an observer to increase positional accuracy.

Compilation of field data: The compilation and preparation of aeromagnetic contour maps were directed by W. J. Dempsey and W. E. Davis. These maps were published in 1949, 1950 and 1951. Magnetic contours on the aeromagnetic map are relative to an arbitrary datum as the airborne magnetometer measured only variations in the total intensity of the earth's magnetic field. The absolute total intensity of the earth's magnetic field can be obtained by adding about 56,000 gammas to a relative intensity value for any point on the map. Information derived from the total intensity and inclination charts and tables of the U. S. Coast and Geodetic Survey (Deel and Howe 1948) for the year 1949 indicate an absolute total intensity of about 56,600 gammas in the Fredericktown area.

Accuracy of position: Under the most favorable conditions the aircraft's position or that of the magnetometer can be determined within 100 feet. This is accomplished by carefully plotting the correlation marks from the continuous-stripfilm to aerial photographs and subsequently transferring these points to the topographic base. Observer check points are used whenever camera malfunction or unidentifiable strip film is encountered.

A short line containing several sharp anomalies with good positional location is flown in opposite directions and 1/2 of the anomaly displacement is applied to each magnetic profile. Lag that is due to the change in air speed over hills in which the flight lines alternate in direction can only be removed during the adjustment of individual profiles during contouring.

Although the aeromagnetic survey was made at a constant barometric altitude, areas of high relief and rugged terrain necessitated a change in survey elevation. The maximum deviation from the 1,800 foot datum was made over Taum Sauk Mountain and the surrounding hills. This mountain necessitated a change to about 2,100 feet. For purposes of magnetic interpretation the radio altimeter record gave the absolute altitude above the rugged terrain of the St. Francois Mountains.

Additional control was obtained for the magnetic record by flying a short line containing low gradient magnetic anomalies and good positional location at the beginning and end of a day's flying. This line is called a calibration line. In addition, base lines were flown across all traverses. These lines were chosen for low magnetic characteristics and good locational features to facilitate reliable intersection data.

The total-intensity map

The aeromagnetic map, corresponding to the area of exposed igneous rocks shown in figures 2 and 2a can be divided into two parts of different magnetic character: an area of low magnetic gradient best developed near (A) in the central part of the area, and a magnetically complex area best developed near (B) in the western part. Comparison of the magnetic intensities with exposed basement rocks shows that the magnetically flat area correlates with granite outcrop, and that the magnetically complex area correlates with volcanic rocks.

in figures 2a and 3

The map shows several types of anomalies: (a) broad high-amplitude anomalies (as much as 2,500 gammas) partly caused by magnetite-bearing volcanic rock and partly by magnetite rich iron deposits such as the one causing the Pea Ridge anomaly (near point shown as 5,175); (b) broad anomalies of relatively low amplitude (less than 600 gammas), such as the one in the one in the Richwoods area (3,169), due to a roof pendant of volcanic rock in granite; (c) small, low-amplitude anomalies (less than 300 gammas), such as the one over a buried knob at Potosi, east of 1795. The low-amplitude anomalies (less than 150 gammas) are commonly caused by topographic relief, and to a lesser degree by lithologic differences, altered zones at intrusive contacts, or local concentration of magnetic minerals in the Precambrian rocks.

Comparison of the groups of anomalies with exposed basement rocks shows the high-amplitude anomalies correlate with magnetite-rich volcanic rocks and in places with magnetite-bearing iron ores. The geologic causes of the intermediate-amplitude anomalies (200 to 600 gammas) are varied, but these anomalies commonly occur over roof pendants of volcanic rock in granite.

Topographic relief of the dissected Precambrian surface or small local variations in magnetic susceptibility of the igneous basement rocks cause many small magnetic highs and lows in the Bonne Terre area (fig. 2a). Larger contrasting tectonic units, such as faulted igneous blocks comprising the mountains and intermountane basins, produce broader and larger highs and lows. In the Bonneterre area aeromagnetic patterns consist of small local anomalies superimposed upon larger and broader anomalies.

The magnitude of magnetic anomalies associated with knobs of volcanic rock is generally twice as large as that of anomalies over comparable surfaces of granite. The distinctive magnetically flat pattern associated with the granite outlines partly rounded structural basins containing Paleozoic carbonate strata (Bellevue, figs. 2a and 3) and shows a distinct gradient sloping southwest. This gradient is interpreted as indicating that the faulted granite blocks are tilted southwestward. The presence of small bodies of granophyre and isolated pendants of volcanic rock complicates the magnetic pattern in areas of relatively low magnetic relief.

The grain of the magnetic pattern in the vicinity of the Indian Creek (3500) and Shirley (near 1795) anomalies indicates subsurface structures in the Precambrian of northeasterly trend; lows indicate faulting of a distinctly northeasterly and northwesterly trend. These magnetic lows associated with fault zones are believed to be caused by rock of negligible magnetic susceptibility. These rocks contain zones of leaching and silicification that have altered magnetic mineral assemblages to nonmagnetic minerals.

The magnitude of broad anomalies caused by changes in susceptibility and related physical properties of rocks is several times that of the anomalies due to topography. Broad anomalies, due to lateral changes in susceptibility over a contact between rocks of contrasting lithology, range in amplitude from 300 to more than 600 gammas. Small anomalies due to topography, shown more clearly in profile than on contour maps, range in amplitude from 30 to 150 gammas (Allingham, 1964).

Aeromagnetic anomalies

In this study, aeromagnetic information is used to solve local and regional geologic problems in Precambrian igneous rocks that are exposed in the St. Francois Mountains or buried beneath the shallow-platform carbonate strata,

The magnetic method is used to distinguish and correlate igneous rock units according to physical rock properties such as susceptibility and remanent magnetism and characteristic patterns observed on contour maps or on profiles. Two approaches are used to study the magnetic properties of these rocks. First laboratory measurements of rock samples yield susceptibility and remanence data for total magnetizations. Secondly these rock properties also are determined from magnetization computed from models simulating known volumes of rocks such as hills or ridges on a magnetically homogeneous terrain. Different magnetic patterns associated with granitic, dioritic, volcanic, or pyroclastic rocks are used to define zoning or boundaries or deduce rock type and trace their subsurface distribution.

The structural implications of anomalies and gradients are another important contribution of aeromagnetic data. The shape or attitude of rock units, their displacement or dislocation in subsurface, delineation of major structural blocks also are deduced from magnetic data.

Although high-amplitude anomalies are used directly as guides to potential iron deposits, the observed field is intensified by mathematical filters in order to emphasize subtle changes in magnetic patterns which can be used to outline areas favorable for exploration of lead deposits.

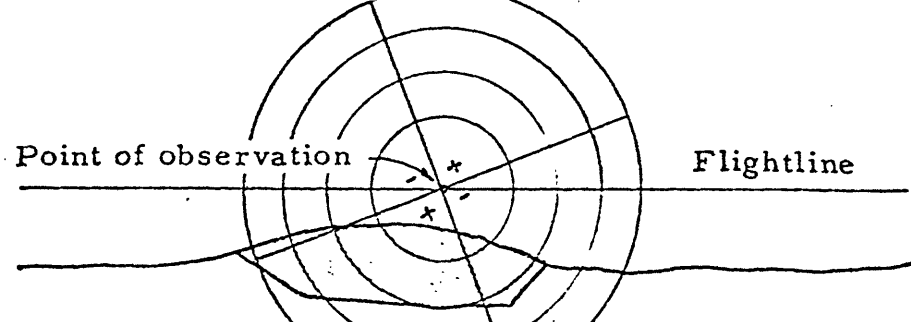
Interpretative techniques

In the interpretation of some total-intensity aeromagnetic anomalies, the interpreter assumes a geologically plausible size, shape, magnetization, and the depth to the top of the geologic feature producing an anomaly. A magnetic field calculated from this assumed model is compared with the observed magnetic field. The parameters are changes until the observed and calculated fields fit.

Magnetic anomalies caused by geologic features whose lengths are at least three times as large as their other dimensions were calculated with the aid of the polar chart of Pirson (1940). Faults and ridges are the commonest geologic features in this category. The intensity of the geomagnetic field (T_0) and its inclination were obtained from charts of the U. S. Coast and Geodetic Survey (1955). Magnetization (KT_0) was computed from the measured susceptibility. Measurements indicated that remanent magnetization was negligible in the anomalies examined in this study. Depth or distance to the exposed Precambrian surface of the magnetometer was obtained from altimeter records. With the value of the magnetization fixed the sizes and shapes of the models were changed to produce the desired fit of the curves.

Magnetic anomalies caused by geologic features whose dimensions are about equal were calculated by one of three methods utilizing slabs, a graphical technique, or polar charts. (fig. 14).

Figure 14 near here



$$\Delta T = KT_0 \Sigma N / 240$$

ΔT = total magnetic intensity

K = susceptibility

T_0 = inducing field of earth

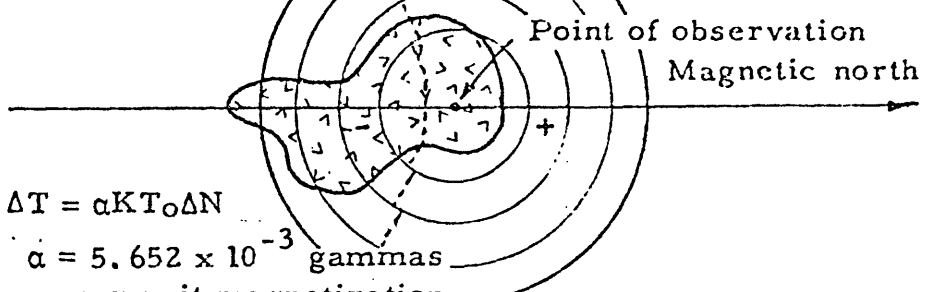
ΣN = total counts

Henderson polar chart

B

Inclination 75°

Depth unit one inch



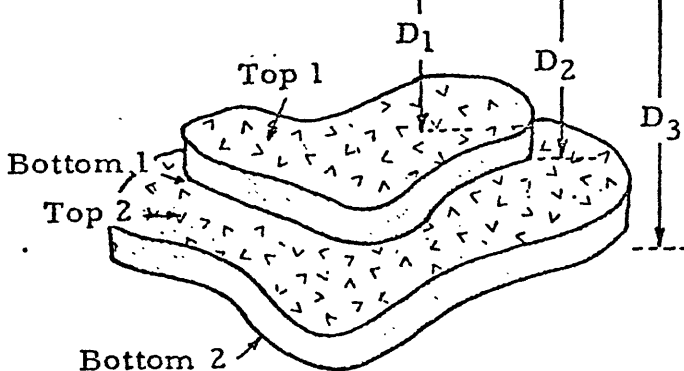
$$\Delta T = \alpha KT_0 \Delta N$$

$\alpha = 5.652 \times 10^{-3}$ gammas
per unit magnetization

Simplified topography

C

Flightline



D

Point	ΣN_{top}	ΣN_{bot}	$=$	ΔN	ΔT

Figure 14.--Use of Polar charts in two- and three-dimensional analyses of aeromagnetic anomalies.

(1) The slab method, outlined by Zietz and Henderson (1956), utilizes small slabs measured in terms of depth units. The field of each slab has been previously calculated. The body is subdivided into horizontal layers according to depth units and the contribution of the slabs are added to obtain the anomaly at a given point.

(2) In the graphical method (Henderson and Zietz, 1957), the body is divided into layers normal to the direction of the inducing field. A lengthy double integration is performed.

(3) A more direct and shorter method is outlined by Henderson (1960b) in which a polar chart is used for rapid computation of the magnetic effect of a three-dimensional body. The body is subdivided into horizontal layers, each outlined by the contour bisecting each layer. The scale of the top and bottom of each layer must be adjusted to agree with that of the chart. The scale change was made by a projector. A chart scale of a depth unit equal to one inch is most convenient. The counts for each layer are tabulated and the total-intensity field, AT computed.

The depth or distance from the airborne magnetometer in the plane of observation to the magnetic source rocks in the basement were estimated by the method outlined by Vacquier and others (1951). The shape characteristics of the observed aeromagnetic field are compared with theoretical anomalies of prismatic models. The horizontal extent of the steepest gradient is used as a first approximation for the dimensions of the model. The estimates are then refined by an index.

Table 2 lists some depths in the sedimentary basins. Local drilling

Table 2 near here

data corroborates some of these estimated depths.

For sharp high-amplitude cylindrical anomalies, empirical factors from magnetic-doublet curves was used to calculate the depth to the source rocks. (Henderson and Zietz, 1958).

Table 2. Depths to magnetic sources in the basement estimated from aeromagnetic anomalies observed over the northern basins.

Anomaly	Quadrangle	Depth or distance to Precambrian (feet)	Altitude of Precambrian Surface (feet)	
			Estimated	Known
Cave Spring	Union	1000	900	1005
Little Boone	Sullivan	1050	850	
Mineral Hill	Sullivan	1650	160	-360
Vilander	Sullivan	1750	50	
Pea Ridge	Sullivan		-100	
Little Pilot Knob	Richwoods	1900	-100	-110
Indian Creek	Richwoods	1750	50	S.L.
Rogue Creek	Richwoods	1850	-50	S.L.
Aptus	Richwoods	2200	-400	
North Richwoods	Richwoods	2800	-1000	-700 ⁺
Cove Creek	St. Clair	1900	-100	
Pyatt	Berryman	1075	725	
Huzzah	Berryman	1900	-100	
Butts Ford	Berryman	1200	600	S.L.

* Distance from aircraft magnetometer to the Precambrian source.

Table 2. (Continued)

1								
2								
3								
4								
5								
6								
7								
8								
9								
10								
11								
12								
13								
14								
15								
16								
17								
18								
19								
20								
21								
22								
23								
24								
25								
Clear Crrk	Berryman	1600	200					
Kelly Hollow	Berryman	2000	-200					
Fourche a Renault	Potosi	1800	S.L.	+25				
Potosi	Potosi	1900	-100	-135	+			
Wallen Creek	Potosi	2400	-600	-300				
Shifley	Potosi	1900	-100	200				
Little Lost Creek	Potosi	1500	300	250				
Palmer	Potosi	1350	450	426				
Compton Branch	Potosi	1250	550					
Prospect	Bonne Terre	2000	-200	200				
Hopewell	Bonne Terre	2200	-400					
Three Hill Cr. West	Bonne Terre	1800	S.L.					
Three Hill Cr. East	Bonne Terre	1200	600					
Chicken Farm Knob	Bonne Terre	1500	300	200	+			
French Village	Farmington	1550	250					
Jaydee	Farmington	1200	600					
Farmington-South	Fredericktown	1600	200	290				

The throw or vertical displacement of some gravity faults can be estimated from characteristic magnetic profiles or estimated by use (written commun.) of a simple formula devised by R. G. Henderson. Anomalies over slab models can be applied to gravity faults of moderate vertical displacement, such as the Simms Mountain fault, Big River fault zone, Wolf Creek fault, the Palmer fault Complex and the St. Genevieve fault system.

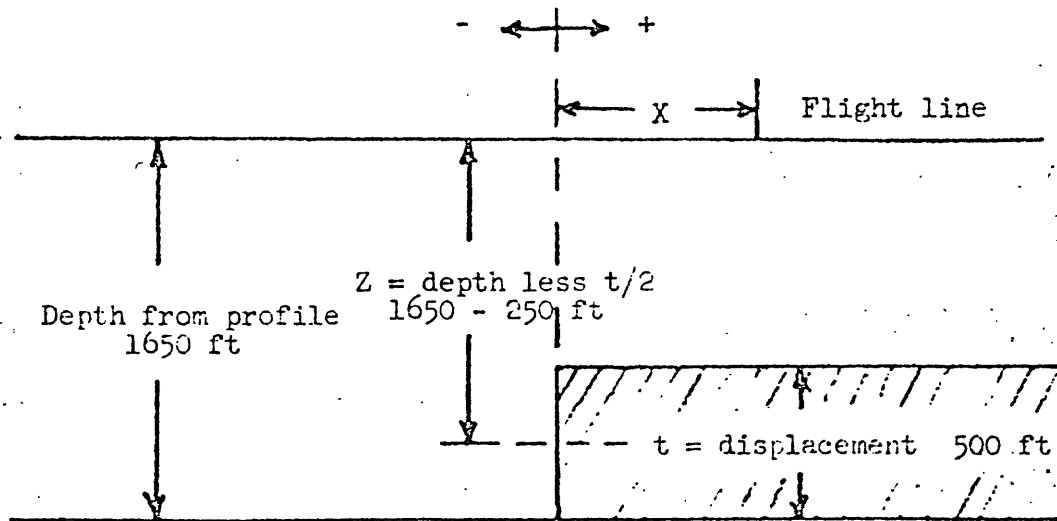
Induction theory used in the formula assumes a normal magnetization in the direction of the earth's field. The sedimentary rocks are assumed to be non-magnetic, and the magnetic rocks are assumed to be homogeneous. For reasonable accuracy, the ratio of the displacement or thickness of the slab to the depth of burial, should be (t/z) less than unity for errors smaller than 2%. The general expression for the total intensity field is given by:

$$\Delta T = 2kT_0 \frac{t}{z} (\cos^2 I \sin \alpha - \sin^2 I$$

$$(2 \cos I \sin I \sin \alpha) \left[\frac{-x/z}{1 + (x/z)} 2 + \frac{1}{1 + (x/z)^2} \right]$$

The parameters are given in Figure 15, where z is the depth to the center of the up-thrown block.

Figure 15 near here



$\alpha = 45^\circ$ angle between magnetic north and traverse across strike of fault

$T_0 =$ Earth's field 5.66×10^4 gammas

$k =$ susceptibility of granite 1.7×10^{-3} cgs

$I =$ inclination of Earth's field 70°

$t/Z = 500/1400$ error less than $1/4\%$

Figure 15.--Diagram showing the parameters used to compute the displacement of normal faults in basement rocks.

If we assume that the granite is homogeneous and that the sedimentary rocks are ^{non-} magnetic, the parameters (Fig. 15) produce an anomaly of 65 gammas. The granite at Jonca Creek, however, has magnetic characteristics similar to the granitic rocks near Fredericktown, so that the computed anomaly is about 130 gammas. The residual anomaly across the Wolf Creek fault exceeds 100 gammas after the magnetic contrast between the granites has been removed; the observed residual anomaly is almost the same as the computed anomaly.

The thickness of some isolated volcanic units are quickly estimated by use of a cylindrical model where the total intensity anomaly, areal extent and depth to top of the magnetic unit are known. The expression for thickness is approximated by

$$\Delta T \approx \frac{2\pi k T_0}{\rho} \left[(z + \ell) / [(z + \ell)^2 + r^2] \right]^{1/2} \left[\frac{1}{2} - \frac{z}{(z^2 + r^2)^{1/2}} \right]$$

where ℓ = thickness
 r = radius of body
 $-z$ = depth to top
 kT_0 = magnetization of body

At Taum Sauk Mountain, the anomaly ranges from 450 gammas on the south slope to 650 gammas on the north slope.

Substituting $z = 650$ feet
 $r = 1.3 \times 10^4$ feet
 $T_0 = 5.7 \times 10^4$ gammas
 $k = 2 \times 10^{-3}$ cgs

the thickness ℓ will approach infinity for $\Delta T = 670$ gammas or $1 \gg 1.5 \times 10^3$ feet. An analysis of the anomalies in the Ironton area (see Fig. 76) verified a thick sequence of volcanic rocks for this area.

Although continued, derivative and residual anomalies provide a high degree of resolution, Skeels (1947, p. 43-44) showed that computed anomalies do not permit a unique interpretation or define a particular distribution of magnetic rock but rather permit a qualitative appraisal of an area. Computed anomalies, such as derivatives and continuous fields are not only difficult to interpret, they may also amplify errors in the observed field.

Downward continuation intensifies the observed field as the magnetic surface is approached. Peters (1949, p. 308) in his direct approach to magnetic interpretation used the magnetic intensity continued to the basement level to compute the magnetic potential and, thus, calculate directly from the observed field a distribution of subsurface magnetic rocks which account for the observed field. At the basement level, broad magnetic variations in the field due to susceptibility contrast can be removed. In this study the field was continued to the level of the ground surface and then continued to the level of the Precambrian surface.

Derivatives of the observed field are a measure of the change in gradient. The use of the derivative method in geophysical interpretation has been demonstrated by Evjen (1936), Peters (1949), Henderson and Zietz (1949a), Elkins (1951), p. 45-48) and others. In this study a second-vertical derivative of the observed magnetic field was made for purposes of comparison. The regional component of the observed field changes systematically resulting in a smooth surface, whereas the residual or local component may change in an irregular or non-systematic way resulting in small highs and lows.

Residual or local anomalies can be separated from the observed total-intensity field by conventional graphical methods outlined by Nettleton (1954, p. 3-5) or by analytical methods summarized by Krumbein (1956; 1959). To obtain residual anomalies the regional gradient must be subtracted from the total-intensity field. In the graphic method a smooth curve or surface representing the regional anomaly is obtained by graphically smoothing the observed data. Differences between the regional and the observed data are plotted as residual anomalies. By using the analytic methods of Swartz (1954), Oldham and Sutherland (1955) and others, an elementary undulating surface polynomial is fitted to the observed data by least squares, which results in a smooth field. Polynomial surfaces of higher order, fifth or seventh, more closely fit the observed anomalies. In the separation of residual or local anomalies from the total-intensity field the analysis is independent of the relation between grid and trend orientation.

computer
The program of regional gradients used by the U. S. Geological Survey: (1) calculates the n coefficients by least-squares analysis for a selected degree surface fit to the observed data, (2) prints out coordinates, observed value, calculated value representing the regional field, and the residual for each observation, (3) computes the sum of the squares of the residuals, and the standard error.

The methods herein outlined permit a rapid analysis of low amplitude magnetic anomalies associated with basement structure.

Data and calculations

Computation processes for continuation and derivatives and those for residual anomalies were programmed for the electronic computers by James Marsheck and Walter Anderson of the U. S. Geological Survey.

A grid, having an interval corresponding to the spacing between flight lines, was laid over contour map of the observed aeromagnetic field. Magnetic information was interpolated at each grid intersection and tabulated for punch cards. The computations were done on Burroughs 205 and 220 electronic computers. Data from the printout sheet of the computer were recompiled and contoured.

The grid spacing for the continuation and residual maps was 1000 feet, whereas the spacing the derivative maps was 2000 feet. Contouring was improved by computing intermediate points. These were obtained by migrating the grid one-half the grid interval along ordinate and abscissa.

The residual anomaly is affected by the relative size of the grid interval. Krumbein (1956, p. 2183) gives an empirical rule for selecting grid spacing. Spacing should be at least twice as large as the average area represented by control points. With a 1/4-mile spacing of control points, the average area is 1/16 square mile. Double the area is 1/8 square mile. This suggests that a grid spacing between 1/3 and 1/2 mile should be satisfactory, although the validity of Krumbein's rule has not been carefully checked.

Depths to the igneous basement rocks were made in the Bonneterre area and elsewhere in the mining district. These depths assuming induction theory, were estimated by the method described by Vacquier and others (1951, p. 11-15). The Chicken Farm anomaly, shown in Figure 83, was one of the anomalies used for determination of depth. The average estimated depth of 1500 ft was deducted from the flight altitude of 1900 ft to place the surface at 400 ft above sea level. The altitude of the knob of 500 ft was known from drilling data. These estimates of depth were within 10 percent of the actual distance between the airborne magnetometer and the Precambrian surface.

Grid spacing depends upon the density of data and the areal extent of the gradient, and shape of the anomalies. The shallow depth of burial of the basement rocks and resulting short distance from the plane of observation limited the grid interval to about one-half the depth of burial or 1000 feet.

During the computation of residual anomalies the first, third, fifth and seventh degree surfaces, representing the regional fields in the Bonneterre area, were fitted to the observed data and the first 3 surfaces were contoured. The standard error decreases as follows:

1st degree	96.0 gammas	Where error = $[R^2/(N-1)]^{1/2}$
3rd degree	76.9 gammas	R = residuals
5th degree	66.1 gammas	N = number of observed values
7th degree	64.6 gammas	

Further decrease in the standard error did not justify additional computation or contouring beyond the fifth degree surface.

Characteristic anomalies

In order to understand and quickly interpret total-intensity aeromagnetic anomalies shown in profile, groups of anomalies characteristic of commonly observed geologic features were constructed.. The geologic features of interest generally are shear zones, normal faults, vertical and inclined contacts between granitic and volcanic rocks, thin slabs of volcanic rocks, rectangular blocks and cylinders of volcanic rock of infinite thickness, and valleys in volcanic or granophyric rocks. A thin mantle of sedimentary strata and residuum of cherty soil partly or completely cover many of these geologic structures. By simple comparison of the computed profiles over simple geometry with the observed aeromagnetic profiles, a plausible geologic structure can be readily deduced.

The dimensions, shape and depth of burial of the models were varied in order to approximate as many of the physical and geologic conditions as possible. Induction theory was applied to the models, as measurements of the magnetic properties of the rocks indicated that remanence was unimportant in many localities. Average magnetic susceptibilities for granitic and volcanic rocks were selected for computing curves. Computations were further simplified because the distance from the magnetic detector to the source usually ranged between 1000 to 2000 ft. Polar charts and formulas were used to integrate models and calculate curves. Model computations were also simplified where one dimension was effectively infinite, that is, one horizontal dimension was two and one half times longer than the other dimensions.

Many geologic observers believe that faults and related fractures serve as major channelways for the upward migration of ore-bearing fluids. The search for faults using aeromagnetic information is facilitated by comparison of these observations with computed profiles over models of faults and contacts. The models in Figure 16

Figure 16 near here

represent vertical fault zones of different dimensions and depths. The two profiles for each model represent the magnetic effects of zones in granite and volcanic rocks. Generally the anomalies observed over these faults have small amplitudes. These models simulate major fault zones in igneous rocks having magnetizations typical of the Ozark region. The magnetite in the sheared rock has altered to nonmagnetic assemblages. The negligible susceptibility causes a characteristic low. The observed aeromagnetic profile over the Simms Mountain fault zone (Irondale fault of Buckley) between Doerun and Knoblick is shown in Figure 17. Total intensity magnetic profiles

Figure 17 near here

over normal faults (Figure 18) shows the change in gradient at depths

Figure 18 near here

between 1200 and 1800 ft.

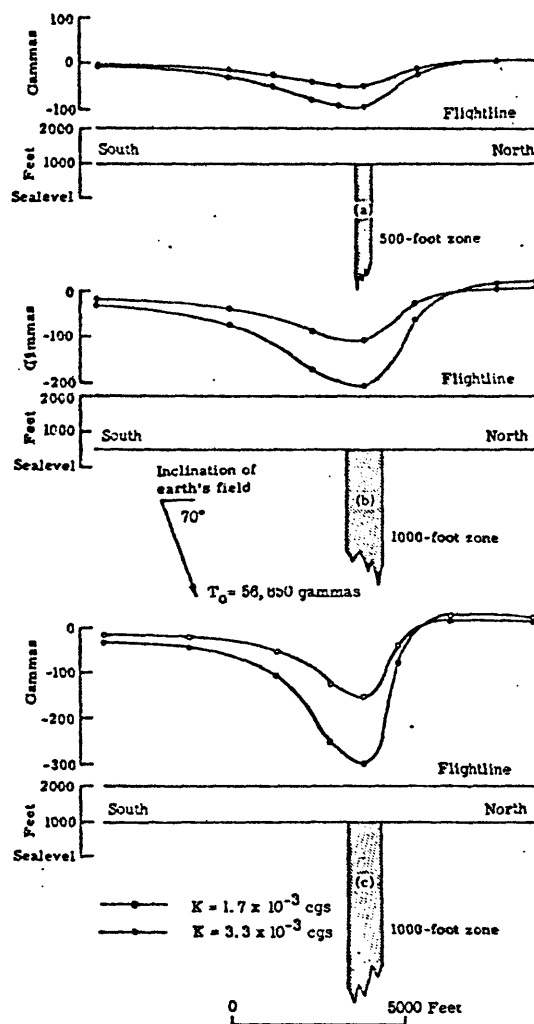


Figure 16.--Characteristic magnetic profiles across vertical fault zones.

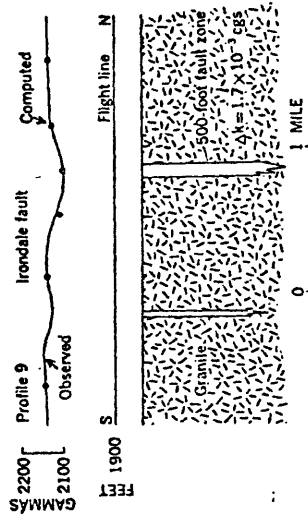


Figure 17.--Width of the Simms Mountain fault zone estimated from aeromagnetic data.

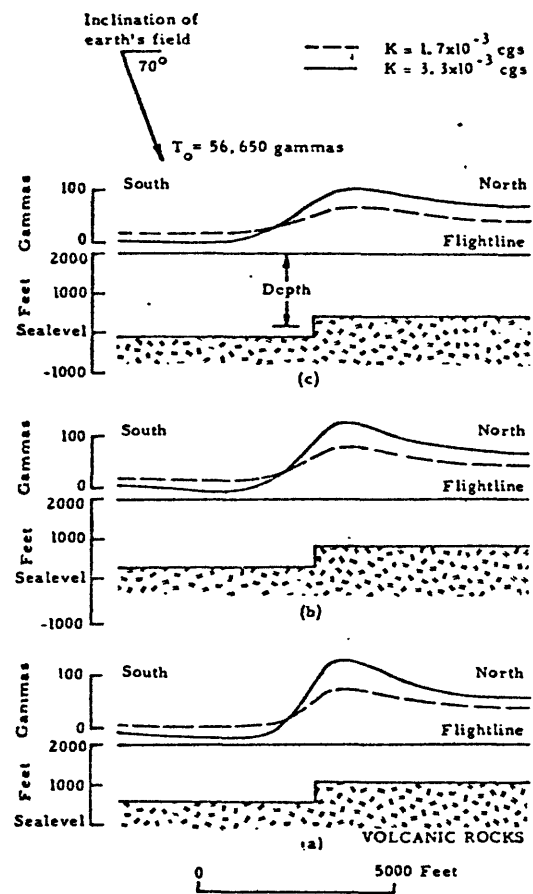


Figure 18.--Characteristic total-intensity magnetic profiles over normal faults.

An aeromagnetic interpretation of the Palmer fault between Shoal and Huzzah Creeks, where the fault has a vertical displacement of 400 ft, is shown in Figure 19. The nature of the Palmer fault

Figure 19 near here

complex produced an irregular assortment of upthrown and downdropped blocks of basement, which locally complicates interpretation.

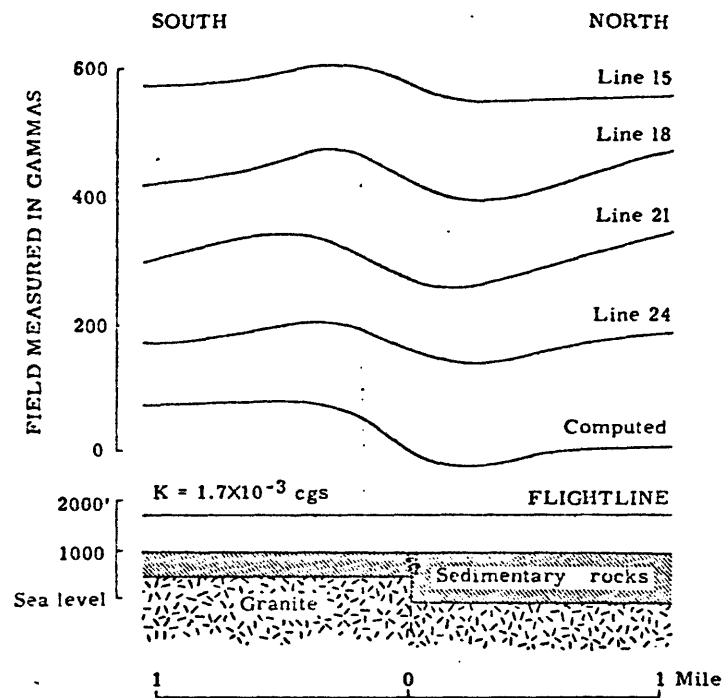


Figure 19.--Aeromagnetic interpretation of the Palmer fault zone.

The attitude of some contacts between rocks of, known or inferred contrasting magnetic susceptibility and lithology can be determined from aero-magnetic data. The contact may be intrusive or faulted. Typical profiles of vertical or inclined contacts, shown in Figure 20, 21, and 22 can be used to deduce the relations of buried or obscure contacts

Figures 20, 21, 22 near here

between volcanic and granitic rocks. The typical set of profiles (Fig. 20) shows the anomalies over contacts of magnetically contrasting rocks. The distinction between dipping and vertical contacts is subtle. Where the volcanic sequence is thick, the dip of the contact is estimated from the steepness and position of the magnetic gradient in relation to the contact. The magnetic contrast between rock units, however, can change the gradient. The increasing susceptibility (induced magnetism) shown in Figure 21 changes the gradient of profiles over vertical contacts of infinite depth extent. The attitude and location of the contact between granophyric and porphyritic rock of the Musco group and the coarse-grained red granite of the Bevos group can be determined north of Fredericktown by comparison of the computed magnetic profile with the observed profile. Figure 23 shows the inclination of the

Figure 23 near here

intrusive contact near Pine Mountain between Fredericktown and Ironton to be about 30° (A) and a vertical contact westward (B) from Flatwood.

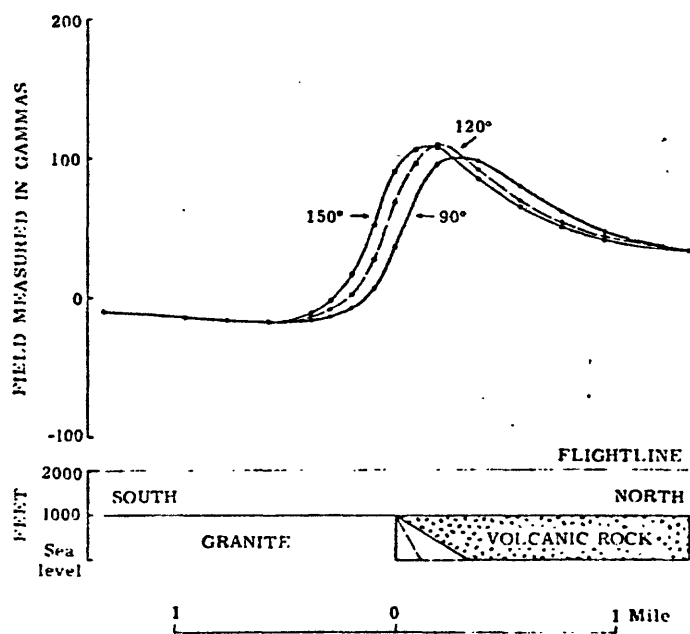
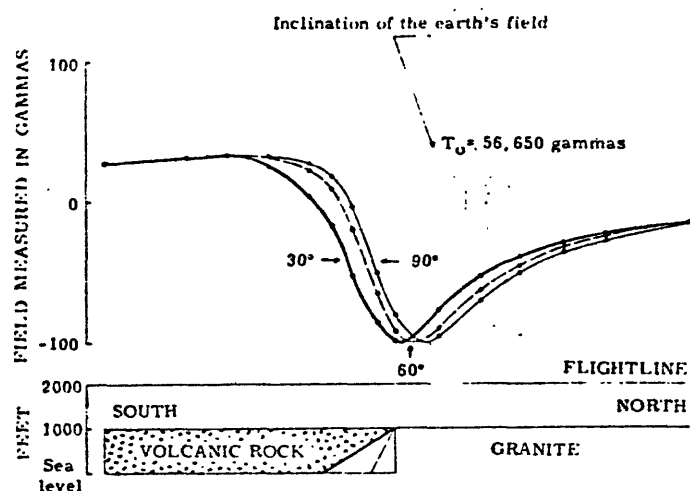


Figure 20.--Magnetic effect of inclined contacts between granite and volcanic rocks.

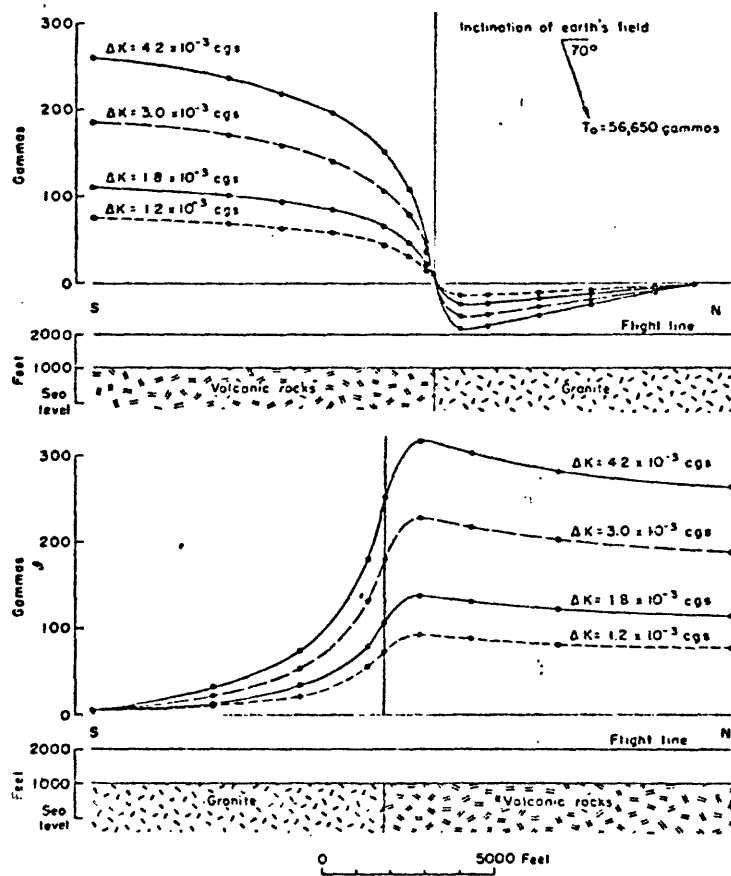


Figure 21.--Characteristic total-intensity magnetic profiles in the magnetic meridian over vertical contacts showing the effects of varied rock susceptibilities.

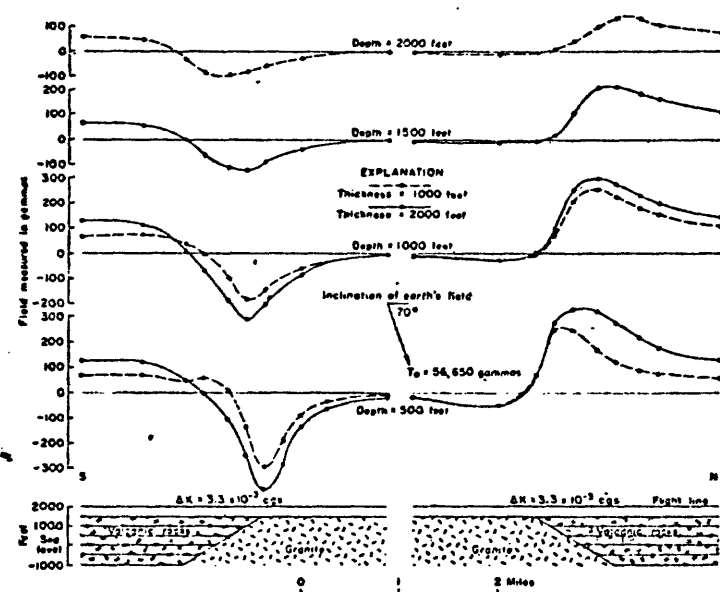


Figure 22.--Characteristic effects of ends of volcanic flows at different thicknesses and depths.

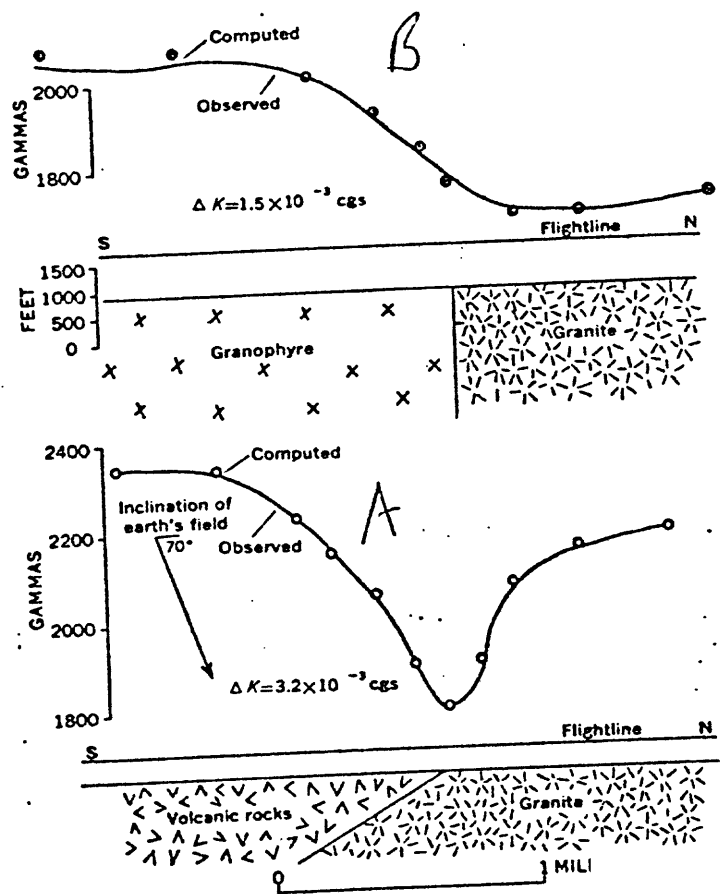


Figure 23.--Aeromagnetic profiles over contacts between granitic and volcanic rocks near Flatwoods area.

148 p. 148 a follows

Slab models of Zietz and Henderson (1956) can be used to find the thickness and approximate areal extent of thin volcanic flows. A comparison of an aeromagnetic profile over volcanic flows at Grassy Mountain, Des Arc quadrangle, with computed profiles of slabs gives a flow thickness of about 1200 ft. and delineates partly buried contacts with intrusive granite. The contribution of partly exposed volcanic rocks near Minimum to the total-intensity field is shown in Figure 24.

Figure 24 near here

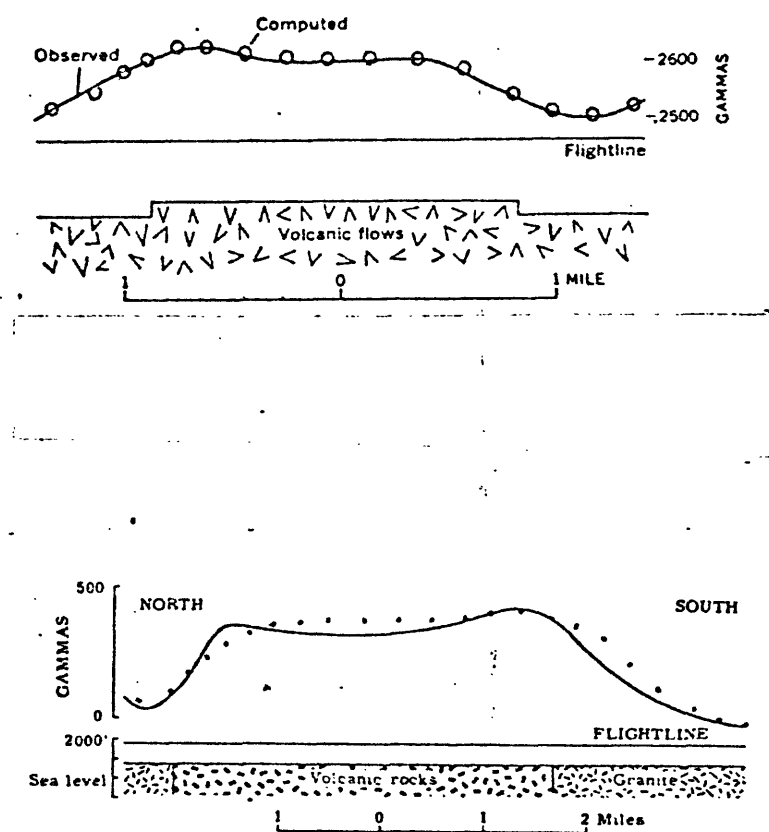


Figure 24.--Aeromagnetic profiles over volcanic flows near Minimum and Criswell, Missouri.

Similarly a comparison of computed profiles of slabs with aeromagnetic profiles over volcanic flows near Criswell gives the relief and areal extent of a hill on a buried volcanic terrane.

The characteristic magnetic curves in normalized form over an infinite prism, (Figure 25) was used to interpret a large aeromagnetic anomaly near Shirley (Figure 26). Prismatic models presented by

Figures 25 and 26 near here

Vacquier and others (1951, p. 65-147) are useful in this type of interpretation. The structure inferred from the Shirley anomaly is interpreted as a magnetic volcanic unit contrasting with less magnetic volcanic rock and granite of low susceptibility. The more magnetic rock has low topographic relief but this relief on the Precambrian basement is not indicated by inflections on the profile. The 200-ft of relief on the basement surface merely contributes to the total-intensity anomaly. The magnetic contrast is mainly between rhyodacite ($k = 5.3 \times 10^{-3}$ emu/cm³) and trachyte ($k = 6.1 \times 10^{-3}$ emu/cm³) on the southside and trachyte and granite (1.1×10^{-3} emu/cm³) on the northside.

Comparisons of observed magnetic profiles with computed "normalized" profiles over cylinders of infinite depth extent, shown in Figure 27 were used for estimating the diameters of some magnetic

Figures 27 and 28 near here

bodies. A cylindrical model gave an approximation to an anomaly

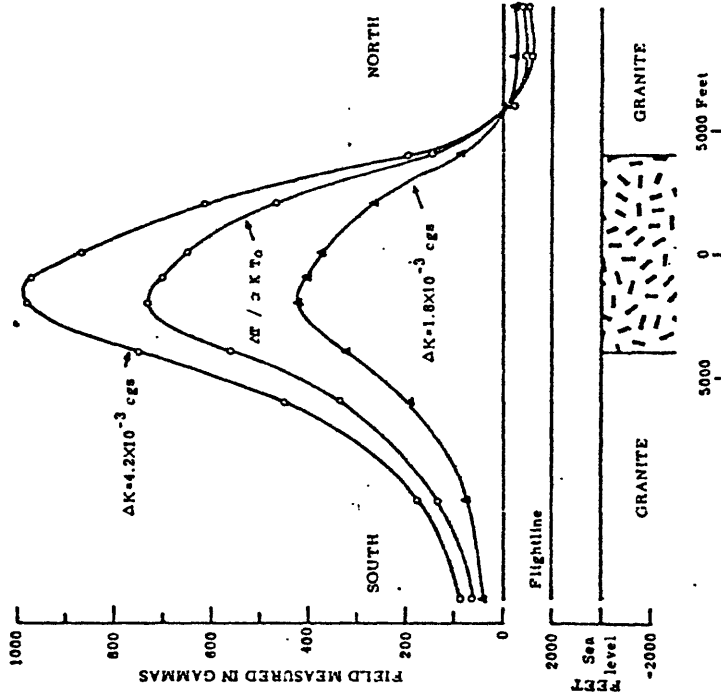


Figure 25.—Prismatic model used to approximate aeromagnetic anomalies of the type near Shirley, Missouri.

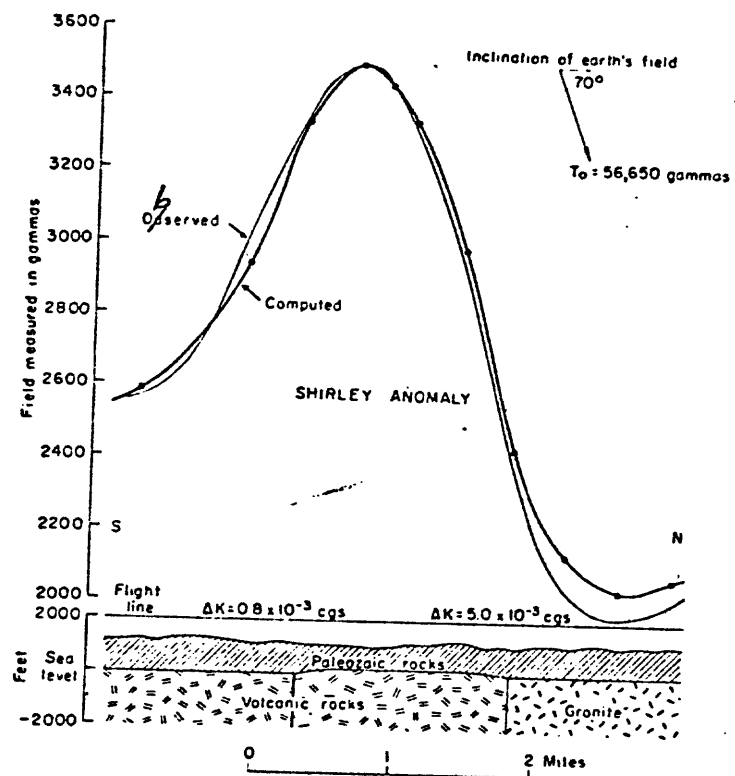


Figure 26.--Interpretation of the high-amplitude anomaly near Shirley, Missouri.

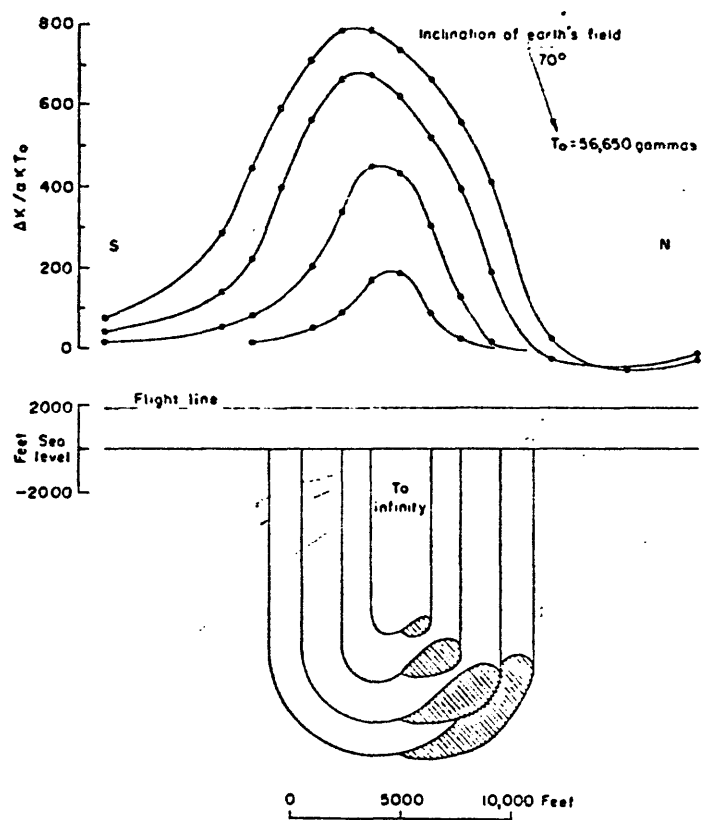


Figure 27.--Magnetic profiles over cylindrical models of infinite depth extent.

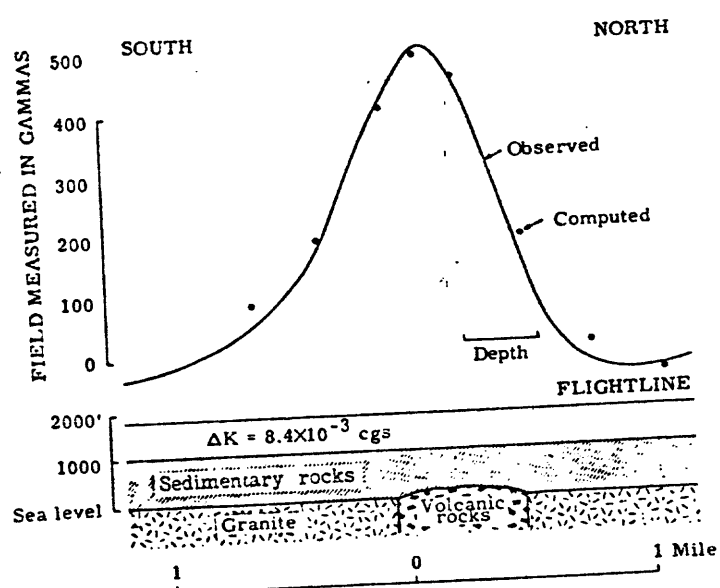


Figure 28.--Aeromagnetic anomaly associated with a plug-like feature near Pyatt.

believed to be associated with a volcanic plug near Pyatt (Fig. 28).

Interpretations in volcanic flows produce distinctive lows in magnetic profiles. A series of profiles, shown in figure 29,

Figures 29 and 30 near here

were computed to illustrate eroded or isolated flows. Figure 30 shows the aeromagnetic anomaly that results from a postulated discontinuity in the buried volcanic flows at Cedar Creek in the Berryman quadrangle.

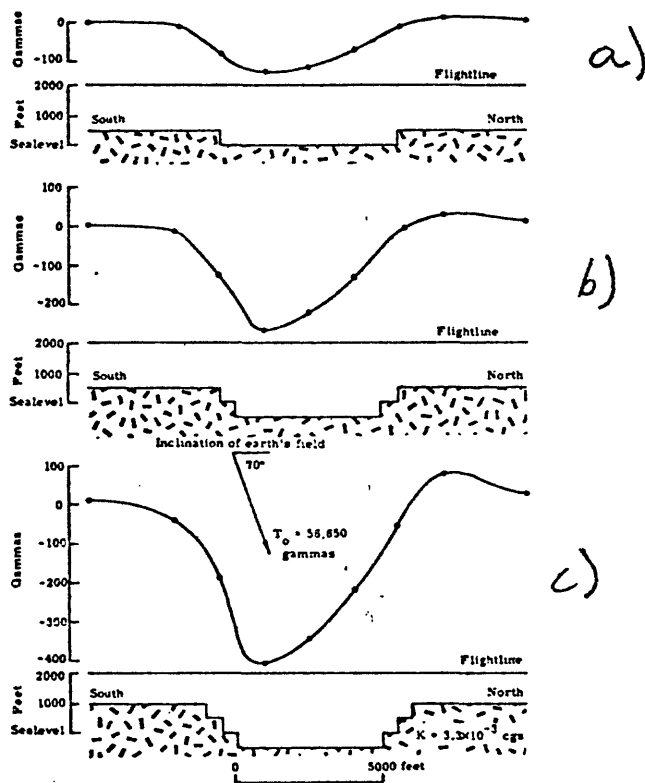


Figure 29.--Magnetic profiles over erosional areas in volcanic flows.

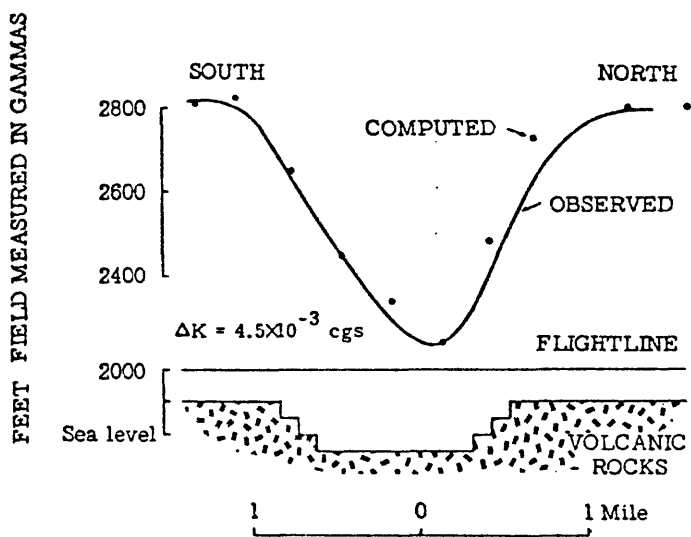


Figure 30.--Aeromagnetic anomaly at Cedar Creek caused by an erosional discontinuity in volcanic flows.

Rock relations

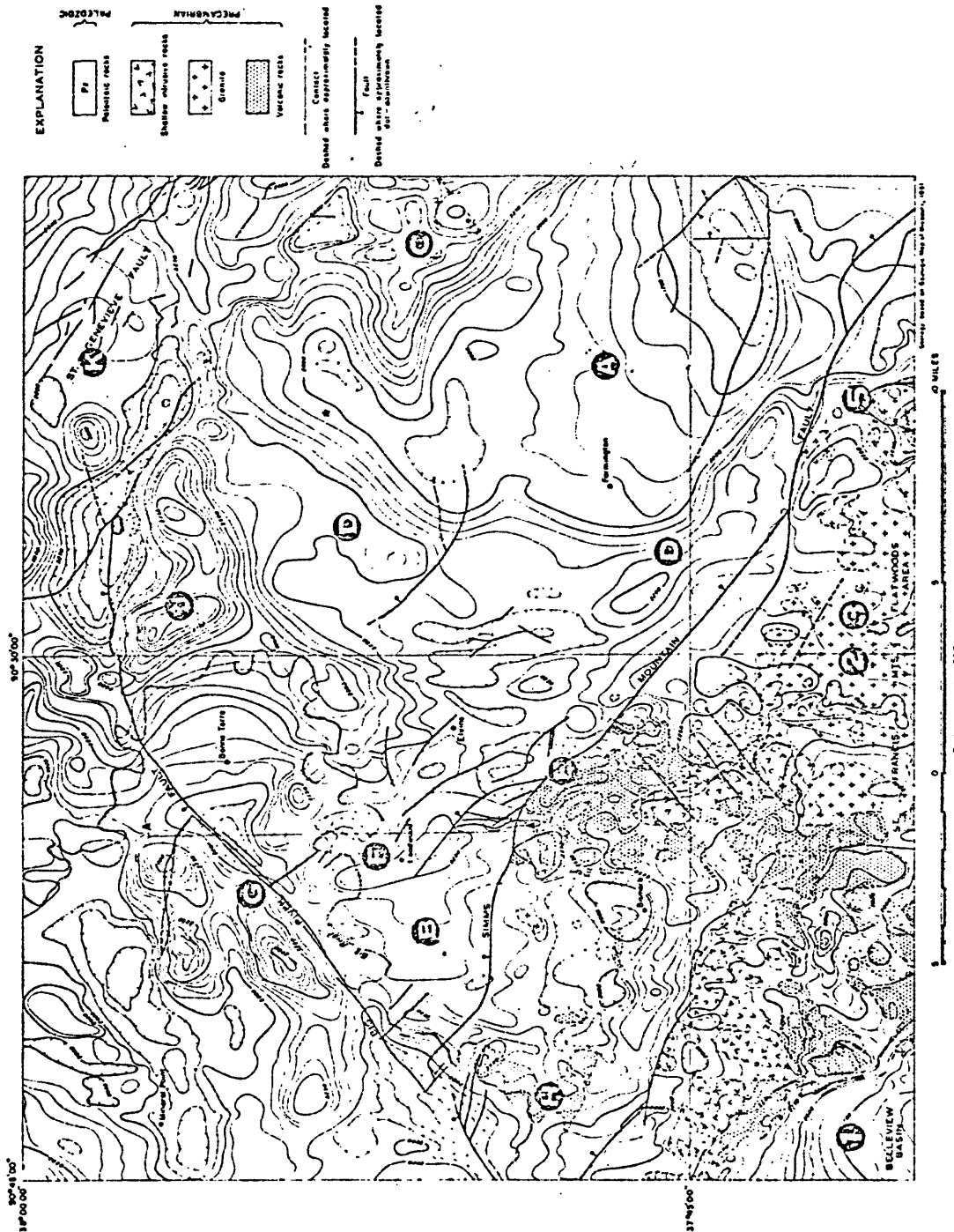
The aeromagnetic map covering an area of buried Precambrian (Figs. 2a, igneous rock and 31), show that this area can be divided into

Figure 31 near here

(a) a magnetically flat area underlain by granite of low susceptibility (shown at D), and (b) a magnetically complex area underlain by older volcanic rocks of high susceptibility that form near-surface features (shown at E, F, G). The magnetic pattern associated with the border of the ^{Bellevue} basin (1) results mainly from the contrasting magnetic character of granite and volcanic rock.

The granitic rocks were divided into groups by susceptibility (Fig. 8) and according to magnetic patterns (Fig. 31) shown in areas 1, 2-3, and 5. The granite underlying the Farmington anticline (A) corresponds to group 1 that floors the Bellevue basin. The buried granite (B) west of the "Lead Belt" is similar to the granite in the Flatwoods area (groups 2-3). Similarly, the granitic rocks at Jonca Creek (C) are correspond to the more magnetic phases (groups 3-4). Granophyre and granite porphyry (D) that rim the less magnetic granite (A) are similar to the granitic phases near Fredericktown (group 5).

The volcanic rocks and granite porphyry at Simms Mountain (E) extend northward in subsurface to Leadwood (F) at the west boundary of the mining district and westward to Hughes Mountain and Irondale (H). These rocks form a horseshoe-shaped feature that partly enclose the granite (B). Near the Big River fault zone, large magnetic pendants of volcanic rock (G and J) in the roof of the granite are detected in subsurface by their associated anomalies.



Aeromagnetic profiles are used to deduce plausible geometric relations and lithologies as an aid in mapping areal geology. These relations are verified by fitting computed profiles to observed data by two- or three-dimensional analyses of the suggested geometry (Pirson, 1940; Henderson and Zietz, 1956, 1957; Henderson, 1960b).

Anomalies greater than 200 to 300 gammas result from contrasting lithologies in addition to topographic relief. Large roof pendants of volcanic rock in a granite terrain typify these anomalies. The upper profile A-A' (Fig. 32) in the section from Russell Mountain to Buford

Figure 32 near here

Mountain shows a difference in level of about 1000 to 1300 gammas between the magnetic anomaly over granite and that over volcanic rock.

Topography has little magnetic effect in this area, because the tuffs and other pyroclastic rocks that cap these hills such as Buford Mountain, function as a nonmagnetic window. The underlying ash flows, rhyolite, porphyry, and andesite cause the aeromagnetic anomaly. The low in the magnetic profile between Russell

Mountains and Charles Mountain is due to thinned volcanic rock, the result of granite intrusion as inferred from granophyre in Stouts Creek. The profile A-A' across the eastern part of the Bellevue basin shows the magnetic effect of granite between volcanic rocks of higher magnetic susceptibility. The anomaly over Buford Mountains results from volcanic rock in contact with the granite, granophyre, and granite porphyry. Trachyte of Buford Mountain (lower part, fig. 42a) has a high susceptibility, which contrasts sharply with that of the granite. A sharp low in the profile suggests a zone of crushed non-magnetic rock between the porphyry and trachyte. Diabase that has reversed remanence can produce a similar anomaly.

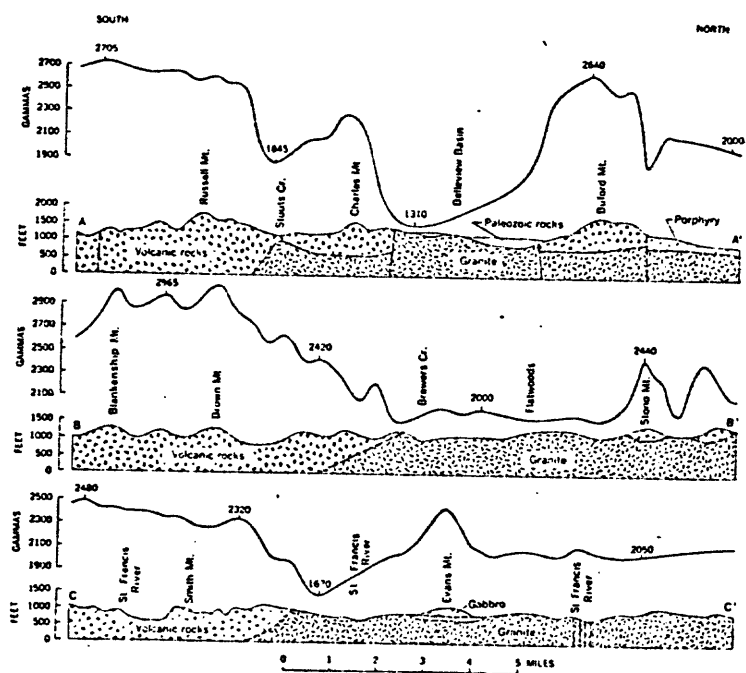


Figure 32.--Subsurface structure and lithology deduced from aeromagnetic profiles over the St. Francois Mountains.

The section from Blankenship Mountain to Stono Mountain, profile (fig. 32), B-B', shows a difference in magnitude of about 1000 gammas between anomalies over volcanic rock and granite. The 50-to 200-gamma anomalies near Blankenship and Brown Mountains are examples of anomalies due partly to topographic relief of the volcanic rocks. An observed concentration of iron minerals near the intrusive contact between volcanic rock and granite, however, produces the small anomaly south of Brewers Creek. The granite in this area produces uniformly flat magnetic profiles, which merely show a very low regional gradient of about seven gammas per mile. For the anomalies over small volcanic pendants at Stono Mountain, the difference in total-intensity amplitude is about 500 gammas. The effect of topography and magnetic contrast in rock type produce these anomalies.

A section from Marlow Mountain to Flatwoods (Fig. 32 C-C')

shows that the magnetic intensity is about 500 gammas higher over volcanic rock than over granite. The shape and magnitude of the anomaly over the southward-dipping contact between granite and volcanic rock consequently differs from that over a vertical contact (Figs. 20 and 23b). In this area the attitude of intrusive contacts can be determined from magnetic data. The anomaly over Evans Mountain is greater than that over a comparable hill on volcanic rocks because of the underlying gabbro. Gabbroic phases of diabase, which contains titaniferous spinels, commonly intruded the granite-rhyolite contact. The 50-gamma anomaly at the St. Francis River north of Evans Mountain is caused by a swarm of diabase dikes of easterly trend. The magnetic profile over the granite in the Flatwoods area north of Evans Mountain is uniformly flat. Instead of the present geologic interpretation, a shallow (low angle) dipping contact near "1620" low is inferred from the magnetic data by use of profiles in figures 20 and 22.

Structural relations

Many structural relations, mainly in subsurface, can be deduced from the aeromagnetic map (Figures 2a and 90). These relationships are discussed in terms of topographic features, roof pendants at the top of the batholith, zones of fracturing and intermontane basins. Some relationships are distinguished and interpreted by the magnetic gradient between magnetically contrasting rock units.

In Figure 90, the magnetically flat granite at Flatwoods (1) is dotted by magnetic volcanic pendants and granophytic sheets. This area contrasts sharply with the thick magnetic volcanic and pyroclastic sequence near Ironton (2). Similarly the relatively nonmagnetic granite underlying the Farmington anticline (3) produces a magnetic gradient between the less dense and more magnetic granite at Jonca Creek (4) and the more magnetic granite at Flatwoods (1). These gradients not only help to distinguish rock types but permit these rocks to be divided into structural blocks, such as the Avon block (3).

Lows and small inflections in magnetic profiles help extend knowledge of faulting, by tracing them in subsurface and estimating their vertical displacements. The structural implications of the aeromagnetic patterns associated with the St. Genevieve fault zone (5), Big River fault (6), Palmer fault complex (8), and Simm Mountain fault system (9) are analyzed. The relations of these faults to granite-floored intermontane basins, such as Bellevue valley (9), Sabula (10), Coldwater (11), etc., are examined by use of magnetic lineaments of gradients.

The structural relations in mining areas, such as iron deposits at Shepherd Mountain (2) and Mt. Cottoner (12), and lead deposits in the Leadwood area (13) and Fredericktown - Mine La Motte areas, are discussed in the chapter on the relation of aeromagnetic anomalies to mineral deposits. The subsurface diorite pluton near Avon is discussed in the chapter on regional features.

Topographic anomalies

An aeromagnetic anomaly caused by topographic relief on a magnetically homogeneous terrane is designated as a topography anomaly. Many of the hills are almost equidimensional (Fig. 33), which

Figure 33 near here

necessitates the use of a three-dimensional methods such as that devised by Henderson and Zietz (1957) or Henderson (1960b). Figure 34

Figure 34 near here

illustrates the magnetic effect of exposed conical hills of granitic and volcanic rock in the St. Francois Mountains.

Buck Mountain is a hill of coarse-grained red granite, described in detail by Robertson and Tolman (1969). The granite contains 0.5-0.6% accessory magnetite and has an average magnetic susceptibility of 1.7×10^{-3} emu/cm³ units. Remanent magnetization measurements of the granite showed a negligible intensity and a random direction. In computing the anomaly only induction was assumed to produce the anomalies. The susceptibility used in computing the magnetization was an average of samples collected from the hills and nearby outcrops, as shown in Figure 11.

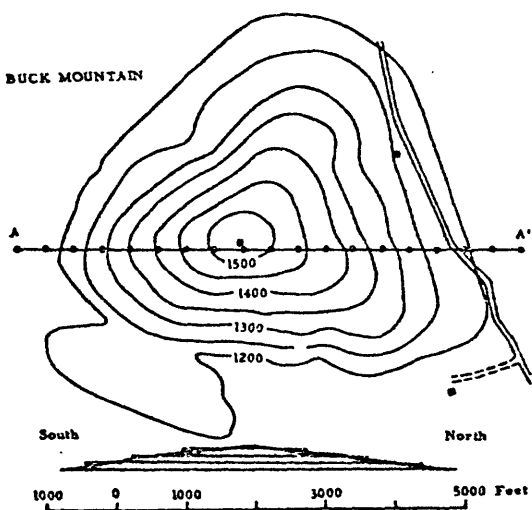


Figure 33.--Topography of a granite knob showing the irregular three-dimensional model used in computations.

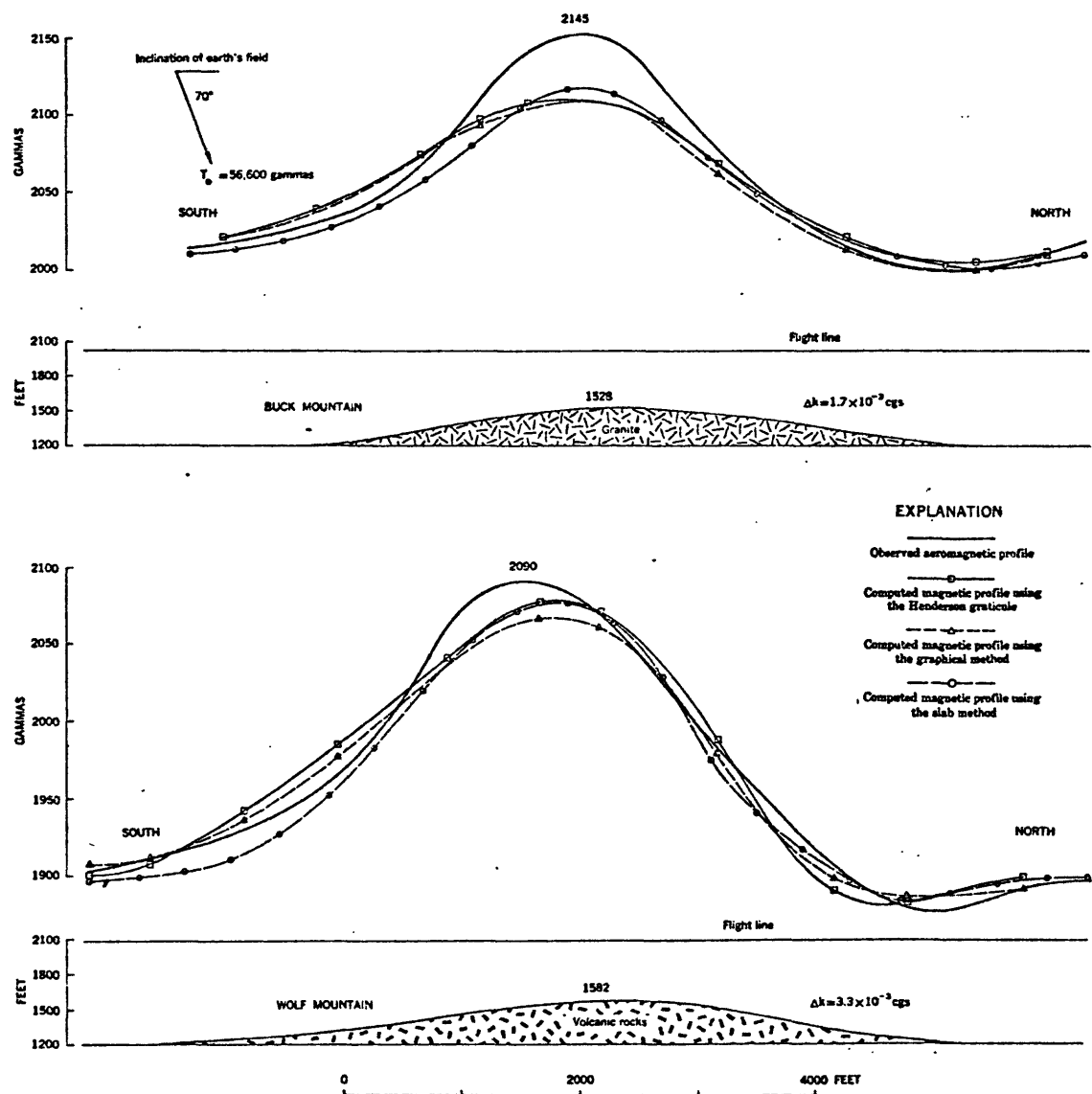


Figure 34.--The magnetic effect of topographic relief by three-dimensional techniques.

The aeromagnetic anomaly observed over the granite of Buck Mountain has an amplitude of about 150 gammas. The computed anomaly has about two-thirds of this amplitude. Discrepancies between the observed and computed anomalies may result (1) from unobserved inhomogenieties in the granite hill, (2) from a small susceptibility contrast in the granite of the valley and of the hill, (3) from a disturbing geometry at depth, and (4) from an increase in contributing topographic relief caused by weathering of granite in valleys and on the flanks of hills. The susceptibility of weathered granite or granite wash is about the same as that of the sedimentary rocks of the intermontane basins. All the methods used to compute theoretical anomalies gave similar results. For bodies of irregular shape, the graticle of Henderson (1960b) gave the quickest and best-fitting curves.

The volcanic rocks of Wolf Mountain include rhyolite, dacite, breccia, and trachyte. The average susceptibility of these flows and pyroclastic rocks, as shown by Figure 9, is about 3.3×10^{-3} emu/cm³. Magnetic profiles computed by different methods compare favorably with each other and with the observed profile. The amplitude of the anomaly observed over the volcanic rocks of Wolf Mountain is about 200 gammas. This value is close to the maximum amplitude of the topographic anomalies in this region, as no relief greater than Wolf Mountain is likely. In the St. Francois Mountains, an anomaly over a hill of volcanic rock has twice the magnitude of that over a comparable hill of granite. Magnetic susceptibility of these rocks confirms this difference in the observed magnetic fields. The amplitudes of the observed and computed anomalies over the granophyre or microgranite at Mt. Devon, shown in Figure 35 are the same magnitude or about 170 gammas.

The granophyre and fine-grained porphyritic granite are believed to represent an early chilled phase, or more likely a late shallow intrusive phase of the batholith. The iron did not react to form abundant ferromagnesian minerals but formed dust-like magnetite similar to that observed in the volcanic rocks. These fine-grained granites are more magnetic than the coarse-grained phases (see fig. 8) and similar in magnetic properties to the volcanic rocks (fig. 9).

Figure 35 near here

The anomaly resulting from the granophyre is equivalent in magnitude to the observed and computed anomaly over volcanic rock of College Hill south of the town of Ironton. The presence of the large mafic dike on the north side of Mt. Devon described by Muilenburg and Goldich (1933) does not affect the computed curves, because both the host rock and dike have about the same susceptibilities.

Table 3 summarizes some of the topographic anomalies observed

Table 3 near here

in the St. Francois Mountains. The amplitudes of magnetic anomalies were correlated with hills of small topographic relief and different types of rock. The topography of some hills accounts for only part of the related magnetic anomalies. Igneous complexes produce most of the magnetic anomalies observed over hills such as Knob Lick; Buckner and Smith Mountains in the Fredericktown quadrangle (fig. 2a).

Evans, Matthews, Tin, and Crane Mountains are volcanic roof pendants ranging from thin plates to deep-rooted features. A combination of topography and magnetic contrast between volcanic and granitic rocks produces aeromagnetic anomalies associated with pendants.

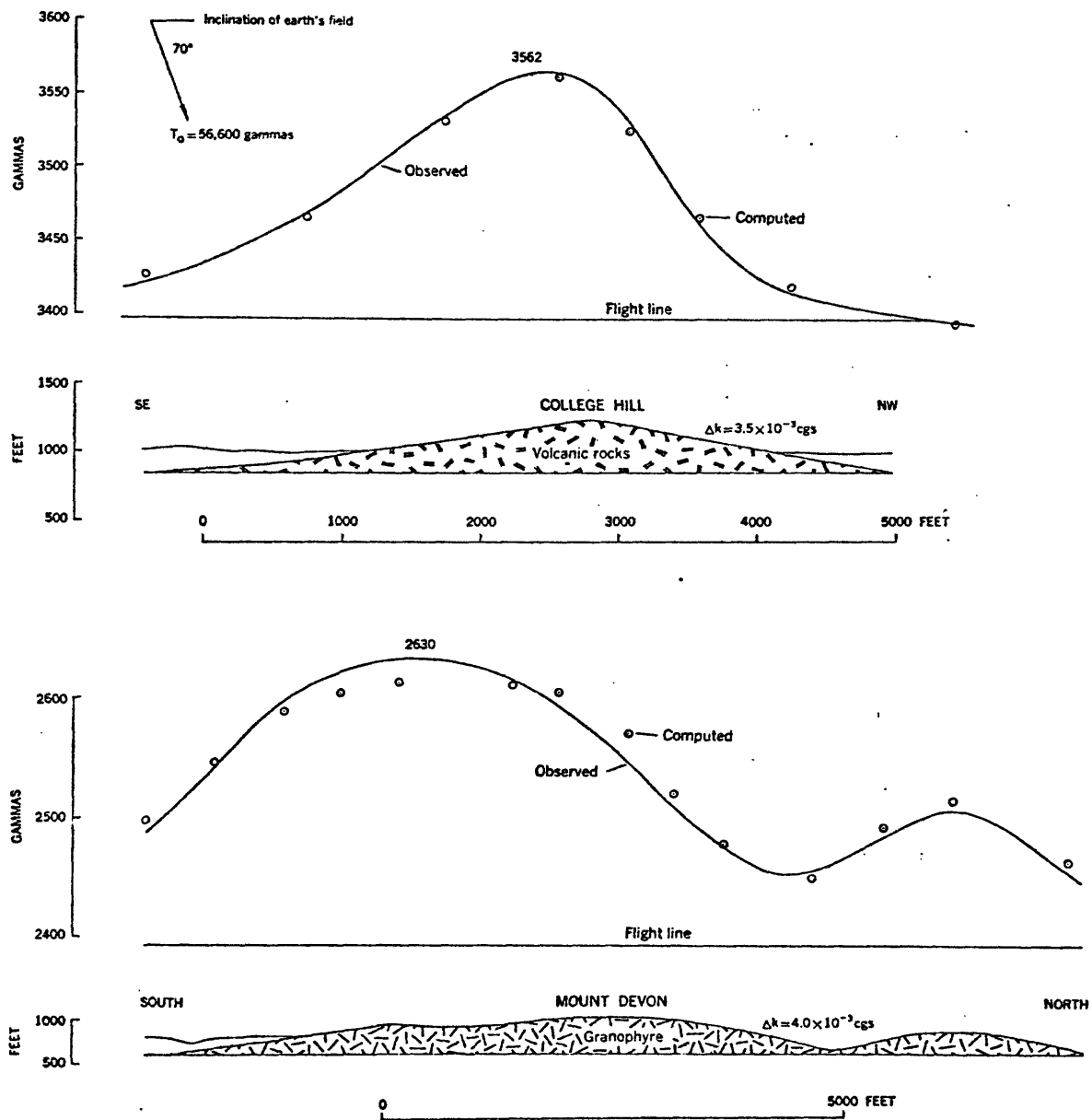


Figure 35.--Magnetic profiles computed from two-dimensional models showing the effect of topography.

Table 3. Correlation of Precambrian topography and low amplitude magnetic anomalies (Continued)

Copper mine Hill	Fredericktown	Sec. 6, T. 33N. R. 7E.	880	920	120	0.5x0.7	granophyre	50
Atien Hill	"	Sec. 29, T. 35N. R. 5E.	940	860	80+	0.5x0.6	granite	40
Buck Mountain	Trenton	Sec. 7, T. 34N. R. 5E.	1528	450	330	0.7x1.0	granophyre	140
Bread Tray Mountain	"	Sec. 1, T. 34N. R. 5E.	1425	450	225	0.7x1.5	granophyre	90
King Mountain	"	Sec. 2, T. 34N. R. 5E.	1427	450	225	0.8x1.3	granophyre	90
Liberty Hill	"	Sec. 30, T. 33N. R. 5E.	1405	475	400	0.8x1.5	ryolite	120
Red Hill	"	Secs. 26, 27, T. 33N. R. 4E.	1370	475	375	1x1.5	volcanic	260 +
College Hill	"	Secs. 5, 6, T. 33N. R. 4E.	1240	560	250+	0.4x0.8	volcanic	120
White Peak	"	Sec. 21, T. 33N. R. 4E.	1160	640	200	0.5x0.7	volcanic	90
Buck Mountain	"	Sec. 33, T. 34N. R. 3E.	1625	475	425	0.8x1	ryolite	175
East Charles Mountain	"	Sec. 28, T. 34N. R. 3E.	1665	475	365	0.7x1.2	volcanic	200
East Anderson Mountain	"	Secs. 22, 27, T. 34N. R. 4E.	1365	500	320	1 x 1	trachyte andesite	140
East Trilby Mountain	"	Sec. 10, T. 34N. R. 4E.	1436	475	335	0.7x1.2	volcanic	180

Table 3. Correlation of Precambrian topography and low amplitude magnetic anomalies

Name	Quadrangle	Location	Peak altitude	Depth in feet	Relief in feet	Dimensions in miles	Rock	Magnetic relief in gamma
Evans Mountain	Fredericktown	Sec. 34, T. 34N. R. 5E.	1222	580	400	1 x 2	Rhyolite	400
Blue Mountain	"	Sec. 16, T. 33N., R. 5E.	1380	500	480	0.8 x 1.5	volcanic	450
Murphy Hill	"	Secs. 15, 16, T. 34N. R. 5E.	1020	780	240	0.6 x 2	granophyre	250
Tin Oak Hill	"	Sec. 4, T. 33N. R. 7E.	880	920	100+	0.5 x 0.5	granophyre	120
Bald Hill	"	Sec. 30, T. 34N. R. 7E.	998	800	200'	0.6 x 0.6	granophyre	80
Catherine Knob	"	Sec. 6, T. 33N. R. 7E.	940	860	180'	0.6 x 0.6	granophyre	60
Bald Knob	"	Sec. 15, T. 33N. R. 5E.	1064	735	260	0.4 x 0.4	volcanic	60
Haskins Knob	"	Sec. 20, T. 33N. R. 6E.	1024	775	225	0.4 x 0.5	volcanic	60
Tin Mountain	"	Sec. 30, T. 33N. R. 6E.	1136	665	435	0.7 x 1.0	volcanic	280
Mount Devon	"	Sec. 23, T. 33N. R. 6E.	1107	700	410	1 x 1	granophyre	200
Stringtown Hill	"	Sec. 4, T. 33N. R. 7E.	820	980	40+	0.3 x 1	granophyre	45
Holliday Mountain	"	Sec. 4, T. 33N. R. 6E.	1090	710	290	0.4 x 0.8	granite	75
Pine Mountain	"	Sec. 19, T. 33N. R. 6E.	900	900	300	1 x 1	volcanic	60

101-2
101-2
101-2
101-2

Table Correlation of Precambrian topography and low amplitude magnetic anomalies (Continued)

East Middlebrook Hill	Ironton	Sec. 7, T. 34N. R. 4E.	1365	500	250	0.6x0.7	volcanic	80
Golf Mountain	"	Sec. 3, T. 34N. R. 4E.	1382	500	380	0.9x1.3	volcanic	190
Brown Mountain	"	Sec. 1, T. 34N. R. 4E.	1650	475	550	1.2x1.5	trachyte andesite	200 ⁺
Mark Hill	"	Sec. 30, T. 35N. R. 4E.	1190,	610	100+	0.3x0.4	granophyre	100
North Buford Mountain	"	Sec. 20, 21, T. 35N. R. 3E.	1609	475	400	1 x 1	trachyte	210
Sierras Mountain	Bonne Terre	Sec. 26, T. 36N. R. 4E.	1460	500	450	1x1.5	volcanic	150
Middle Mountain	"	Sec. 34, T. 36N. R. 4E.	1530	475	550	1 x 1	volcanic	170
West Mountain	"	Sec. 33, T. 36N. R. 4E.	1260	540	260	1 x 1	volcanic	80
North Biernack Hill	"	Sec. 30, T. 36N. R. 4E.	1120	680	120	0.3x1	granophyre	100
Butterton Hill	Des Arc	Sec. 3, T. 32N. R. 4E.	970	830	150	0.3x0.8	volcanic	150
Blue Hill	"	Sec. 11, T. 32N. R. 4E.	960	840	230	0.5x0.7	volcanic	200
North Jewett Hills	"	Sec. 32, T. 32N. R. 5E.	1000	800	300	0.8x1	volcanic	70
Lunk Hill	"	Sec. 1, T. 30N. R. 3E.	1100	700	400	1 x 1	rhylolite	120
Table Mountain	"	Sec. 13, T. 30N. R. 3E.	960	840	660	1.5x1.5	dallenite	380
							volcanic ridge	
							edge of gray basin	
							167b, 167c	167c

Table 3. Correlation of Precambrian topography and low amplitude magnetic anomalies (Continued).

Des Arc Hill	Des Arc	Sec. 8, T. 30N. R. 4E.	860	940	460	1 x 1	dellenite	200
Des Arc Mountain	w w	Sec. 21, T. 30N. R. 4E.	1367	500	770	1.3 x 1.6	dellenite	260
Middle Des Arc Mtn.	w w	Sec. 23, T. 30N. R. 4E.	1240	560	840	1.2 x 1.2	dellenite	330
Mudlick Mtn.	w w	Sec. 20, T. 30N. R. 5E.	1260	540	840	1.1 x 2	dellenite	220+
Reed Bend Hill	Goldwater	Sec. 34, T. 31N. R. 5E.	740	1060	250	0.5 x 0.5	volcanic	50
Cedar Knoll	w	Sec. 27, T. 31N. R. 6E.	810	990	210	0.6 x 0.7	volcanic	160
Buckhorn Hill	w	Sec. 32, T. 31N. R. 7E.	810	930	250	0.7 x 1	volcanic	100
Twelve Mile Hill	w	Sec. 2, T. 31N. R. 6E.	1090	710	390	0.8 x 1.5	volcanic	230
Little Grassy Mountain	South	Sec. 20, T. 32N. R. 6E.	1170	630	370	1 x 1	volcanic	185
Antioch Hill	w	Sec. 24, T. 32N. R. 6E.	1000	800	200	0.5 x 0.7	volcanic	220
Little Cedar Mountain	North	Sec. 9, T. 32N. R. 6E.	1161	640	300	0.7 x 1	rhyolite	350
Matthews Mountain	w	Sec. 2, T. 33N. R. 6E.	1140	475	500	1 x 1.2	rhyolite	450
Burns Mountain	w	Sec. 16, T. 32N. R. 7E.	1170	630	270	1 x 1	volcanic	275
Legion South	Higdon	Sec. 5, T. 33N. R. 8E.	1000	800	200	0.7 x 1.5	granophyre	75
Legion West	w	Sec. 36, T. 34N. R. 7E.	1140	660	330	1 x 1.5	granophyre	110
							p4	168

J. P. Fletcher

Taum Sauk, Hogan and Ketcherside Mountains in southwestern Ironton quadrangle are layered pyroclastic units, mainly ash-flow tuffs of low magnetic susceptibility. These pyroclastic rocks act as a magnetic window and do not produce topographic anomalies, whereas the more mafic diabase and gabbro underlying some volcanic flows produce the broad magnetic anomaly shown in Figure 2a.

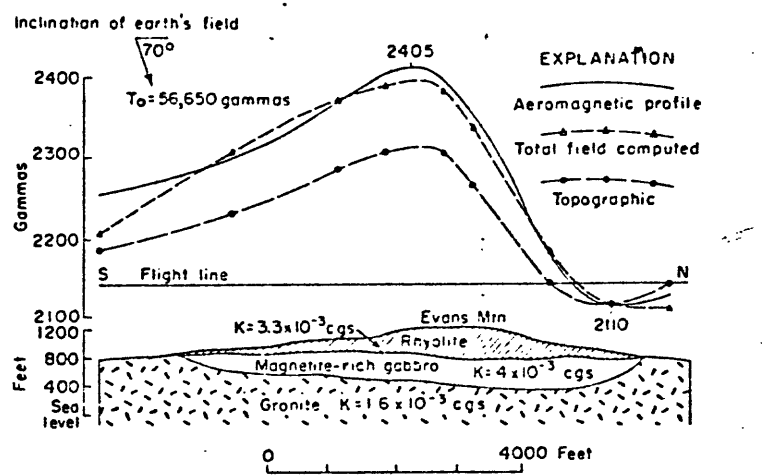


Figure 36.--The magnetic expression of a rhyolite hill and a gabbro sill on granite terrain at Evans Mountain.

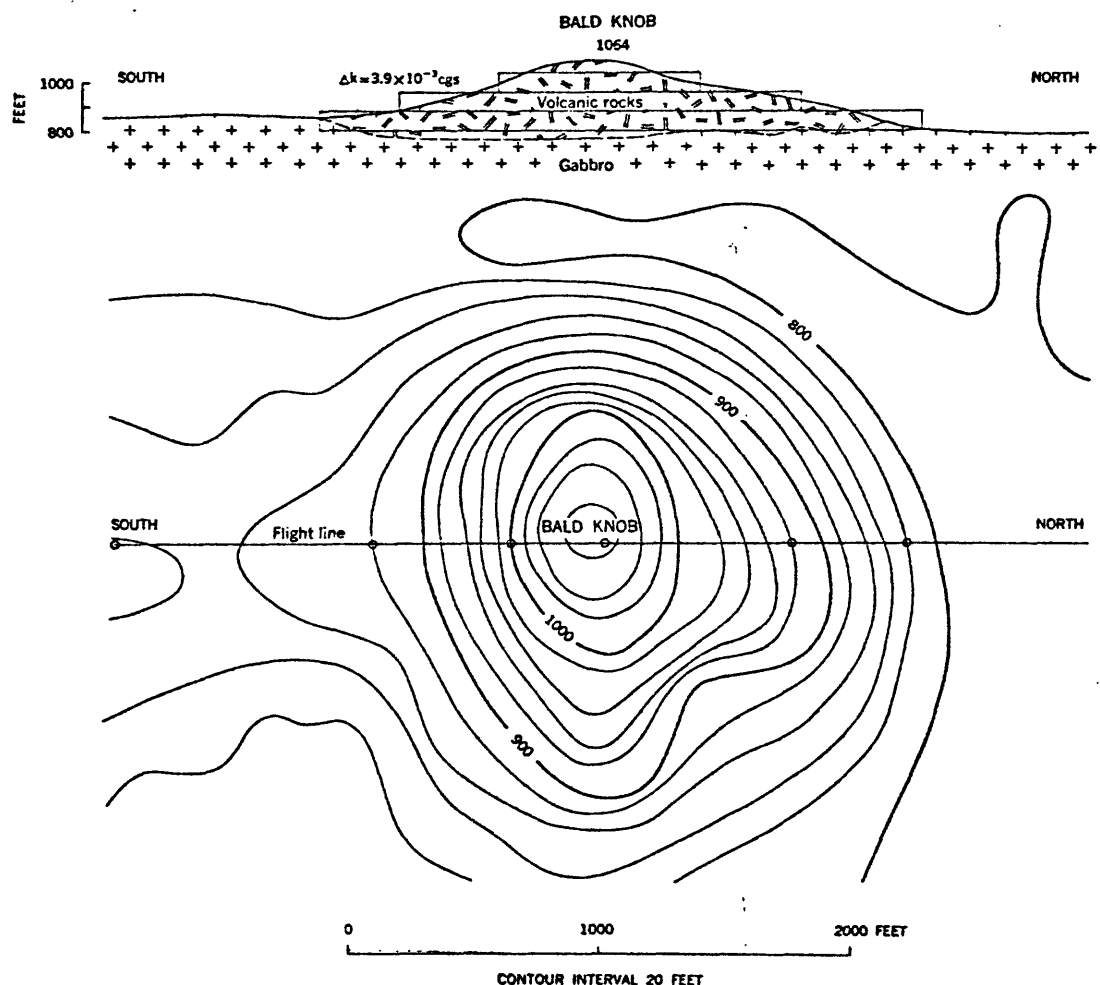
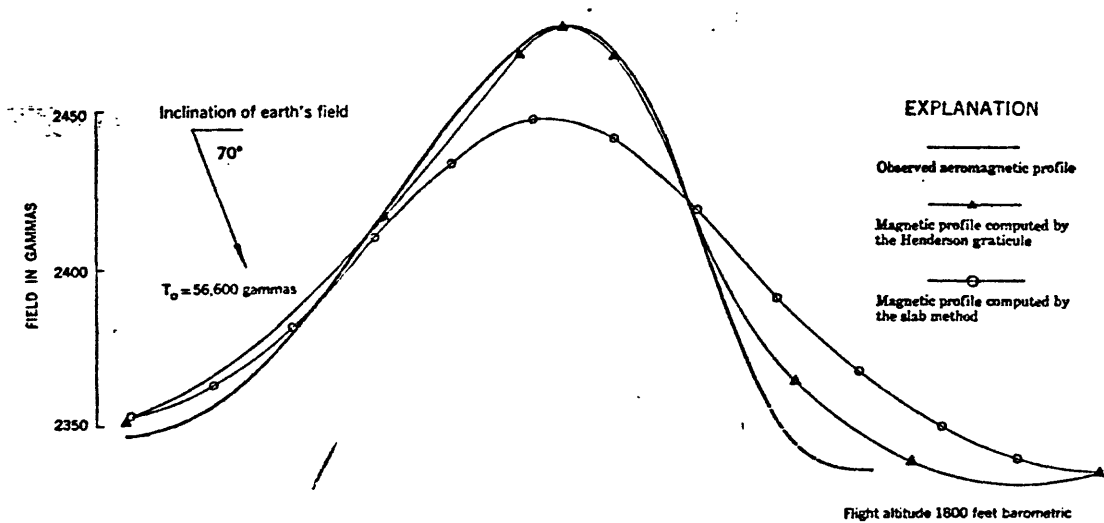


Figure 37.--The magnetic effect of volcanic rocks on gabbro terrain at Bald Knob.

The amplitude of the anomaly is about 140 gammas. Computations show that the hill of volcanic rock accounts for most of the aeromagnetic anomaly; thus, the pendant can extend only a short distance below the present surface of the gabbro. Although the volcanic rock increases in magnetite content near the gabbro contact, the model was treated as a homogeneous body and assigned an average susceptibility (3.9×10^{-3} emu/cm³) for computations. Numerical integration by the Henderson graticule gave the best approximation to the observed magnetic profile.

At Tin Mountain (Fig. 38) the structure of a volcanic roof

Figure 38 near here

pendant was obtained from aeromagnetic data. The gabbroic sill has about the same magnetic properties as the volcanic rocks.

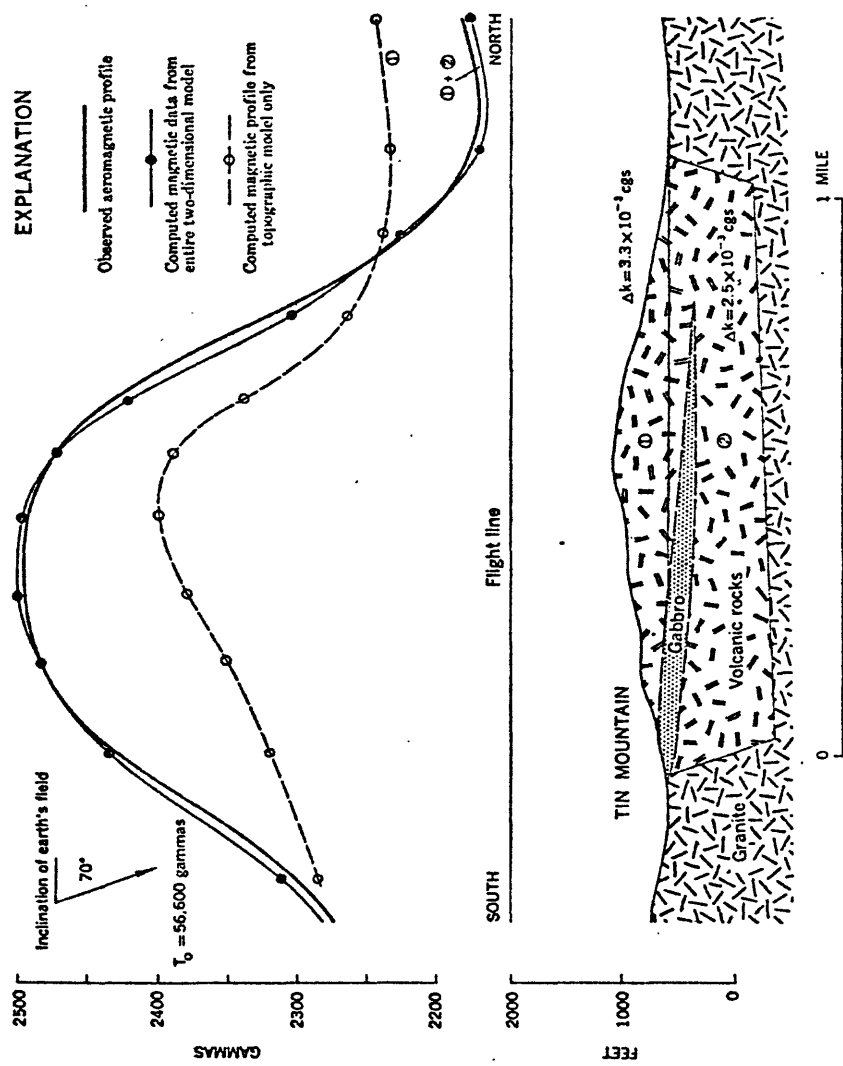


Figure 38.—Subsurface structure of a roof pendant at Tin Mountain from aeromagnetic data.

Topographic relief of the mountain (1) accounts for about 50 percent of the total anomaly. By adding a slab (2) to the model, equivalent to 1000 feet of volcanic rock, the computed data match the observed magnetic profile; therefore it seems that the combined effect of topography and lithologic contrast may have produced the anomaly.

The roots of some pendants of volcanic rocks extend into the roof of the enclosing granite host. At Crane Mountain, the volcanic rocks comprise a mixed sequence of rhyolite, trachyte, and andesite flows and tuffs that contain small veins of magnetite. The rock has high susceptibility because of disseminated magnetite. If the amount of vein magnetite is assumed to be small, the model extends to about 3,000 feet below the surface of the ground (Figure 39). A shallow-roofed model suggests near-surface iron deposits and an associated sharp, high-amplitude anomaly.

In section, roof pendants in the exposed Precambrian core of the St. Francois Mountains do not confirm the common concept of being thick or deep-rooted geologic features. According to model studies, most of the pendants are thin or shallow isolated features, a contribution to structural geology.

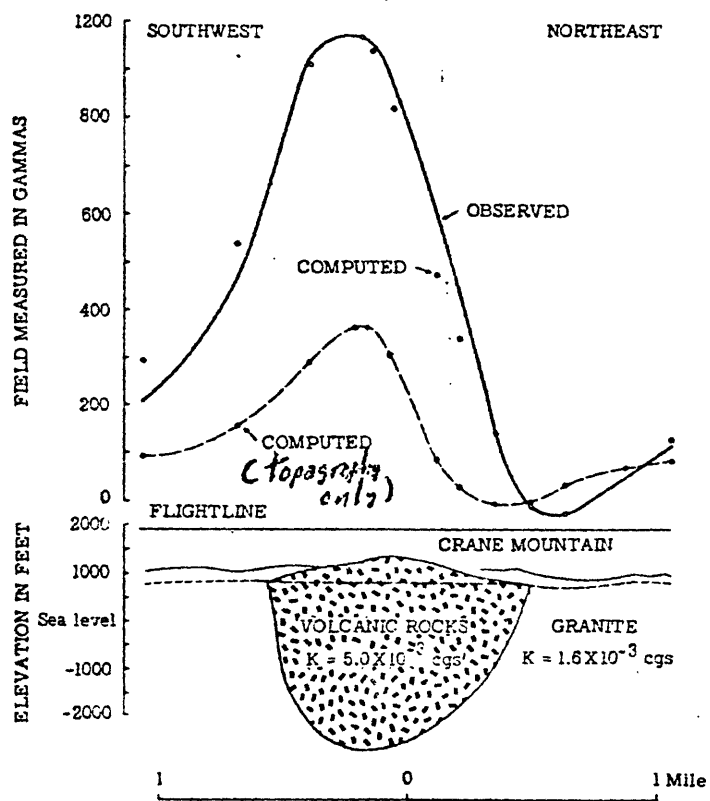


Figure 39 --Magnetic profiles showing the effect of topography and deep-rooted subsurface structure of volcanic rocks at Crane Mountain.

Faults and basins

Brown (1958, p. 7) believes that faults and related fractures served as major channelways for the upward migration of ore-bearing fluids; thus, recognition of faulting from patterns of magnetic anomalies should be useful in mineral exploration. Generally the anomalies observed over known faults are small. Major fault zones containing altered magnetic minerals can be detected from a series of closed lows on contour maps, by inflections, or by lows in magnetic profiles. Interpretation of aeromagnetic data is facilitated by comparison with characteristic profiles across models of faults.

Two types of faults or their combination are observed: (1) strike-slip or shear such as the fault in Barren Hollow Creek (T. 33 N., R. 5E), and normal or gravity such as the Simms Mountain system, Big River fault zone, St. Genevieve fault complex, etc. The diagrammatic section (Fig. 39a) showing fault blocks in the St.

Figure 39a near here

Genevieve system illustrates the type magnetic anomaly associated with different rock sequences. The vertical displacement ranges from 250 ft to 1200 ft and is commonly distributed among several parallel faults of the fractured complex (Weller and St. Clair, 1928, p. 256).

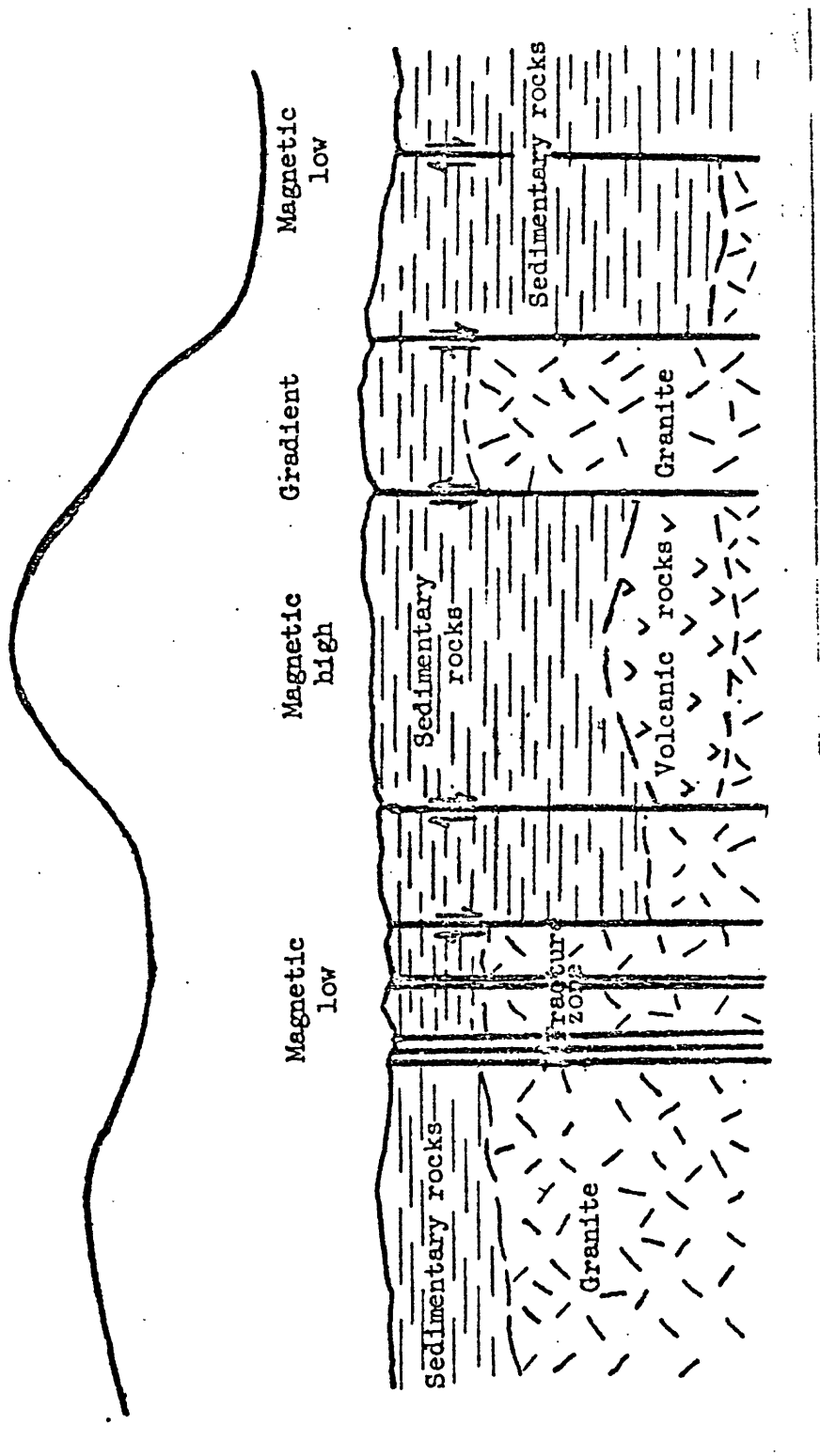


Figure 39 a.—Diagrammatic section showing aeromagnetic anomalies over the complex St. Genevieve fault zone.

The Big River fault zone (D) and the Simms Mountain fault zone (E) (Figs. 31 and 40) bound the main lead-producing area. These major fault

Figure 40 near here

zones contain leached, silicified, or oxidized rock of negligible magnetic susceptibility where the magnetic minerals have altered to nonmagnetic assemblages. The narrow fault of small displacement near Mitchell knob produces a small dip in the magnetic profile. The shallow, granite-floored Leadwood basin produces a broad low-amplitude anomaly. The Big River fault zone contains a relatively wide zone of nonmagnetic rock flanked by magnetic volcanic rocks. The large susceptibility contrast produces a magnetic low.

The Simms Mountain fault zone has vertical displacements as much as 600 ft and is an example of combined shearing and normal faulting in granite (Fig. 41). The volcanic pendant of Simms Mountain produces

Figure 41 near here

the observed anomaly; however, the combined effect of the nonmagnetic fault zone and vertical displacement in the granite broadens the low in the magnetic profile. The magnetic contribution of sheared rock is very low or comparable to the Irondale branch of the Simms Mountain fault system near Irondale (Figs. 31 and 40).

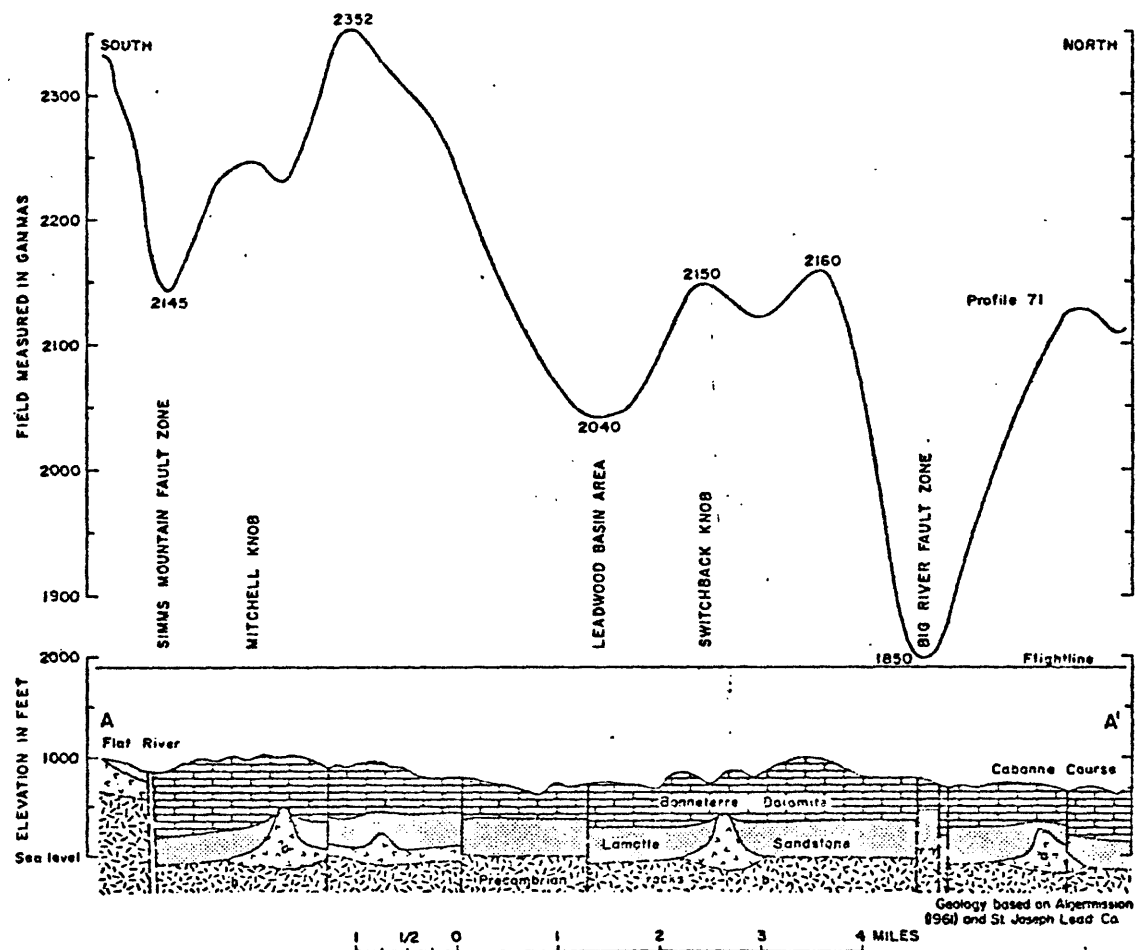


Figure 40.--Aeromagnetic profile from Flat River to Cabanne Course, showing the effect of basement topography and major fault zones.

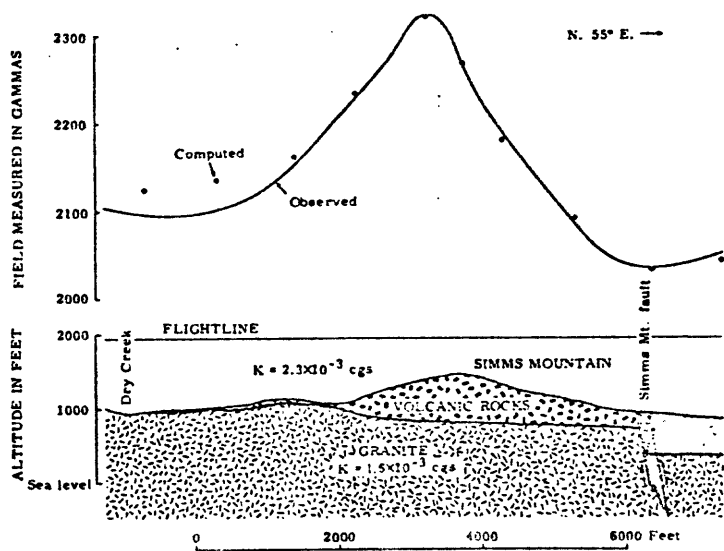


Figure 41.--Subsurface structure of the volcanic roof pendant and fault zone at Simms Mountain deduced from aeromagnetic data.

Graves (1938, p. 133) postulated a fault on the southwest flank of Buford Mountain. The most convincing evidence for a fault scarp in the Precambrian rocks is the alignment of volcanic ridges or nearly straight boundaries on the eastern side and zones of crushed or sheared granite near the contact with the sedimentary strata of the basin. The Ironton fault (Fig. 42), the name proposed by Graves for

Figure 42 near here

the Buford Mountain scarp, produces only part of the observed magnetic anomaly. The large susceptibility contrast between granophytic and sedimentary rocks produces the main magnetic gradient.

Several shallow intermontane basins, such as in Bellevue valley, Sabula area, Farmington area, and Swan Branch area, flank the St. Francois Mountains (Figs. 2a and 31). The elongate Bellevue valley is underlain by Cambrian strata, floored by granitic rocks and surrounded by volcanic ridges as represented by the model in (a) Figure 43.

Figure 43 near here

The distinctive magnetically flat pattern associated with granite clearly defines the boundaries of the basin. The magnetic pattern shows a gradient to the north and northwest. Interpretation of this pattern indicates that large blocks of granite are down-dropped and tilted. The present basins are now partly bounded by fault scarps.

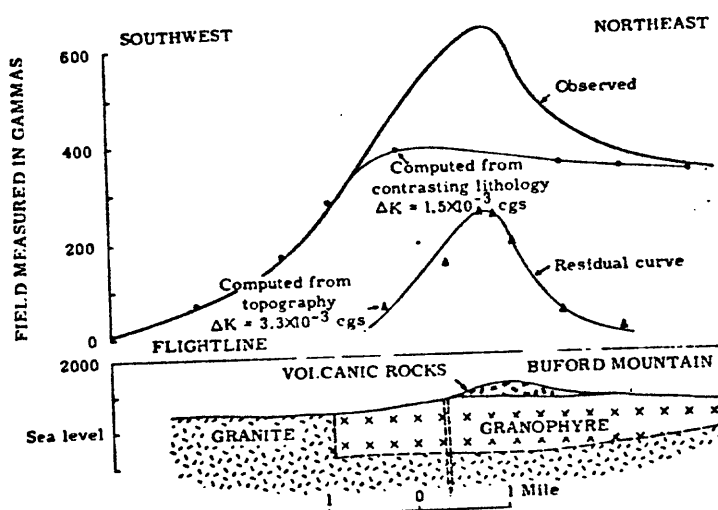


Figure 42.--Aeromagnetic profile over a ridge of trachyte and pyroclastic rocks at Buford Mountain.

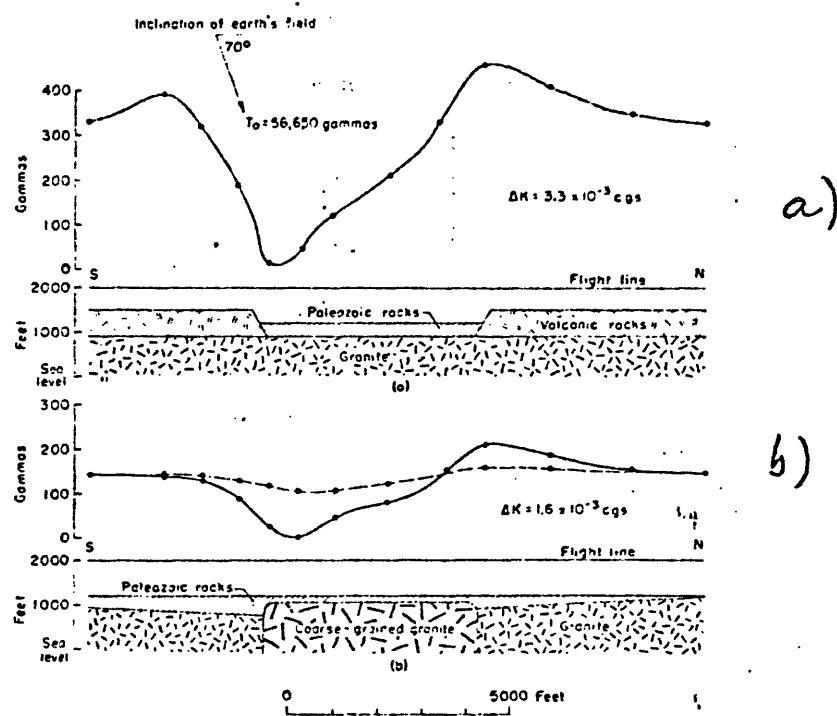


Figure 43.--Computed magnetic profiles over models of representing (a) the shallow Bellevue basin and (b) the Farmington anticline.

According to the magnetic gradient, the vertically faulted contact between the coarse-grained granite and the granite porphyry (granophytic) is west of Buford Mountain and beneath the valley strata. (fig. 42) The coarsely crystalline granite has a weak remanent component opposite to the present geomagnetic field. The magnetic contrast between the granitic rocks together with this remanent component cause the magnetic low associated with the shallow Bellevue basin. A similar magnetic pattern is observed over the Farmington area (figs. 2a, 31 and 43). The magnetic contrast between two types of granitic rock as shown by the models in Figure 43, (b) rather than contrast between Cambrian strata and granite (a) is believed to produce this anomaly. East of the Castor River (Liberty area), a large eastward-trending magnetic low reflects a sand-filled basin according to drilling information (Robert Uhley, written communication, 1960). The sand pinch-out line was determined from this magnetic and drill data, and a favorable area for mineral exploration was outlined.

Granite underlying the Bellevue Valley, Sabula area, Farmington area, Swan Branch area, and Indian Creek basin area may also represent high-level intrusions or cupolas. Erosion partly exposed this broad area of silica-rich granite of low magnetic susceptibility.

Relations to mineral deposits

Large concentrations of magnetite are sources of several high-amplitude aeromagnetic anomalies in southeastern Missouri. The relations between the 3000-gamma anomaly and the magnetite deposit at Pea Ridge was studied (Fig. 44) and similar analyses applied to other high-amplitude anomalies as potential iron deposits.

Ground magnetic surveys have been used as a guide in developing ore bodies and revealing the presence of buried knobs (Powers and others, 1953). Scharon (1952) recognized that airborne magnetic surveys also show a correlation with buried igneous knobs and ridges associated with lead deposits in the Fredericktown area.

Aeromagnetic anomalies are indirectly related to structures that localize lead deposits in carbonate strata. Hills and ridges cause low-amplitude anomalies. This topographic relief controlled sedimentary structures such as reefs, breccias, lagoonal muds and solution features that localized galena. Faults in the basement, postulated as channelways for ore-bearing fluids, cause low-amplitude anomalies.

Iron deposits

Precambrian iron deposits occur as fissure filling and replacement veins in the form of hematite, magnetite, and martite according to Hayes (1959b). The magnetite ore bodies at Pea Ridge (Snyder and Wagner, 1961, p. 92) and at Iron Mountain (Murphy and Mejia, 1961, p. 132) are cut by mafic dikes; thus iron mineralization is Precambrian in age. Because of the magnetic and high density, properties of the minerals, magnetic and gravity surveys have been used to look for deposits in southeastern Missouri. Two iron deposits in the Bourbon-Sullivan-Pea Ridge area were disclosed by an aeromagnetic survey made by the U. S. Geological Survey in 1948 (Eng. Min. Jour., 1958). A gravity survey of the same area by Gregson (1958) indicated a northwest-trending Precambrian ridge that appeared to be associated with these iron deposits (high density contrast).

Ore bodies at Pea Ridge, Iron Mountain and Pilot Knob were truncated by the Precambrian erosion that produced basal conglomerates of hematite boulders. The Ozark Ore Company used the gravity method to locate a conglomerate ore body near Pilot Knob (John E. Murphy, oral communication). In this study the aeromagnetic method was applied to three areas, Pea Ridge, Cottoner Mountain, and Kratz Spring (Sullivan area).

Pea Ridge anomaly

An aeromagnetic survey by the U. S. Geological Survey of the Sullivan quadrangle (Dempsey and Meuschke, 1951) resulted in the discovery of the large iron deposit at Pea Ridge. Drilling by the St. Joseph Lead Company intersected a magnetite ore body.

The aeromagnetic anomaly observed over the magnetite deposit at Pea Ridge is shown in Figure 44. The depth to the top of the deposit

Figure 44 near here

from the plane of observation, (1800 ft. altitude) was estimated by the method of Vacquier and others (1951) to be 2200 ft. A second- vertical derivative map (Figure 45) gives about 2000 ft. The depth

Figure 45 near here

below ground surface to the magnetic source in the Precambrian base- ment is 1400 ft., which corresponds to the depth from drilling (Eng. Min. Jour., 1958). The Pea Ridge deposit is a tabular body about 200-300 ft wide, over 2000 ft long, and dipping steeply northward. It extends from 1400 ft to more than 3000 ft in depth (Beveridge, 1958a, b).

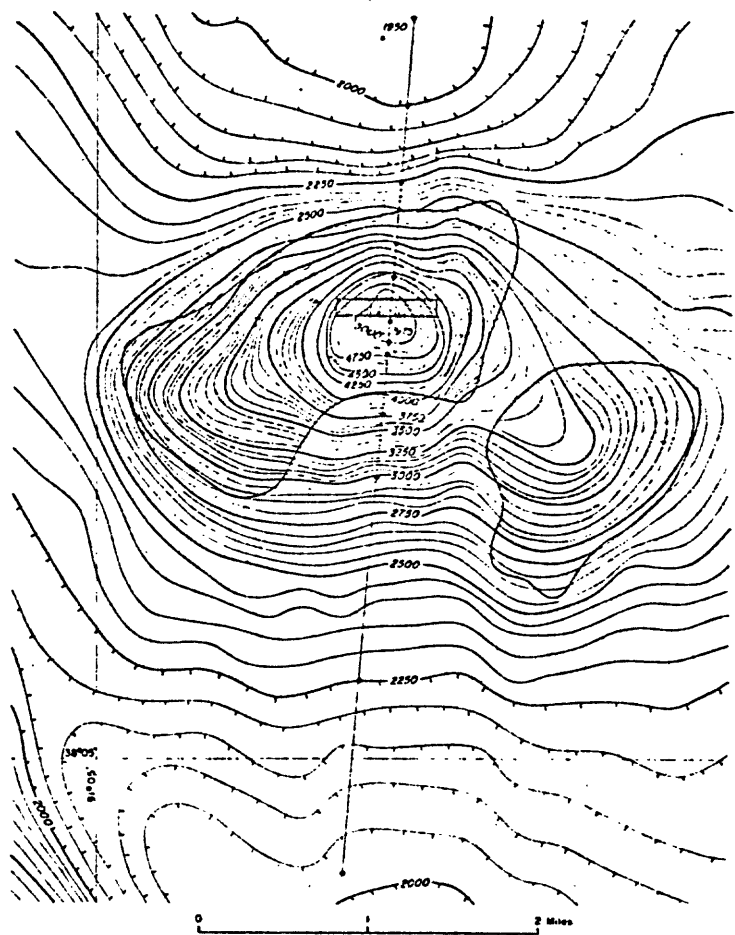


Figure 44.--The high aeromagnetic anomaly at Pea Ridge, Missouri, caused by a large magnetite-rich iron deposit.

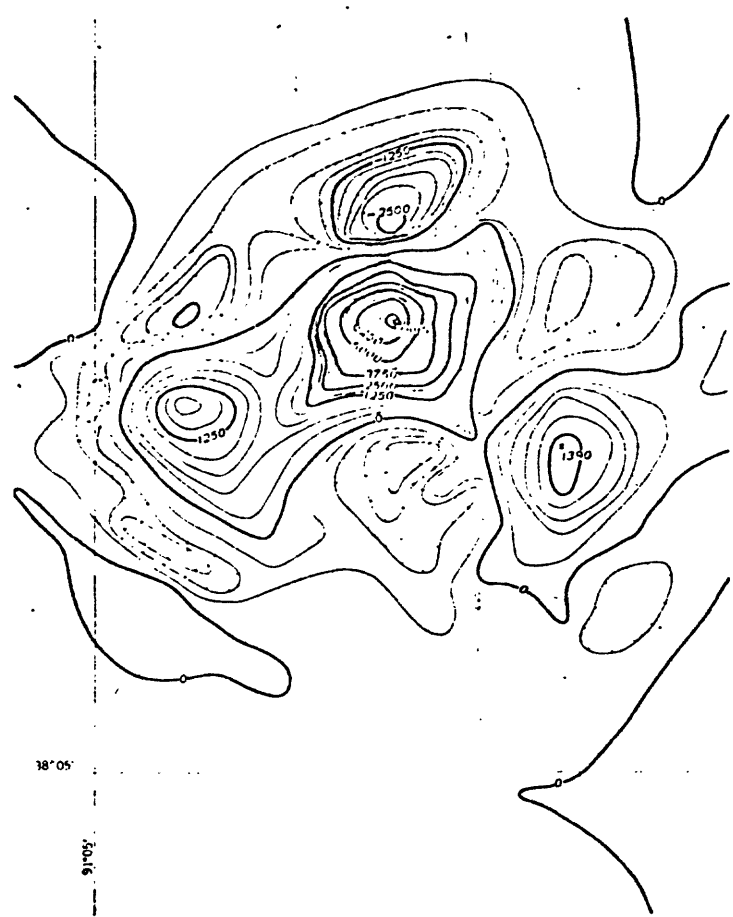


Figure 45.--Second-vertical derivative of the Pea Ridge anomaly at 1/2-mile spacing suggesting an arcuate deposit.

The 2400-gamma contour, which connects the Pea Ridge anomaly with the broad anomaly associated with volcanic rocks, suggests that the anomaly consists of two parts: a volcanic plug or stock-like body of intrusive felsite, and the iron ore body, (figs. 2a and 44). An approximation to volcanic plug was made by connecting the 3100-gamma contour on the south side of the anomaly with the 2200-gamma contour on the north side. The zero contour of second-vertical derivative map (Fig. 45) outlines the volcanic rocks and, in detail, suggests an east-west iron deposit. By selecting a wider spacing for the derivative map (Fig. 46),

Figure 46 near here

the interpreter postulated an arcuate sheet-like magnetite deposit. The remanent magnetization was assumed to be in the direction of the earth's field, because of the normal shape of the magnetic anomaly. A sheet-like body extending to great depth (infinity) and at least 2 depth units in length was used to simulate the ore body and accounts for 85 percent of the observed anomaly (Fig. 47). A cylindrical model

Figure 47 near here

would give comparable results.

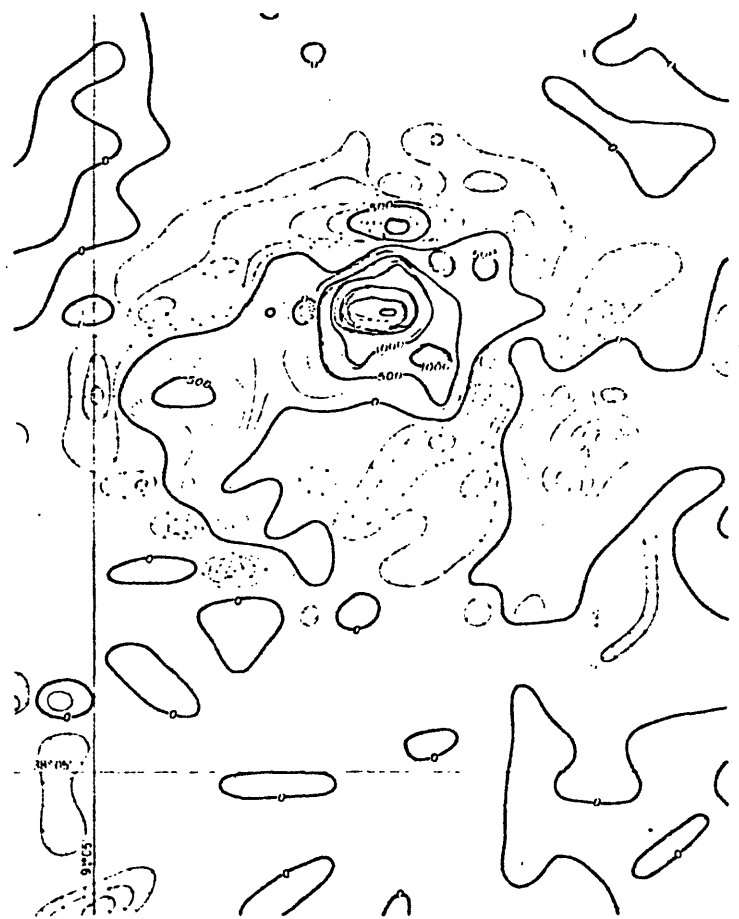


Figure 46.—Second-vertical derivative of the Pea Ridge anomaly at 1/4-mile spacing suggesting a linear deposit.

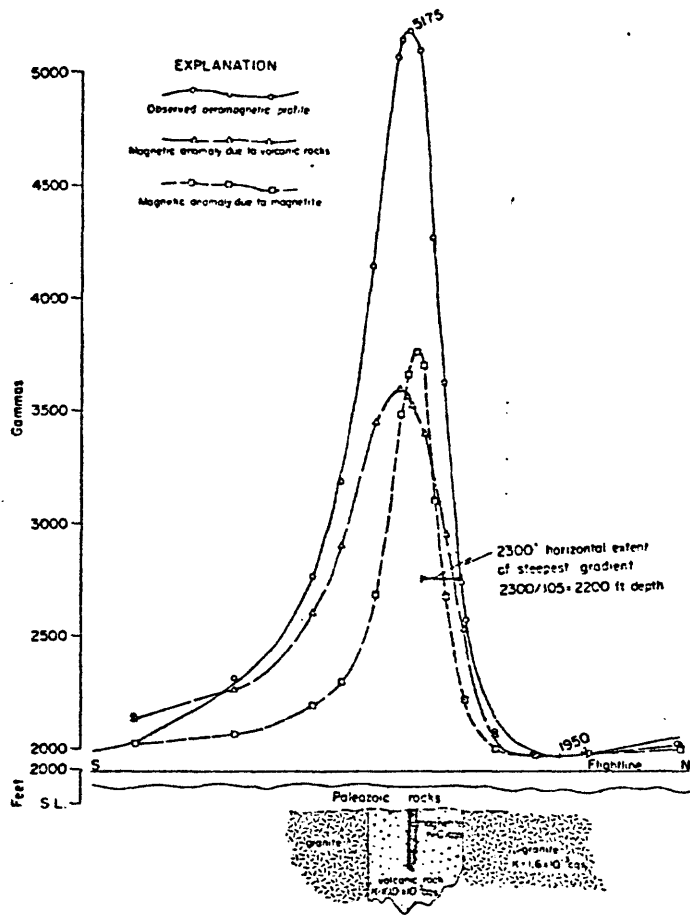


Figure 47.--Magnetic anomalies caused by volcanic rocks and magnetite body at Pea Ridge.

Susceptibility measurements (Fig. 48) were made of intrusive

Figure 48 near here

rhyolite porphyry from the drilling of the Bourbon magnetic anomaly (McMillan, 1946). A susceptibility of about 11×10^{-3} emu/cm³ was estimated for the magnetite-rich volcanic rock. The magnetization of the host rock was computed from this value. The structural control interpreted from the aeromagnetic information was to be a magnetite-filled shear zone in a plug of hypabyssal rock, probably identified as porphyry.

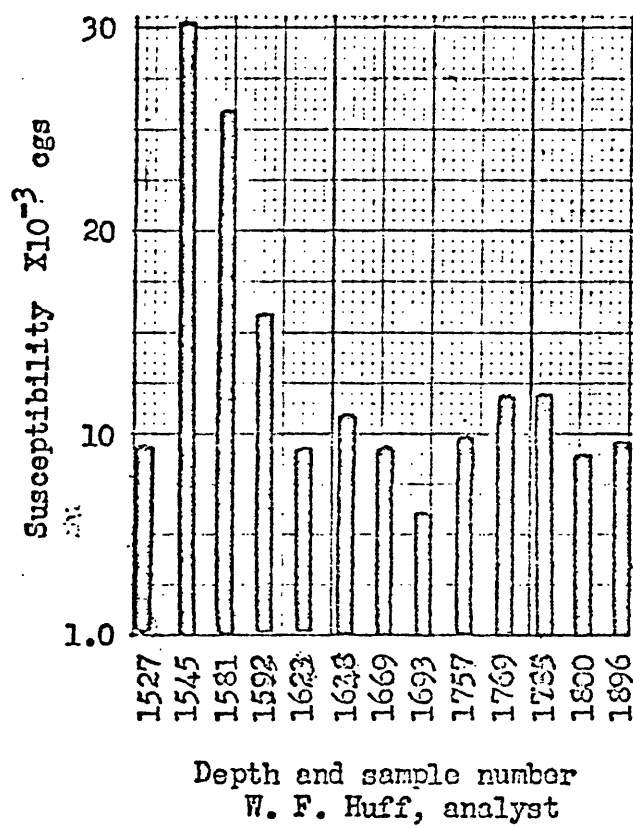


Figure 48.--Susceptibility measurements of rhyolite cored from the U.S. Bureau of Mines drill hole (BN-1) near Bourbon.

Cottoner Mountain anomaly

A high-amplitude anomaly was observed over the east flank of Cottoner Mountain about 3 miles northwest of Marquand (figs. 2a and 49). Like

Figure 49 near here

mineral zoning around a deposit, a rectangular prism of magnetite-rich volcanic rock sets in an elongate block of volcanic rock, the core of which is a potential iron deposit. Depths calculated to the magnetic rock indicate a near-surface deposit. The Starkey mine on the northeast side of Cottoner Mountain further corroborates this postulated mineral-bearing rock. The old prospect is on a steep magnetic gradient marking a change in lithology and a possible zone of fracture. The prospect is outside of the main magnetic unit and according to Grave (1945, p. 364-365) contains pyrite at the contact between Precambrian felsite and Cambrian dolomite. The magnetic rocks is controlled by a northwest-trending fracture system as inferred from the magnetic gradient on the southwest side of the anomaly (A-A, fig. 49).

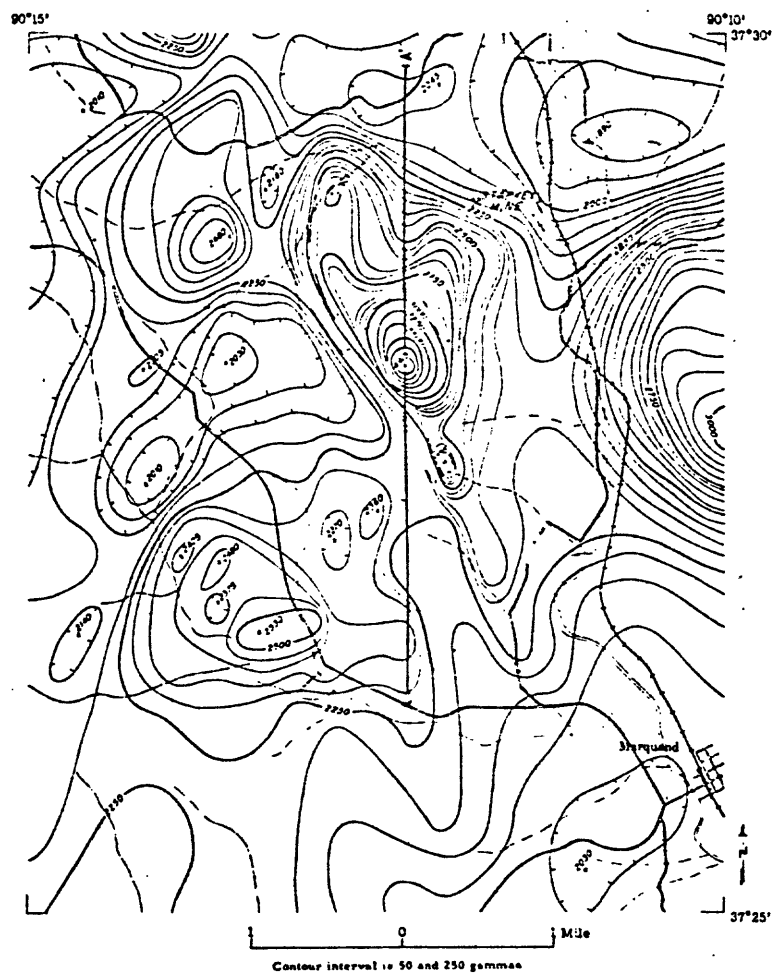


Figure 49.--The high-amplitude aeromagnetic anomaly at Cottoner Mountain near Marquand.

Northwest-trending fracture zones are shown by a series of lows (A-A') in a second-vertical derivative map of the magnetic field (Fig. 50). These alined lows seem to be partly offset by northeast-

Figure 50 near here

trending fractures as inferred from lows of the derivative map. The outline of the magnetic rock is also shown by the derivatives.

The southwest boundary of the magnetic unit probably is faulted as shown by the abrupt break in the observed profile (Fig. 51). The

Figure 51 near here

profile also suggests that a potential deposit could dip slightly northward. This deposit resembles the Canadian deposit at Marmora described by Bower (1960, p. 6 and 10). The Cottoner Mountain anomaly is believed to be a mineralized volcanic vent.



Figure 50.--Second-vertical derivative of the Mt. Cottoner anomaly near Marquand.

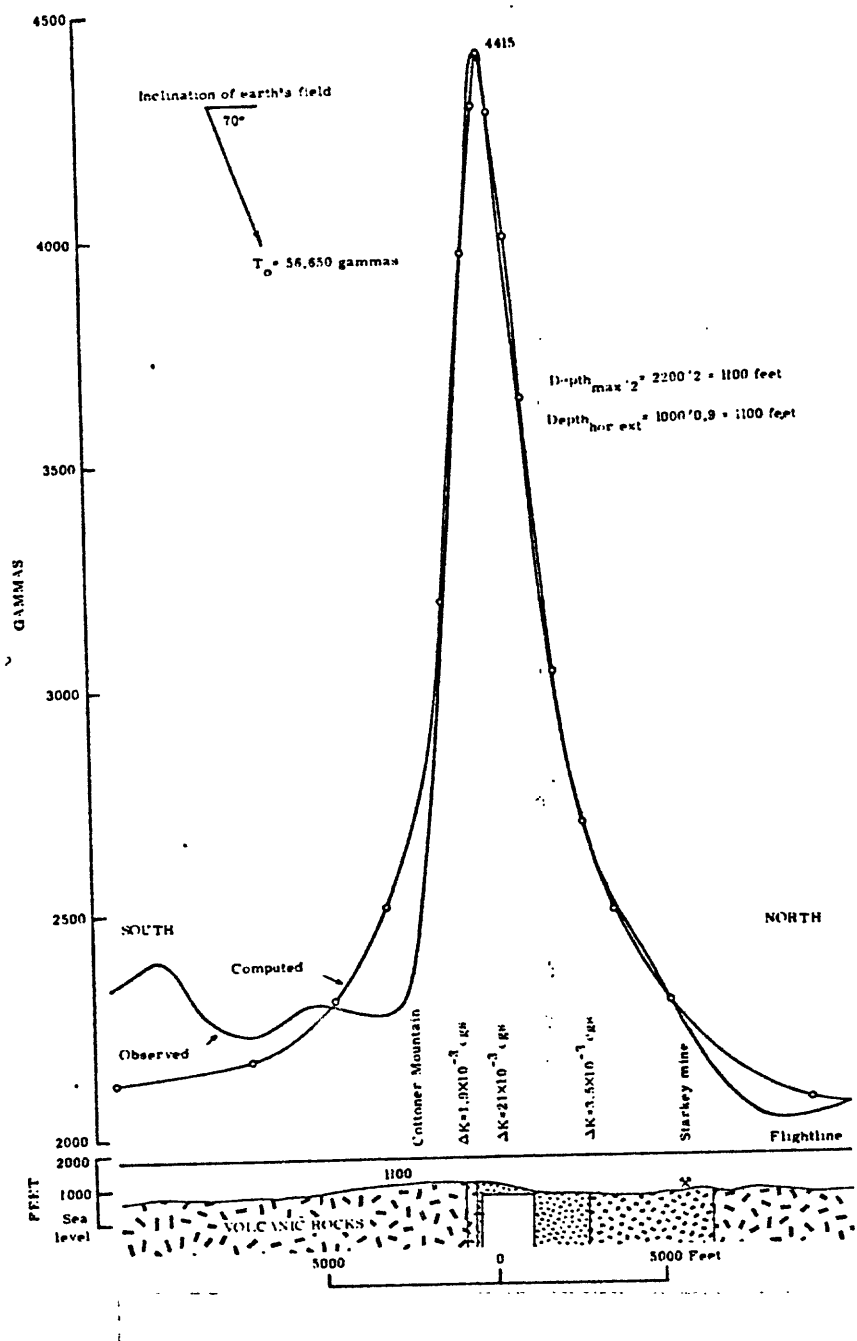


Figure 51.--Interpretation of a total-intensity aeromagnetic profile over a potential iron deposit at Cottontree Mountain.

Kratz Spring anomaly

Subsurface structure in the Sullivan-Bourbon area was investigated by Searight, Williams, and Hendricks (1954) in connection with ground magnetic surveys. The structure in this area consists of broad northwestward trending anticlines and synclines modified by minor series of faults, which trend northward. The trends of the magnetic highs that are associated with the basement rocks have no relation to these structures in the sedimentary strata.

The gravity survey of Gregson (1958) outlined the more dense, near-surface volcanic rocks in the vicinity of Sullivan and Bourbon. A drill hole penetrated rhyolite porphyry at a depth of 25 ft in the $NE_{\frac{1}{4}}$, $NW_{\frac{1}{4}}$, $NW_{\frac{1}{4}}$ of sec. 18, T. 40N, R. 2W (fig. 2a). From a few samples, Frank (1958) suggested that high thermoremanent magnetization (TRM) and high susceptibility for the Precambrian rocks in the Sullivan area represent about 5% magnetite.

A large aeromagnetic anomaly was observed near Kratz Spring School, about 4 miles northwest of Sullivan on the nose of a gravity gradient: there the volcanic rocks appear to plunge northward. The interpretation of this anomaly is shown in Figure 52. Thin deposits

Figure 52 near here

of sedimentary strata cover the magnetite-rich volcanic rocks. The main magnetic gradient (Line 17, Fig. 52) is produced by magnetic contrast across a sloping contact in the volcanic basement rocks. The 1500-gamma anomaly is believed to be caused by a nearly vertical magnetite deposit in the volcanic host rock. The postulated iron deposit seems to be controlled by east-west fractures and is elongate in this direction. The magnetite-bearing deposit dips northward.

Shepherd Mountain anomaly

Shepherd Mountain produces a high-amplitude anomaly northwest of Ironton. This magnetic feature is part of a large arcuate anomaly that connects, College Hill, Crane, Anderson, Oak and Charles Mountains. The arcuate anomaly surrounds Arcadia Valley, which like Bellevue basin, is believed to be floored by coarse-grained granite, is believed to which represent an eroded cupola of the batholith that intruded the volcanic rocks.

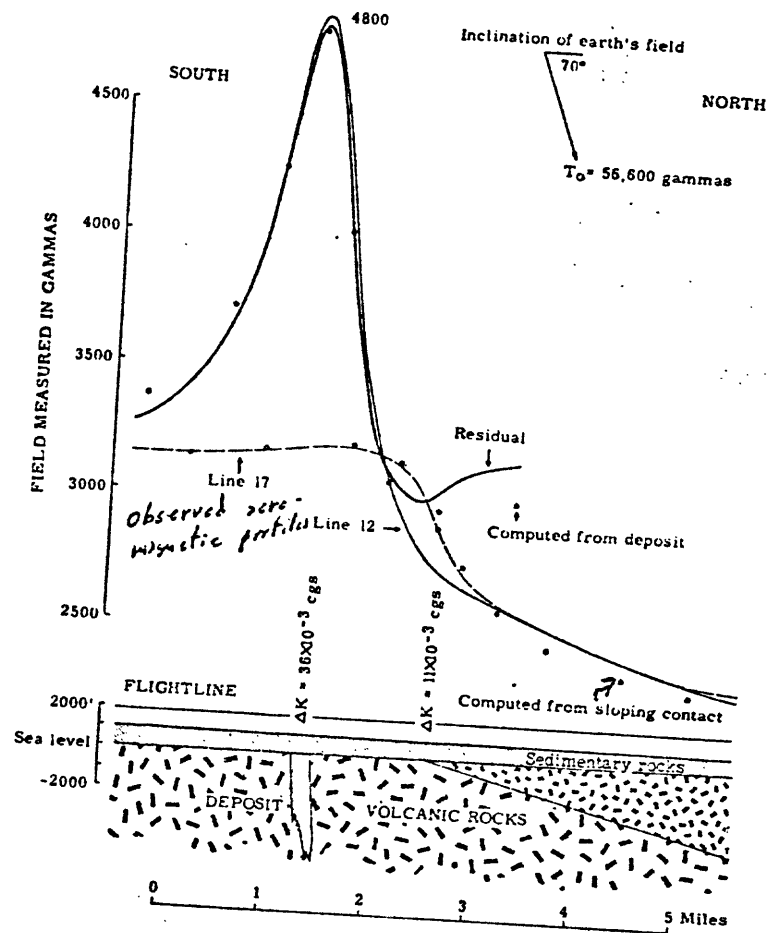


Figure 52.--The Kratz Spring aeromagnetic anomaly, Union quadrangle, that suggests a potential buried iron deposit.

202

(p. 202a follows)

A sheet of gabbroic rock, observed at the base of the hill, also indicates the proximity of the batholith's roof.

Susceptibility measurements of some volcanic rocks cored in the Ironton area indicate an average magnetic susceptibility of about 9×10^{-3} emu/cm³ (fig. 52a).

Figure 52a near here

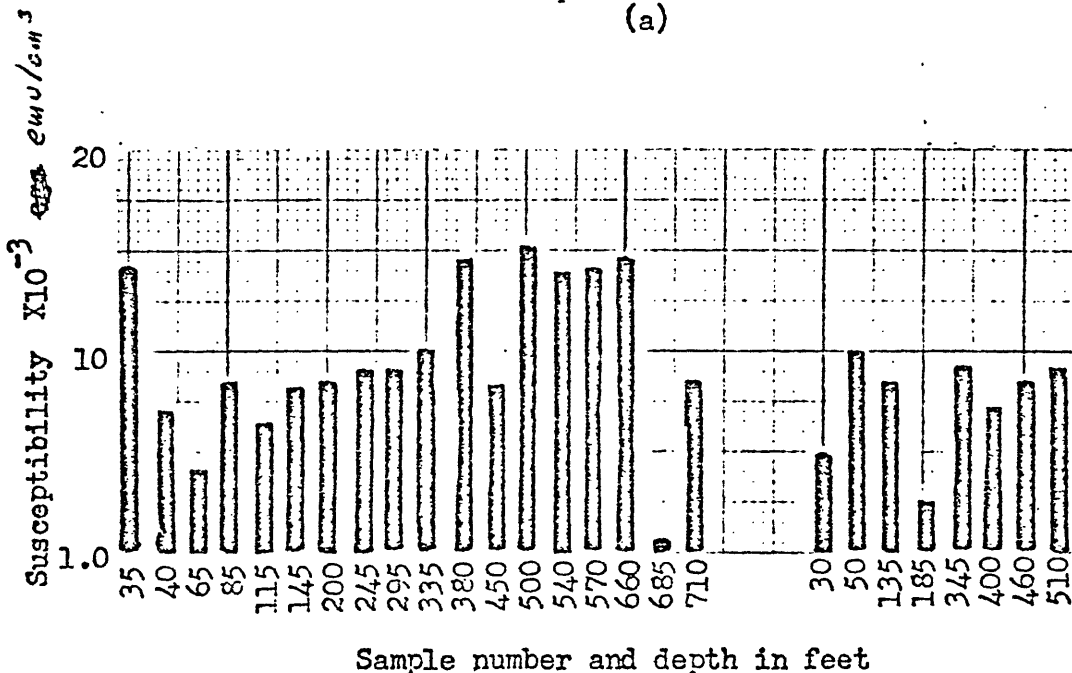
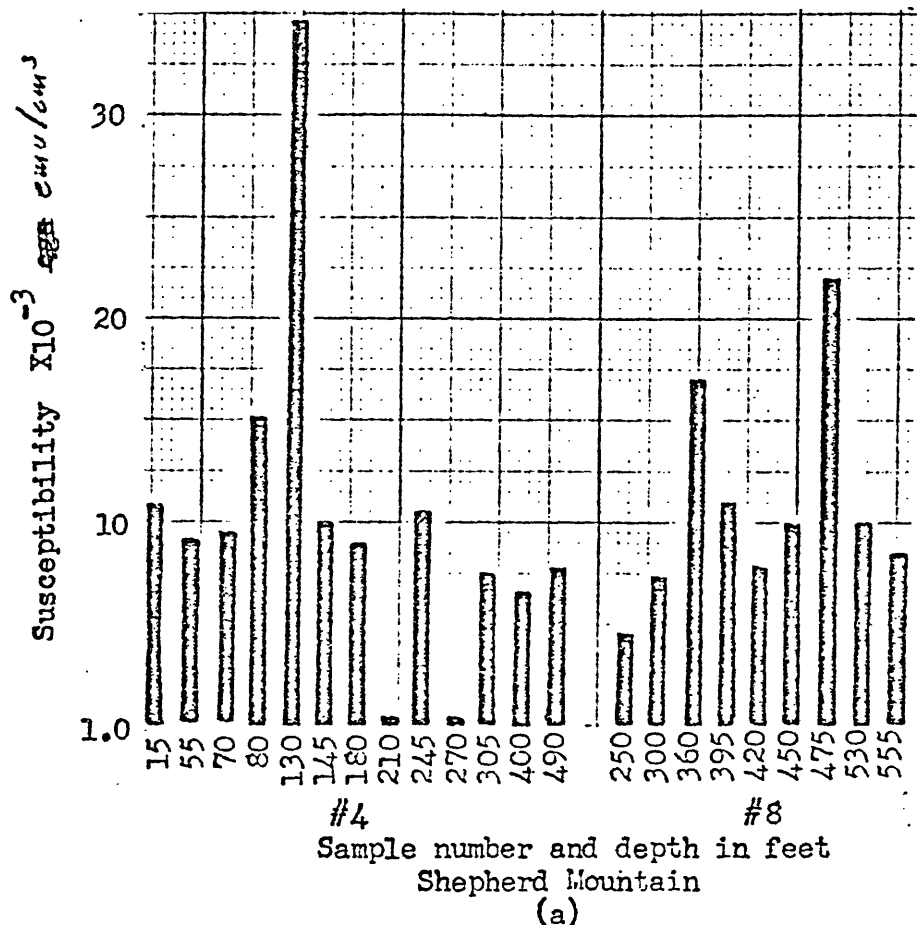


Figure 52-a Susceptibility measurements of rhyolite core from drill holes at Shepherd Mountain (a), Russell Mountain (b), and Anderson Mountain (c).

The magnetic rhyolitic and andesitic rocks of Shepherd Mountain contribute substantially to the observed anomaly; a large residual anomaly remains after deducting the magnetic effect of the volcanic rocks.

The remanent component of the volcanic rocks was

computed from the residual total intensity anomaly by using a rectangular model (Zietz and Andreasen, written commun.) for Shepherd Mountain. The mean direction of magnetism for these volcanic rocks is about N.20E. The dip is normally about the same as the present field.

Three open cuts expose northeast trending fissure veins of magnetite and specularite on the west and north slopes near the crest of the mountain (Crane, 1912, p. 121 and 132). About 75,000 tons of from specular iron ore was mined, three vertical fissure veins on Shepherd Mountain according to Crane (1912, p. 131-134). The veins contain a mixture of hematite and magnetite. The size of the veins ranging in width from 2 to 30 ft cannot account for the residual anomaly, which exceeds 1000 gammas in amplitude. A large buried deposit can be inferred from the residual The small magnetic contribution of Pilot Knob to the main anomaly seems to corroborate a hidden deposit on Shepherd Mountain.

The magnetic

partly mined
effect of two small veins in the rhyolite of nearby Cedar Hill also is negligible. Nason (1892, p. 307) reported a production of 25,000 tons of hematite ore from these veins.

204 (p 206 folio)

Two smaller anomalies were detected on a westward-trending spur of the arcuate magnetic anomalies. These two anomalies were observed over Russell and Vail Mountains between secs. 2 and 3 and in the $S\frac{1}{2}$ sec. 1, T.33N., R.3E. The anomalies are associated with concentrations of specularite and magnetite. About 3000 tons of iron ore was reported mined from a narrow east-west vein in the $SW\frac{1}{4}$ sec. 3, T.33N., R.3E., on Russell Mountain in the vicinity of the aeromagnetic anomaly (Crane, 1912, p. 137). Detailed ground magnetic and gravity surveys are needed to pinpoint the sources of these anomalies. Core from a drill hole at Vail Mountain contains specks and tiny veins of magnetite. The susceptibility of these samples ranges from 11.5×10^{-3} to 34×10^{-3} emu/cm³ and is similar to the results from Russell Mountain (Fig. 52a).

Iron Mountain anomaly

Iron Mountain is rhyolite porphyry a hill that rises 300 ft above the surrounding valleys. Mineralized andesite in the southwestern part of the hill contain the iron deposits, which were described by Murphy and Mejia (1961). These deposits, mainly hematite and 10-20% magnetite, are controlled by a dome-like collapse structure. The vertical part of the deposit accounts for the narrow anomaly, whereas the horizontal section contributes very little to the total-intensity field.

The aeromagnetic anomaly associated with the iron deposit is not as impressive as the Shepherd Mountain anomaly, although the data outlines an arcuate band of volcanic rock around a magnetic low over the valley similar to that at Ironton.

Lead and zinc deposits

The Bonne Terre quadrangle and adjacent areas were part of the extensive airborne surveys covering the lead mining region. The purpose of these surveys was to evaluate the aeromagnetic method as a rapid means of examining large areas for new deposits of lead. The success of surveys in exploration depended upon the association of these widespread deposits with sedimentary or structural features and topographic relief of the magnetic Precambrian basement rocks. In this study, various analytical techniques were applied to aeromagnetic data over mine workings in order to find the technique, which gave the best correlation and was, therefore, the most suitable method for exploration for lead deposits.

The area of the present investigation covers about 55 square miles of the main mining district (Fig. 2a) on the northern flank of the St. Francois Mountains. Parts of this study in the St. Francois Mountains (Allingham, 1958, 1960, and 1964) show that hills and ridges of the exposed Precambrian igneous rocks produce small magnetic anomalies having amplitudes of less than 200 gammas. The present phase of this study of the Bonneterre area indicates that the subsurface topography and structure of the basement rocks surrounding the Ozark uplift produce similar magnetic anomalies; thus these results are applicable to the entire mining region.

The complete system of automatic computation devised by Henderson (1960) was applied to total-intensity aeromagnetic data to continue the observed field downward towards its source, to calculate vertical derivatives of high resolving power, and to separate small residual anomalies. Computations were made by electronic digital computing equipment which enhanced this direct approach to interpretation by speedily processing the magnetic data. These computed anomalies permitted greater definition of basement topography and thereby extended the qualitative analysis of magnetic data.

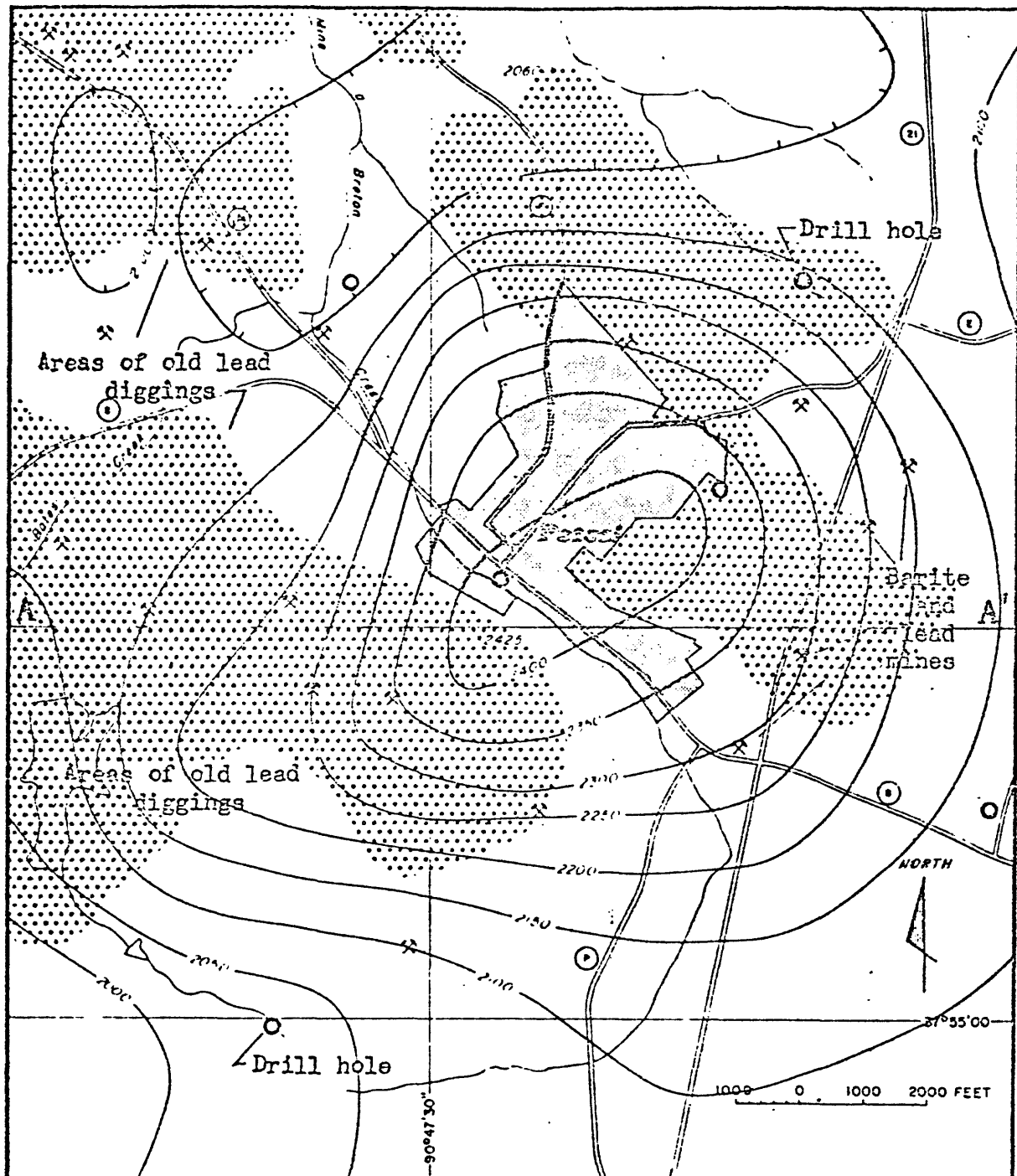
Potosi area

In the barite area of Washington County many joint-controlled deposits, classified as filled fissures and replacement veins, were mined for galena. Crystals of coarse-grained aggregates of galena fill these fissures. Many veinlets are paper thin but they are numerous over small areas, as shown by Dake (1930, p. 228, pl. 24). Ball (1916) and Winslow (1894, p. 678) give accounts of the joint-controlled and residual lead deposits in the Potosi, Palmer, and Richwoods areas. The shallow residual deposits are at the base of the residuum overlying the Potosi Dolomite.

The barite mines that surround Potosi, are the site of one of the oldest lead producing areas in the United States. Mine a Burton, which adjoins Potosi on the south was developed about 1779 according to Schoolcraft (1819, p. 19). From 1798 to 1816 about $\frac{1}{2}$ million pounds of metallic lead were smelted locally. Lead was mined from residual deposits in the clay and cherty residuum at the top of the Potosi Dolomite. The ore and residuum accumulated at the top of the dolomite as the carbonate strata weathered and dissolved away. Areas of lead and barite mine workings surround the town of Potosi (Fig. 53) and ring the broad aeromagnetic anomaly

Figure 53 near here

associated with buried Precambrian igneous rocks.



Drilling data from St. Joseph
Lead Co. and Dake (1930).

Figure 53.--Total-intensity aeromagnetic anomaly at Potosi showing the distribution of residual lead and barite deposits.

This simple isolated aeromagnetic anomaly associated with a mining area was studied using the direct method of interpretation suggested by Peters (1949). The system of Henderson (1960) was applied to the Potosi anomaly (Fig. 53) with encouraging results.

Subsurface structural relief on top of the Lamotte Sandstone is about 135 ft southwest of Potosi and decreases to 50 ft northeast of Potosi. The amplitude of the magnetic anomaly is about 350 gammas. Depth to the magnetic source determined by the method of Vacquier and others (1951) is about 1900 ft; basement is estimated to be about 100 ft below sea level. This value is within 10% of the depth estimated from the top of the Lamotte Sandstone, which is about sea level. The basement relief is unknown but would be greater than the 50-135 ft relief of the overlying sandstone. From model studies (Table 3), the volcanic rocks were estimated having as much as 300 ft of relief. The zero contour of the second- vertical derivative map (Fig. 54) outlines the inferred subcrop of volcanic rock which is

Figure 54 near here

believed to be the source of the magnetic anomaly. The dimensions of this anomaly, about 800 ft square, approximates a 4x5 prism in depth units according to the method of Vacquier. The average value of the horizontal extent of steepest gradient is between 1900 ft and 2000 ft. The writer will present evidence to support an interpretation of a volcanic roof pendant as the cause of the Potosi anomaly.

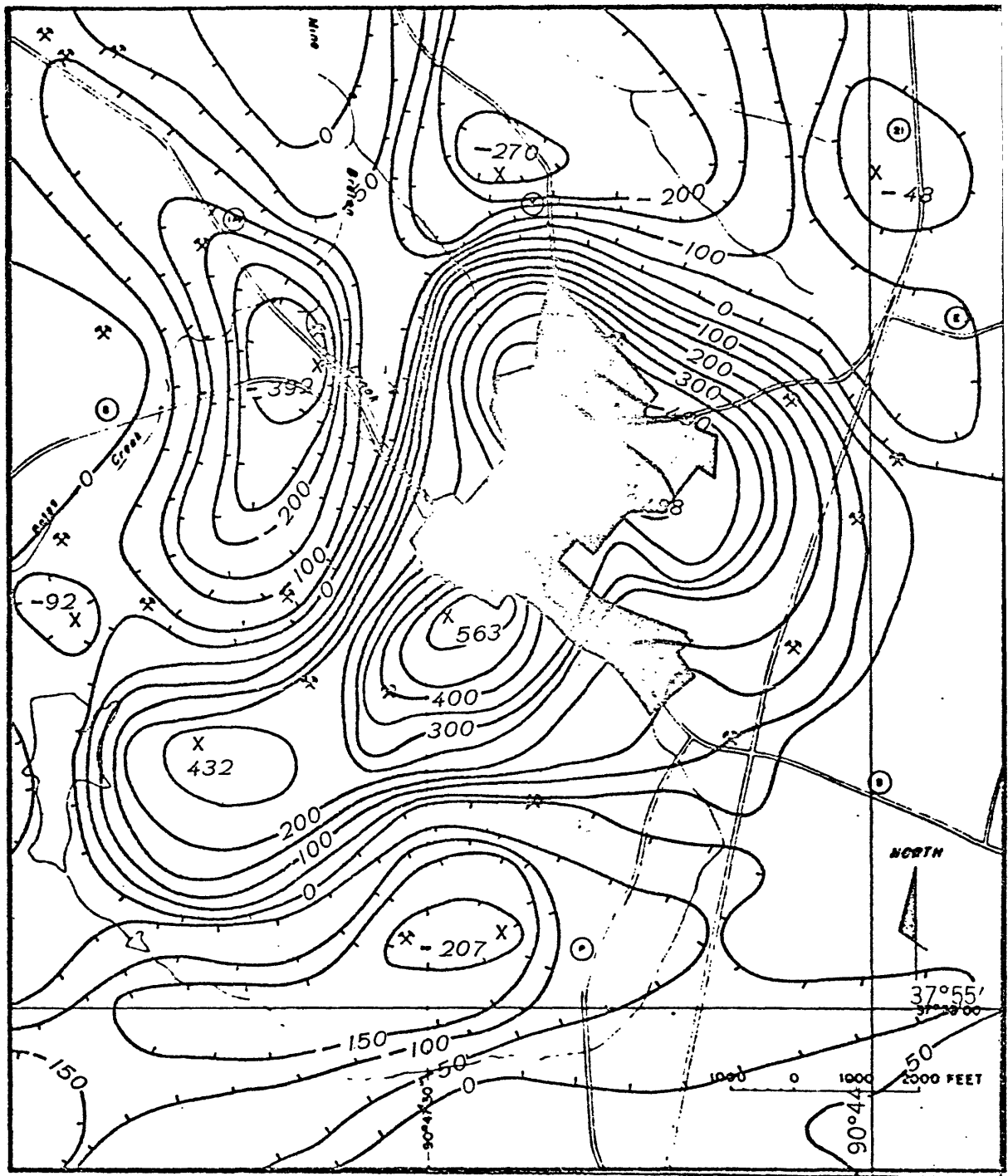


Figure 54.--Second-vertical derivative of the Potosi anomaly at 3,000-ft grid spacing showing the magnetic gradient that outlines the source rock.

Lead and barite deposits are compared with the observed anomaly (Fig. 53) and the derived magnetic data (Figs. 54-58). Comparison was first made with derivative maps having different grid spacings. In order to determine the optimum grid spacing, three different grids were selected for derivatives (Figs. 54-56). Spacing greater than the

Figures 54-56 near here

distance between the magnetometer and source rock (3000 ft) resulted in an intensified but poorly defined generalized anomaly. A smaller grid spacing (1000 ft) produced small closures of questionable value and a loss of definition in the original anomaly. Grid spacing equivalent to the depth to basement (2000 ft) produced a derivative map of high resolving power and good definition (Fig. 55). The boundaries of the source rock were clearly defined by the magnetic gradients. The anomaly separates into four highs (A,B,C,D, fig. 58).

Continuation of the field towards its source (Figs. 57 and 58) not

Figures 57 and 58 near here

only revealed the same features as the second-vertical derivative map but also improved the postulated of the subsurface rock distribution. The observed field was continued downward for three levels. The field continued down 1000 ft is equivalent to a ground survey. Continuation to this level steepened the gradients caused by the boundaries of the source rocks. (Fig. 59).

Figure 59 near here

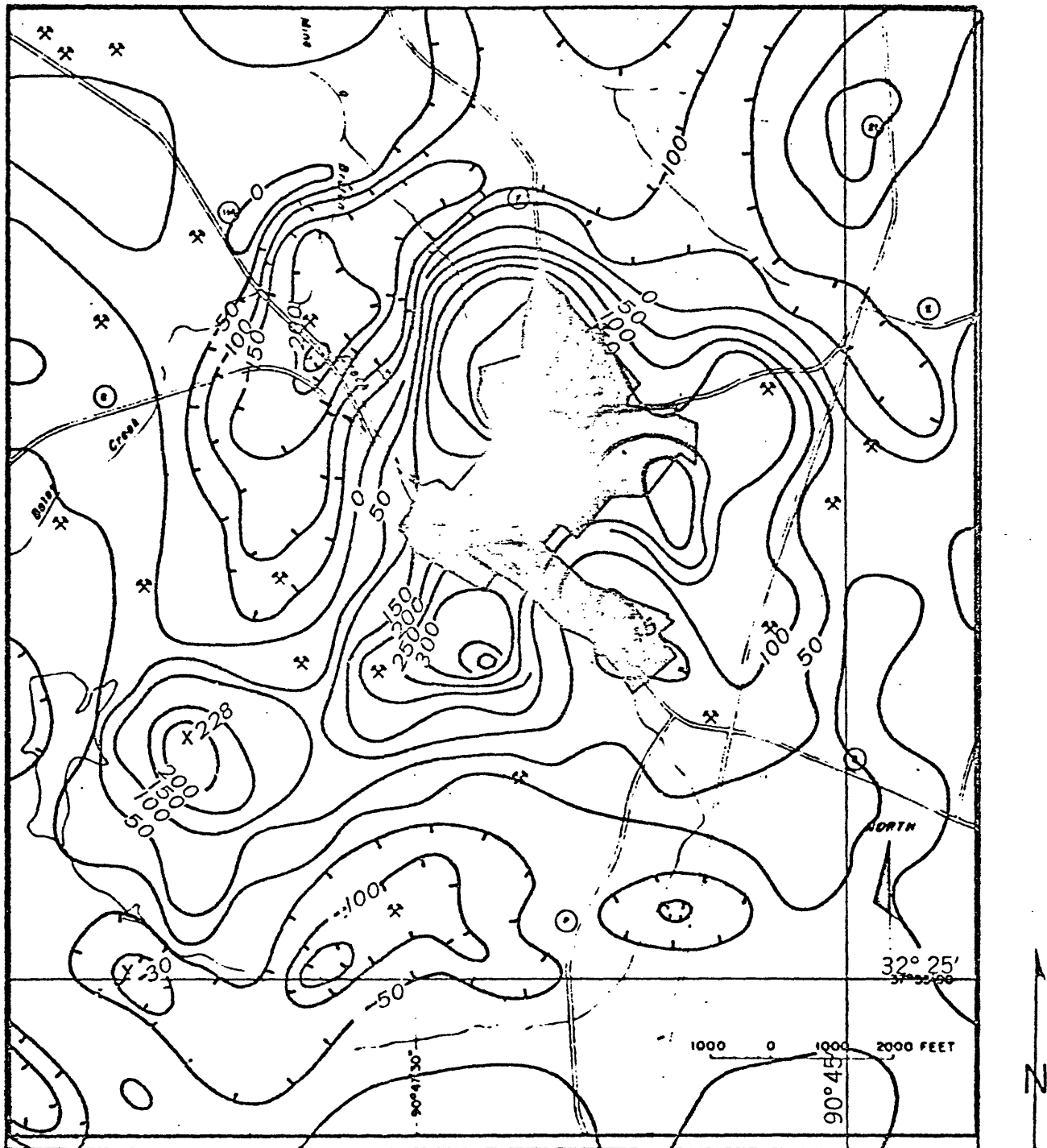


Figure 55.--Second-vertical derivative of the Potosi anomaly at 2,000-ft grid spacing.

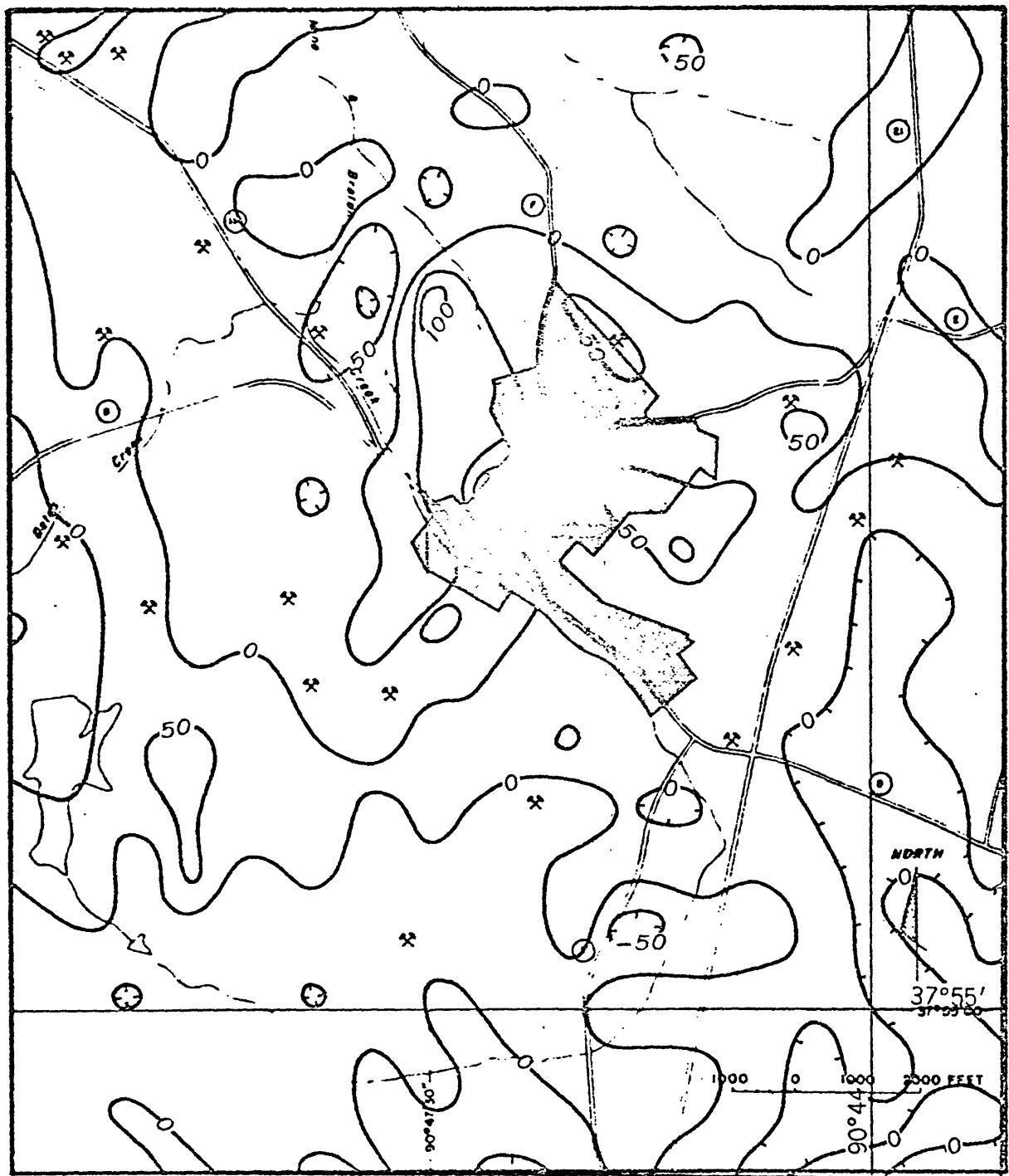


Figure 56.—Second-vertical derivative of the Potosi anomaly at 1,000-ft grid spacing.

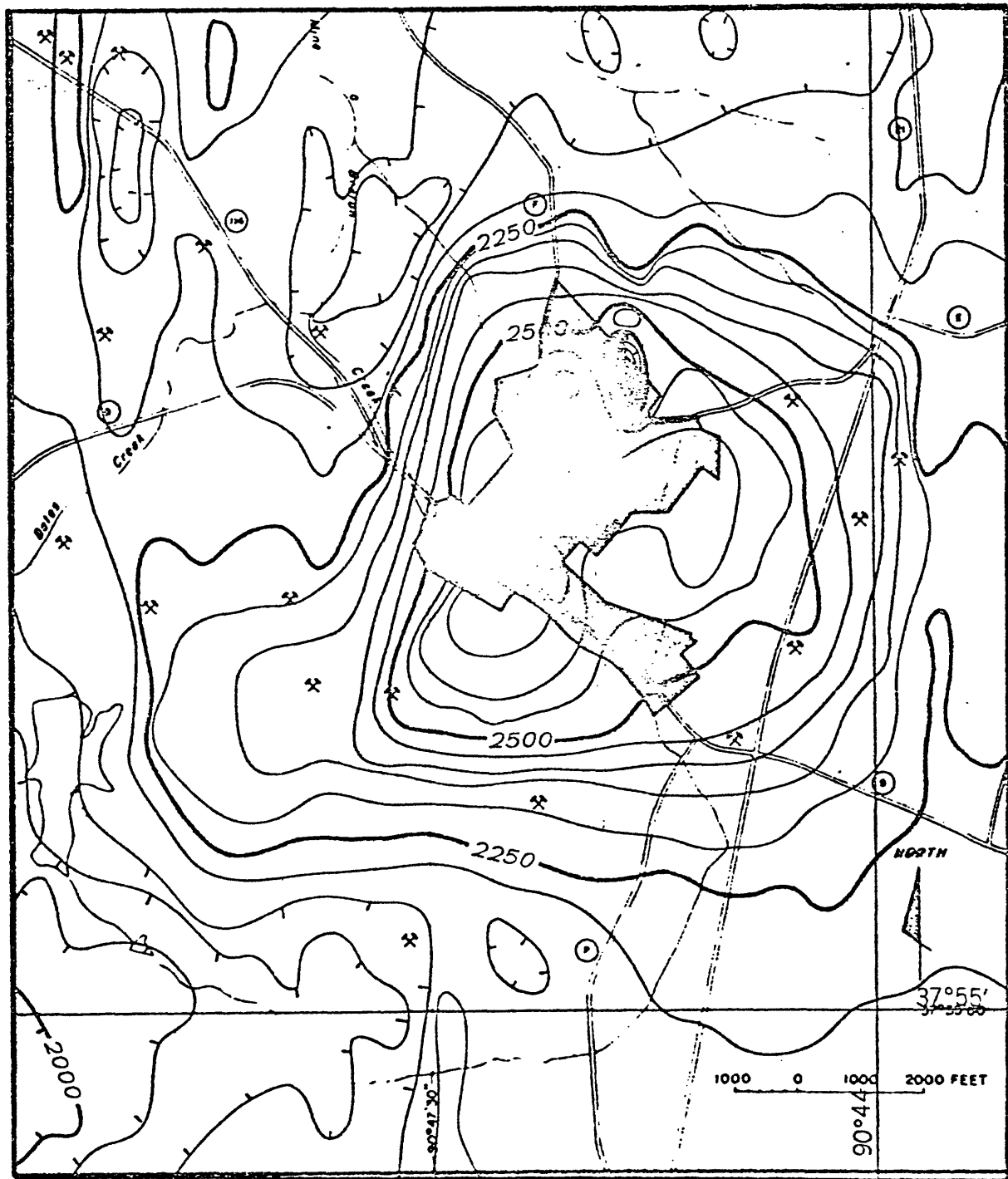


Figure 57.—Potosi anomaly continued downward to 900 ft above sea level.

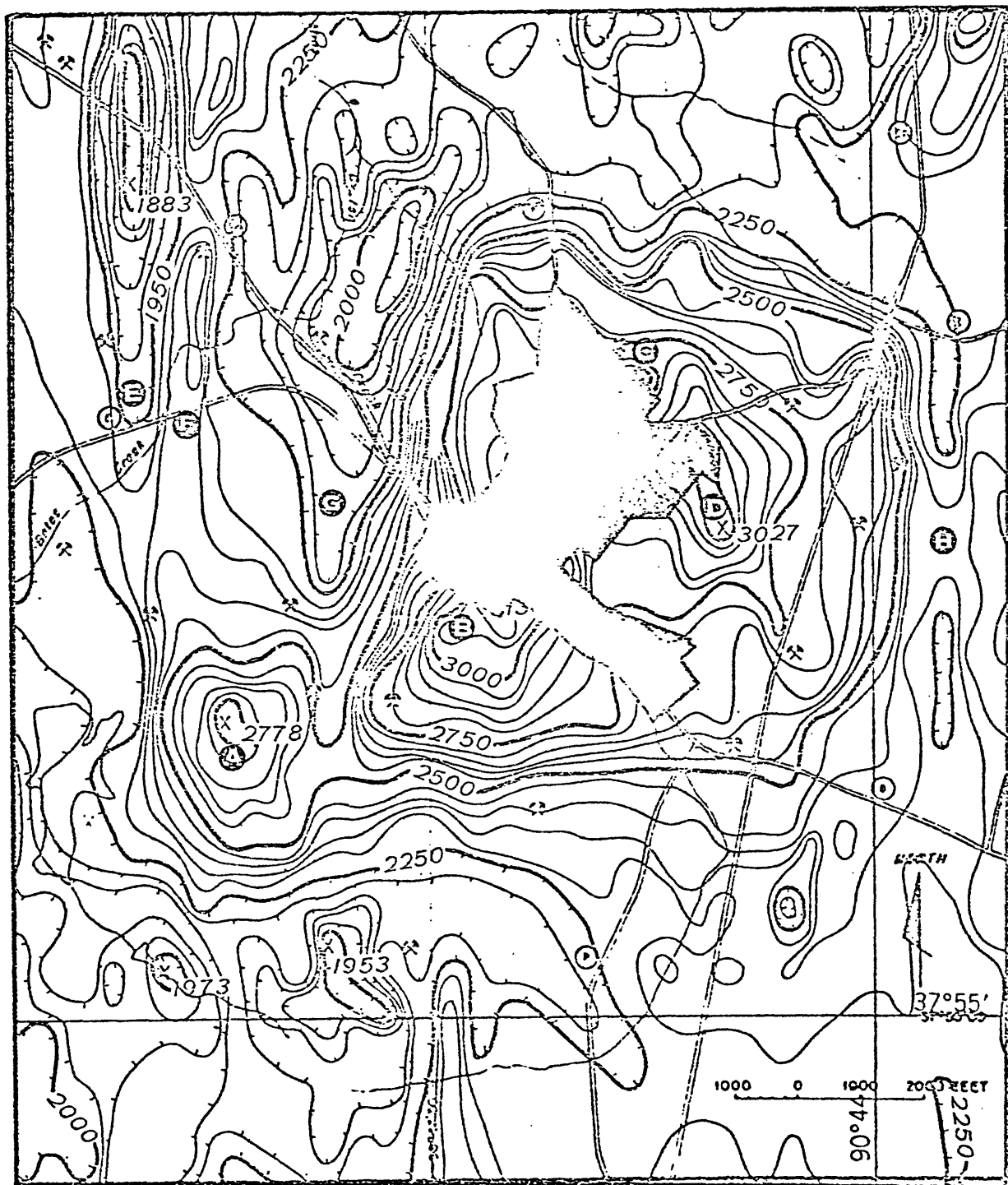


Figure 58.--Potosi anomaly continued downward to 100 ft below sea level, near the Precambrian surface.

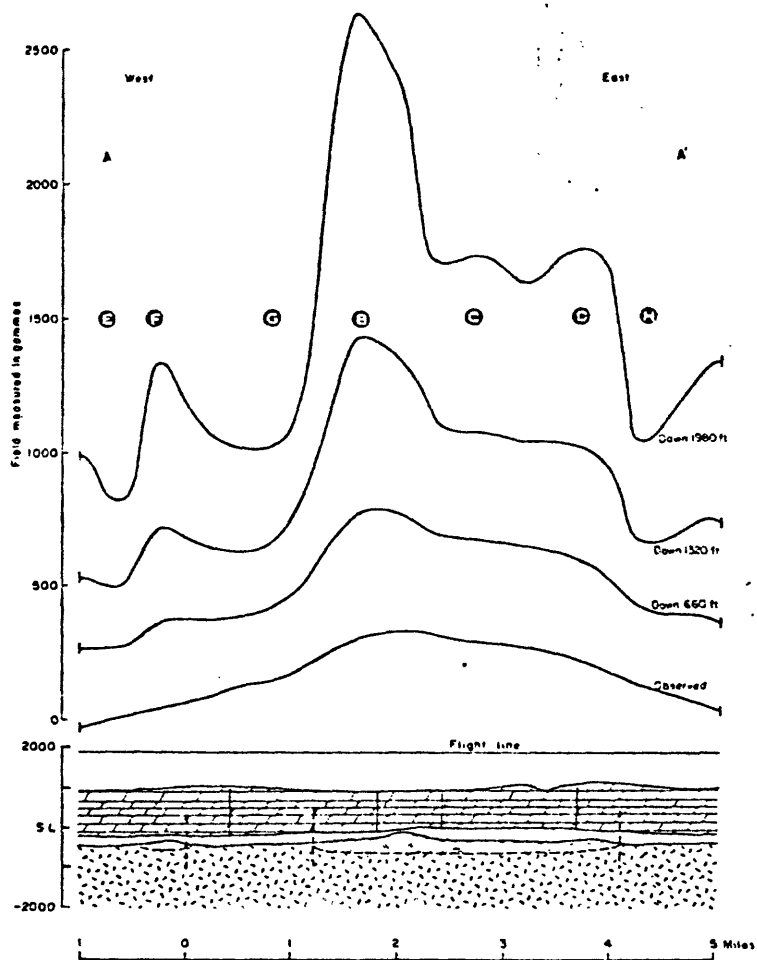


Figure 59.--Magnetic profiles across the anomaly at Potosi showing the effect of downward continuation.

Continuation of the magnetic field to the second level or about the Precambrian surface outlined basement features believed to be caused by buried igneous topography. The intensity of the anomaly implies a block of volcanic rock on a granite terrain. Like the derivative map, the continuation map shows a magnetic high centered on Potosi and surrounded by elongate lows. Subsurface knobs and ridges are inferred from several smaller highs.

Linear features obscure on the observed field are clearly shown by the continuation map. The magnetic low, (E, figs. 55 and 58) defines a probable north-south trending fault zone. The narrow high adjoining the low implies a ridge (F) that extends northwest from the knob. Two other northward-trending fracture zones are inferred from the continuation map. The magnetic gradient and linear lows, (G) and (H) at the border of the anomaly mark the subsurface trace of the buried zones of fracturing. Most of the mining is localized along the steep magnetic gradients in the vicinity of Potosi.

The magnetic gradients at the boundaries of the magnetic rock permit calculation of a maximum depth to this source. The level generating the steepest gradient without oscillations of the field is the depth to the source or magnetic basement. The second-vertical derivative of this level is mainly zero.

A roof pendant of volcanic rock, partly isolated by faulting and erosion, is believed to cause the Potosi anomaly. Peripheral fracturing of the overlying dolomite provided a structural environment for the lead deposits.

The eastern mining area

Development of fracture patterns and depositional features were controlled by knobs on the magnetic Precambrian surface. The resistant, magnetic pendants occur within a more easily eroded, less magnetic granitic terrain. The aeromagnetic map (Figs. 2a and 60) shows that

Figure 60 near here

some anomalies of low amplitude and small areal extent correlate with these hills and ridges of fine-grained Precambrian granitic and volcanic rocks.

The aeromagnetic and geologic map shows several important features related to the main mineralized area enclosed by the towns of Bonne Terre, Leadwood, and Elvins. The Big River fault and Simms Mountain fault bound the mines on the northwest and southwest. The hypabyssal rocks (granite and rhyolite porphyries) at Hughes Mountain (lower left, fig. 60) can be traced northward under the Paleozoic sedimentary rocks to Irondale (B) by contoured magnetic data.

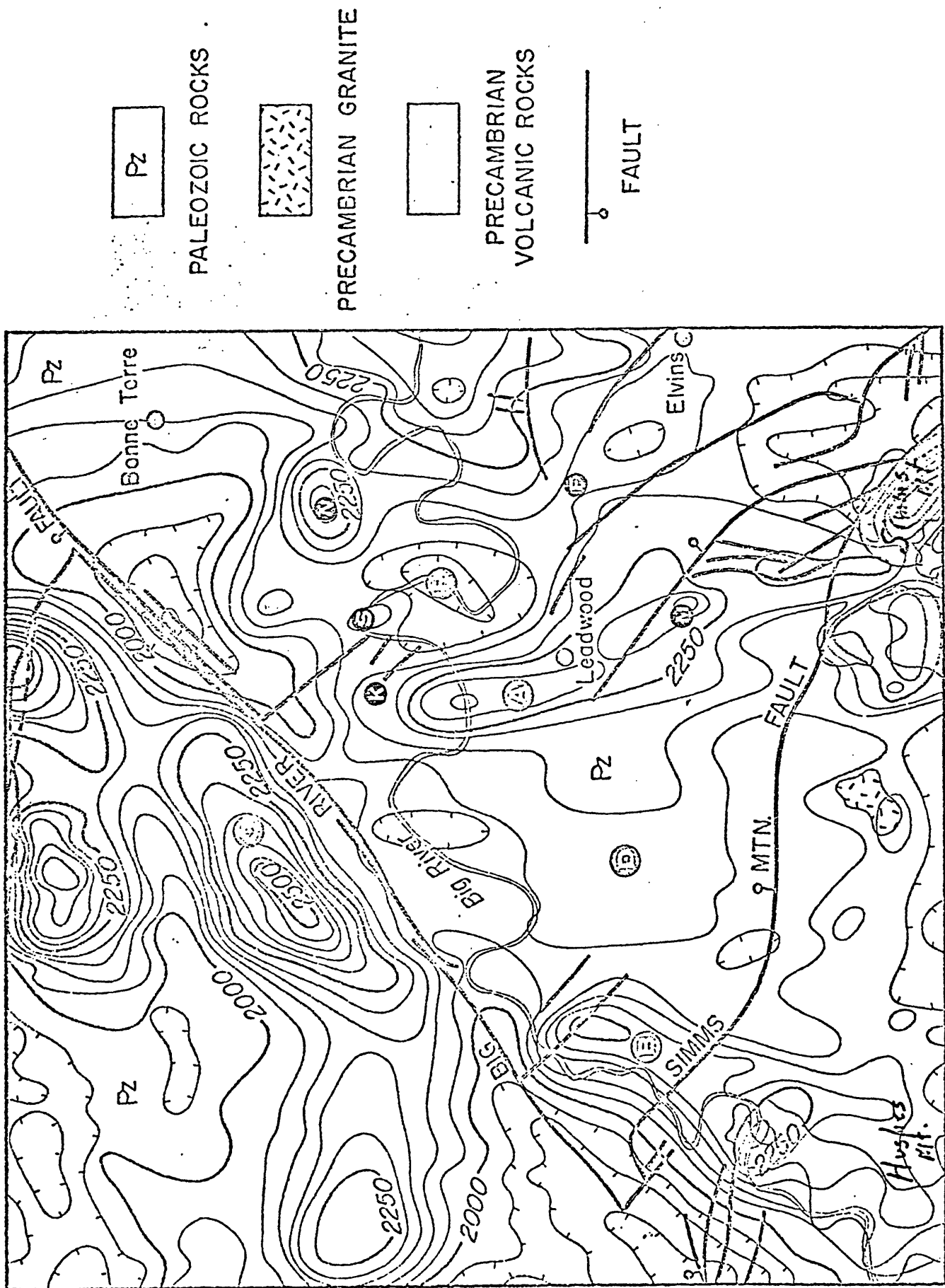


Figure 60.—Aeromagnetic and geologic map showing the major features of the main mining area near Bonne Terre, Missouri.

Similar rocks at Simms Mountain (lower right) also can be traced in subsurface by the magnetic contours to the Leadwood area (A).

Buried volcanic rocks (C) are recognized by the associated magnetic anomaly, especially its relative amplitude. The flat or low magnetic gradient near (D) discloses the buried coarse-grained granite. Similarly, a broad magnetic low indicates the granite-floored shallow basin (E) east of Leadwood. The Big River and Simms Mountain fault zones can be traced by an alignment of magnetic lows.

Irondale anomaly

The aeromagnetic anomaly at Irondale permits correlation with Precambrian igneous rock exposed at Hughes Mountain and its subsurface extension northeastward under Paleozoic strata to the Big River fault (Fig. 61). The rhyolite porphyry at Hughes Mountain produces a small

Figure 61 near here

indefinite magnetic anomaly. The saddle between two granite knobs to the east causes a small magnetic low.

A well-defined magnetic gradient parallels the sides of the subsurface ridge from Hughes Mountain. The best correlation is in the vicinity of Irondale. Similarly, aeromagnetic data show that the volcanic rocks exposed at Simms Mountain continue in subsurface north of the Simms Mountain fault zone (figs. 2a, 60 and 61). These rocks north of the fault zone form thin roof pendants and are cut by northwest-trending faults.

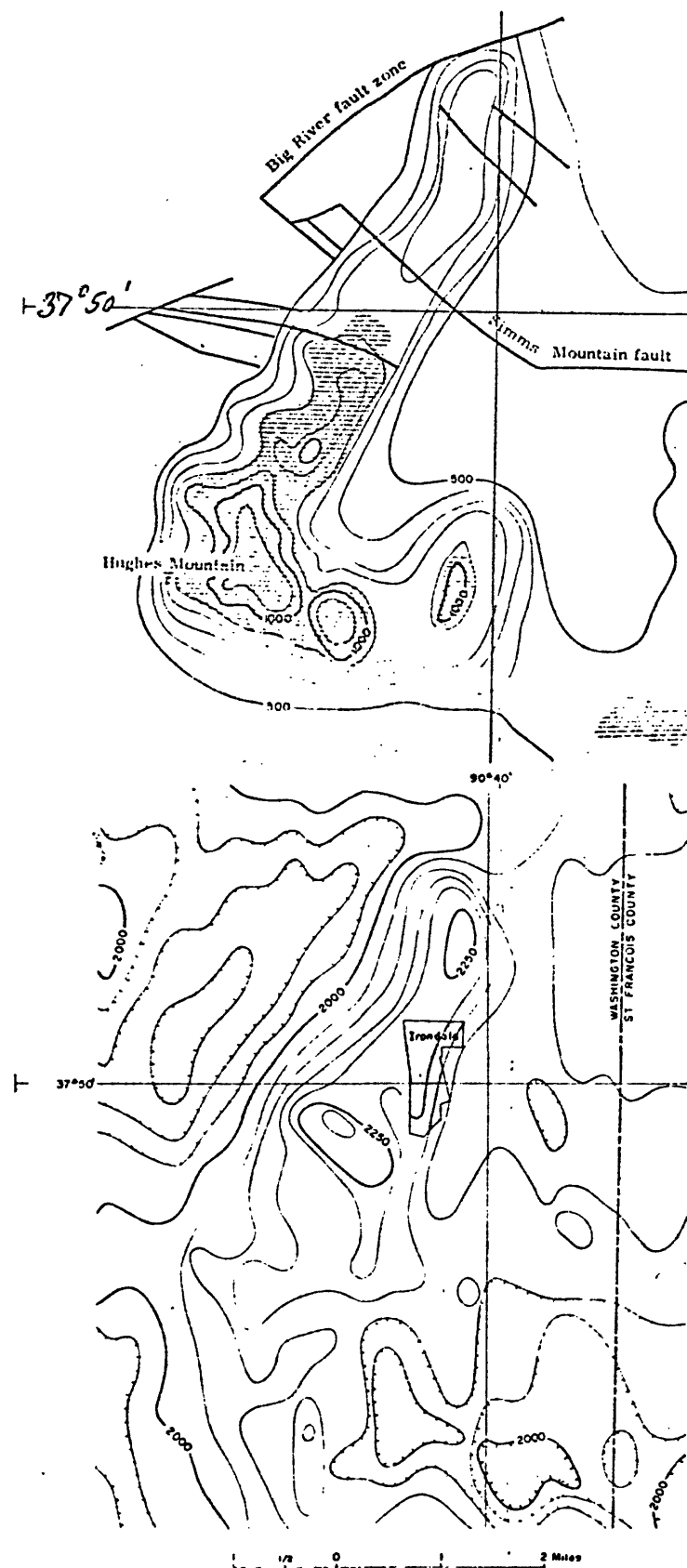


Figure 61.--Aeromagnetic (below) data showing correlation with Precambrian outcrop, subsurface topography, and faults (above) at Irondale, Missouri.

Bonne Terre area

The triangular area enclosed by the towns of Bonne Terre, Leadwood, and Elvins is the heart of the Lead Belt and is designated the Bonne Terre area. The geologic and aeromagnetic map of this part of the mining region (figs. 2a and 60) shows that the main mineralized area is bounded by the Big River fault on the northwest and the Simms Mountain fault on the south. Small subsidiary faults cross the area of extensive mine workings.

Relatively nonmagnetic granitic rocks cause a characteristic low magnetic gradient, such as the magnetically flat area (D) west of Leadwood. Rounded negative anomalies of low amplitude disclose the flat shallow basins underlain by granite. These basins received sedimentary breccias and argillaceous strata at their margins. Breccias are host rocks for major lead deposits. Northeast of Leadwood mines border a flat basin-like area, which is surrounded by Leadwood, Schultz, and Switchback knobs (figs. 60 and 65). A broad magnetic low marks this area (E). A similar low between Elvins and Leadwood correlates with the Owl Creek basin (F), which is partly bordered by mines.

Volcanic rocks associated with the elongate anomaly (A) between Schultz and Mitchell Knobs (figs. 60 and 65) are recognized in subsurface by the contrasting magnetic pattern of moderate amplitude. The writer believes that the combined effect of topographic relief on granophyre volcanic rocks and the magnetic contrast between the granite and these rocks causes the elongate anomaly extending from Schultz Knob (K) to Mitchell Knob (M) near Leadwood.

Relief on the basement surface such as hills of rhyolite cause the small anomalies that are observed over Switchback (S, figs, 60 and 65) and Chicken Farm (N) knobs (figs. 40, 60, and 63). These Precambrian hills

Figures 63 near here

are interpreted as roof pendants. The 50-gamma anomaly observed over Switchback Knob was produced by a thin pendant of resistant rhyolite porphyry in the granite.

A larger and thicker pendant of volcanic rock than Switchback Knob (S, fig. 60) caused the large magnetic anomaly over Chicken Farm Knob (N, figs. 60 and 63). This anomaly yielded reliable depths to its magnetic source; a distance that was useful in selecting a grid spacing for the derived fields. Despite an apparently favorable environment, the sedimentary strata around this knob are barren of lead minerals.

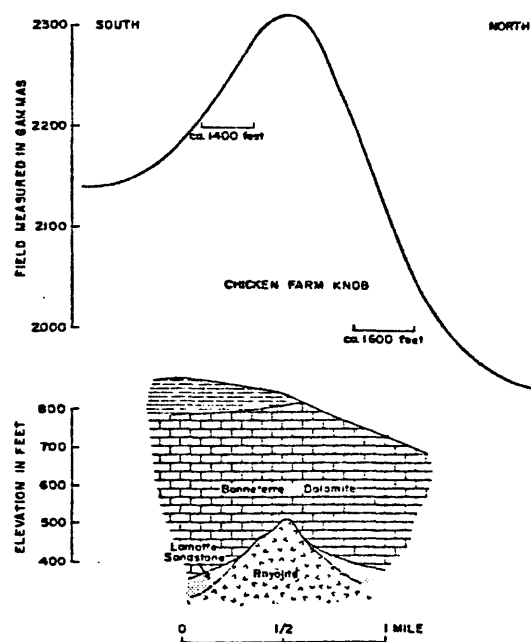


Figure 63.—Aeromagnetic profile showing the effect of topography and estimated depth to basement at Chicken Farm Knob.

Recognition of faulting is important in mineral exploration where the faults controlled movement of ore-bearing fluids. Anomalies observed over some faults are very small and, in places, are obscured by larger anomalies resulting from susceptibility contrast between rock units. A minor northwestward trending fault at Mitchell knob, shown in Figure 40, produced only a small dip in the magnetic profile. In some major fault zones, the magnetic minerals have been altered to nonmagnetic assemblages by meteoric waters or ore-bearing fluids circulating through the sheared or crushed rock. The major faults can be correlated from a series of closed lows on the contour map (Figure 60) or by pronounced dips in magnetic profiles (Figure 40), such as observed over the Big River and Simms Mountain fault zones.

Anomalies and mines

According to Snyder and Odell (1958, p. 905-906), two structural elements, exclusive of faults, controlled lead deposits in the Bonne-terre area. These structures are depositional ridges and shallow basins. Hills or knobs of granite, granophyre, or rhyolite controlled depositional ridges, sand bars, benches, and organic reefs along their crests. Small magnetic anomalies correlate with the hills. Because of the indirect relation of these anomalies to lead deposits in the sedimentary structures, the relation between some anomalies and mine workings is less pronounced than their correlation with basement relief.

The relations among an ore deposit, a buried hill, and its magnetic anomaly is illustrated by the first important lead deposit in the main mining district, St. Joseph Mines (Bonne Terre mine) whose historic workings partly parallel and wrap around an elongate fine-grained granite knob at Bonne Terre (Fig. 64). The ore was

Figure 64 near here

structurally controlled by a sedimentary ridge-reef complex that trends northeastward and southwestward from the basement knob (Eckelmann, Brown, and Kulp, 1957). The knob causes an elongate 50-gamma anomaly. The nearly east-west trend of this narrow anomaly is inferred from several nested north-south profiles, spaced about $\frac{1}{4}$ -mile apart.

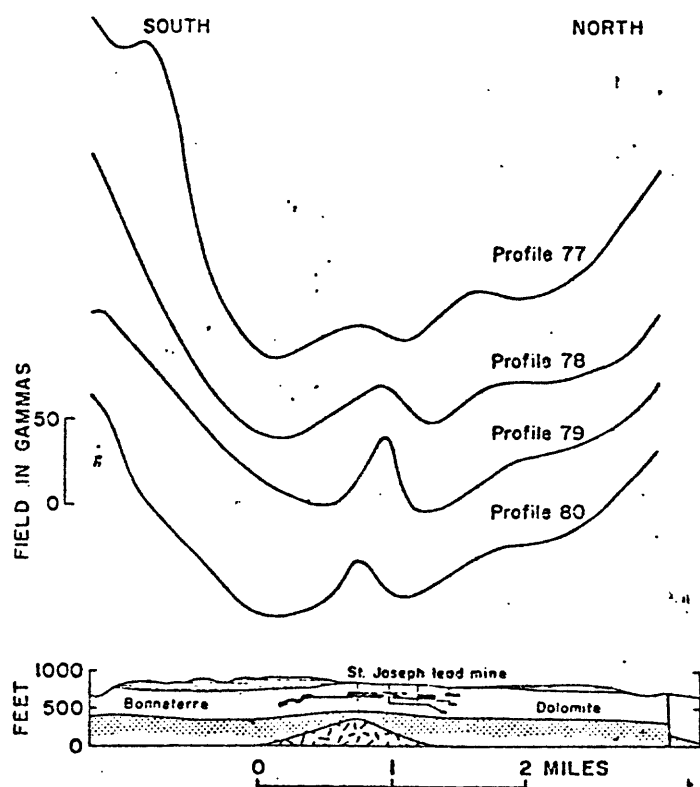


Figure 64.--Aeromagnetic profiles over a granite knob at Bonne Terre showing low amplitude and continuity of the magnetic anomaly and its correlation with mine workings.

The total-intensity aeromagnetic map (fig. 65) of the Bonne Terre

Figure 65 near here

area shows the relationships of mine workings, buried knobs, and faults. The mined area is underlain partly by eroded granophyre that form several knobs. The elongate anomaly between Schultz (K) and Mitchell (M) Knobs correlates with the mined areas extending eastward from the knobs in the vicinity of Leadwood. A linear lead deposit parallels the elongate anomaly northwestward and wraps sinously around Schultz Knob. A 40-gamma anomaly, observed in profile, correlates with Leadwood Knob. This knob partly controlled a large northeastward-trending ore body. Mine workings extend southwestward from a small isolated rhyolite hill called Switchback Knob. The rhyolite causes a small-amplitude anomaly.

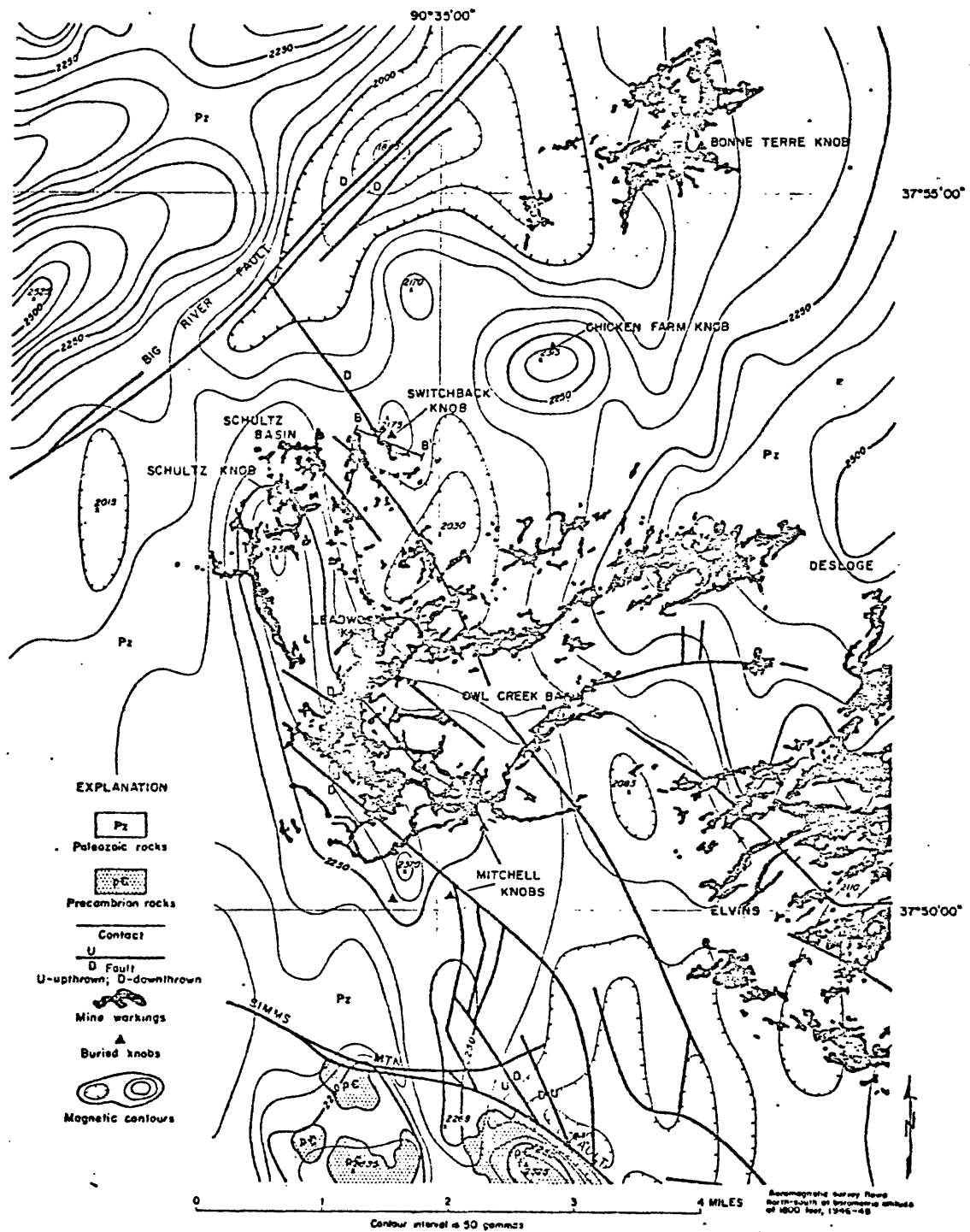


Figure 65.--Total-intensity aeromagnetic map of the Bonne Terre area, southeastern Missouri showing its relation to faults, mine workings, and buried knobs.

Analysis of anomalies

The correlation of small magnetic anomalies with geologic or physiographic features obviously is enhanced where their amplitudes can be emphasized. Ground magnetic surveys place the detector closer to the magnetic basement rocks; hence, the anomalies are higher in amplitude and more easily separated from surrounding anomalies. Ground magnetic surveys generally have greater resolving power, where background noise is low, than their aeromagnetic counterpart and have been used extensively for locating basement knobs (Buehler, 1932, p. 50). In this study, however, analytical methods were used to emphasize small amplitude anomalies of aeromagnetic data.

The usefulness of residuals (Fig. 66) derivatives (Fig. 67), and downward continuation (Fig. 68), of observed aeromagnetic data in

Figures 66, 67, 68 near here

mineral exploration was assessed by comparing the relation of these computed fields with (1) the location of mine workings for correlation with ore-bearing structures; (2) known buried Precambrian hills; and (3) zones of faulting. The computed fields also were compared with observed data to determine their relative resolving power.

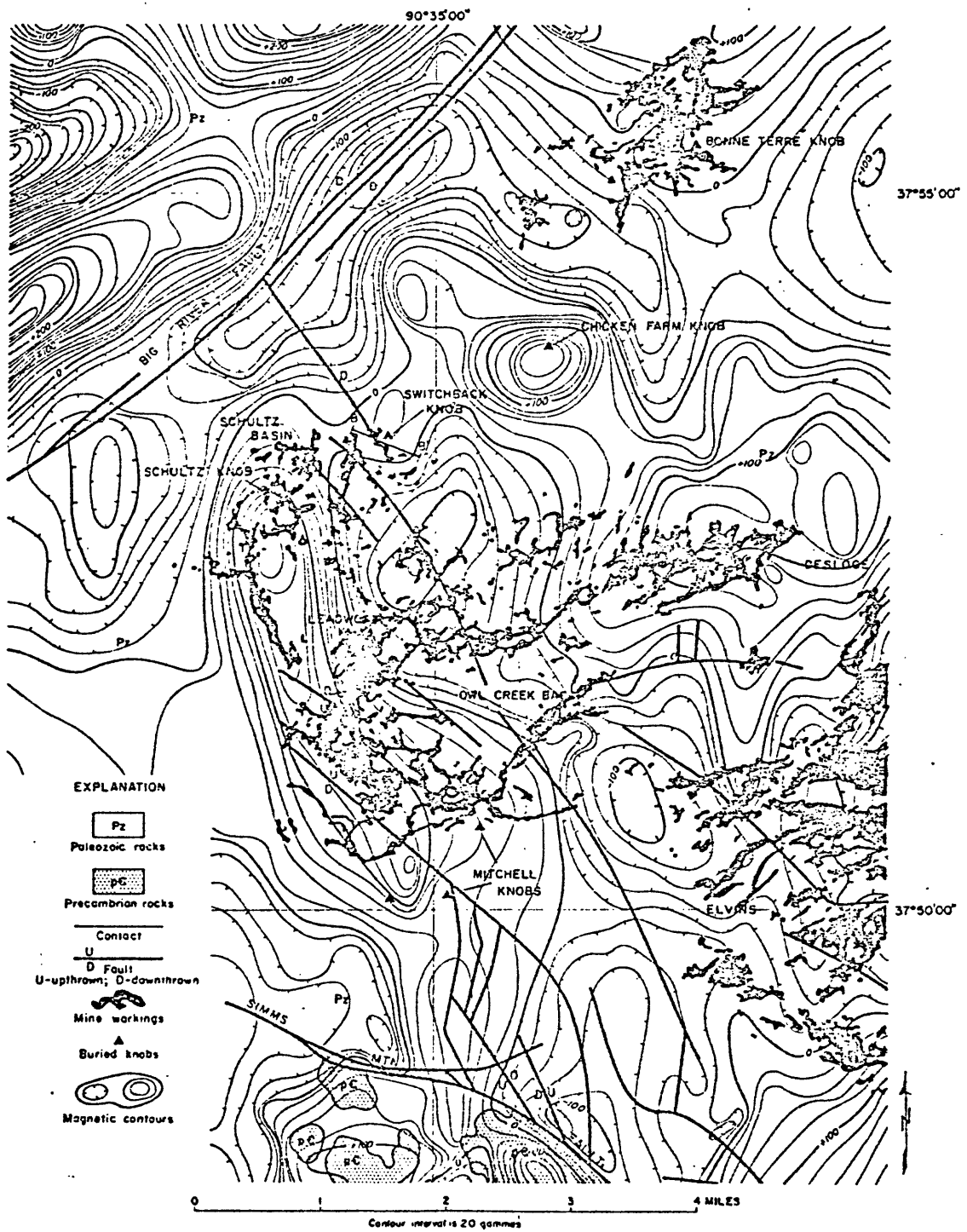


Figure 66.--Residual anomalies from the third-degree representation of the geomagnetic field in the Bonne Terre area.



Figure 67.--Second-vertical derivative of the observed magnetic field in the Bonne Terre area.

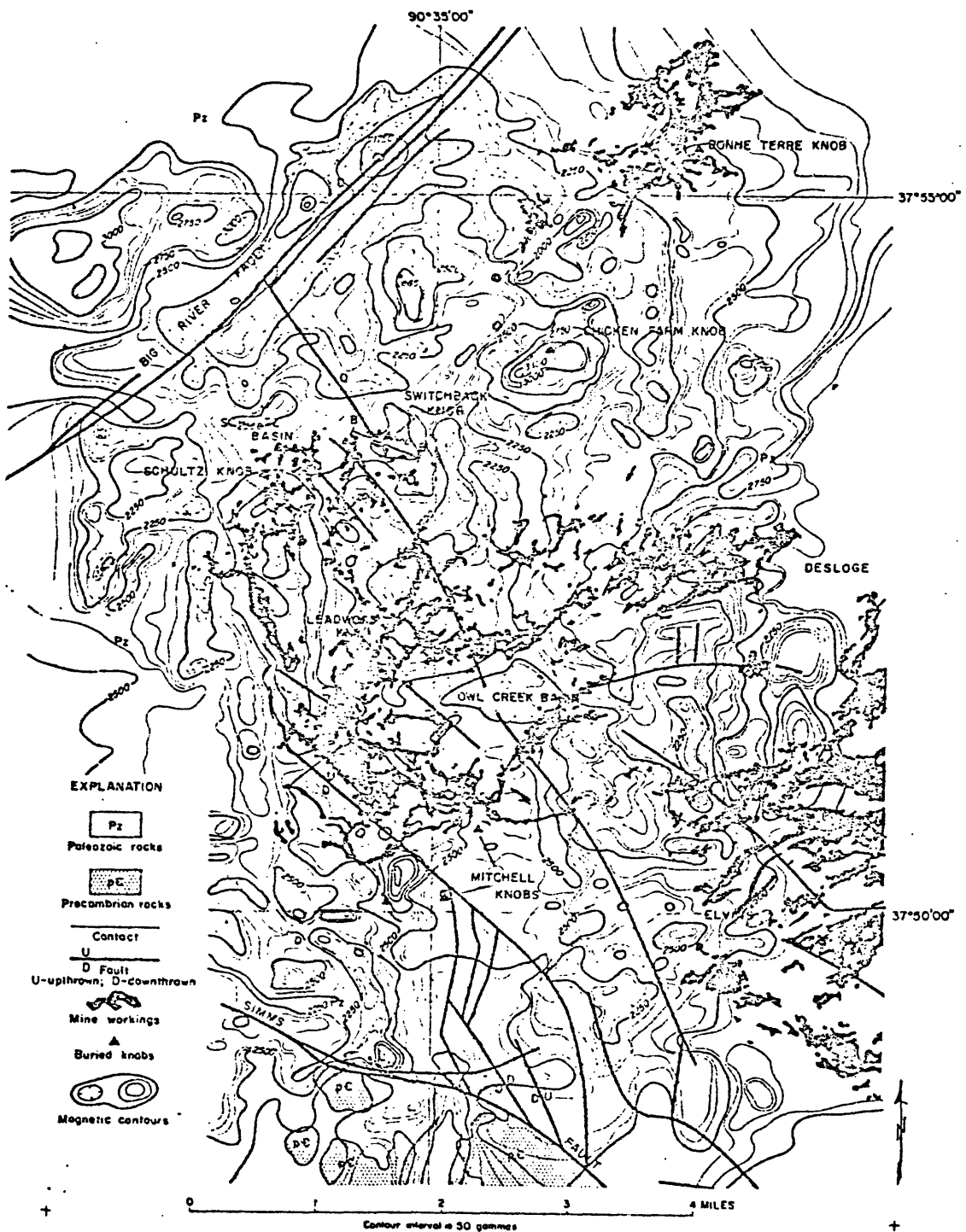


Figure 68.--Aeromagnetic field in the Bonne Terre area continued downward to 100 ft below sea level, about average Precambrian surface level.

The mine workings between Mitchell knob and Schultz knob correlate best with the total-intensity field continued to about basement level, (Fig. 68) The second-vertical derivative map (Fig. 67) also shows good correspondance between the well-defined anomalies and the mines. The correlation between the residual anomalies map (Fig. 66) and the mines has not improved over that shown by the observed total intensity field.

The southwest ridge of Leadwood Knob correlates with the continued anomaly and to a lesser degree correlates with the derivative anomaly. Correlation is lacking with the residual anomaly. Schultz Knob correlates with continued anomaly but is not indicated by the derivative or residual anomaly maps. Switchback Knob correlates best with the continued anomaly but also correlates with derivative anomaly.

The total-intensity field continued downward 2000 ft or about to basement level aided correlation between basement hills and the small anomalies by increasing the amplitudes and marking the areal extent of the anomalies. The anomalies associated with basement rocks from Mitchell to Schultz Knobs, over Chicken Farm Knob, and over the Big River fault zone would still be easily detected by the airborne magnetometer if the Precambrian basement was buried by an additional 1000 ft strata.

The nonmagnetic rocks in the wide shear zone of the Big River fault system produce magnetic lows. The trace of the Big River fault, shown in the northwest part of the maps, parallels elongate lows of the continued and derivative anomaly maps. The fault partly correlates with the northeastward trend of the magnetic gradient and partly with the lows of the residual anomaly map. Narrow northwestward trending faults of small displacements, shown in the south part of the maps, appear to correlate with the continued field.

The flat basin-like areas between the town of Elvins and Schultz Knob correlate with the derived anomaly maps. The basins seem to correlate best with the continued anomalies.

Although the regional fields are mathematically derived, the 3rd degree surface representing the regional field, shown in Figure 69

Fig. 69 near here

appears to be caused by structural features in the basement. Faults are believed to bound these structural blocks. Faulting and tilting of large blocks of basement rocks prior to sedimentations provided sufficient local relief for the development of a maturely dissected landscape of ridges and rounded hills (Tarr, 1936, p. 716-717). Leadwood is the flat saddle of the regional magnetic field; hence, the residual anomalies in this area change little from anomalies of the observed field. Lead deposits are associated with the southeast part of the map covered by the large magnetic low.

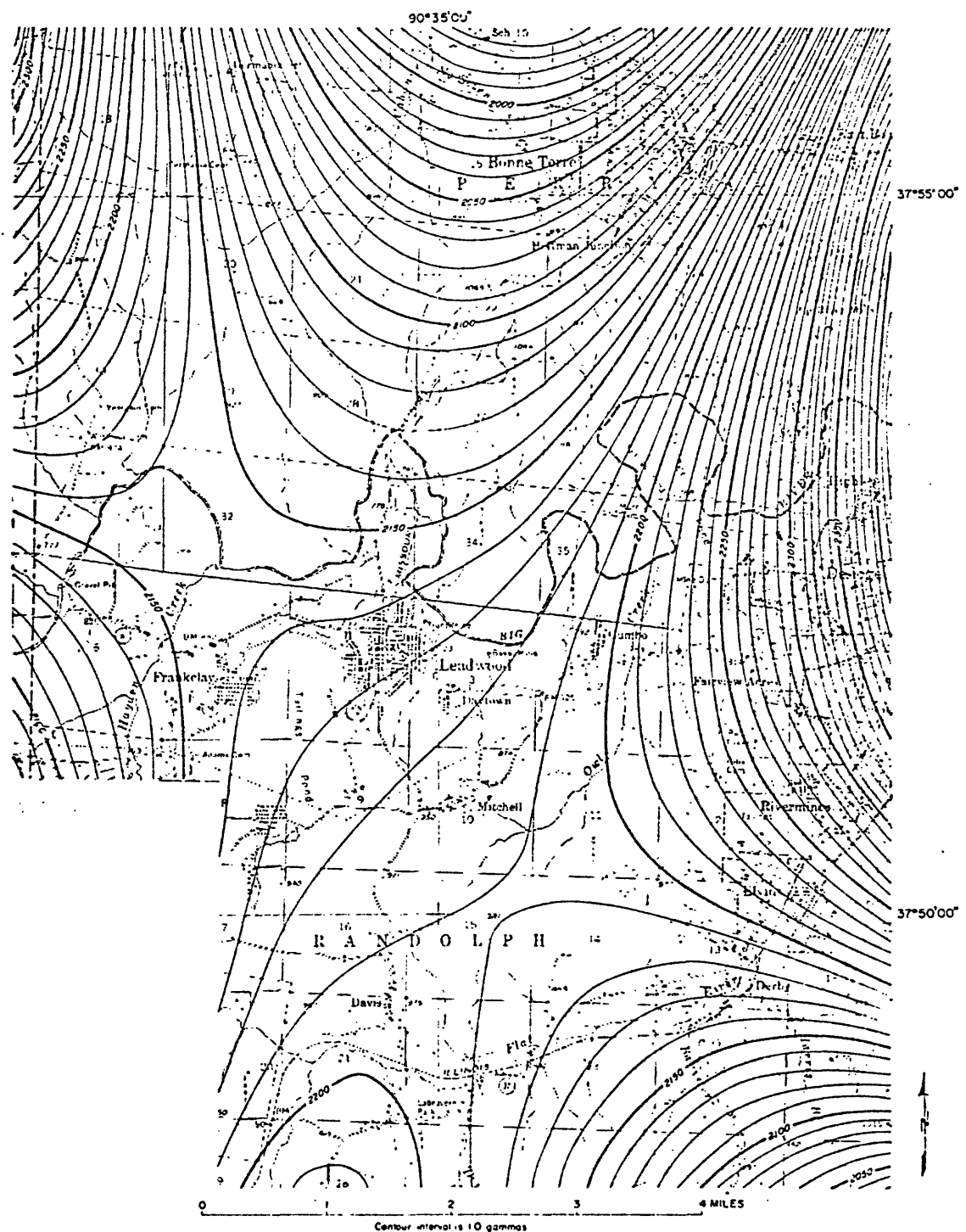


Figure 69.--Third-degree polynomial representation of the geomagnetic field in the Bonne Terre area.

The correlation between magnetic and geologic data is further demonstrated by the profiles A-A' of derived magnetic fields over rhyolite of Switchback Knob, shown in Figure 70. The zero points

Fig. 70 near here

on the second-derivative profile of the observed field project into the geologic section at the extremities of mine workings in nearby lead deposits. Points on the profile that represent the 250-gamma/length² values correlate with the pinchout line of the Lamotte Sandstone and the projection of the mine workings. The relative resolving power of the derived magnetic fields are also shown by the profile over Switchback Knob. All the anomalies are intensified by the second-vertical derivative, because of its high resolving power. The profile of the field continued downward to the Precambrian surface, however, shows greater resolution than the second-derivative profile. Profiles A-A' of the derived magnetic fields over Chicken Farm Knob (Figure 71).

Figure 71 near here

show about the same relations as the profiles over the mineral-bearing area of Switchback Knob. These profiles show a broad anomaly. The second-vertical derivative of the data continued downward shows asymmetry in the topography, however the lack of mineral-bearing structures at Chicken Farm Knob are not indicated by the magnetic data.

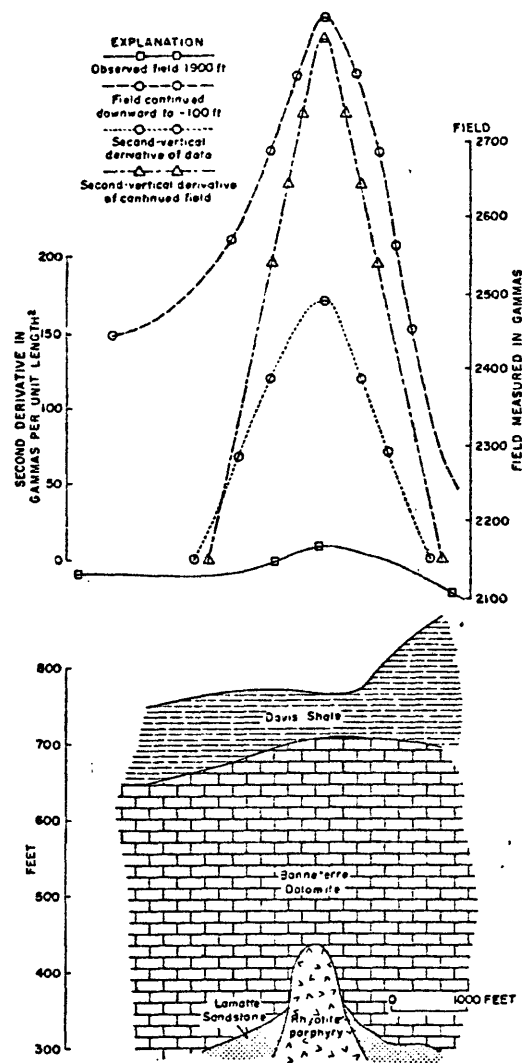


Figure 70.--Profiles of derived magnetic fields over the rhyolite pendant of Switchback knob.

242

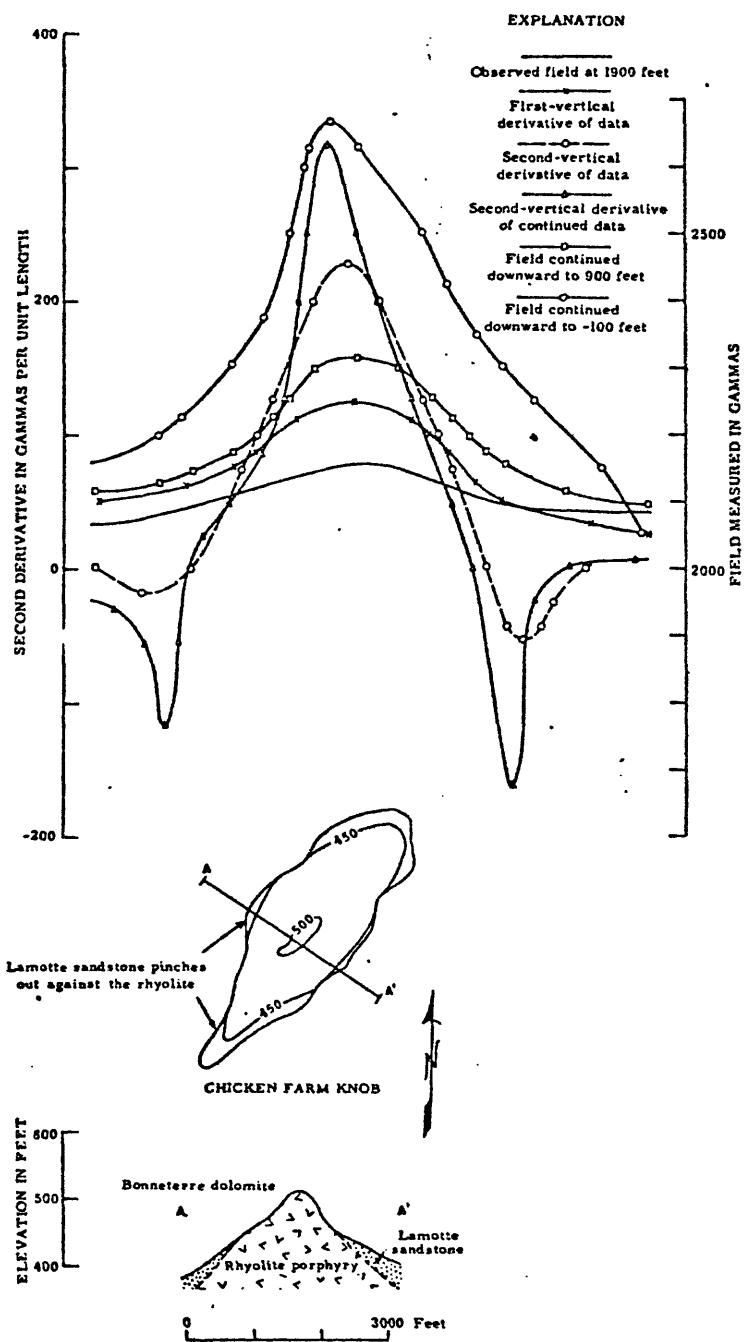


Figure 71.--Profiles of derived magnetic field over the rhyolite pendant of Chicken Farm Knob.

243

In the Bonne Terre area where subsurface geologic information is abundant, topographic relief and major dislocations of the basement rocks and overlying sedimentary strata correlate with anomalies of the derived magnetic fields. Buried basement topography, especially in areas of isolated roof pendants is better defined by downward continuation rather than by derivatives or by residuals of the observed data. Downward continuation has greater resolving power than the other methods. Where the gradient of the continued field and the vertical derivatives steepen in profile, presence of the pinch-out line of the Lamotte Sandstone is more likely: this steepening may be a useful guide in delineating areas for exploration.

These interpretative techniques can be used on aeromagnetic data elsewhere in southeastern Missouri to deduce likely areas of buried topography and faults, and thus delineate areas favorable for further lead exploration.

Detailed aeromagnetic data

In areas of buried hills, profiles disclose details of the small-amplitude anomalies associated with basement relief that may be lost in contouring aeromagnetic information. A special map having a 20-gamma contour interval was prepared of the Bonne Terre area. The anomaly map (Fig. 72) shows a striking correlation with buried knobs,

Figure 72 near here

basins, and faults.

Contours show clearly the bifurcation in the Mitchell Knob (M, fig. 60) The small subsurface knobs at Gumpo (G) and south of Owl Creek (N, fig. 60) cause small anomalies that are shown by closed contours. Similarly Leadwood Knob (L) and the elongate ridge at Bonne Terre (T) are indicated by the contour map. Other anomalies are also strikingly delineated by contours.

Granite-floored basins, such as Leadwood (D), Owl Creek (O) and Elvins (E) are outlined by broad lows. Faults are more clearly defined by profiles (Fig. 40) but are also marked by gradients on the contour map.

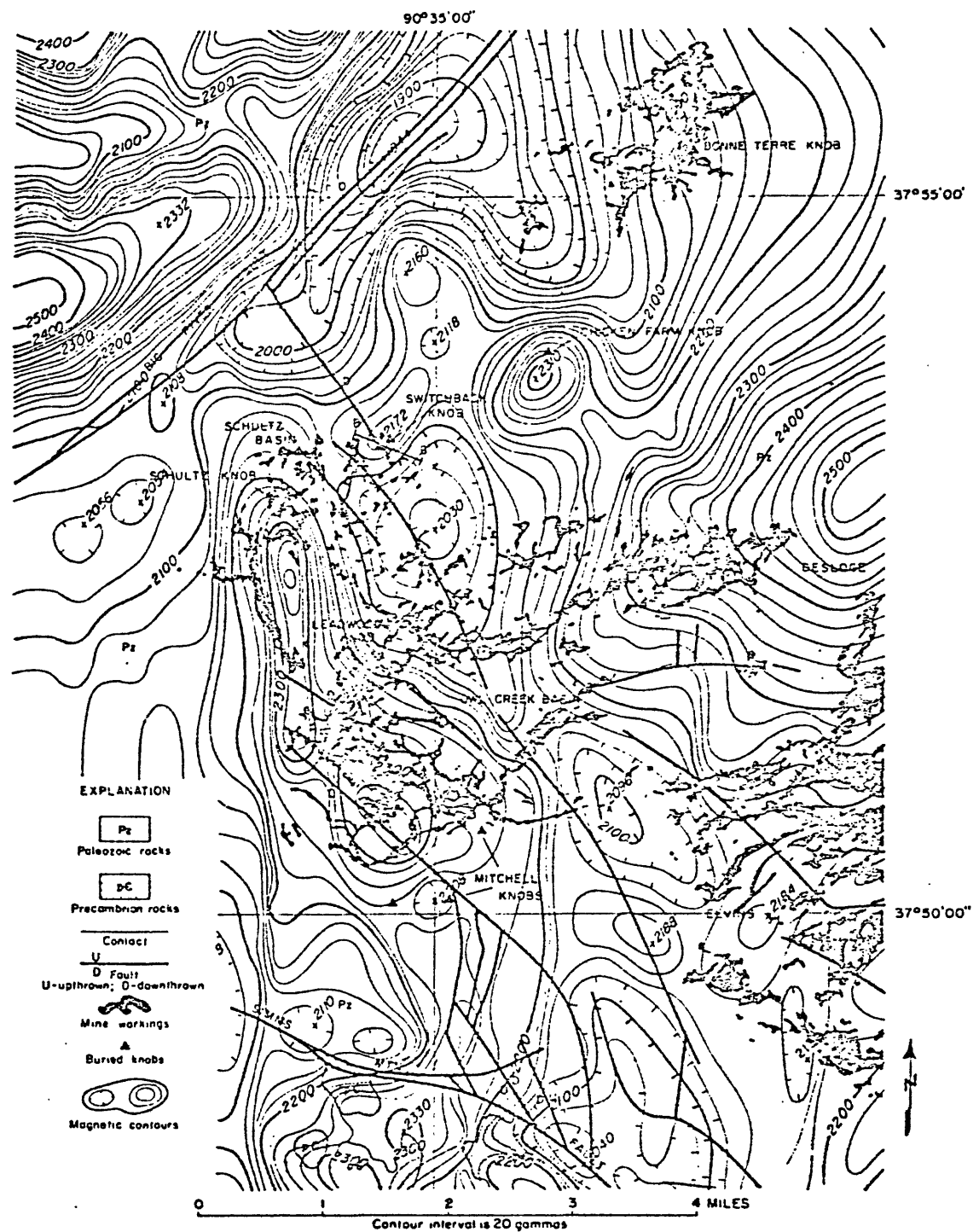


Figure 72.—Detailed total intensity aeromagnetic map of the Bonne Terre area having a 20-gamma contour interval.

In detail (Fig. 73 and 73a) Schultz Knob is on the nose of the

Figure 73 near here

elongate north-trending anomaly. The Leadwood anomaly is associated with a spur of Leadwood Knob. The mine workings wrap around the elongate anomaly, extend eastward from Leadwood anomaly and wrap around the Leadwood low.

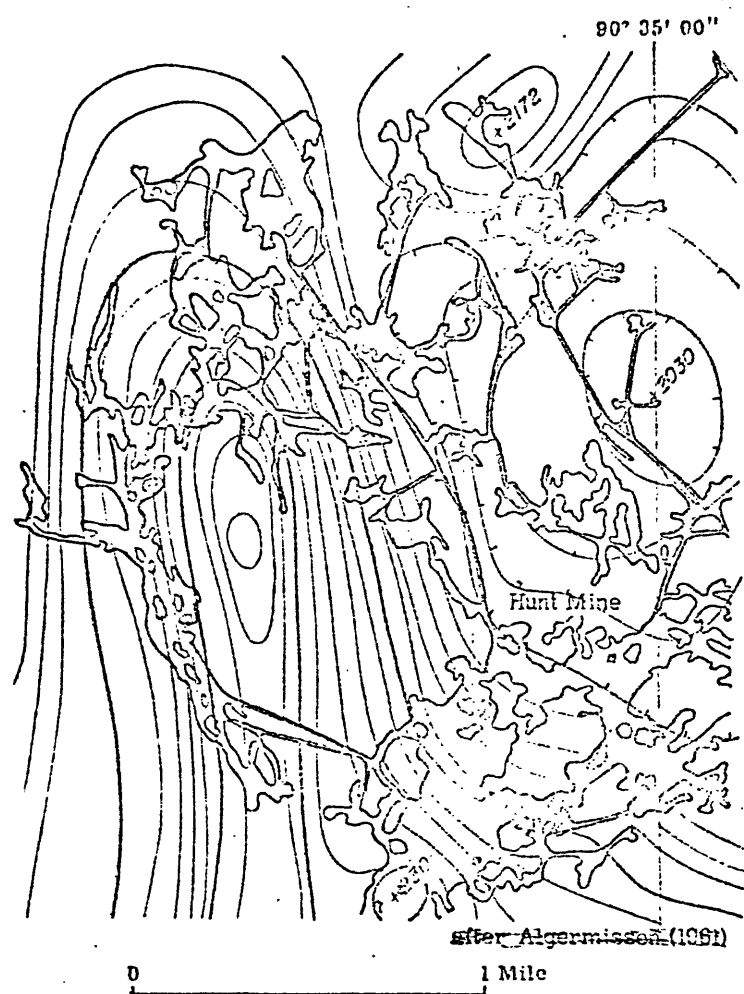


Figure 73.--Correlation of aeromagnetic data and mine workings at Leadwood, Missouri.

Relations to regional features

The northern basin encompasses a broad area northwest of the old lead belt near Leadwood, Bonne Terre, and Elvins on the north flank of the St. Francois Mountains. This basin is floored by granite which is inferred from low magnetic gradients and low-amplitude anomalies of the aeromagnetic map (Fig. 2a).

According to correlations of magnetic and geologic data in the St. Francois Mountains, volcanic roof pendants, ridges, and knobs produce aeromagnetic anomalies of moderate amplitude at Three Hill Creek, Potosi, Indian Creek, Mineral Fork, Richwoods, and elsewhere. The erosion pattern in the St. Francois Mountains demonstrates that three areas have the best likelihood of topographic relief. The importance of this basement relief to lead-bearing sedimentary structures was established in the Bonne Terre mining area (Allingham, *In press*).

(fig. 2a)

The aeromagnetic anomaly extending basinward from Little Pilot Knob to Indian Creek is one of the dominant features of this northern basin. The magnetic anomaly bifurcates near Indian Creek; it extends southeastward towards Three Hill Creek area and northward towards the Richwoods area. The geologic significance of these anomalies ~~are~~ is described in detail because of their importance in mineral exploration.

Sources of volcanic rocks

The large areal extent of volcanic rocks, especially subsurface, prompts some speculation about the source of these rocks. Isolated volcanic vents or ring-like caldera structures might be detected by examination of magnetic anomalies. Brecciated rock in volcanic vents or fissure zones are possible hosts for iron mineralization as well as sources of volcanic rocks. Anomalies, such as those observed over Cottoner, Russell, Shepherd, and Iron Mountains, may represent dilatant fissure zones or vents filled with breccia or volcanic debris in which magnetite and other iron minerals are concentrated (Table 4).

Table 4 near here

These broad high-amplitude anomalies including the Pea Ridge anomaly form a lineament of northwesterly trend and are probably located along a zone of weakness, at the intersections of northeastward-trending fracture zones, and near the contact between granite and volcanic rock. All of these anomalies appear to be related to plug-like volcanic bodies.

Table 4. High-amplitude anomalies related to possible mineralized volcanic structures

Name	Location	Total Intensity	Altitude	Vertical Intensity	(gammas)	(gammas)
1. Mt. Cottoner	37°28'	90°12'	1100		800	
2. Shepherd Mt.	37°37'	90°38'	1800		2400	
3. Boss-Bixby	37°37'	91°91'	2150		3500	
4. Pea Ridge	38°07'	91°03'	3225			
5. Bourbon	38°08'	91°14'	5800			
6. Kratz (Cave Spring)	38°16'	91°12'	1600		2200	

Belle anomaly

The total-intensity aeromagnetic anomaly at Belle, Missouri, outlines a buried circular feature in the basement (Fig. 74). But for

Figure 74 near here

small areal size, the anomaly resembles those associated with ring-like zoned intrusions of quartz monzonite in Maine and Wisconsin (Allingham, 1960, 1961). In areal extent the circular feature more closely resembles the moat and dome of calderas at Timber Mountain, Nevada (Boynton et al 1963) and in the Jemez Mountains (Cordell and Joesting, (written commun.)). The breaks in the circular magnetic high imply a northeast-trending graben. The moat is inferred from the magnetic lows enclosing this ring-like structure.

Depths from aeromagnetic data corroborate the structure contour on the igneous basement prepared by Grenia (1960). Some topographic expression had to be added to fit the observed anomaly (Fig. 75); this

Figure 75 near here

interpretation conforms to the characteristic resistant nature of volcanic rocks of producing hills on weathered, eroded Precambrian terrain.

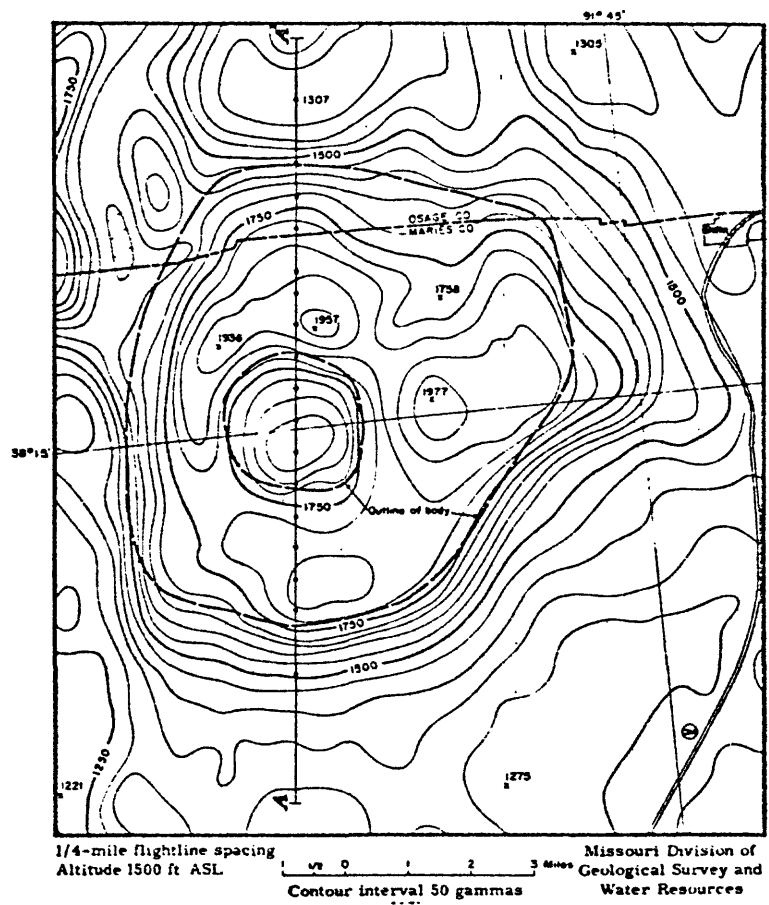


Figure 74.--The circular aeromagnetic anomaly at Belle, Missouri.

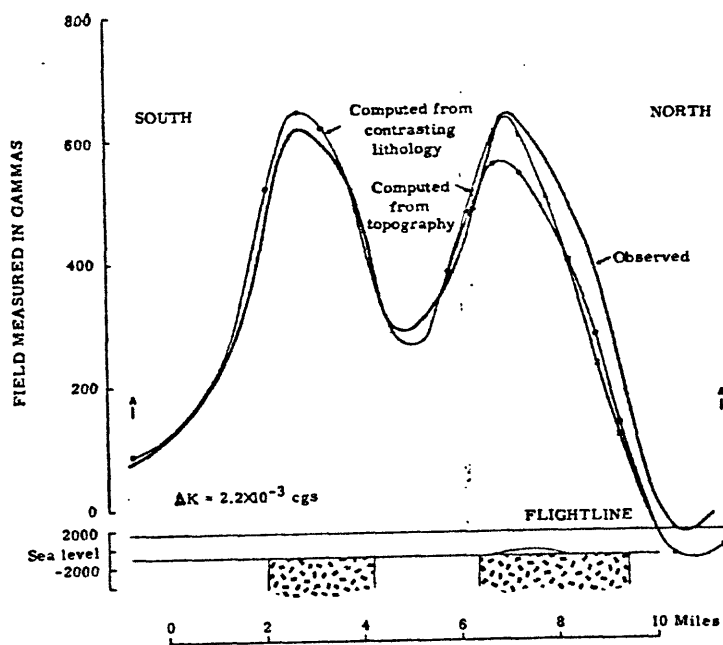


Figure 75.--Magnetic profiles across the Belle anomaly showing dimensions of magnetically contrasting rock.

Many other circular features are shown on the vertical intensity magnetic map of Missouri (Farnham, 1943) and are presented in Table 5.

Table 5 near here

The author believes that these ring-like features may be magnetically zoned igneous intrusions or calderas in different stages of erosion.

Table 5. Ring-like magnetic anomalies in Missouri

Name	N. Lat.	Location	W. Long.	Diameter Miles	Vert. Intensity gamma
1. Bend		38.2°	91.8	8	500
2. Shamrock		39.0°	91.7	10	400
3. Edina		40.2°	92.1	8	500
4. Adair		40.3°	92.4	8	350
5. Glenwood		40.5°	92.5	6	350
6. Lemons		40.5°	93.1	6	400
7. Carrollton		39.4°	93.6	6	700
8. Harrelson		38.8°	94.5	12	800
9. Mt Hulda		38.4°	93.3	8	400
10. Neosho	36.9°N		94.3	6	300

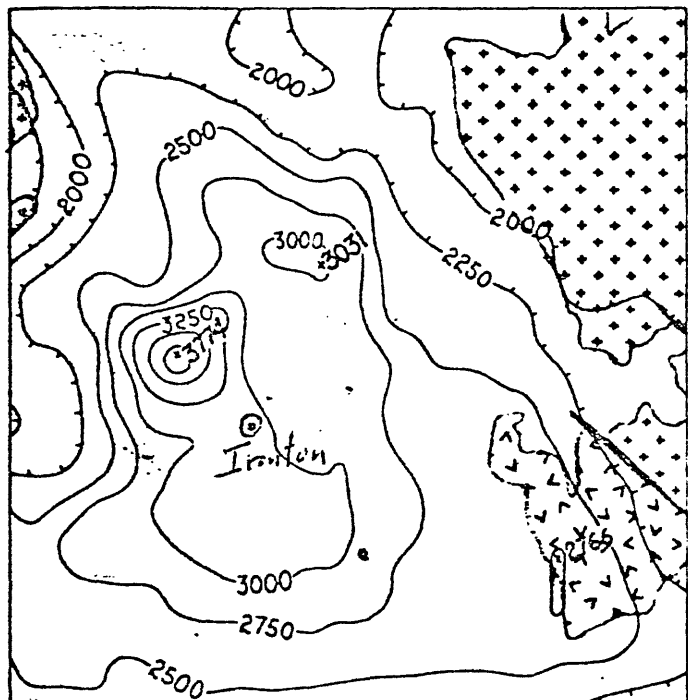
Ironton anomaly

The total-intensity aeromagnetic field in the Ironton area was continued upward and downward for correlation of three levels of data with exposed igneous geology (Fig. 76). Continuation of the fields

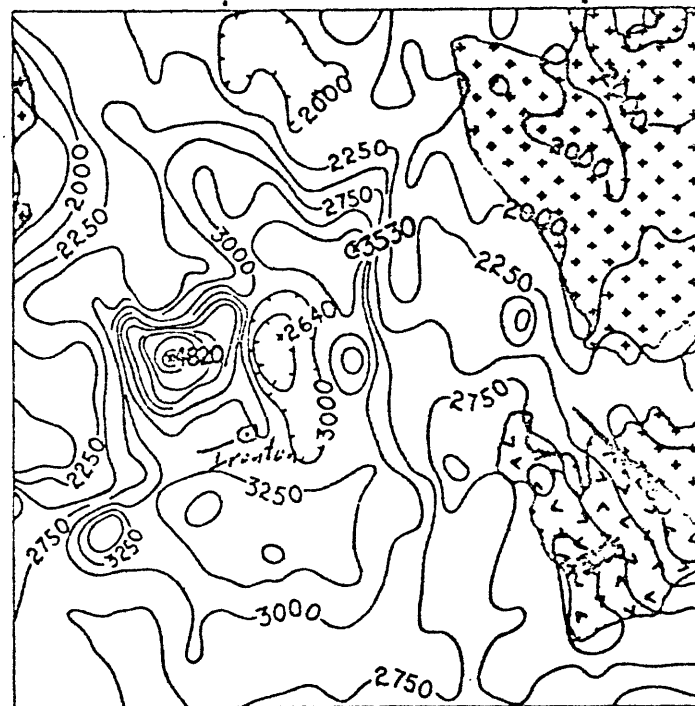
Figure 76 near here

was done by digital computer using the technique of Henderson (1960) to simulate magnetic data observed at different altitudes. The geology is generalized to four types of rock: granite, granite porphyry (granophyre), volcanic rocks (felsite and pyroclastic sedimentary detritus), and Paleozoic rocks of the shallow intermontane basins. Upward continuation to 3300 ft showed the area of highest magnetic intensity, which was interpreted as the thickest volcanic rocks having a north-south axis. The 2000-gamma contour marks the contact between granite and volcanic rocks. The Shepherd Mountain anomaly in the central part of the map, although diminished in amplitude, is nearly 800 gammas. The residual anomaly, less the effect of topography, represents magnetite-rich rock and a potential iron deposit (see fig. 52).

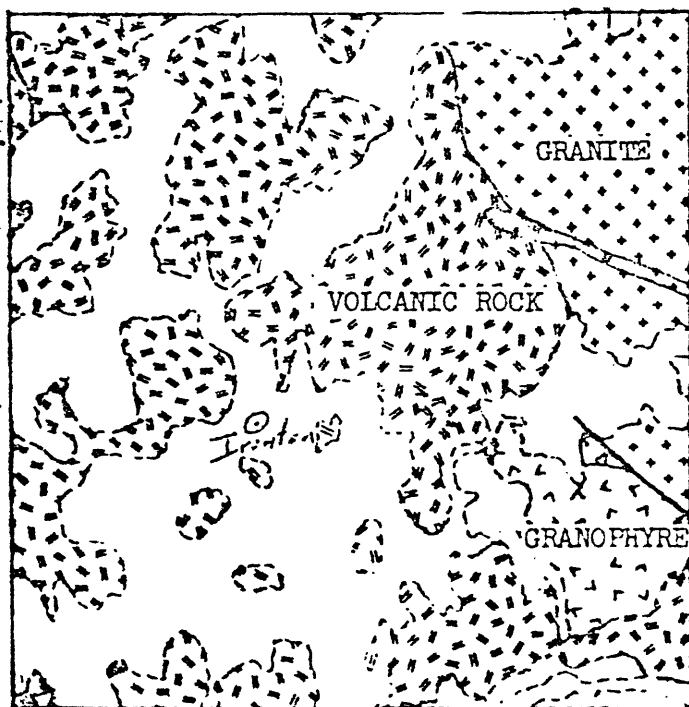
357



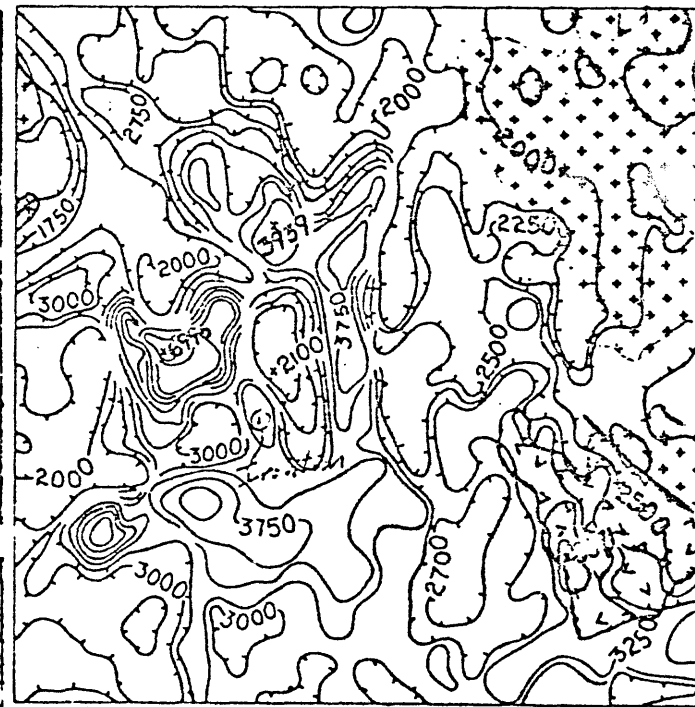
Plane of observation at 3300 feet



Plane of observation at 2000 feet



Igneous geologic



Plane of observation at 700 feet

Figure 76.--Correlation of exposed igneous rocks and derived magnetic fields in the Ironton area.

Downward continuation emphasizes anomalies related to the volcanic terrain, nevertheless the same anomalies, whether real, spurious, or less well-defined, were observed in the aeromagnetic field. The arcuate magnetic high outlines the volcanic ridge from Russell Mountain to Middlebrook Hill. Shepherd Mountain anomaly has an impressive amplitude of 4,000 gammas (Ironton quadrangle, fig. 2a). A thinner sequence of volcanic rocks surrounds this zone of magnetic highs. Magnetic lows partly define the areas of thin volcanic rocks. The magnetic highs may mark the sites of vents for the extrusive rocks. These fractured vents could provide loci for iron mineralization.

The magnetic effect of the thick block of volcanic rock in the Ironton area was isolated for interpretation by upward continuation. The synclinal nature of this block was corroborated by applying the unfolding test of Graham (1957) to the remanent magnetism of the rocks at its border (Ku and Scharon, 1965).

Indian Creek anomaly

Dark, dense trachyte exposed at Little Pilot Knob extends north-eastward in subsurface to form a resistant buried ridge near Indian Creek. The trachyte is more calcic and mafic than felsites of the St. Francois Mountains. Plagioclase is andesine; hornblende content ranges from 5-7%. This rock in outcrop and drill core has abundant large grains of disseminated magnetite as an accessory mineral. The magnetite content of the rock ranges from 0.5 to 5% but generally is less than 3.5%. Magnetite is considered to be a late phase of the trachyte that may have been mobilized and redeposited by metasonatic or hydrothermal processes related to emplacement of the granite batholith.

The trachyte has a high magnetic susceptibility that ranges from 3.5×10^{-3} to 15.4×10^{-3} emu/cm³ (Fig. 77 and Table 2). The total-intensity aeromagnetic anomaly exceeded 900 gammas, whereas ground magnetic surveys made by the Missouri Geological Survey (Cowie, 1946) showed anomalies having vertical intensities as much as 60,000 gammas near Little Pilot Knob. Variations in ground measurements are attributed to effects of lightning on the remanent magnetization of the outcropping trachyte. Deviations in compass readings corroborated the possible residual magnetic effect of lightning on the exposed volcanic rock. According to measurements of oriented samples, Cowie believes remanent magnetism is the major contributor to the anomaly at Little Pilot Knob. His average susceptibility of 6×10^{-3} emu/cm³ is in close agreement with the values obtained by the author.

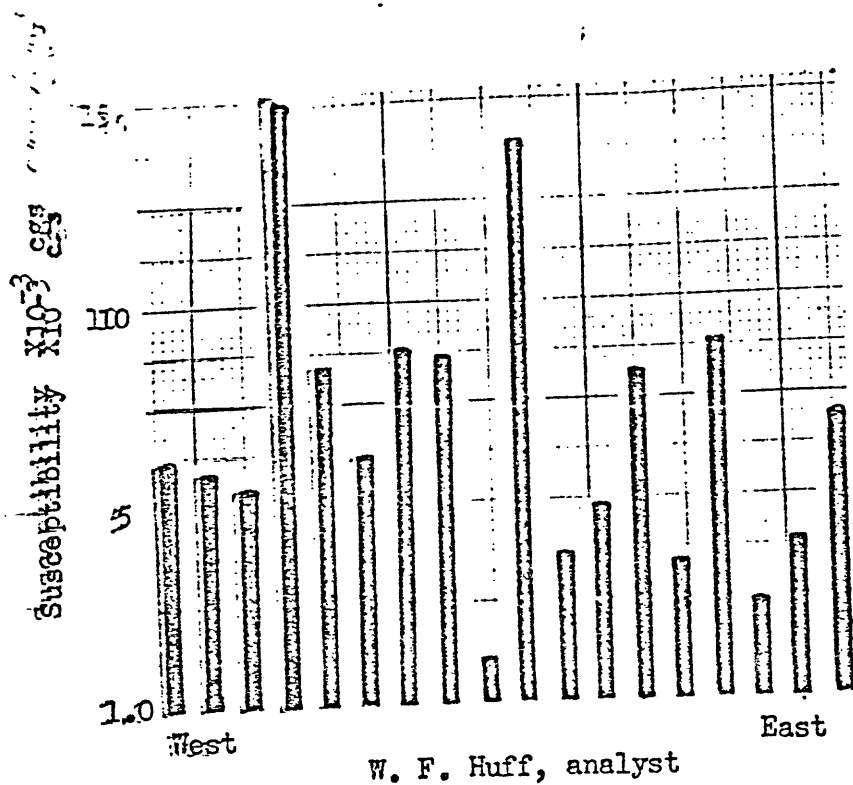


Figure 77.--Susceptibility of trachytic rocks cored from a buried ridge near Indian Creek, Missouri.

The correlation between the aeromagnetic anomaly and subsurface topography of the Precambrian volcanic rocks is shown in Figure 78.

Figure 78 near here

The magnetic gradients outline ridge of the volcanic rocks. This ridge can be represented by a prism of infinite depth (Fig. 79). The contacts here

Figure 79 near here

seem to be nearly vertical. Faulted contacts are inferred from the magnetic profiles. The magnitude of the anomaly indicates a rock of high susceptibility containing an abnormally high concentration of magnetite. Sufficient iron minerals may be present to warrant exploring these magnetic highs for potential iron deposits.

The buried ridge formed a platform for the accumulation of algal reefs and inter-reef detritus, which localized long, linear lead deposits on the flanks and saddles of the ridge (Snyder and Emery, 1956). According to Bain (1953) the Indian Creek Mine is now a major producer of lead. He states that the ore zone is about 4,000 ft long, 500-600 ft wide, and as much as 150 ft thick.

The grain of the magnetic pattern in the vicinity of the Indian Creek and Shirley anomalies indicates subsurface structures in the Precambrian of northeasterly trend; lows indicate faulting of a distinctly northeasterly trend and the magnetic highs are related to topographic or structural relief of similar trend. This interpretation is partly substantiated by out crop and subsurface drill data in the vicinity of Indian Creek and areas to the southwest.

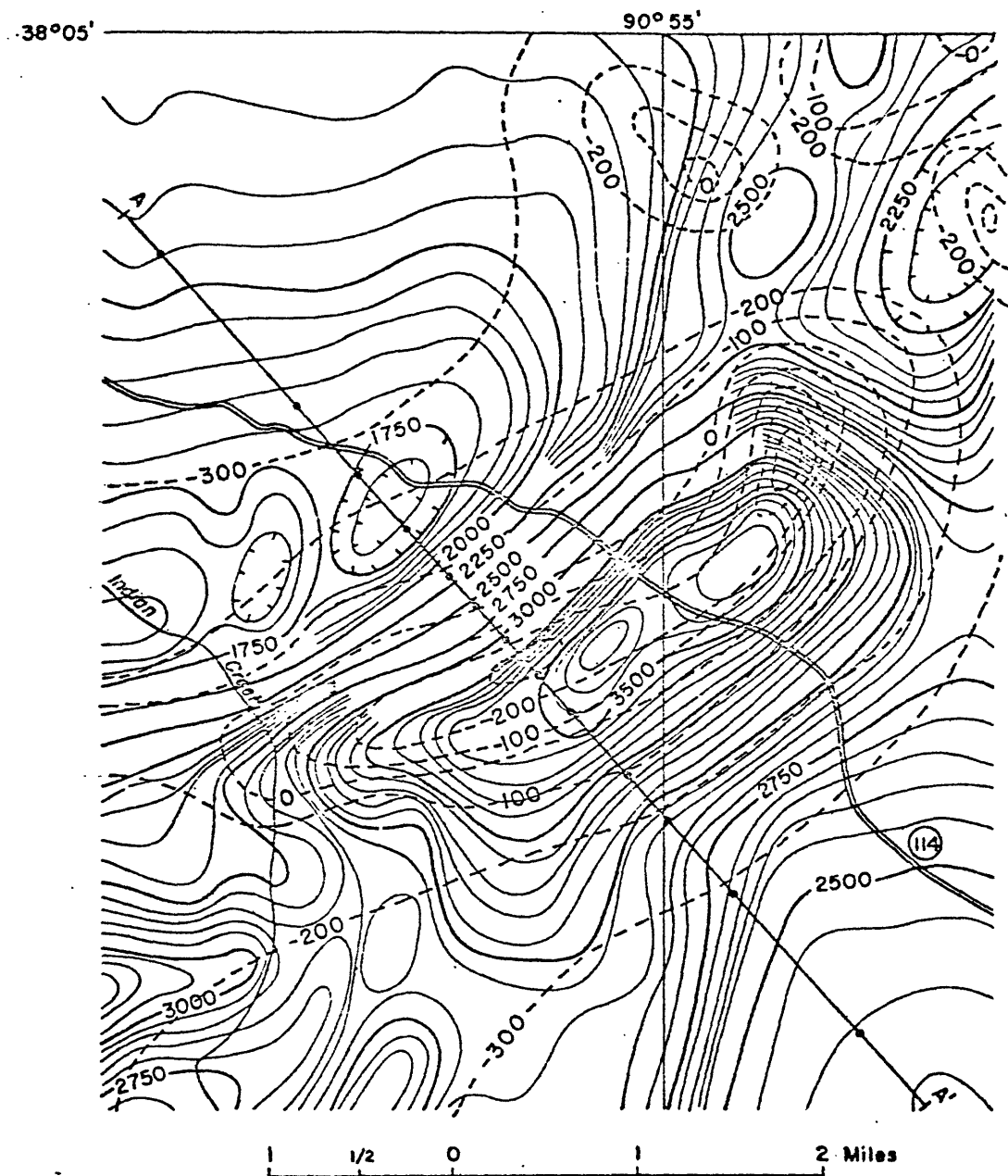


Figure 78.--Correlation between aeromagnetic anomaly (solid) and subsurface topography (dashed) of Precambrian rocks near Indian Creek.

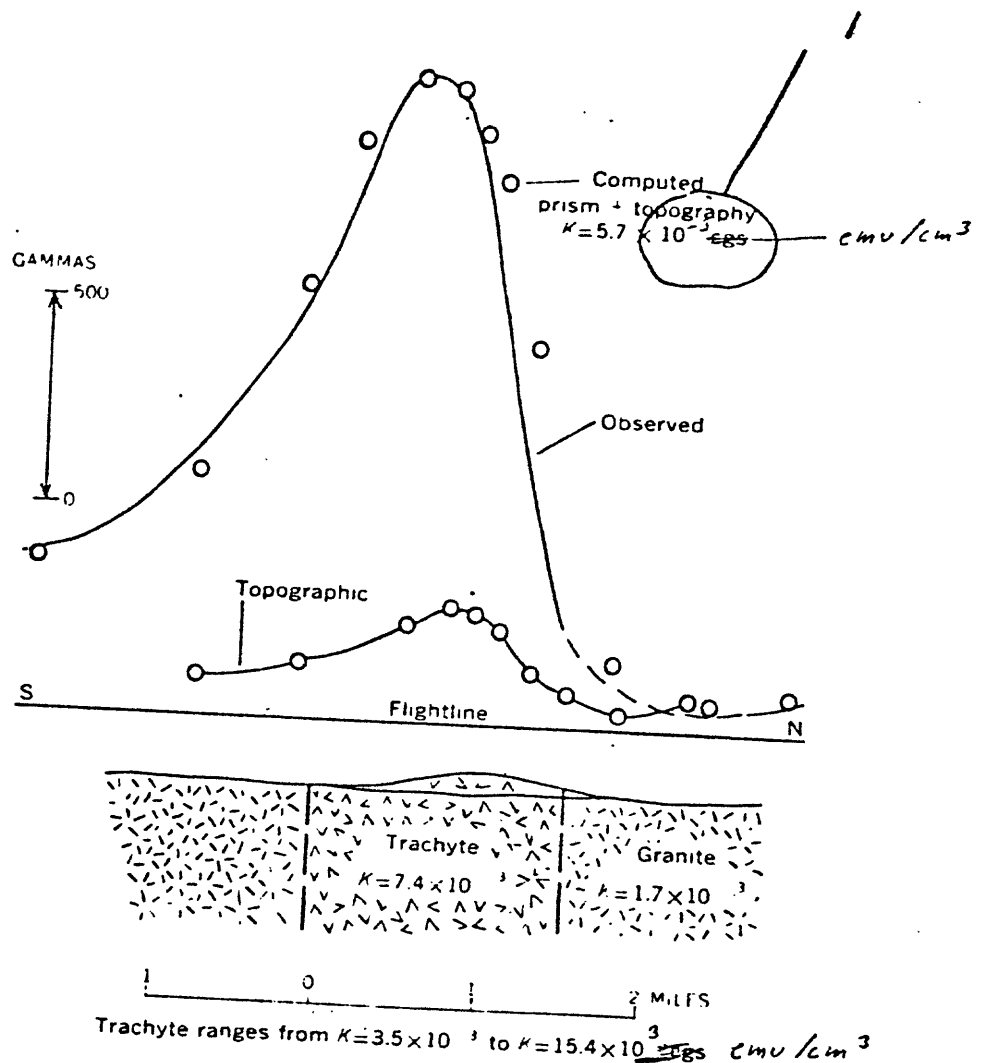


Figure 79.--Aeromagnetic profile over a ridge of trachyte of high susceptibility near Indian Creek.

Richwoods anomaly

Near Richwoods two nearly parallel magnetic anomalies are connected at the northern end to form a horseshoe-shaped feature (Fig. 80). Buried volcanic ridges are believed to produce this anomaly.

Figure 80 near here

These volcanic rocks represent roof pendants in the granite basement that floors most of the northern basins. The analytical methods demonstrated in the Bonne Terre mining area were applied to the Richwoods anomaly.

Both continuation of the observed field downward and the second-
vertical derivative outline the buried magnetic source by emphasizing anomalies
in the observed field (Figs. 81, 82, 83). Drilling by the St. Joseph Lead

Figures 81, 82, and 83 near here

Company indicated that the top of the Lamotte Sandstone is about 350 to 450 ft below sea level. Drilling information also indicates the presence of a basement ridge. Continuation of the field downward to about the level of the Precambrian basement produced the sharpest and best defined anomalies (Fig. 82). Alineament of magnetic lows and steep gradients implied possible fault zones in the basement. Ground measurements compare favorably with the aeromagnetic field continued to about ground level (Fig. 84). Residual lead deposits were mined in

Figure 84 near here

the vicinity of the town of Richwoods (Litton, 1855, p. 53-54) (Fig. 84). Between 1845 and 1854 two furnaces at Richwoods yielded about 500 tons of lead annually (Schoolcraft, 1819, p. 55). The pattern of the total-intensity anomaly, which has a magnitude of as much as 500 gammas in a distance of two miles, continued nearly to the Precambrian surface resembles the field observed over exposed volcanic rocks. The anomalies having the steepest gradients (fig. 84) are the most promising for the subsurface exploration of lead.

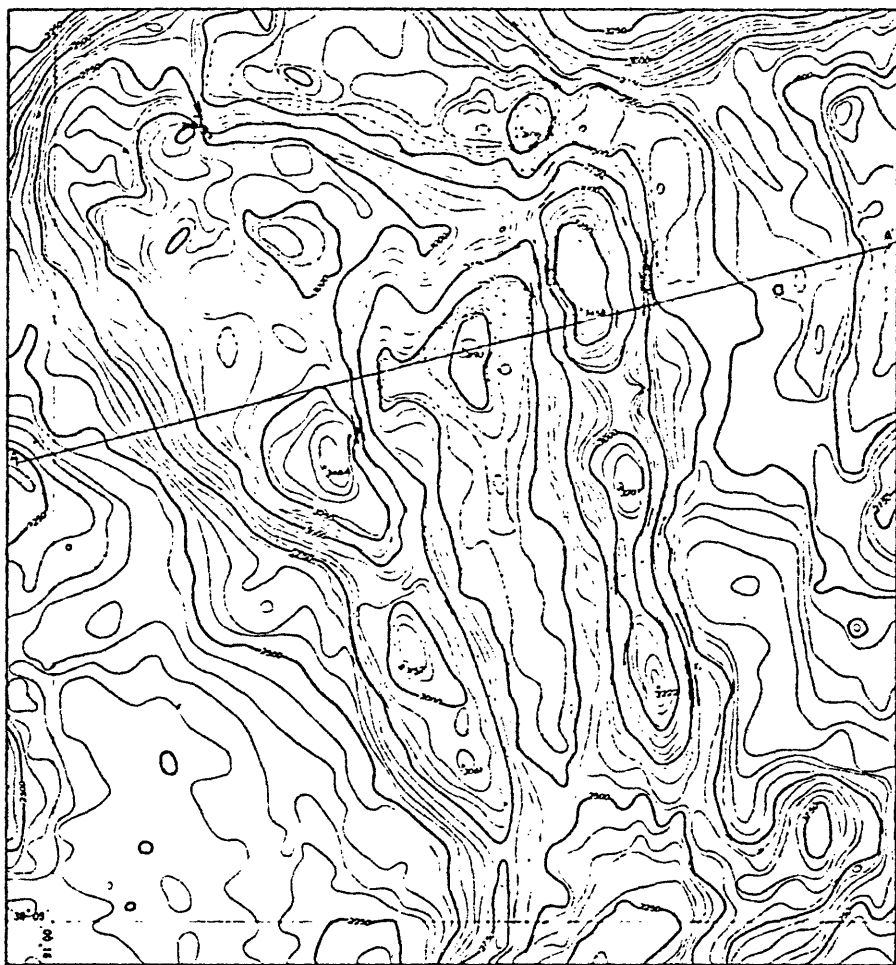


Figure 81.—Field of the Richwoods anomaly continued downward to 700 ft, about ground level.

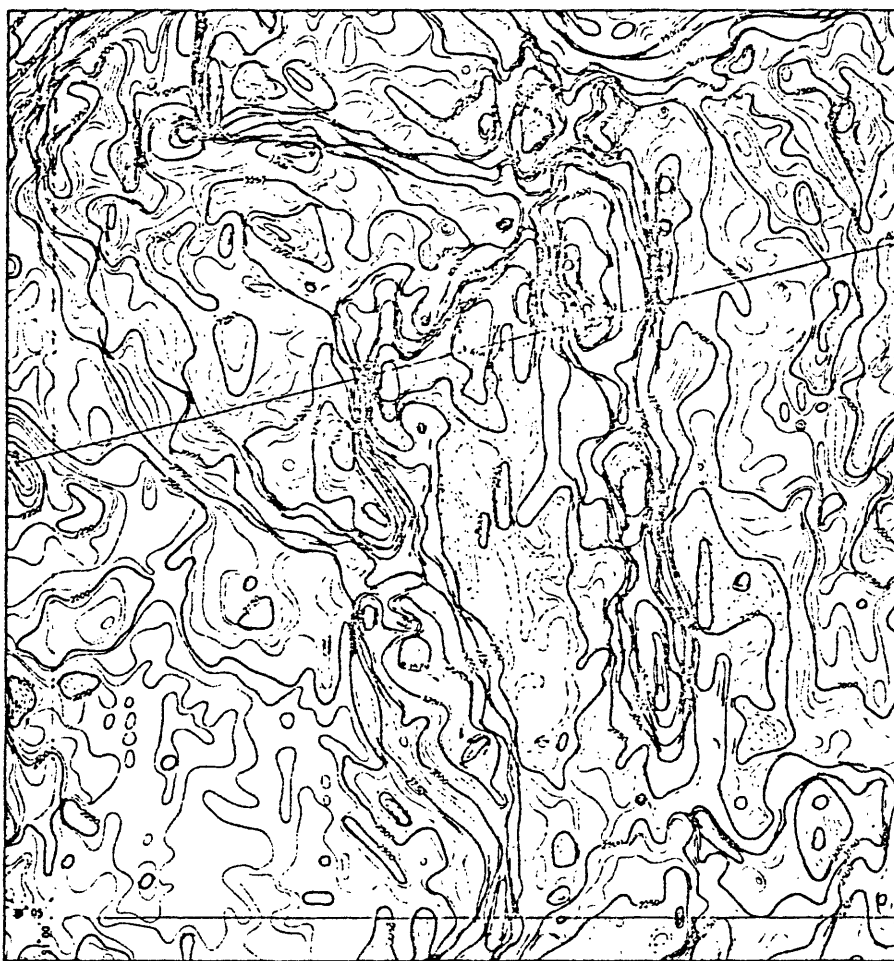


Figure 82.--Field of the Richwoods anomaly continued downward to 600 ft below sea level, nearly the Precambrian surface level.

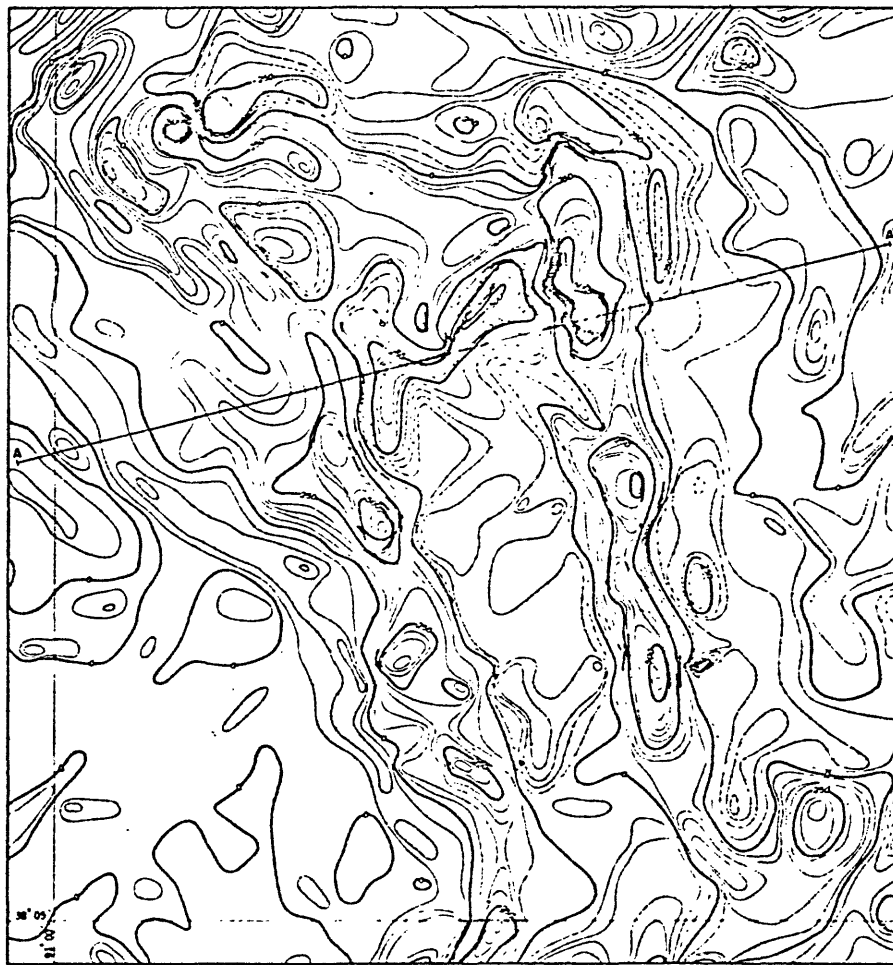


Figure 83.--Second-vertical derivative of the observed field in the Richwoods area.

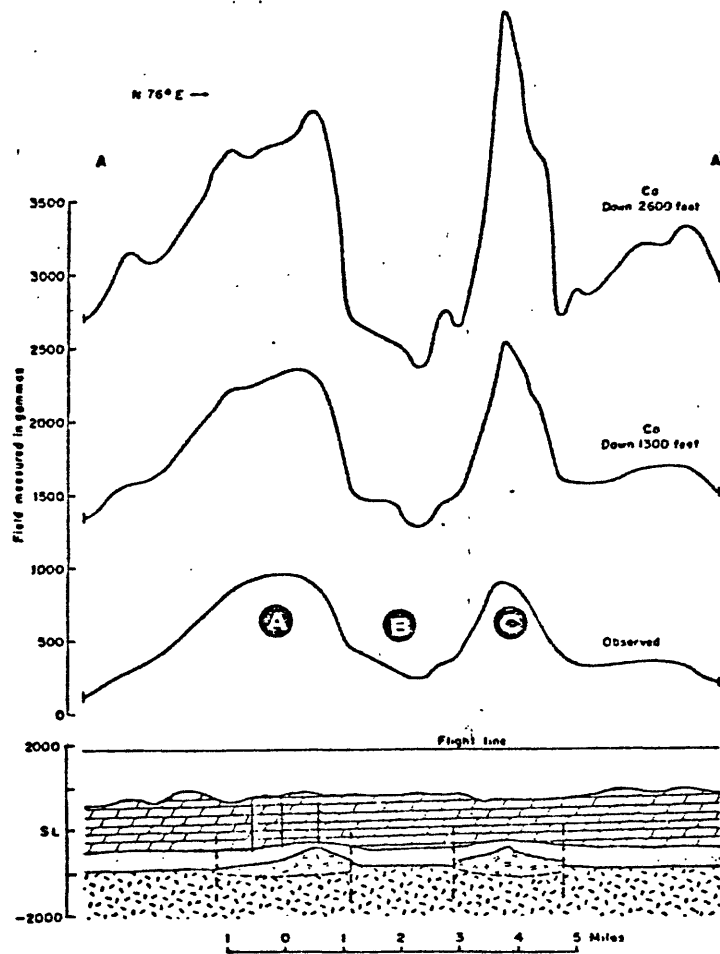


Figure 84.—Profiles across the Richwoods aeromagnetic anomaly showing the effect of downward continuation on the total-intensity field.

Avon anomaly

A buried pluton of diorite near Avon is believed to cause^{the observed} nearly circular magnetic anomaly of about 1000 gammas (Fig. 3). The pluton borders the southeast edge of the Avon structural block of Graves, which corresponds to the Farmington anticline of Weller and St. Clair. (1928). The Avon block is partly underlain by relatively nonmagnetic granite, which is joined on the east by the fine grained magnetic granite of Jonca Creek. The diorite intruded a zone of fracture in a large pendant of volcanic rock south of the arcuate Wolf Creek-Greasy Creek fault. These effusive rocks are in contact with granite similar to the red granite at Flatwoods (Fig. 2a). This granite merges with the granophytic rocks of the Fredericktown area. Tarr and Keller (1933, p. 815-825) described a diabase dike of post-Devonian age, which parallels the southeastern border of the Avon block. Rust (1937) mapped many igneous pipes north of the diorite pluton and concluded that they were diatremes. These mafic post-Devonian pipes are magnetically zoned according to Kidwell (1947). Holmes (1950) outlined these elliptically shaped pipes by the magnetic highs associated with magnetite concentrated at their borders. These small mafic intrusions may be genetically related to the diorite intrusion.

1 In profile (fig. 85), the nonmagnetic granite, in contact with

2 _____
3 Figure 85 near here

4 _____
5 more magnetic volcanic and fine-grained granitic rocks, produces a
6 characteristic aeromagnetic low. Magnetite-rich diorite produces most
7 of the observed anomaly. Some of the faults result in small irregulari-
8 ties of dips in the profile, especially the Higdon fault zone.

9 Granophyre produces a magnetic anomaly of the same magnitude as the
10 volcanic rock.

11

12

13

14

15-

16

17

18

19

20-

21

22

23

24

25-

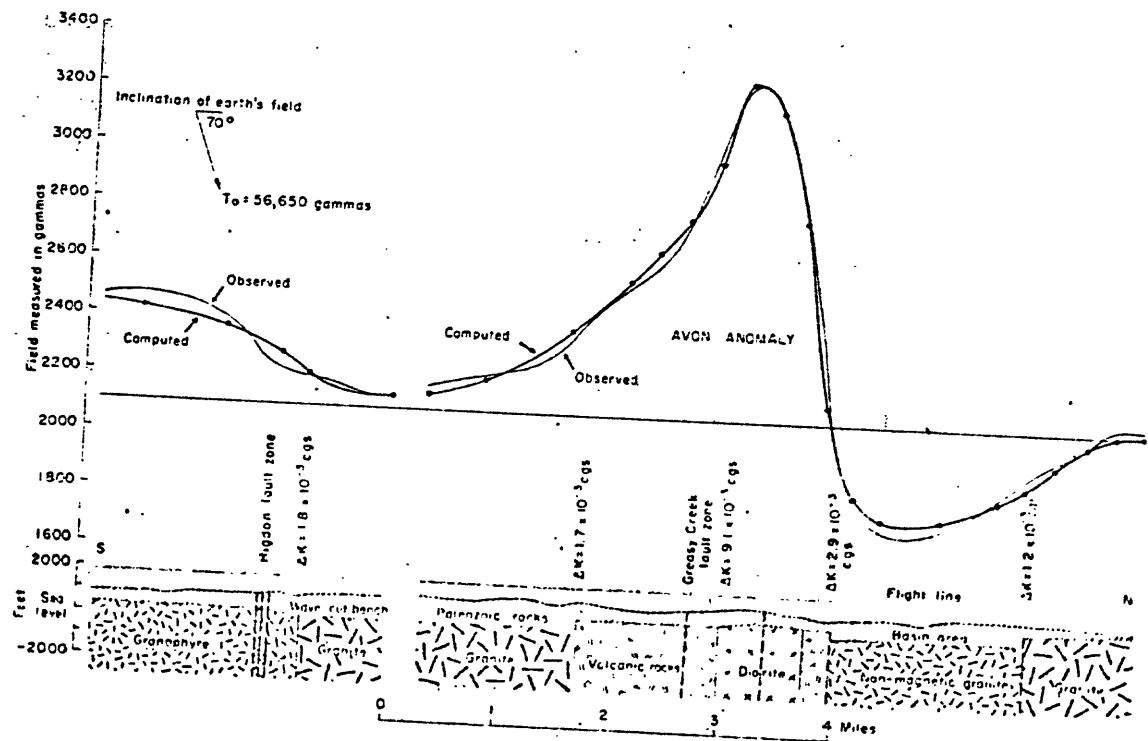


Figure 85.--Subsurface structure and intrusive relationships near Avon.

Gabbroic rocks

Numerous mafic dikes in the St. Francois Mountains were located by Haworth (1896), Koch (1932) and Wing (1932). Denham (1934) showed that the diabase at Skrainka intruded the contact between the granite and rhyolite. Jenke (1948) petrologically subdivided the mafic rocks in the Fredericktown quadrangle and discussed their intrusive relations.

According to D. H. Amos (written communication, 1960), the sheet-like gabbro bodies in the Ironton, Fredericktown, and Edgehill quadrangles range from 70-750 feet thick and dip from nearly horizontal to about 30° . The gross body has an east-west synclinal structure; the upper and lower contacts are parallel. The gabbroic rocks are sill-like bodies emplaced along the contact between the rhyolite pendants and the roof of the granite batholith. Plagioclase and augite, with or without olivine, are the major silicate minerals according to Desborough and Amos (1961).

Analysis of the gabbro sheet locally shows the body to dip steeply instead of the shallow dip indicated by the geologic relations. At Evans Mt., the contact between the gabbro and granite is well-exposed and dips 25-30° southward. East of this locality, magnetic information indicates a change from nearly vertical to about 45° southward. The magnetic anomalies range from 30 to 100 gammas. The magnetic susceptibility ranges from 0.3 to 12×10^{-3} emu/cm³. Olivine diabase contains about 3.5-5% magnetite and ilmenite in a 1:1 ratio according to D. H. Amos. Where the sills have differentiated, the gabbroic phases contain 7-10% magnetite. Where the body is thick and coarsely granular, the gabbro can be traced in granite by magnetic data. Multiple or thin sheets of gabbro cannot be resolved or traced by aeromagnetic profiles, mainly because of the low magnetite content or oxidation of the magnetite. Thick sequences of volcanic rock tend to mask the magnetic expression of the mafic sills.

Locally the gabbroic sills can be traced by patterns on the aeromagnetic profiles. The best magnetic expression of these mafic sills is shown in the southeastern part of the Ironton quadrangle by an arcuate magnetic gradient over Rock Creek and the drainage into Patterson Creek. A diabase sill is outlined a magnetic gradient from Carver Creek road northwestward to the Devils' Toll-Gate.

The gabbroic body that surrounds Bald Knob (Figs. 2a and 37) causes an aeromagnetic gradient southeastward around Smith Mountains to join a mafic sill on the west and north sides of Tin Mountain (Fig. 38), eastward to Hawkins Knob and then along the granite-rhyolite contact to Matthews Creek. The magnetic profiles also indicate that the gabbroic units at Holliday and Bevos Mountains are connected. The anomaly continues southeastward to Barnes Creek and then to the west side of Buckner Mountain. Figures 2, 2a, and 3 show the relationship between the gabbro and associated magnetic gradients.

The carbonate and clastic strata of the Ozark uplift are typical of a stable platform and shallow depositional environment. The relations of these flat-lying sedimentary beds to the Precambrian rocks show that the igneous terrain of the St. Francois Mountains has been a slightly positive area since Precambrian time.

The local distribution of epicenters of earthquakes on the flanks of the Ozark uplift appears to be related to zones of faulting according to Heinrich (1937, 1946, 1949, 1950, 1951 a,b). Heinrich (1941) stated that 85% of all seismic activity in Missouri originates in two areas: about 60% from the New Madrid area and 25% from the St. Marys area (Ste. Genevieve zone). The Ste. Genevieve fault system is one of the most seismically active fracture zones. Other epicenters are distributed along the northwest and southeast flanks of the uplift. The epicenters on the southeast flank are probably related to basement fractures at the margin of the Mississippi embayment (Heinrich, 1946). Epicenters on the Black Creek fault southwest of Bourbon and on the Moselle fault near Union further indicate that other major fractures surrounding the core of the Ozark uplift are seismically active.

Additional zones of faulting can be postulated from the association of earthquake epicenters and known faulting in the mid-continent region (Fig. 86). The west-trending Rough Creek fault system bifurcates east

Figure 86 near here

of the Ozark uplift. The fault trends northwestward as the Ste. Genevieve fault zone and southwestward as a buried seismically active fault zone. The St. Francois Mountains seems to buttress the stresses that are released through regional faults. The Palmer fault complex is the western extension of the Rough Creek system.

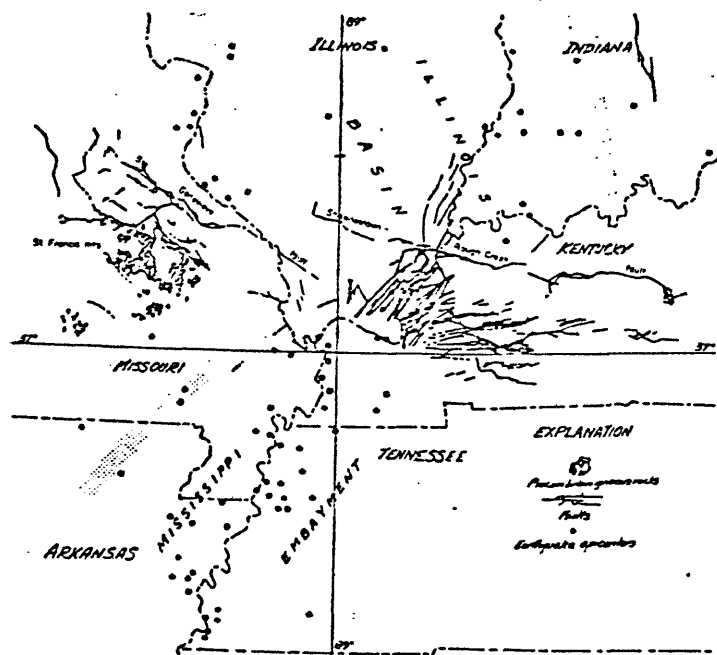


Figure 86.—Relations of faults and earthquake epicenters at the margins of the St. Francois Mountains, Mississippi embayment, and western Kentucky.

The crustal thickness in the Ozark region was estimated by Walter (1940). From an earthquake study, he obtained a thickness of 39 km. The crustal thickness at the boundary between the Ozark uplift and the embayment Mississippi was investigated by Reinhart and Meyer (1961). Their crustal models show a thick crust of 41-43 km associated with an area (fig. 89), of low elevation. Differences in the gravity anomalies, as much as 40 mgal in the isostatic anomalies, are difficult to reconcile with models having almost the same crustal thickness. Their models also show an intermediate boundary at about 10-11 km.

The general subsurface geologic structure of the Precambrian rocks in the core of this cratonic dome can be inferred from gravity and aeromagnetic information. Contrasts in the density, magnetic properties of the volcanic and granitic rocks permit a qualitative discussion of the grain or gross pattern of anomalies in relation to regional geologic features. Maps showing the exposed Precambrian geology, gravity anomalies, alignment of physiographic features, and trends of magnetic anomalies (Figs. 87, 88, and 89) were correlated in order to postulate subsurface Precambrian structural elements and lithologic units in southeastern Missouri. These structural features in the basement rocks are known to control or localize some mineral deposits such as iron in the Precambrian volcanic rocks and lead in the lower Cambrian strata.

Local gravity anomalies do not correlate with surface lithology of the thin sequence of sedimentary rocks.

(Gerlach and Scharon, 1960). These anomalies correlate with buried Precambrian topography according to Algermissen (1961). Gravity anomalies (Fig. 89) show good correlation with broad geologic units. A northwest trending rectangular gravity high correlates with some outcropping and subsurface volcanic and granitic rocks of the St. Francois Mountains. The high extends from Wayne County northwestward to the northern part of Franklin County.

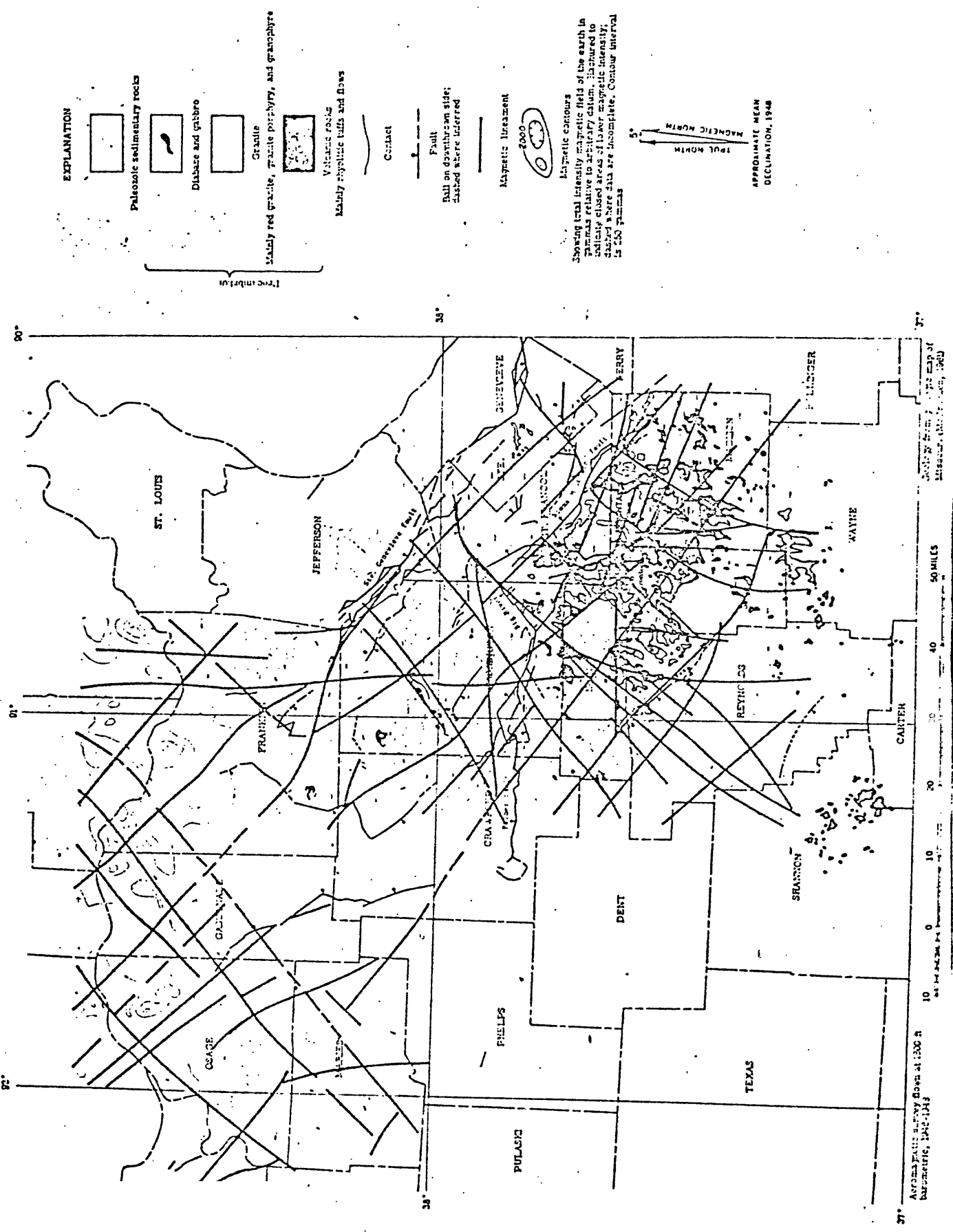


Figure 87.—Magnetic lineaments and exposed Precambrian rocks in southeastern Missouri.

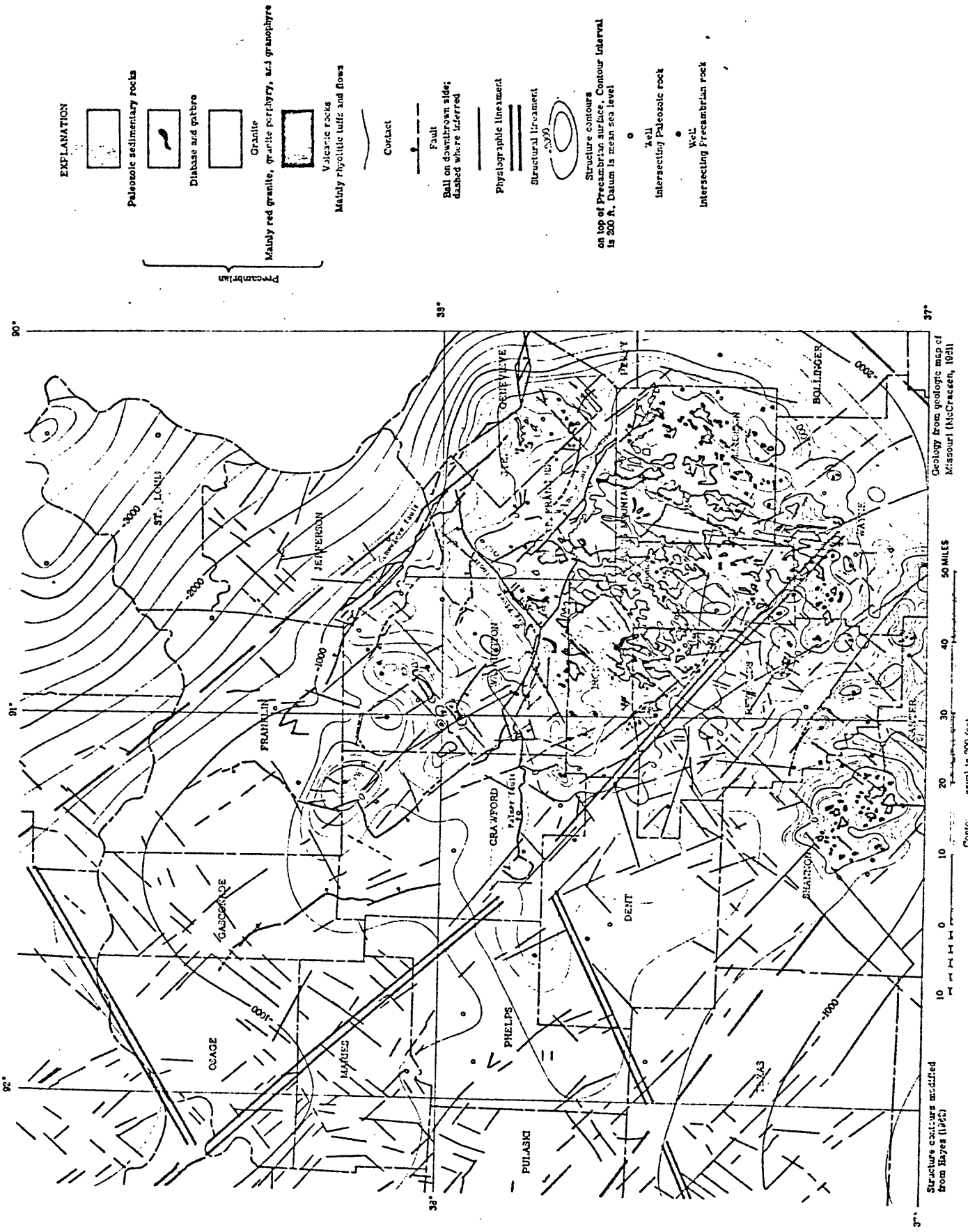


Figure 88.—Fracture systems, structural lineaments, and contours on

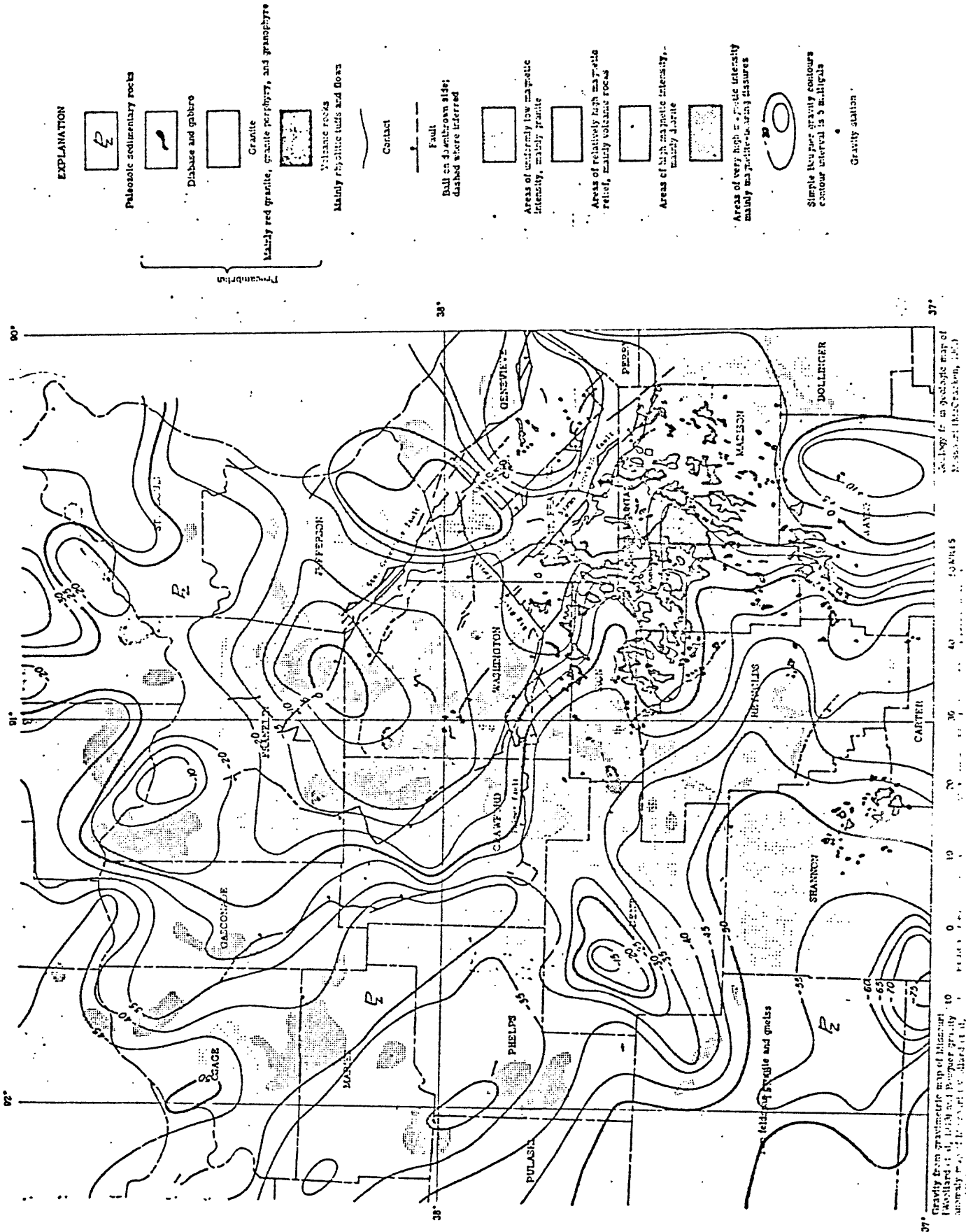


Figure 89.--Bouguer gravity, major subsurface magnetic units and inferred lithology.

Sources of the gravity anomalies are believed to be in the Precambrian basement rock. Depths estimated from the western gradient of the gravity high and the gradient over the Farmington Anticline, between St. Francois and St. Genevieve Counties, indicate shallow sources in the crust. Several thousand feet of sedimentary strata are needed to produce the 10 milligal anomaly observed in Washington and Franklin Counties. The source of this gravity high is not necessarily exposed or near-surface rocks but might be due to more mafic rock at depth.

Granite of Jonca Creek in St. Genevieve County is less dense as inferred from the corresponding gravity low. The large low west and southwest of the St. Francois Mountains in Texas, Howell and Shannon Counties is believed to be low-density granite.

Three small gravity highs in the northwest parts of Dent, Phelps, and Marie Counties ^{respectively} are believed to be caused by diorite intrusions. These anomalies are aligned on northwest trending gravity feature west of the St. Francois Mountains. The high in Dent County appears to correlate with dioritic rock detected in drilling samples (Grenia, 1960). The isolated highs in northwestern Phelps and Maries Counties probably are produced by the same mafic rock.

The physiographic lineaments show a rhombic pattern similar to the magnetic trends. Some lineaments coincide or parallel the magnetic trends. Correlation of physiographic patterns with known faulting is less pronounced. These lineaments trend northwestward and northeastward. The draping effect of the thin Paleozoic sedimentary cover against the Precambrian blocks (Fig. 86) shows in the rhombic pattern. These patterns reflect joint-controlled drainage and the effect of the buried Precambrian ridges (Zarzavatjian, 1958). Major structural lineaments that bound the St. Francois Mountains block parallel the direction of magnetic lineaments.

Magnetic lineaments trend predominantly northeastward and northwestward to form a rectangular or rhombic pattern. Comparison of trends of anomalies or gradients with faults show a good correlation. The St. Genevieve fault zone, Wolf Creek fault, and some small faults were extended beyond present mapping by use of aeromagnetic lineaments. These magnetic trends also outline granite-floored basins at Belleville (A), Sabula (B), and Goodwater (C) in Figure 3. Faults deduced from aeromagnetic data include the faults postulated by Graves (1932) for the Ironton area. Although the faulted coarse-grained granite seem to have subsided in areas such as the Belleville and Sabula basins, the buried coarse-grained granite block northwest of Avon seems to have been uplifted to form the Farmington anticline.

The magnetic gradients used to deduce fracture systems (Fig. 90)

Figure 90 near here

represent sharp contrasts between magnetic and nonmagnetic units.

Vertical intrusive contacts cause similar gradients. These contacts are magnetically indistinguishable from fault contacts except where fracture zones also cause magnetic lows as well as linear gradients such as associated with the Big River fault zone (figs. 3 and 60). Aeromagnetic patterns are locally more informative for near surface rock units than the gravity data. Areas of low magnetic relief containing small, low-amplitude anomalies that partly border the higher magnetic relief of the St. Francois Mountains may be used to outline areas of possible Cambrian archipelago environment (fig. 91), which is a locus of lead mineralization.

Figure 91 near here

Such an area may be the newly developed lead-mining area that extends southward from Czar Knob and Viburnum towards Oates (fig. 2a). The gross magnetic pattern is useful in distinguishing favorable basement structures; it does not indicate the sedimentary environment directly.

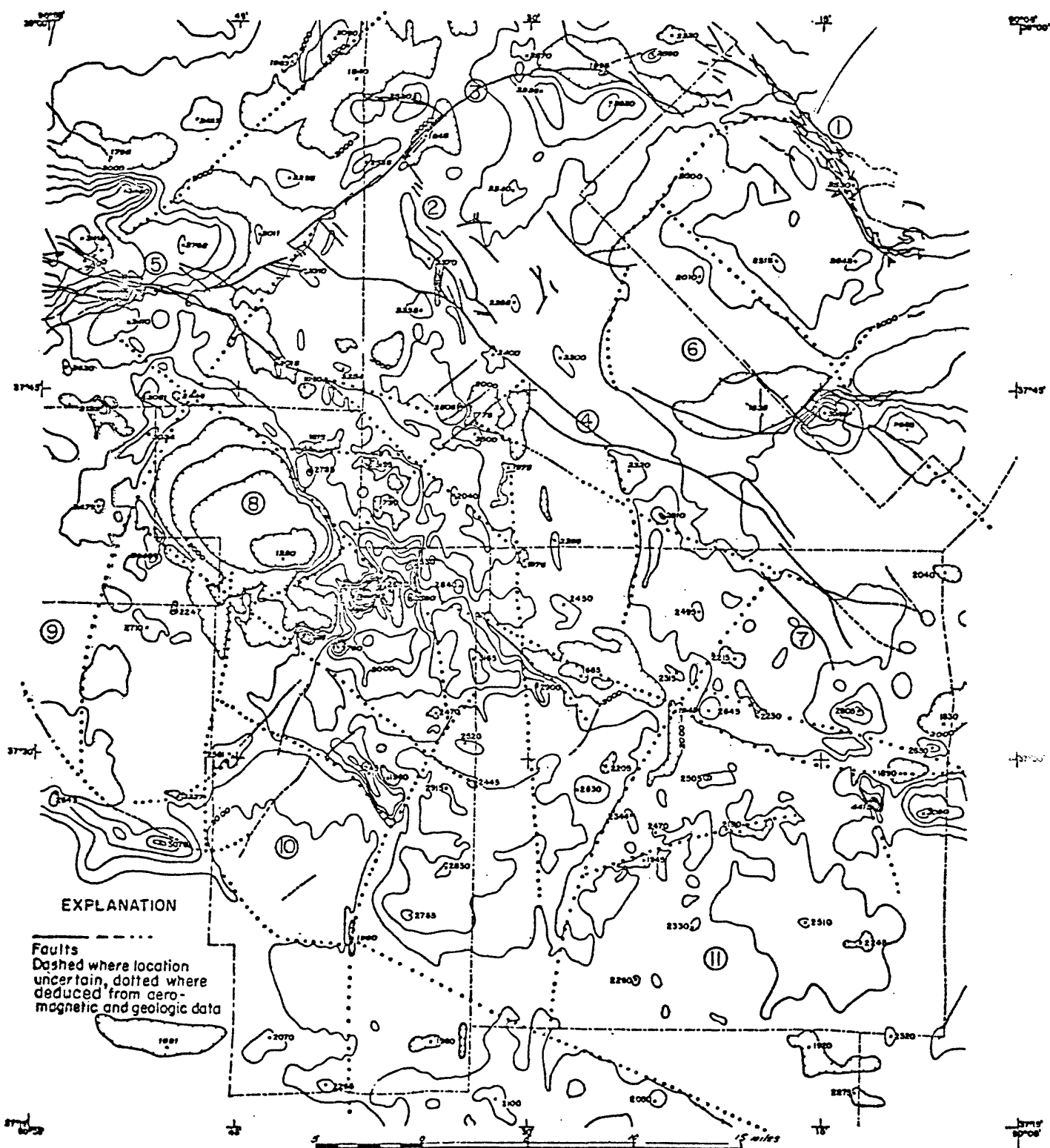


Figure 90.--Fractures deduced from aeromagnetic and geologic information.

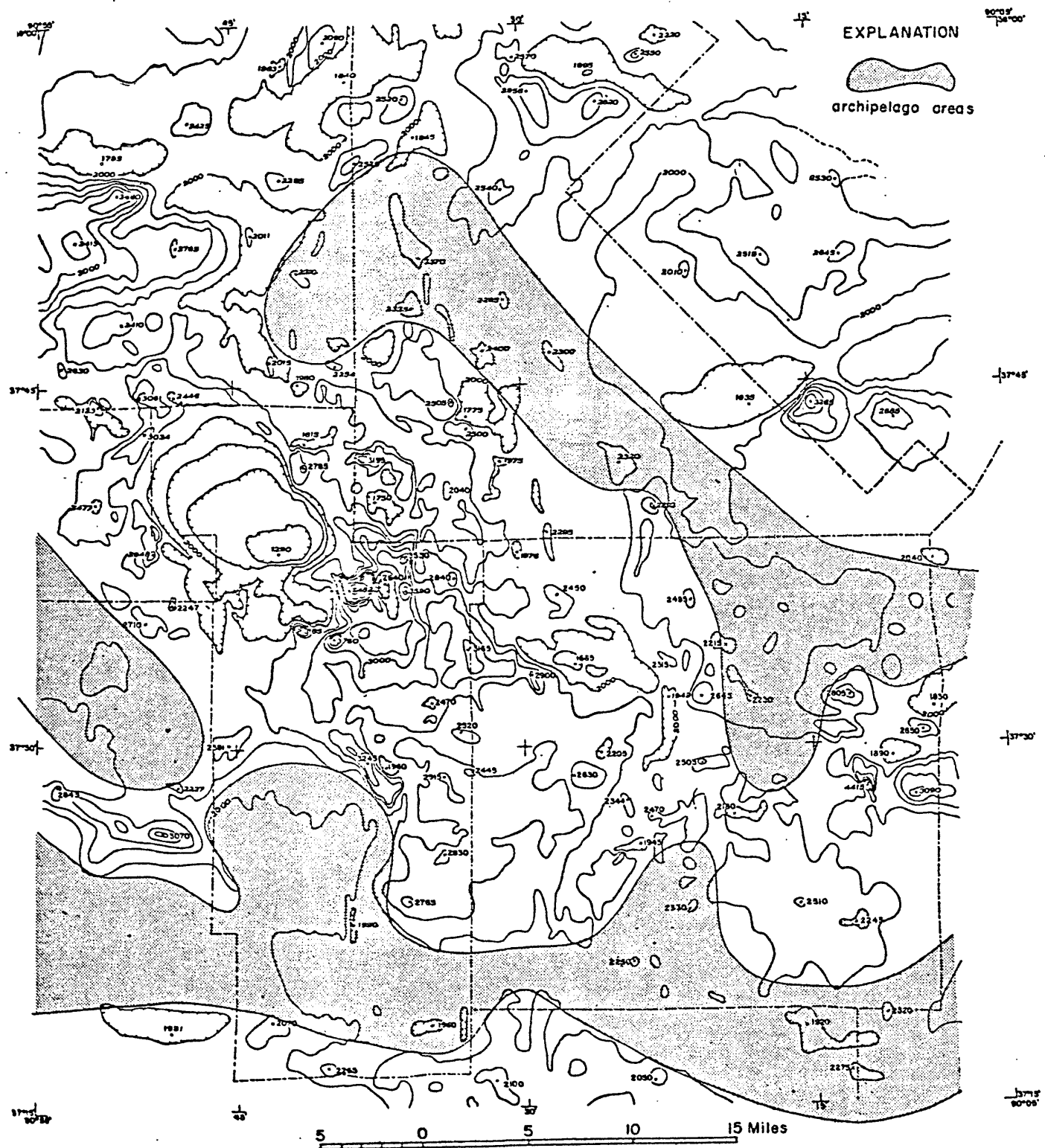


Figure 91.--Areas of postulated archipelago environment surrounding the St. Francois Mountains.

Resume and conclusions

The development of a mature landscape on the Precambrian surface left resistant hills of volcanic pendants on a granite terrane. The St. Francois Mountains formed an archipelago environment at the time this area was inundated by Cambrian seas. Atolls, wave-cut benches, sand bars, and shallow platforms permitted building of reefs and deposits of interlagoonal debris. A rhombic pattern of faults and major zones of fracture provided channelways for mineral-bearing solutions to reach sedimentary structures in the dolomitic limestone.

A study of the aeromagnetic information over the St. Francois Mountains shows that magnetic anomalies are useful in distinguishing (a) areas having potential economic iron deposits, (b) borders of basins having possible archipelago environments, (c) knobs and ridges having suitable sedimentary structures for localizing deposits of galena, (d) areas of faulting, (e) the attitude of igneous contacts, (f) subsurface configuration of volcanic pendants, and (g) different granitic rocks. These data are not only helpful in disclosing regional structures and thereby aiding the field geologist in mapping but are also helpful in delineating sites favorable for mineral exploration.

Many low-amplitude anomalies, up to 200 gammas in amplitude, are caused by topographic relief of the Precambrian surface. Some intermediate anomalies, 200-600 gammas in amplitude, are caused by lithologic inhomogeneities as well as topography. Low- to intermediate-amplitude anomalies should therefore be examined geologically where they are related to resistant igneous rocks that have topographic relief, which may structurally control economic mineral deposits in the overlying carbonate strata.

In the Bonneterre area, where subsurface geologic information is abundant, topography and major dislocations of the basement rocks and overlying sandstone correlate well with anomalies of the derived magnetic fields. The application of automatic computation to aeromagnetic data speeded interpretation of selected areas.

Magnetic relief of low-amplitude aeromagnetic anomalies was exaggerated by preparation of vertical derivatives or by continuation of the field downward. Contour maps of these intensified fields resembled or correlate with the Precambrian surface but do not uniquely define the configuration of the basement. Fields continued toward their source showed large vertical oscillations in profile where the field was continued to a depth beyond the basement contact; thus, continuation indirectly corroborated calculated depths to basement. Continuation of the aeromagnetic field to a level near the surface of the Precambrian rocks increased the amplitude of small low-amplitude anomalies whereby they were more easily distinguished from broad magnetic anomalies. Buried basement topography especially in areas of isolated volcanic roof pendants, was better defined by downward continuation rather than by derivatives or residuals of observed data. Downward continuation had greater resolving power than the other methods. As the gradient of the continued field and the vertical derivatives steepen in profile, presence of the pinchout line of the sand is more likely. This technique may be a useful guide in delineating more favorable areas for exploration. Continuation downward to the Precambrian surface yielded the best correlation with extensive mine workings in the lead district. The relations between these deposits and magnetic anomalies are useful guides for exploring the Ozark uplift.

The need for some conventional ground magnetic surveys, which are time-consuming and expensive, can be eliminated by simulating data at ground level by downward continuation of aeromagnetic data, unless the added resolving power of being closer to the source is needed.

These interpretative techniques can be used on aeromagnetic data elsewhere in the mining district of southeastern Missouri to deduce areas of likely buried topography and faults and, thus, to delineate areas favorable for exploration of ore deposits.

The shallow sedimentary basins surround the St. Francois Mountains are potential areas of exploration for lead deposits. The area enclosed by the sea level contour on the Precambrian surface encompasses many of these shallow basins.

References

1 Ade-Hall, J. M., 1965, The magnetic properties of some submarine oceanic
2 lavas: Royal Astron. Soc. Geophys. Jour., v. 9, no. 1, p. 85-91.

3 Algermissen, S. T., 1961, Underground and surface gravity survey,
4 Leadwood, Missouri: Geophysics, v. 26, no. 2, p. 158-168.

5 Allen, V. T., and Fahey, J. J., 1952, New occurrences of minerals at
6 Iron Mountain, Missouri: Am. Mineralogist, v. 37, p. 736-743.

7 Allen, V. T., Hurley, P. M., Fairbairn, H. W., and Pinson, W. H.,
8 1959, Age of Precambrian igneous rocks of Missouri: Geol. Soc.
9 America Bull., v. 70, no. 12, p. 1560-61.

10 Allingham, J. W., 1958, Low-amplitude anomalies in S. E. Missouri
11 [Abs.]: Geophysics, v. 25, no. 5, p. 1057.

12 _____, 1960, Interpretation of aeromagnetic anomalies in
13 southeast Missouri: Art. 95 in U. S. Geol. Survey Prof. Paper
14 400-B, p. B216-B219.

15 _____, 1961, Aeromagnetic interpretation of zoned intru-
16 sions in Northern Maine: Art. 387 in U. S. Geol. Survey Prof.
17 Paper 424-D, p. D265-266.

18 _____, 1964, Low-amplitude aeromagnetic anomalies in
19 southeastern Missouri: Geophysics, v. 29, no. 4, p. 537-552.

20 _____, (in press), Aeromagnetic anomalies in the Bonne
21 Terre area of the southeast Missouri Mining district: Geophysics

22 Allingham, J. W., and Bates, R. G., 1961, Use of geophysical data to
23 interpret geology in Precambrian rocks of Central Wisconsin:
24 Art. 394 in U. S. Geol. Survey Prof. Paper 424-D, p. D-292-296.

Anderson, L. A., 1961, A remanent magnetometer and magnetic susceptibility bridge: Art. 282 in U.S. Geol. Survey Prof. Paper 424-C, p. C370-C372.

Anderson, R. E., 1962, Igneous petrology of the Taum Sauk area, Missouri: unpublished Ph. D. thesis, Washington Univ., St. Louis, 100 p.

Anderson, R. E., and Scharon, H. L., 1961, Notes on the geology of the Taum Sauk area in Guidebook to the Geology of the St. Francois Mountain area: Mo. Div. Geol. Survey and Water Res. Rept. Inv. 26, p. 119-121.

Bain, C. K., 1963, St. Joseph Lead's Indian Creek Development: Mining Eng., v. 5, no. 9, p. 899-904.

Bain, H. F., 1901, Lead and zinc deposits of the Ozark region: U. S. Geol. Survey 22nd Ann. Rept., pt. 2, p. 23-227.

Ball, S. H., 1961, Lead mines of Washington County, Missouri: Min. and Sci. Press, v. 113, no. 22, p. 807-810.

Beckman, H. C., 1927, Water resources of Missouri: Mo. Bur. Geol. and Mines, v. 20, 2nd Ser., 424pp.

Beveridge, T. R., 1958a, Basic research at Missouri Geological Survey leads to Pea Ridge iron ore discovery: Mo. Engineer, v. 22, no. 1 12, p. 4-5.

_____, 1958b, Pea Ridge iron discovery: Mo. Div. Geol. Survey and Water Res., 6th Bienn. Rept. State Geologist, 1956-1958, p. 5-6.

Bonham, L. C., 1948, The geology of the southwest part of the Ironton quadrangle, Missouri: unpublished M.S. thesis, Washington Univ., St. Louis,

Bower, M. E., 1960, Geophysical interpretation of the magnetic anomaly at Marmora, Ontario: Canada Geol. Survey Paper 59-4, 11 p.

Branson, E. B., 1944, The geology of Missouri: Missouri Univ. Studies, Quart., v. 19, no. 3, 535 p.

Breitnwicher, R. H., and Richter, J. B., 1953, Geology of the northern half of the Marquand quadrangle, Madison and Bollinger Counties, Missouri: unpublished M.A.A. thesis, Univ. of Michigan, Ann Arbor.

Bridge, Josiah, 1930, Geology of the Eminence and Cardareva quadrangles: Mo. Bur. Geol. and Mines, v. 24, 2d. ser., p. 59-64.

_____, 1937, The correlation of the Upper Cambrian sections of Missouri and Texas with the section in the Upper Mississippi Valley: U. S. Geol. Survey Prof. Paper 186-L, p. 233-237

Bridge, Josiah, and Dake, C. L., 1929, Initial dips peripheral to resurrected hills: Missouri Bur. Geol. and Mines, 55th Bienn. Rept., State Geologist, 1927-1928, app. 1, p. 93-99.

Broadhead, C. G., 1877, Southeast Missouri lead district: Am. Inst. Mining Engineers Trans., v. 5, p. 100-107.

_____, 1889, The geological history of the Ozark uplift: Am. Geologist, v. 3, p. 6-13.

Brown, J. S., 1958, Southeast Missouri lead belt in Geol. Soc. America Guidebook, St. Louis, meeting, 1958, p. 1-7.

Brown, J. S., and Snyder, F. G., 1958, Discussion of lead isotope data for southeast Missouri (abs.): Econ. Geology, v. 54, no. 7, p. 1345.

Buckley, E. R., 1908, lead and zinc resources of Missouri: Am. Min. Cong. Proc., 10th Ann. Sess., Rpt. Proc., p. 282-297.

_____, 1909, Geology of the disseminated lead deposits of St. Francois and Washington Counties: Mo. Bur. Geol. and Mines, v. 9, 2nd ser., 2 pt., 259 p.

Buckley, E. A., and Buehler, H. A., 1904, Quarrying industry of Missouri: Mo. Bur. Geology and Mines, v. 2, 2d. Ser., 434 p.

Buehler, H. A., 1907, The lime and cement resources of Missouri: Mo. Bur. Geol. and Mines, v. 6, 2nd Ser., 255 p.

_____, 1919, Geology and mineral deposits of the Ozark region: Am. Inst. Mining Metall. Engineers Trans., v. 58, p. 389-408.

_____, 1832, The disseminated-lead district of southeastern Missouri: Intermat. Geol. Cong. 16th, U. S., Guidebook 2, p. 44-45.

Burgchardt, C. R., 1952, Geology of the northwest portion of the Richwoods Quadrangle, Missouri: Unpublished M.A. thesis, Univ. of Iowa, Iowa City.

Burke, R. F., 1951, The geology and mineralogy of St. Clair mining district, Franklin and Washington Counties, Missouri: unpublished M. A. thesis, Univ. of Missouri, School of Mines and Met., Rolla.

Chandick, K. C., 1950, A detailed gravimetric survey of an area immediately south and east of St. Charles, Missouri:

Unpublished M. A. thesis, St. Louis Univ., St. Louis.

Chauvenet, Regis, 1874, Chemical analyses: Mo. Geol. Survey Rept. 1873-1874, p. 706-734.

Clark, E. L., Scofield, N. L., and Koenig, J. W., 1956, Bibliography of the geology of Missouri 1945-1955: Mo. Div. Geol. Survey and Water Res., v. 38, 2d ser., 146 p.

Clark, S. K., and Royds, J. S., 1948, Structural trends and fault systems in Eastern Interior Basin: Am. Assoc. Petroleum Geologists Bull., v. 32, no. 9, p. 1728-1749.

Cobb, H. 1874, Notes on the history of lead mining in Missouri: Mo. Geol. Survey Rept., 1873-74, p. 672-685.

Collier, J. E., 1953, Geography of the northern Ozark border region in Missouri: Mo. Univ. Studies, Quart., v. 26, no. 1.

Cowie, R. H., 1946, Report on a magnetic anomaly in Washington County, Missouri: Mo. Div. Geol. Survey and Water Res., open-file report, 11 p.

Cozzens, A. B., 1941, The iron industry of Missouri: Mo. Historical Rev., v. 35, no. 4, p. 509-538.

Crane, G. W., 1912, The iron ores of Missouri: Missouri Bur. of Geol. and Mines, v. 10 2d ser. 434 p.

Crowe, H. M., 1938, The geology of the western third of the Coldwater quadrangle, Missouri: unpublished M. S. thesis, Washington Univ., St. Louis.

Curtis, A. D., and Dott, R. H., Jr., 1951, The geology of the northern half of the Coldwater quadrangle, Madison County, Missouri: Unpublished M. A. thesis, Univ. of Michigan, Ann Arbor.

Dake, C. L., 1930, Geology of the Potosi and Edgehill quadrangles: Mo. Bur. Geol. and Mines, v. 23, 2nd Ser., 233 p.

Dake, C. L., and Bridge, Josiah, 1926, Early diastrophic events in the Ozarks (abs.): Geol. Soc. America Bull., v. 38, p. 157-158.

_____, 1932, Buried and resurrected hills of Central Ozarks: Am. Assoc. Petroleum Geologists Bull., v. 16, no. 7, p. 629-652.

Davis, G. L., Tilton, G. R., Aldrich, L. T. and Wetherill, G. W., 1958, The age of rocks and minerals: Annual report of the Director of the Geophysical Laboratory, 1957-1958, Carnegie Inst. of Wash., p. 176-181.

Degenfelder, G. J., 1950, Geology of the southwest portion of the Berryman quadrangle, Missouri: unpublished M. A. Thesis, Univ. of Iowa, Iowa City, Iowa.

Deel, S. A., and Howe, H. H., 1948, United States magnetic tables and magnetic charts for 1945: U.S. Coast and Geod. Survey Ser. 667, 137 p.

Dempsey, W. J., and Meuschke, J. L., 1951, Total-intensity aeromagnetic map of the Sullivan and part of the Union quadrangles, Missouri: U.S. Geol. Survey Geophys. Inv. Map GP78.

Dempsey, W. J., and Duffner, R. T., 1949, A total-intensity aeromagnetic map of Coldwater quadrangle, Missouri: U. S. Geol. Survey Geophys. Inv. Map.

_____, 1949b, Total-intensity aeromagnetic map of Des Arc quadrangle, Missouri: U. S. Geol. Survey Geophys. Inv. Map.

_____, 1949c, Total-intensity aeromagnetic map of Fredericktown quadrangle, Missouri: U. S. Geol. Survey Geophys. Inv. Map.

_____, 1949d, Total-intensity aeromagnetic map of Ironton quadrangle, Missouri: U. S. Geological Survey Geophys. Inv. Map.

Denham, R. L., 1934, Igneous rocks at Skrainka, Madison County, Missouri: unpublished M. S. thesis, 49 p., Washington Univ., St. Louis.

Desborough, G. A., and Amos, D. H., 1961, Ilvaite: A late magmatic occurrence in gabbroic rocks of southeastern Missouri: Am. Mineralogist, v. 46, p. 1509-1511.

Doan, E. B., Paseur, J. E., and Fosberg, F. R., 1960, Basic aspects, in military geology of the Nujako archipelago, Ryukyu-Retto, Part I: Military Geology Branch, U. S. Geological Survey, for Intell. Div., Office of the Engineer, CHQ, Far East Command, pl. 30-114.

Dobrin, M. B., 1952, Introduction to Geophysical Prospecting: New York, McGraw-Hill, 435 p.

Doell, R. R., and Cox, Allan, 1961, Paleomagnetism in Advanced in Geophysics: New York, Academic Press, v. 8, p. 221-313.

Farnham, F. C., 1943, Magnetic map of Missouri showing anomalies of vertical intensity: Mo. Geol. Survey and Water Res. Map.

Hardley, A. J., 1962, Structural geology of North America: New York, Harper & Row, 743 p.

Eckelmann, F. D., Kulp, J. L., and Brown, J. S., 1956, Lead Isotopes and the pattern of mineralization in southeast Missouri (abs.): Geol. Soc. America Bull., v. 67, no. 12, pt. 2, p. 1689-1690.

Eckelmann, F. D., Brown, J. S., and Kulp, J. L., 1957, Relationships between lead isotope composition, pattern of mineralization, and composition of ore solutions in the Bonne Terre Mine, southeastern Missouri (abs.): Am. Geophys. Union Trans., v. 38, no. 3, p. 390.

Elkins, T. A., 1951, The second derivative method of gravity interpretation: Geophysics, v. 16, p. 29-50.

Erickson, J. W., 1950, The geology of the northwest quarter of the Berryman quadrangle, Missouri: unpublished M. S. thesis, Univ. of Iowa, Iowa City.

Evjen, H. M., 1936, The place of the vertical gradient in gravity interpretation: Geophysics, v. 1, p. 127-136.

→ Farnham, F. C., Muilenberg, G. A., Reinoehl, C. O., and Grohskopf, J. G., 1931, Geophysical prospecting: Mo. Bur. Geol. and Mines, Bienn. Rept. State Geologist, 1929-30, app. 3, p. 146-151.

Farnham, F. C., and Van Nostrand, R. G., 1941, Some measurements of magnetic susceptibility of rocks [abs.]: Mo. Acad. Sci. Proc. 1940, v. 6, no. 4, p. 90-91.

Fenneman, N. M., 1938, Physiography of eastern United States: New York, McGraw-Hill Book Co.

Fisher, R., 1953, Dispersion on a sphere: Royal Soc. London Proc., Ser. A, v. 217, p. 295.

← Ford, R. J., 1962, Geophysical interpretation of an airborne field intensity survey: unpublished M. A. thesis, St. Louis Univ., St. Louis.

Fox, J. H., 1953, A magnetic study of a northeastern Ozark fold: unpublished M. A. thesis, St. Louis Univ., St. Louis.

Frank, A. J., 1948, Faulting on the northeastern flank of the Ozarks [abs.]: Geol. Soc. America J. Ll., v. 59, p. 1322.

_____, 1958, Magnetic data and petrographic analyses of Precambrian rocks of Missouri [abs.]: Geol. Soc. America Bull., v. 69, no. 12, p. 1566-67.

French, G. B., 1956, Pre-Cambrian geology of the Washington County area, Missouri: unpublished M. A. thesis. Univ. of Missouri, School of Mines and Met., Rolla.

Gabriel, W. J., 1950, A bedrock topography survey by the electrical resistivity method: unpublished M. S. thesis, St. Louis Univ., St. Louis.

Gage, J. R., 1874, Lead mines, southeast Missouri: Mo. Geol. Survey Rept. 1873-74, p. 602-637.

Gallaher, J. A., 1900, Preliminary report on the structural and economic geology of Missouri: Mo. Bur. Geol. and Mines, 259 p.

Ganguli, D., 1955, Gravity survey of part of St. Clair quadrangle, Missouri: unpublished M. A. thesis, St. Louis Univ., St. Louis.

Gerlach, G. S., and Scharon, H. L., 1960, A regional gravity of the St. Francois Mountains of Missouri (abs.): Jour. Geophys. Research, v. 65, no. 8, p. 2492-2493.

Grave, O. R., 1943, Manganese deposits of Missouri: Mo. Geol. Survey and Water Res., 62nd Bienn. Rept. State Geologist, 1941-1942, p. 7

Giles, A. W., 1939, Structural features of the Mississippi Valley region and their relation to mineralization: Geol. Soc. America Spec. Paper no. 24, p. 39-49.

Goebel, E. D., 1951, Paleozoic formations of the Ironton Quadrangle, Missouri: unpublished M. S. thesis, Univ. of Iowa, Iowa City.

Gooding, A. M., 1951, Geology of the southwest portion of the Richwoods Quadrangle, Missouri: unpublished M. S. thesis, Univ. of Iowa, Iowa City.

Graham, J. W., and others, 1957, Stress-induced magnetizations of some rocks with analysed magnetic minerals: Jour. Geophys. Research, v. 62, p. 465.

Graves, H. B., Jr., 1938, The Precambrian structure of Missouri: St. Louis Acad. Sci. Trans., v. 29, no. 5, p. 111-164.

Grave, O. R., 1945, Pyrite deposits of Missouri: Mo. Geol. Survey and Water Res., v. 30, 2nd ser., 482 p.

Green, R., 1960, Remanent magnetization and the interpretation of Magnetic anomalies: Geophys. Prosp., v. 8, p. 98.

Greger, D. K., 1945, Bibliography of the geology of Missouri: Mo. Geol. Survey and Water Res., v. 31, 2d ser., 294 p.

Gregson, V. G., 1958, A regional gravity survey of parts of Franklin, Crawford, and Washington Counties, Missouri: unpublished M. S. thesis, Washington Univ., St. Louis.

Grenia, J. D., 1960, Precambrian topography and rock types: Mo. Geol. Survey and Water Res. Map.

Hall, D. H., 1962, Least squares in magnetic and gravity interpretation:
Am. Geophys. Union Trans., v. 39, no. 1, p. 35-39.

Haworth, Erasmus, 1888, Contribution to Archaean geology of Missouri:
Am. Geologist, v. 1, p. 280-297; p. 363-382.

_____, 1891, Age and origin of crystalline rocks of Missouri: Mo. Geol. Survey Bull. v. 5, p. 11-42.

_____, 1895, Crystalline rocks of Missouri: Mo. Geol. Survey, v. 8, p. 81-224.

_____, 1896, Archean rocks: Mo. Geol. Survey, v. 9, pt. 3, p. 15-27, 54-68; pt. 4, p. 24-55.

Hayes, W. C., 1947, Geology of the Ozark-Martin mine area, Madison County, Missouri: unpublished M. A. thesis, Univ. of Missouri, School of Mines and Met., Rolla.

_____, 1951, Cambrian iron deposits of Missouri: unpublished Ph. D. thesis, Univ. of Iowa, Iowa City.

_____, 1959a, A compilation of chemical analyses, precambrian rocks of Missouri: Mo. Geol. Survey and Water Res., Misc. Pub.

_____, 1959b, Geology and exploration of Missouri iron deposits [abs.]: Mining Eng., v. 11, no. 1, p. 13.

_____, 1961, Physiographic features of the St. Francois Mountains in Guidebook to the Geology of the St. Francois Mountain area: Mo. Div. Geol. Survey and Water Res. Rept. Inv. No. 26, p. 115-118.

Hayes

304

Hays, Walter, 1961, A paleomagnetic investigation of some Precambrian igneous rocks of southeast Missouri: unpublished Ph. D. thesis, Washington Univ., St. Louis, 194 p.

Hays, W. W., and Scharon, H. L., 1963, An example of the influence of remanent magnetization on magnetic intensity measurements: *Geophysics*, v. 28, no. 6, p. 1037-1048.

Heinrich, R. R., 1937, Seismic activity in the St. Marys (Missouri) region since 1910: *Seismol. Soc. America Bull.*, v. 27, p. 245-250.

_____, 1941, A contribution to the seismic history of Missouri: *Seismol. Soc. America Bull.*, v. 31, no. 3, p. 187-224.

_____, 1946, Northeastern Ozark earthquakes: *Am. Geophys. Union Trans.*, v. 27, p. 320-323.

_____, 1949, Three Ozark earthquakes: *Seismol. Soc. America Bull.*, v. 39, no. 1, p. 1-8.

_____, 1950, Earthquakes in the Sta. Genevieve (Missouri) fault zone: *Earthquake Notes*, v. 21, no. 3, p. 17-18.

_____, 1951a, The northern limits of the New Madrid earthquake region: *Earthquake Notes*, v. 22, no. 1, p. 1-3.

_____, 1951b, A north central Ozark earthquake: *Earthquake Notes*, v. 22, no. 4, p. 35-36.

Henderson, R. G., 1960a, A comprehensive system of automatic computation in magnetic and gravity interpretation: *Geophysics*, v. 25, no. 3, p. 569-585.

_____, 1960b, Polar charts for evaluating magnetic anomalies of three-dimensional bodies: Art. 52 in U. S. Geol. Survey Prof. Paper 400-B, p. B112-B114.

Henderson, R. G., and Zietz, Isidore, 1949a, The computation of second vertical derivatives of geomagnetic fields: Geophysics, v. 14, no. 4, p. 508-516.

_____, 1949b, The upward continuation of anomalies in total magnetic intensity fields: Geophysics, v. 13, p. 517-534.

_____, 1957, Graphical calculation of total-intensity anomalies of three-dimensional bodies: Geophysics, v. 22, no. 4, p. 887-904.

Heyl, A. V., Brock, M. R., Jolly, J. L., and Wells, C. E., 1965, Regional structure of the Southeast Missouri and Illinois-Kentucky mineral districts: U.S. Geol. Survey Bull. 1202-B, p. Bl-b20.

_____, 1958, Mangetic-doublet theory in the analysis of total-intensity anomalies: U. S. Geol. Survey Bull. 1052-D, p. 159-186.

Hershey, O. H., 1901 Peneplains of the Ozark highland: Am. Geologist, v. 27, p. 25-41.

Heyl, A. V., Agnew, A. F., Lyons, E. J., and Behre, C. H., Jr., 1959, The geology of the upper Mississippi Valley zinc-lead district (Ill.-Iowa-Wisc.): U. S. Geol. Survey Prof. Paper 309, 310 p.

Holmes, C. R., 1950, Magnetic fields associated with igneous types in the Central Ozarks: Mining Eng., v. 20, no. 11, p. 1143-1446.

Howell, F. B., et, al., 1944, Correlation of the Cambrian Formations of North America: Geol. Soc. America Bull., v. 55, no. 8, p. 993-1003.

Hsu, I-Chi, 1962, Paleomagnetic investigations of some of the Precambrian volcanic rocks in the St. Francois Mountains, Missouri: unpublished M. A. thesis, Washington Univ., St. Louis, 37 p.

Ireland, H. A., 1955, Precambrian surface in southeastern Oklahoma and parts of adjacent states: Am. Assoc. Petroleum Geologists Bull., v. 39, no. 4, p. 468-483.

Irving, E., 1964, Paleomagnetism: New York, John Wiley & Sons, px 399 p.

James, J. A., 1948, Geology of the Berryman area, Washington County, Missouri: unpublished M. S. thesis, Univ. of Missouri, School of Mines and Met., Rolla.

_____, 1949, Geologic relationships of the ore deposits of the Fredericktown area, Missouri: Mo. Geol. Survey and Water Res. Rept. Inv. No. 8, p. 1-23,

Irving, E., Stott, P. M., and Ward, M. A., 1961, Demagnetization of igneous rocks by alternating magnetic fields: Phil. Mag., v. 6, p. 225-241. 307

_____, 1952, Structural environments of the lead deposits
in the southeastern Missouri mining district: Econ. Geology,
v. 47, no. 6, p. 650-660.

Jenke, A. L., 1948, An investigation of the basic rocks in the
Fredericktown quadrangle, Missouri: unpublished M. S. thesis,
Washington Univ., St. Louis.

Johnson, H. N., 1950, Sequence occupancy of the St. Francis mining
region (historical): unpublished Ph. D. thesis, Washington Univ.,
St. Louis.

Kailasam, L. N., 1953, Geophysical investigations of a near-surface
geologic structure in the neighborhood of Saint Charles, Missouri:
unpublished M. A. thesis, St. Louis Univ., St. Louis.

Keiser, H. D., 1930, Mine La Motte: A historic lead property in south-
east Missouri: Eng. Mining Jour., v. 130, no. 3, p. 110-114.

Keller, Fred, Jr., Henderson, J. R., Dempsey, W. J., and Duffner, R. T.,
1950, Total-intensity aeromagnetic map of Bonneterre quadrangle:
U. S. Geol. Survey Geophys. Inv. Map GP-14.

Keller, W. D., 1945, Common rocks and minerals of Missouri: Univ. of
Missouri Bull., v. 46, no. 5, (Arts and Sci., no. 1), 78 p.

Keyes, C. R., 1896, Geographic relations of the granites and
porphyries in the eastern part of the Ozarks: Geol. Soc. America
Bull., v. 7, no. p. 363-376.

_____, 1910, Controlling factors of ore localization in
the Ozark region: Econ. Geology, v. 5, no. 7, p. 683-688.

Kidwell, A. L., 1942, The igneous geology of Ste. Genevieve County, Missouri: unpublished M. S. thesis, Washington Univ., St. Louis.

_____, 1947, Post-Devonian igneous activity in southeastern Missouri: No. Geol. Survey and Water Res., Rept. Inv. no. 4, 83 p.

King, H., 1851, Remarks on geology of State of Missouri: Am. Assoc. Adv. Sci. Proc., v. 5, 182-200.

King, P. B., 1951, The tectonics of Middle North America: Princeton, Princeton Univ. Press, 191 p.

Koch, H. L., 1932, The igneous geology of the western half of the St. Francois Mountains: unpublished M. S., Washington Univ., St. Louis, 81 p.

Krumbein, W. C., 1956, Regional and local components in facies maps: Am. Assoc. Petroleum Geologists Bull., v. 40, no. 9, p. 2163-2194.

_____, 1959, Trend surface analysis of contour-type maps with irregular control-point spacing: Jour. Geophys. Research, v. 64, no. 7, p. 823-834.

Ku, C. C., and Scharon, H. L., 1965, Application of paleomagnetics to the tectonics of the St. Francois Mountains, Missouri (abs.): Am. Geophys. Union Trans., v. 46, no. 1, p. 66.

Lake, M. C., 1932, The iron ore deposits of Iron Mountain: Int. Geol. Cong., 16th, U. S., Guidebook 2, p. 56-57.

Leaf H. W., 1955, A magnetometer survey of the magnetic highs to the east of St. Clair, Missouri: Unpublished M. A. thesis, St. Louis Univ., St. Louis.

Litton, Abram, 1855, Preliminary report on principal mines in Franklin, Jefferson, Washington, St. Francois, and Madison Counties, Missouri: Mo. Geol. Survey, 1st and 2d. Ann. Rept., pt. 2, p. 71-94.

Londsdale, E. H., 1894, Topography of granite and porphyry region of Missouri: Iowa Acad. Sci. Proc., v. 1, pt. 4, p. 43-48.

Marbut, C. F., 1896, Physical features of Missouri: Mo. Geol. Survey, v. 10, p. 13-109.

_____ ; 1916, Characteristics of soil and its relation to geology [abs.], Geol. Soc. America Bull., v. 27, p. 114-115.

McCracken, M. H., et al, 1961, Geologic map of Missouri: Mo. Div. Geol. Survey and Water Res., 1:600,000.

McEvilly, T. V., 1957, Abnormal sedimentary susceptibilities in Eastern Missouri: Geophys. Soc. Tulsa Proc., v. 4, p. 60-69.

McMillan, W. D., 1946, Exploration of the Bourbon magnetic anomaly, Crawford County, Missouri: U. S. Bur. Mines Rept. Inv. 3961, 9 p.

Melton, F. A., 1931, Post-Pennsylvania denudation of the Ozark dome: Am. Jour. Sci., 5th ser., v. 21, p. 214-219.

Meyers, Charles, 1939, The Geology of the Pilot Knob, Missouri, iron mineralization: unpublished M. S. thesis, Washington Univ., St. Louis.

Moss, R. G., 1936, Buried precambrian surfaces in the United States: Geol. Soc. America Bull., v. 47, no. p. 935-966.

Mumme, W. G., 1964, Negative total-intensity magnetic anomalies in the southeast of South Australia: Jour. Geophys. Research, v. 69, no. 2, p. 309-315.

Muilenburg, G. A., and Goldich, S. S., 1933, Petrography and petrology of the Mount Devon diabase porphyry: Am. Jour. Sci., 5th ser., v. 26, no. 153, p. 355-367.

Muilenburg, G. A., and Beveridge, T. R., 1954, Guidebook of the 17th Regional Field Conference of the Kansas Geological Society: Mo. Geol. Survey and Water Res. Rept. Inv. no. 17, p. 14-44.

Murphy, J. E., and Mejia, V. M., 1961, Underground geology at Iron Mountain in Guidebook to the Geology of the St. Francois Mountain area: Mo. Div. Geol. Survey and Water Res. Rept. Inv. No. 26, p. 129-137.

Nagata, Takesi, 1961, Rock magnetism: Tokyo, Maruzen Co. 350 p.

Nason, F. L., 1892, A report on the iron ores of Missouri: Mo. Geol. Survey, v. 2, 366 p.

_____, 1901, The geological relations and the age of the St. Joseph: Am. Jour. Sci., 4th Ser., v. 12, p. 358-361.

Neal, D. A., 1956, A gravity and magnetic survey in southeastern Missouri: unpublished M. A. thesis, St. Louis Univ., St. Louis.

Nettleton, L. L., 1954, Regionals, residuals, and structures: Geophysics, v. 19, p. 23-45.

Ohle, E. L., Jr., 1952, Geology of the Hayden Creek lead mine, southeast Missouri: Min. Eng., v. 4, no. 5, p. 477-483.

Ohle, E. L., and Brown, J. S., [Editors]- 1954, Geologic problems in the southeast Missouri lead district: Geol. Soc. America Bull., v. 65, no. 3, p. 201-222; no. 9, p. 935-936.

_____, E. L., Jr., 1959 Some considerations in determining the origin of ore deposits of the Mississippi Valley type: Econ. Geology, v. 54, no. 5, p. 769-789.

Oldham, C. H. G., and Sutherland, D. B., 1955, Orthogonal polynomials: their use in estimating the regional effect: *Geophysics*, v. 20, p. 295-306.

Parizek, E. J., 1949, The geology of the Tiff and Vineland quadrangles of southeast Missouri: unpublished Ph. D. thesis, Univ. of Iowa, Iowa City.

Peters, L. J., 1949, The direct approach to magnetic interpretation and its practical application: *Geophysics*, v. 14, p. 290-320.

Petrie, W. L., 1951, Geology of the southeast portion of the Sullivan quadrangle, Missouri: unpublished M. S. thesis, Univ. of Iowa, Iowa City.

Pilkford, P. J., 1953, Geology of the southeast portion of the Richwoods quadrangle, Missouri: unpublished M. S. thesis, Univ. of Iowa, Iowa City,

Pike, R. V., 1929, The geology of a portion of the Crystal City quadrangle, Missouri: unpublished M. S. thesis, Univ. of Chicago, Chicago.

Pirson, S. J., 1940, Polar charts for interpreting magnetic anomalies: *Am. Inst. Mining Metall. Engineers Trans.*, v. 138, p. 173-185.

Powers, Harold, Scharon, H. L., and Tolman, Carl, 1953, Geophysical case history, Fredericktown lead district, Missouri: *Mining Eng.*, v. 5, no. 3, p. 317-320.

Pampelly, Raphael, 1873, Notes on geology of Pilot Knob and its vicinity: *Mo. Geol. Survey*, v. 1 p. 3-28,

Reinhard, J. S., and Meyer, R. P., 1961, Explosion studies of continental structure: Carnegie Inst. of Wash. Publ. 622, 409 p.

Richards, M. E., 1946, Magnetic surveying in progress in Missouri iron ore areas: Skillings Mining Rev., v. 34, no. 38, p. 1.

Ridge, J. D., 1957, The iron ores of Iron Mountain, Missouri: Mineral Industries, v. 26, no. 9, p. 1-6.

Robertson, Forbes, 1940, Flow sequence in the felsite rocks in the eastern Ironton quadrangle [Abs.]: Mo. Acad. Sci. Proc., v. 6, no. 4, p. 83-84.

_____, and Tolman, Carl, 1948, High-potash volcanic rocks, St. Francois Mountains, Missouri [Abs.]: Geol. Soc. America Bull., v. 59, no. 12, pt. 2, p. 1347.

_____, 1969, Exposed Precambrian rocks of Missouri in Hayes, W. C. [Editor], Precambrian Rocks of Missouri: Mo. Div. Geol. Survey and Water Res., 2nd Ser.

Ross, C. S., and Smith, R. L., 1961, Ash-flow tuffs: Their origin, geologic relations and identification, U. S. Geol. Survey Prof. Paper 366, 81 p.

Rust, G. W., 1937, Preliminary notes on explosive volcanism in southeast Missouri: Jour. Geology, v. 45, no. 1, p. 48-75.

Sauer, C. O., 1920, The geography of the Ozark Highland of Missouri: Geol. Soc. Chicago Bull., v. 7, 245 p.

Scharon, H. L., 1962, Correlation of geology and geophysical data in the search of Mississippi lead deposits [Abs.]: Geol. Soc. America Bull., v. 63, no. 12, pt. 2, p. 1384.

_____, Hays, Walter, and Anderson, R. E., 1961, Paleomagnetic investigations in the St. Francois Mountains in Guidebook to the Geology of the St. Francois Mountain area: Mo. Div. Geol. Survey and Water Res. Rept. Inv. no. 26, p. 106-014.

Schmidt, Adolph, 1873, Iron ores of Missouri: Mo. Geol. Survey Rpt., v. 1, p. 50-214.

_____, 1874, The lead region of central Missouri: Mo. Geol. Survey Rept. 1873-1874, v. 1, p. 503-577.

Schoolcraft, H. R., 1819, A view of the lead mines of Missouri (including observations on the mineralogy, geology, antiquities, soil, climate, population and productions of Missouri and Arkansas, and other sections of the western country): 299 p., New York.

Searight, T. K., Williams, J. H., and Hendrix, J. S., 1954, The structure of the Bourbon-Sullivan area, Crawford, Franklin, and Washington Counties: Mo. Div. Geol. Survey and Water Res. Rept. Inv. no. 16, 14 p.

Shumard, B. F., 1873, Geological description of St. Genevieve County: Mo. Geol. Survey Rpt. 1851-1871, p. 290-303.

Singewald, J. T., Jr., and Milton, Charles, 1929, Origin of iron ores of Iron Mountain and Pilot Knob, Missouri: Am. Inst. Mining Metall. Engineers Trans., v., p. 330-340.

Skeels, D. C., 1947, Ambiguity in gravity interpretation: Geophysics v. 13, no. 1, p. 43-56.

Slichter, L. B., 1942, Magnetic properties of rocks: Geol. Soc. America, Spec. Paper, no. 36, p. 295-296.

Snyder, F. G., and Emery, J. A., 1956, Geology in development and mining, southeast Missouri lead belt: Mining Engg, v. 8, no. 12, p. 1216-1224.

Snyder, F. G., and Odell, J. W., 1958, Sedimentary breccias in the southeast Missouri lead district: Geol. Soc. America Bull., v. 69, no. 7, p. 899-926.

Snyder, F. G., and Wagner, R. E., 1961, Precambrian of southeast Missouri: Status and problems in Guidebook to the Geology of the St. Francois Mountain area: Mo. Div. Geol. Survey and Water Res. Rept. Inv. no. 26, p. 84-94.

Sosman, R. B., and Hostetter, J. C., 1917, The ferrous iron content and magnetic susceptibility of some artificial and natural oxides of iron: Am. Inst. Mining Engineers Trans., v. 58, p. 341.

Spurr, J. E., 1926, The southeast Missouri ore magmatic district: Eng. Mining Jour., v. 122, no. 25, p. 2-12, 968-975.

_____, 1927, Iron ores of Iron Mountain and Pilot Knob: Eng. Mining Jour., v. 123, no. 8, p. 363-3661

Steel, A. A., 1910, The geology, mining, and preparation of barite in Washington County, Missouri: Am. Inst. Min. Engineers Bull., v. 38, p. 85-117.

Steinhart, J. S., and Meyer, R. P., 1961, Explosion studies of continental structure: Carnegie Inst. Washington Pub. no. 622, p. 226-247.

Stickel, J. F., Jr., 1949, The igneous geology of the Bonne Terre quadrangle: Unpublished A. M. thesis, Washington Univ., St. Louis.

Stose, G. W., 1932, Geo-logic map of the United States: U. S. Geol. Survey Geologic Map.

Swartz, C. A., 1954, Some geometrical properties of residual maps: Geophysics, v. 19, p. 46-70.

Swallow, G. C., 1855, First and Second annual report of the geological survey of Missouri: Mo. Geol. Survey, 440 p.

Tarr, W. A., 1918, The barite deposits of Missouri and the geology of the barite district: Univ. of Missouri Studies, v. 3, no. 1.

_____, 1932, Intrusive relationship of the granite to the rhyolite (porphyry) of southeastern Missouri: Geol. Soc. America Bull., v. 43, no. 4, p. 965-992.

_____, 1936, Origin of the southeastern Missouri lead deposits, Econ. Geology, v. 31, no. 7, p. 712-754; pt. 2, no. 8, p. 832-866.

_____, and Keller, W. D., 1933, Post-Devonian igneous intrusion in southeastern Missouri: Jour. Geology, v. 41, p. 815-823.

Thomas, L. F., 1924, Climate of St. Louis: Wash. Univ. Studies, v. 12, Ser. 1,

Tolman, Carl, 1929, Igneous rocks of the Mississippi Valley lead-zinc districts: Geol. Soc. America, Spec. Paper no. 24, p. 71-103.

_____, 1933, The geology of the Silver Mine area, Madison County, Missouri: Mo. Bur. Geol. and Mines, Bienn. Rept. of the State Geologist to the 57th Gen. Assembly, 1931-32, app. 1, p. 1-39.

Tolman, C. F., and Robertson, Forbes, 1969, Exposed Precambrian rocks in southeast Missouri: Missouri Geol. Survey and Water Res. Rept. Inv., no. 44, 63 p.

Tolman, Carl, and Koch, H. L., 1936, The accessory minerals of the granites of Missouri: Washington Univ. Studies, new ser., no. 9, p. 11-50.

Tolman, Carl, and Meyer, Charles, 1939, Pre-Cambrian iron mineralization in southeast Missouri (Abs.): Econ. Geology, v. 34, no. 8, p. 946-947.

U. S. Coast and Geodetic Survey, 1955, Total intensity chart of the United States 1955.0: Chart No. 3077f.

Vaquier, Victor, Steenland, N. C., Henderson, R. G., and Zietz, Isidore, 1951, Interpretation of aeromagnetic maps: Geol. Soc. America Mem. 47, 151 p.

Vestine, E. H., and David, N., 1945, Analysis and interpretation of geomagnetic anomalies: Terr. Mag. and Atmos. Elect., v. 50, no. 1, p. 1-36.

Wagner, R. E., 1947, "Lead-belt" geology, St. Joseph lead enterprise: Mining and Metallurgy, v. 28, no. 488, p. 366-368.

Walcott, C. D., 1912, New York Potsdam-Hoyt Fauna: Smithsonian Misc. Coll., v. 57, no. 9, p. 251-304.

Walker, T. H., 1942, The geology of the northwest quarter of the Ironton quadrangle: unpublished M. S. thesis Washington Univ., St. Louis.

Walter, E. J., 1940, Earthquake waves, velocities, and travel times, and crustal structure south of Saint Louis: Unpublished M. S. thesis, St. Louis Univ., St. Louis.

Vestine, E. H., LaPorte, Lucile, Lange, Isabelle, Cooper, Caroline, and Hendrix, W. C., 1959, Description of the Earth's main magnetic field and its secular change, 1905-1945: Carnegie Inst. of Wash. Publ. 578, 532 p.

Weigel, W. W., 1965, The inside story of Missouri's exploration boom:
Eng. and Mining Jour. v. 166, no. 11, p. 77-172.

Warfield, R. G., 1953, Stratigraphy and structure of the northeast
quarter of the Richwoods Quadrangle, Missouri: unpublished M. S.
thesis, Univ. of Iowa, Iowa City.

Weller, Stuart, and St. Clair, Stuart, 1928, Geology of Ste. Genevieve
County, Missouri: Mo. Bur. Geol. and Mines, v. 22, 2d. ser.,
p. 248-251.

Weller, J. M., and Workman, L. E., 1948, Structural Development of
Eastern Interior Basins[Abs.]: Am. Assoc. Petroleum Geologists
Bull., v. 32, p. 300.

Werner, Sture, 1945, Determinations of the magnetic susceptibility of
ores and rocks from Swedish iron ore deposits: Sveriges Geol.
Undersökning, Ser. C, No. 472, Arsbok 39, no. 5, 79 p.

Wheeler, H. A., 1896, Clay deposits: Mo. Geol. Survey, v. 11, 1st
Ser., 622 p.

Wilson, M. E., 1922, The occurrence of oil and gas in Missouri: Mo.
Bur. Geol. and Mines, v. 16, 2nd Ser., 284 p.

Wing, R. B., 1932, The igneous rock types of the eastern half of the
St. Francois Mountains: unpublished M. S. thesis, Washington
Univ., St. Louis,

Winslow, Arthur, 1894a, Lead and zinc deposits: Mo. Geol. Survey,
v. 6, p. 432-434.

_____, 1894b, Lead and zinc deposits of Missouri:
Mo. Geol. Survey, v. 7, sec. 2.

_____, 1896, The disseminated lead ores of southeastern
Missouri: U. S. Geol. Survey Bull. 132, 31 p.

Winslow, Arthur, Haworth, Erasmus, and Nason, F. L., 1894, Report on
the Iron Mountain sheet: Mo. Geol. Survey, v. 9, Rpt. 3, 85 p.

Zarzavatjian, P. A., 1958, Detection of Buried basement highs by
airphoto drainage pattern analysis, Reynolds and Wayne Counties,
Missouri: unpublished M. A. thesis, Univ. of Missouri, School
of Mines and Met., Rolla.

Zietz, Isidore, and Henderson, R. G., 1956, A preliminary report of
model studies of magnetic anomalies of three-dimensional bodies:
Geophysical v. 21, no. 3, p. 794-814.